HYDROCLIMATIC VARIABILITY IN THE ROCKY MOUNTAIN REGION

David Changnon
Thomas B. McKee
Nolan J. Doesken

Colorado State University

Climatology Report No. 90-3

DEPARTMENT OF ATMOSPHERIC SCIENCE

PAPER NO. 475

HYDROCLIMATIC VARIABILITY IN THE ROCKY MOUNTAIN REGION

by

David Changnon

Thomas B. McKee

Nolan J. Doesken

Research was supported by
United States Geological Survey
under Grant Number 14-08-0001-G1294 and
the Colorado Agricultural Experiment Station.

Department of Atmospheric Science
Colorado State University
Fort Collins, Colorado
80523

December 1990

Atmospheric Science Paper No. 475

Climatology Report No. 90-3

ABSTRACT

HYDROCLIMATIC VARIABILITY IN THE ROCKY MOUNTAIN REGION

Interrelated hydroclimatic elements were investigated to determine characteristics of the spatial and temporal climate variability in a five-state region located in the Northern Rocky Mountain Region. The study covered a 35-year period from 1951-1985. The study included 1) developing an interrelated hydroclimatic database, 2) analyzing 14 carefully selected watersheds, 3) analyzing all complete and consistent snowpack and precipitation measurement sites in the five-state region, and 4) describing the association of large-scale circulation indices and winter synoptic patterns to hydroclimatic variability in the Rocky Mountains.

A database was developed to provide a foundation for thoroughly analyzing hydroclimatic variability in the Rockies. The three primary hydroclimatic elements analyzed included total water-year streamflow (ST), winter (October 1-March 31) accumulated precipitation (PR), and April 1 snowpack (SN).

The watershed analyses showed wide differences in SN, PR, and ST variability values spatially and these differences were explained by basin exposure, or aspect, to moist air flows. The stable (low variability) basins with a measure of variability less than 0.55 were exposed to prevailing northerly or westerly flow, while unstable basins were exposed to infrequent southerly or easterly flow. Correlation

analysis between hydroclimatic elements within basins identified SN as the best indicator of ST in 11 of 14 watersheds in the Rocky Mountains. Overall SN was determined to be the best monitor of winter climate in the Rockies. The ST data in the West is so affected by man-made diversions that in most areas it is difficult to use as a representative measure of the hydrologic system's behavior.

Using complete SN and PR data sets from across the five-state study area, stable and unstable regions were separated by the 0.55 measure of variability isoline. Nearly, a factor of two difference was observed in the average magnitude of variability in the two types of regions. The stable and unstable regions revealed a relationship of their variability with how the mountain barrier in each region is exposed to moist air flows, as did the 14 watersheds. Furthermore, these regions (based on magnitude of their SN and PR variabilty) represent a new hydroclimatic classification system for the West, one potentially useful in water resource design and management.

Three basic and persistent patterns of annual SN values were found: 1) years with a consistent anomaly over the entire region, either wet or dry; 2) years with a distinct north-to-south gradient; and 3) average years with average as well as isolated areas of wet and dry located throughout the study region. The distribution of SN patterns during the 35-year period showed that wet, dry, and average patterns occurred throughout the period. However, the wet-north/dry-south gradient patterns occurred only before 1974 and dry-north/wet-south gradient patterns did not occur before 1973. The long-term (decadal or longer) wet and dry periods experienced in the northern and

southern regions of the five-state region are due to north-to-south gradient periods.

Large-scale circulations associated with El Nino-Southern Oscillation (ENSO) events provide 10% more SN to unstable sites with south or southwesterly exposure to moist air flow than circulations associated with non-ENSO events, while stable regions with exposures to northerly or westerly moist air flow are 10% drier during ENSO events than in non-ENSO years. Seasonal large-scale atmospheric/oceanic circulations, such as the ENSO and Pacific-North American index, are weakly correlated ($r < +0.60$) to regional-averaged SN. A seasonally averaged PNA index identified 77% of the non-average annual SN patterns, while monthly averaged 700 mb height and dew-point depression probabilities explained 80% of the non-average SN patterns. These large numbers of annual SN patterns identified indicates that both seasonal and monthly averaged indices should be considered as potential predictive tools. Long-term changes in the seasonally averaged values of large-scale indices (during the mid 1970s) occurred at the same time as long-term changes in regionally averaged SN and at the same time changes in the type of north-to-south gradient pattern were experienced. The change that occurred in the mid 1970s in both SN and the seasonal indices suggests they are all dependent on some other physical phenomena that is part of the global ocean-climate system. Since the economic and social impacts resulting from the persistent wet and dry periods are sizable, further research should focus on identifying long-term variability characteristics and understanding the global ocean/climate system.

Based on PR and SN distributions identified earlier, seven 500 mb winter synoptic patterns were identified as the climatological group that explained almost 98% of the daily winter (October 1 - March 31) synoptic maps for the period from October 1950 through March of 1985. The seven patterns included: 1) ridge, which is associated with dry precipitation anomalies across the five-state region, 2) meridional NW, WNW, and zonal, which are associated with potential wet precipitation anomalies across the northern regions, and 3) trough, split-flow, and cut-off, which are associated with potential wet precipitation anomalies across the southern regions. The winter synoptic patterns identified 89% of the non-average SN patterns and were determined to best explain how the annual SN patterns formed. Changes in the frequency of synoptic patterns clearly explained 1) the change in north-to-south gradient years and 2) the change in regionally averaged SN that occurred in the mid 1970s. Some other interesting but inconclusive analyses suggested that 1) spatial variability in SN is associated with the variability in synoptic patterns and 2) large-scale indices such as ENSO and PNA are not always identified by certain synoptic patterns. Further research may find the physical links to these unanswered questions.

ACKNOWLEDGEMENTS

Dave Changnon would like to thank his wife, Suzy, for providing special support by editing drafts of this report, expressing interest in the work and unrelenting encouragement through the course of the research. He also thanks his father, Stan, for developing his interest in atmospheric sciences at an early age and encouraging him to go to graduate school at Colorado State University.

The efforts of Dr. William Gray, Dr. Roger Pielke, and Dr. Jose Salas, in directing the course of the research and making valuable constructive comments on this report, are appreciated.

Special thanks go to Ms. Odie Bliss for help with the draft final report and Ms. Judy Sorbie for drafting several of the figures.

This work was supported by the U.S. Geological Survey under award #14-08-0001-G1294 and the Colorado Agricultural Experiment Station.

TABLE OF CONTENTS

TABLE OF CONTENTS (continued)

CHAPTER 1

INTRODUCTION

Each year the available water stored in the winter snowpack of the Rocky Mountains provides much of the usable surface water in the western United States. Much of the economic and environmental welfare of the West is effected by the availability of water (Weiss, 1982) stored in the winter snowpack and derived from winter precipitation. These surface water resources are controlled directly by climatic factors. Because winter precipitation, winter snowpack and streamflow are interrelated elements and represent parts of the hydrologic cycle and climate system, they will be referred to as hydroclimatic elements.

Recent droughts and periods of excessive runoff tied to wide fluctuations or variability in winter precipitation and snowpack have created difficult problems for those who must design facilities and manage the distribution of the available surface water. The term variability as used in this study is defined as variations in time. Understanding the hydroclimatic variability characteristics of the Rocky Mountain Region is particularly important because winter precipitation stored in the winter snowpack represents 85% of the area's total streamflow (Grant and Kahan, 1974) and is the source of water for the rest of the West. Few studies have examined the relationships of winter snowpack variability to streamflow variability in this region (Meko and Stockton, 1984; Peterson et al, 1987) or the

existing connections between large-scale atmospheric/oceanic circulations and hydroclimatic variability in the Rocky Mountains.

In the last decade a new issue, global climate change, has raised added concerns about the hydroclimatic elements of the area and potential future stresses on the area's water resources. Global climate models allow atmospheric scientists to consider potential ramifications from increased concentrations of trace gases on the hyrologic cycle (Manabe and Weatherald, 1975; Aston, 1984; Yeh et al., 1984; Gleick, 1986; Abramopoulus et al., 1988; Rind, 1988). The effects of possible global climate changes on interannual variability of regional water supplies would be very important, especially in the West where water demands have almost exceeded available water resources (Gleick, 1986). Even now, minor fluctuations in the water supply can produce significant problems.

1. Purpose

The water that is stored in the winter snowpack of the Rocky Mountains is a variable resource for the West. This study focused on three problems: 1) how variable are the three most critical hydroclimatic elements, winter precipitation, snowpack, and streamflow, associated with the resource, 2) what are the characteristics of this variability, and 3) what are the potential causes for this variability. The hypotheses examined were: 1) that the spatial variability of winter precipitation, largely stored as snowpack, and annual streamflow was geographically organized and controlled by major surface physical variables such as elevation, latitude, basin size, and aspect/exposure, as well as frequency of large-scale synoptic patterns, and 2) that the

temporal variability of hydroclimatic elements was affected by some major atmospheric/oceanic circulation indices and the frequency occurrence of certain large-scale synoptic types. The major objectives of this study were to: 1) develop a database for hydroclimatic research in the Rocky Mountains, 2) define and explain the magnitude of variability of key hydroclimatic elements, 3) examine the complex relationship of hydroclimatic elements both spatially and annually, 4) determine the annual patterns of hydroclimatic elements and the association between interannual variability and long-term (decade or longer) variability, and 5) distinguish possible interannual or long-term ties between the identified spatial and temporal variability characteristics of hydroclimatic elements and features of large-scale atmospheric circulation. The results of the study will serve as a basis for better describing temporal fluctuations found between years and multi-year periods on a regional scale, and also as a foundation for improved in-season predictions of annual runoff. Both are essential to manage western surface water resources better and to design future water systems properly.

Previous studies have provided a foundation from which this study has been built. The next section will review studies related to the issues considered in this paper.

2. Review of Hydroclimatic Investigations

Studies of hydroclimatic variability over complex terrain such as the Rocky Mountains have focused on two areas: definition of the spatial and temporal variability of precipitation and streamflow data, and the relationship of temporal variations in precipitation and/or

streamflow data to large-scale atmospheric conditions. A summary of previous work pertinent to these two areas is presented in the following sections. Precipitation studies will be reviewed before streamflow studies in each section.

A. Hydroclimatic Variability

Early studies examined the spatial variability of precipitation across parts of North America. Conrad (1941) and Longely (1952) provided useful discussions about the limitations for describing the variability of precipitation as well as determining how precipitation variability changed across the United States. First, precipitation for periods less than one year is not normally distributed. Second, most of the descriptors of variability vary according to the mean value of precipitation. Longely (1952) discussed four measures of precipitation variability shown below.

coefficient of variation $v_\sigma = \sigma/\bar{x}$ (1)

the relative variability $v_r = \text{m.d.}/\bar{x}$ (2)

$v_Q = Q/\text{Median}$ (3)

and $v = \text{Range}/\text{Median}$ (4)

where: $\sigma = \sqrt{1/N\sum(x_i-\bar{x})^2}$ = standard deviation (5)

$\bar{x} = \sum x_i/N$ = mean (6)

N = number of items in sample

x_i = value for each item in sample

$\text{m.d.} = 1/N\sum|x_i-\bar{x}|$ = mean deviation from the mean (7)

$Q = Q_3-Q_1/2$ = the quartile deviation (8)

$$
\begin{aligned}
Q_3 &= 75\% \text{ (upper quartile) value} \\
Q_1 &= 25\% \text{ (lower quartile) value} \\
\text{Median} &= \text{single middle value in an ordered list} \\
\text{Range} = x_{max} - x_{min} &= \text{range between highest and lowest values in a sample}
\end{aligned} \tag{9}
$$

Longely (1952) considered the relationship between the coefficient of variation and mean precipitation for areas in the U.S. Pacific Northwest. The correlation coefficient relating precipitation to v_σ for July data was -0.68, for December data -0.71, and for annual data -0.48. The author did not consider these correlations to be very strong. However, Longely concluded that out of these four measures of variability, the coefficient of variation was the best choice to compare variability between different stations. The map of the coefficient of variation, as published by Hershfield (1962), illustrates the variability of annual precipitation in the United States. Variability of annual precipitation was identified to generally increase by a factor of three from the wettest locations to the driest.

A study by Marlatt and Reihl (1963) described the variability of annual precipitation in the Upper Colorado River. Their results suggested that the variance of annual precipitation is caused by variations in the number of days having large amounts of precipitation (>0.10") and produced by passing synoptic-scale weather disturbances.

Results also indicated that 50% of the annual precipitation is produced by 16% of the number of days having precipitation per year.

Several studies identified characteristics of precipitation variability. Using the empirical orthogonal function approach, Sellers (1968) determined the dominant monthly precipitation anomaly patterns for the western United States using records from 1931-1966. Only 45% of the variance can be explained by three eigenvectors. The two monthly patterns found to be most common in winter were a consistent anomaly over the West, and a north-to-south gradient with anomalies of opposite sign in the Pacific Northwest and New Mexico. A paper by Bradley (1980) compared temporal fluctuations of temperature to precipitation across the Rocky Mountains. The results indicated that warm winters (above average) experienced below average precipitation while cool winters (below average) were wetter than average during the period from 1891-1978. The correlations between winter temperature and precipitation were poor ($r < +0.50$). Barry (1981) indicated that increases of precipitation with higher elevations is not attributed to more events each winter but to a larger number of events which produce >1" of precipitation. These large precipitation producing events were found to occur during warm-sector periods with southwesterly airflow at 500 mb. He also suggested that storm types and synoptic flow patterns can also introduce major differences in precipitation distribution across highly complex terrain. A multiple regression analysis described by Barry found that the mean winter precipitation amounts are highly correlated ($r = 0.94$) with the combined surface influence of 1) station elevation, 2) maximum relative relief within 8 km radius, 3) exposure (the fractional circumference of

a circle 32 km in radius not containing a barrier more than 300 km higher than the station), and 4) the orientation (the direction of the sector of greatest exposure). Diaz and Fulbright (1981) analyzed United States winter precipitation data using eigenvectors to identify spatial patterns of variability. Their work identified 5 eigenvectors that explained 67% of the variance. The first eigenvector showed a similar sign across the country, but explained only 27.3% of the variance. The second eigenvector identified centers with opposite signs in the northwest and southeast corners of the United States. The third and fifth eigenvectors showed a north-to-south change in signs. The fourth eigenvector identified the western and southeastern parts of the United States with the same sign and the Mississippi Valley with the opposite sign. Although these studies identified annual precipitation patterns, they did not consider 1) using snowpack data, 2) the effect of annual patterns on long-term periods, and 3) the causes of the interannual variability identified in the patterns.

Results from a recent study by Cowie and McKee (1986) considered the role of large, daily precipitation events to explain the precipitation variability in each season and annually. Their results suggested that large events, those that provide 20-25% of the annual precipitation, play a significant role in explaining 81% of annual precipitation variability. Large summer events drive most of the annual variability across low elevation (below 5000') areas of Colorado, while in the mountain regions both large summer and winter events effect variability. Redmond and Koch (1990) identified spatial patterns of annual and semi-annual precipitation variability. The Redmond and Koch study, like that of Sellers (1968), identified a

consistent anomaly pattern that explained the most variance followed by the north-to-south gradient pattern.

Three recent studies examined streamflow variability across the western United States. A study by Meko and Stockton (1984) examined temporal fluctuations in streamflow and their relationship to climate in the West. Opposite streamflow anomalies existed in two regions, the Pacific Northwest and the Southwest. This north-to-south gradient has been identified in other previously discussed studies by Sellers (1968) and Redmond and Koch (1988). However, Meko and Stockton (1984) determined that north-to-south gradient was the predominant pattern with only one winter, 1976-77, exhibiting a common anomaly (dry) pattern over all regions of the West. Lins (1985) identified spatial patterns in streamflow variability using principal component analysis based on United States streamflow data from 1931-1978. Lin's study found five significant components that accounted for only 56% of the total variance: 1) all one type of anomaly, 2) north-to-south gradient pattern, 3) east-to-west gradient pattern, 4) of one sign on the east and west coasts of the United States and an anomaly of the opposite sign in the central U.S., and 5) a negative anomaly in the northeastern U.S. with a positive anomaly elsewhere in the U.S. A paper by Peterson et al. (1987) investigated the time series of streamflow gauges and precipitation stations along the west coast of the United States. They identified a north-to-south gradient in streamflow anomalies as the predominant anomaly pattern. In these streamflow studies causes for the interannual variability were not given and spatial differences in variability were not identified.

B. Relationship of Hydroclimatic Variability to Large-Scale Atmospheric/Oceanic Features

The work addressed here has used time series of sea-surface temperatures (SST), sea-level pressure (SLP), and geopotential height fields (GHF) to identify teleconnections to North American hydroclimatic elements such as precipitation and streamflow. The SST, SLP, and GHF time series are associated with large-scale atmospheric/oceanic circulations such as El Nino-Southern Oscillation (ENSO), Rasmusson and Carpenter (1982); and Pacific-North America pressure anomalies (PNA), Wallace and Gutzler (1981). Studies that discuss the connection of large-scale circulations to precipitation in the United States are examined first.

Several recent studies examined the relationship of PNA to precipitation variability in North America through use of SLP or GHF anomalies in the northern Pacific. Blasing and Lofgren (1980) identified recurrent patterns of seasonal SLP over the North Pacific and western North America using correlation coefficients computed between anomaly maps to determine which seasonal precipitation patterns were related to the SLP patterns. The authors found that the location and strength of the Aleutian Low was an important factor in determining the type and location of seasonal precipitation anomalies in the United States.

A study by Diaz and Namias (1983) examined the relationship of seasonal precipitation anomalies across the United States to concurrent GHF anomalies over the northern Pacific. Few significant correlations were found between seasonal precipitation and mid-tropospheric heights. The strongest correlations between seasonal precipitation and pressure

heights were $+0.11 < r < +0.44$, which are poor. These correlations occurred in the winter and summer.

Cayan and Roads (1984) found significant moderate correlations ($+0.50 < r < +0.80$) between winter West Coast (California to Washington) precipitation and local 700 mb circulation parameters such as zonal wind, height, and dew point data. SLP also had moderate correlations with West Coast seasonal precipitation. Other circulation parameters such as meridional wind and advection of relative vorticity were poorly correlated ($0 < r < +0.50$) to winter precipitation along the West Coast.

Some studies have focused on identifying spatial patterns of temperature and precipitation that are related to both the ENSO and PNA phenomena. Yarnal and Diaz (1986) examined the time series of the ENSO phenomena to winter climatic elements along the West Coast of North America. Pronounced anomalies were detected, and during ENSO events areas in California experienced below-average precipitation, while areas along the Northern British Columbia Coast experienced above average precipitation. Consistent (all wet or all dry) precipitation anomalies were much more difficult to identify during "cold SST" or La Nina events. In this study more climatic anomalies along the West Coast were identified by the PNA index than by ENSO.

A study by Ropelewski and Halpert (1986) identified precipitation and temperature patterns across North America that exhibited a teleconnection to ENSO events. Analysis showed that in the U.S. Pacific Northwest, below-average winter precipitation occurred during 70% of the ENSO events. Analysis in parts of the southeastern United

States showed above-average winter precipitation during 18 of 22 ENSO events.

A study by Kiladis and Diaz (1989) showed how regional precipitation anomalies around the world change signs during the course (24 months) of the ENSO event. Their results, based on 14 ENSO events, indicated that regions in the U.S. Southwest experienced above-average winter precipitation during ENSO events.

A study by Cayan and Peterson (1990) examined the relationship of North Pacific SLP anomalies and ENSO to western North America (California to Alaska) streamflow anomalies. Areal patterns of streamflow were identified and found to be consistent with those discussed by Meko and Stockton (1984), and Lins (1985). Strong north-to-south gradient patterns in streamflow existed. Streamflow patterns along the Pacific Coast were identified to have moderate correlations to PNA. During ENSO events, the streamflow anomalies of following spring seasons were identified as below-average in the U.S. Pacific Northwest, while regions in the U.S. Southwest exhibited above- average flow anomalies. These conclusions compare readily with those of Kiladis and Diaz (1989) that identified positive precipitation anomalies in the southwestern United States during ENSO events.

Few, if any, past studies have examined: 1) the spatial and annual variability characteristics of streamflow, snowpack, and precipitation within a group of near-virgin watersheds, 2) how well snowpack data can monitor hydroclimatic variability in the West, 3) why spatial differences in variability of hydroclimatic elements exist across the Rockies, 4) the time series of annual snowpack patterns, 5) the relationship of north-to-south gradient years to long-term dry and

wet periods and large-scale circulations, 6) whether large-scale indices are associated with patterns of variability, and 7) whether shorter averaging periods (month or less) of large-scale circulations may be better related to hydroclimatic patterns at the surface. This study reported herein will provide answers to these questions.

3. Procedure

This investigation consisted of 1) developing a hydroclimatic database and 2) five interrelated studies, chosen to serve the hypothesis and its objectives. A database was developed to incorporate interrelated physical processes of hydroclimate in the Rockies and to provide a foundation for analyzing variability for the period from 1951-1985. Initial results based on a watershed study herein were used to develop strategies for further studies. Two studies considered the spatial and annual variability across the five-state region. The fourth and fifth studies integrated the results from the preceeding studies. The relationship between the annual and spatial variability of April 1 snowpack and large-scale circulations, including winter synoptic patterns, was examined to discern possible explanations for hydroclimatic variability in the Rockies.

The first part of the study focused on developing a database for hydroclimatic research in the Rocky Mountains. Data sources that represented different processes of hydroclimate were identified and described. Data from three hydroclimatic elements, October 1-March 31 precipitation (PR), April 1 snowpack (SN), and total water-year streamflow (ST), were evaulated and sites then selected for analysis. The physical processes that influence hydroclimatic elements in the

Rockies were discussed and advantages and disadvantages described for each.

The first study focused on the describing the hydroclimatic variability of SN, PR, and ST found within several watersheds located throughout the Rocky Mountains. A watershed selection criteria was developed and used to select watersheds for study. The magnitude of variability for each element within each watershed was then described. The measure of variability was used to explain differences in the spatial variability and identify what physical variables control the spatial variability. Finally, the study considered the relationship of the three elements within each watershed.

The next major analysis focused on observed spatial patterns of variability for all PR and SN located in the five-state region for the period from 1951-1985. First, the variability of all SN and PR sites was computed. These values were used to identify spatial patterns of variability within the five-state region. Physical reasons for the placement of the identified regions were discussed and compared to the results from the watershed study.

The third study identified the spatial patterns of annual SN and PR. Annual patterns of SN and PR were delineated. Regionally averaged annual PR and SN data were related to assess temporal variability traits similar to those described in the watershed study. Next, changes in interannual variability of SN were defined and the distribution of patterns identified. Finally, long-term variability of SN and PR were described, and the possible link of years with north-to-south gradient patterns to long-term dry and wet periods was assessed.

The fourth study considered the relationship of hydroclimatic variability, as described for SN and PR in the prior studies, to that of large-scale atmospheric/oceanic circulation indices in an attempt to determine the potential causes for variability in the Rockies. First, a brief description is presented of five large-scale indices that have teleconnections to weather conditions in North America. The association of ENSO with patterns of SN variability was analyzed. Next, correlations were computed for the relationship of the large-scale circulation indices to the regional SN data. Seasonal and monthly averaged, large-scale indices were used to identify annual SN patterns. Finally, long-term changes in large-scale indices were related to long-term (decadal or longer) changes in SN and north-to-south gradient patterns.

The last study considered the association of Rocky Mountain winter synoptic patterns to the spatial and temporal variability of SN across the five-state region. Winter synoptic patterns that are associated with the Rocky Mountain region are defined and characterized. The frequency of each synoptic pattern will be determined for each year of the study. The spatial and annual patterns of SN variability will linked to the frequency of certain synoptic patterns. The long-term changes in two synoptic patterns are related to long-term changes in SN and the north-to-south-gradient patterns. Finally, the relationships between winter synoptic patterns and ENSO and PNA will be discussed.

CHAPTER II

DEVELOPMENT OF DATABASE FOR HYDROCLIMATIC RESEARCH IN THE ROCKY MOUNTAINS

The five-state study region, located in the central and northern Rockies, was chosen because it represents the water source for six large watersheds in the United States and the streamflow from this region is supplied predominantly from higher elevations through winter precipitation and accumulated snowpack followed by melting and and run-off in the spring and early summer. The six large watersheds include the Missouri (1), the Arkansas (2), the Rio Grande (3), the Colorado (4), the Great Basin (5), and the Columbia (6), see Figure 1. The dark lines represent the boundaries of each large watershed, the watersheds are identified by numbers and the dashed line is the Continental Divide (C.D.). The three primary data sources for study of hydroclimatic variability in this five-state region are precipitation (PR), snowpack (SN), and streamflow (ST). Each of these sources is important for climate. However, each is observed and archived by different federal agencies and used for a variety of puposes. The development of a combined database requires that data sources be identified, data acquired and checked for quality and completeness, individual sites chosen, and limitations of the data recognized.

The objectives of this chapter include: 1) identifying data sources in this five-state region, 2) evaluating data quality and

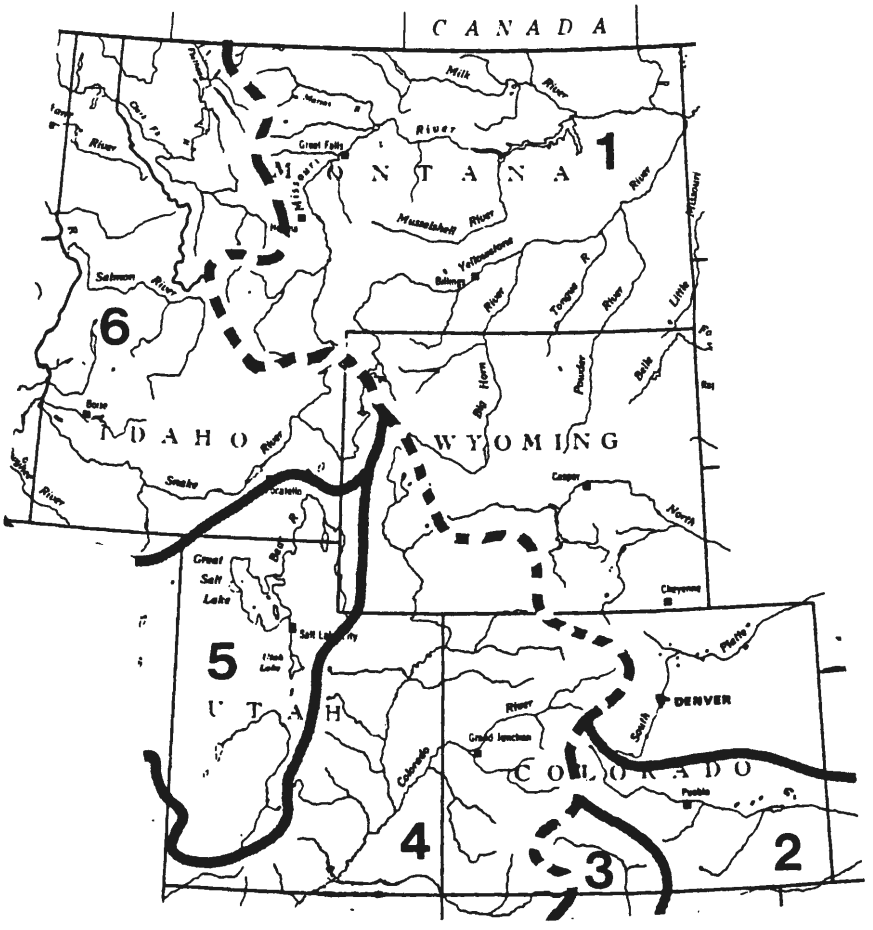

Figure 1. The locations of six major watersheds (numbered) in five-state region. Dark lines separate watersheds and dashed line represents the Continental Divide.

selecting the precipitation (PR), snowpack (SN), and streamflow (ST) sites for study, and 3) discussing the physical processes and data limitations to develop a database.

1. Identify and Describe Data Sources

Three different historical observations directly related to water sources in the five-state region were chosen for study: PR, SN, and ST. The National Ocean and Atmospheric Administration collects PR observations through the National Weather Service (NWS) and archives these observations at the National Climatic Data Center (NCDC) in Asheville, North Carolina. Monthly and daily climatic data were acquired from NCDC for the states of Utah, Wyoming, Idaho, and Montana on magnetic tapes. The climatic data for Colorado was obtained from the Colorado Climate Center. The SN snowcourse observations are collected by the Department of Agriculture through the Soil Conservation Service (SCS) and archived with the SCS in their western center located in Portland, Oregon. Monthly snowcourse data for the five states were obtained by downloading digital data files over a phoneline connection with their central computer system. The Department of the Interior collects ST observations through the United States Geological Survey (USGS) and archives these observations with the USGS in their headquarters located in Reston, Virginia. Monthly streamflow gauge data was obtained via phone hookup to Reston or through USGS water resource books published for each water-year.

The study period of 1951-1985 was chosen for analysis of the data. This period was selected because data studies revealed it was the period with the largest number of continually monitored snowpack sites

and precipitation stations. For detailed study of the watersheds, the period from 1951-1980 was chosen because of limitations in available hydroclimatic data before 1951 and after 1980.

In this study, the period analyzed each year was determined by the winter snowpack accumulating period because high-elevation snowpack in the Rockies represents 85% of the area's total run-off (Grant and Kahan, 1974). To define the length of the winter period, SN data measured around the first of each month (+/- 4 days) from snow courses were analyzed from 25 SN sites throughout the region. At 23 of 25 SN sites the April 1 measurements of snow water equivalent, averaged over the period from 1951-1980, were greater than measurements taken before or after that date. This analysis suggests that snowpack accumulates to a maximum depth after April 1, but often begins to melt before May 1. Thus, the April 1 snowpack (SN) was chosen to represent the snowpack each year throughout the study. The winter accumulation period was arbitrarily chosen to begin October 1, the start of the water year. The October 1-March 31 precipitation (PR) represented the accumulating period up to April 1, the time of the maximum average snowpack measurement, to allow for consistent comparison with SN. The output of the hydrologic cycle in this study was the streamflow. Total water-year (October 1-September 30) streamflow (ST) was chosen to compare with PR and SN. Once these three data sets were chosen, each one's data quality was assessed and the number of sites selected for analysis throughout the study.

2. Evaluation of Data Quality and Selection of Sites

The data of the potential SN sites and PR stations were examined for all sites and stations in the five-state region that had 35 years of data (1951-1985). All annual SN and monthly PR data records were examined thoroughly to identify station relocation or changes in observation technique. Those stations or sites with data showing dramatic shifts, usually identified by double-mass curves, were eliminated from the study, or their raw data was modified using adjacent stations/sites and differences in mass curves as ratios. State climatologists and snow survey supervisors in the five states helped identify stations and sites with inadequate data or data of incomplete quality. Missing data at PR stations and SN sites was estimated for certain stations with nearly complete and consistent records and described below.

Missing SN values were estimated using one, if not two, procedures depending on available data. The most common procedure to estimate April 1 snowpack was to interpolate measurements of the same year, taken from March 1 and May 1, for the station with the missing data. The second procedure, used to cross check procedure one or if March 1 or May 1 values were missing, used SN data from site(s) near the site with missing data and estimated the April 1 value based on interpolations from those alternate sites. SN sites with more than two years of missing April 1 values were not used.

The second procedure described to fill missing SN values also was used to estimate missing PR data. However, care was taken when trying to interpolate values from other sites because most mountainous PR stations were highly affected by local topographic influences (i.e.,

low-elevation valley sites). PR stations with more than twelve winter months (equivalent to two years) of missing data in the 35 years were not used.

Figures 2 and 3 show the distribution of PR stations and SN sites that had complete and consistent records for the 35-year period from 1951-1985. A total of 266 PR stations and 275 SN sites are included. Appendix I provides a table with information regarding station name, number, latitude, longitude, elevation, and median PR value for each site. The median value for stations also shown in Appendix I is plotted on the five-state map to indicate how the median state varies from one location to another. In Appendix II, both the table and the map provide similar information for the SN sites. An examination of Figures 2 and 3 reveals that the two types of observations are not generally co-located. PR stations have been placed to provide a monitor of climate and are spatially distributed and located where people can make daily observations. The result is a distinct bias toward valley locations and lower elevations. SN sites have been specifically designed to monitor snow for the projection of seasonal streamflow (Soil Conservation Service and National Weather Service) and are usually located at higher elevations and measured once a month.

The number of ST gauges selected for studying hydroclimatic variability was limited by several problems within watersheds (discussed in the next section) throughout the Rocky Mountains. Based on a basin selection criteria described in Chapter 3, 14 watersheds were chosen to examine the variability of each element, PR, SN, and ST, as well as to relate the elements to one another within each watershed for the period from 1951-1980.

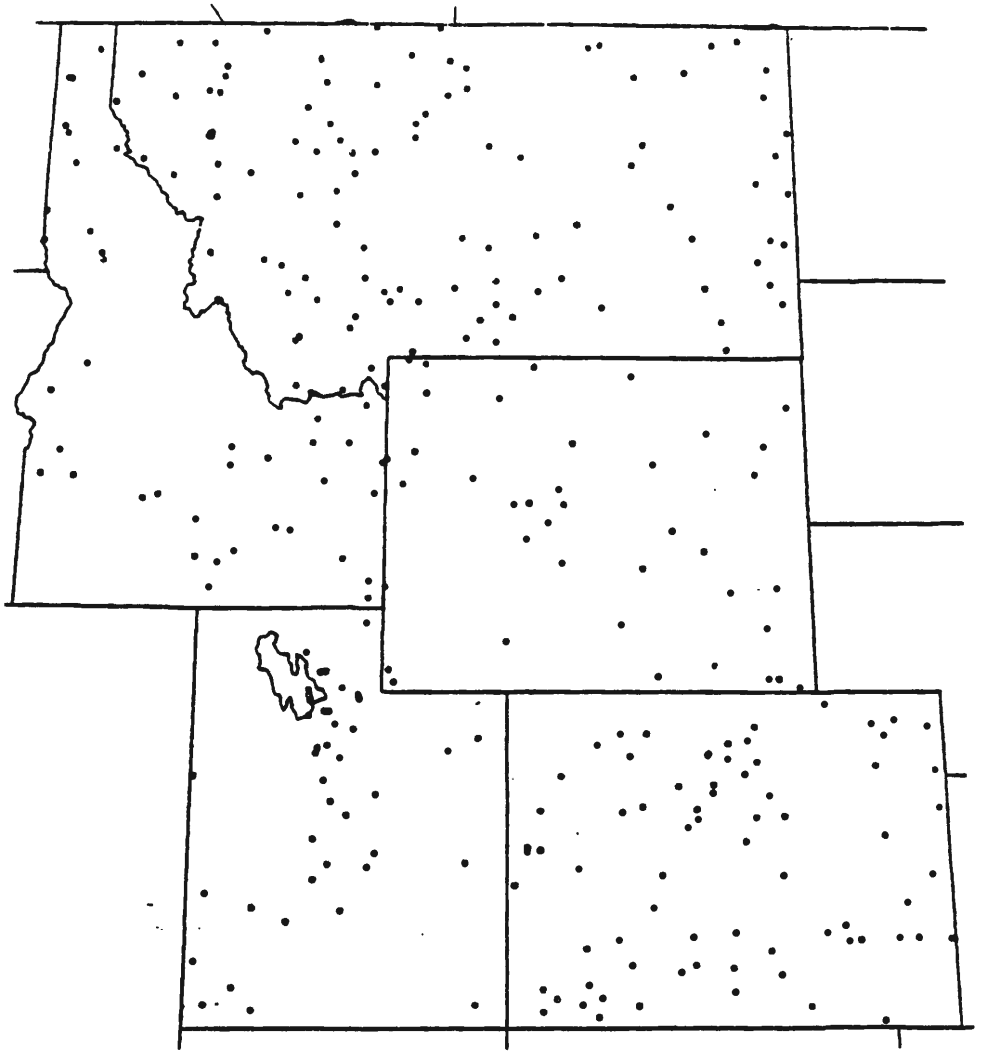

Figure 2. Distribution of 266 PR stations used in study.

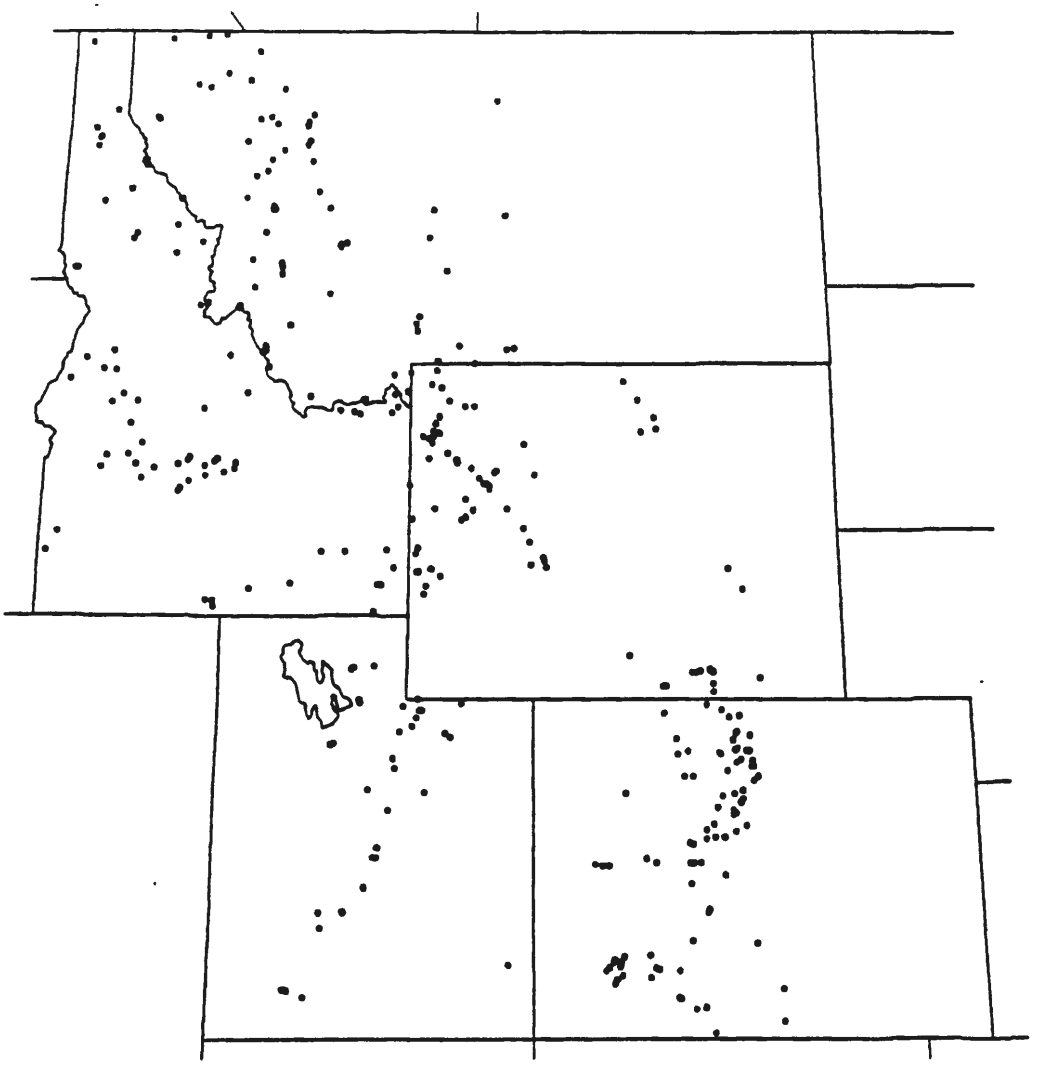

Figure 3. Distribution of 275 SN sites used in study.

3. Physical Variables and Data Limitations

An objective of this research was to determine the surface physical variables that explained the hydroclimatic variability. The physical variables influencing hydroclimatic variability in the five-state region are remarkably diverse. In this part of the study physical variables are described and their influence relative to hydroclimatic elements discussed. Each hydroclimatic element is different with unique characteristics. These characteristics are stated as advantages and disadvantages for each hydroclimatic element.

The study attempted to stratify the PR data into descriptive categories, including latitude, and elevation. These descriptors were identified for each station and watershed. Latitude is related primarily to the large-scale atmospheric circulation and storm track that varies with time. Elevation is important because wetter locations are generally higher. Aspect defines the direction of the inflowing air that causes upward vertical motion. Aspect is important at all latitudes because the vertical motion caused by the terrain is often greater than the lifting associated with synoptic-scale storms.

Table 1 shows the distribution of 266 PR stations and 275 SN sites by approximate latitude (states from north to south) and elevation. One observation is that PR stations and SN sites rise from Idaho and Montana in the north to Colorado in the south. This is related to the general elevation trend in Rocky Mountains such that Colorado is the highest elevation state.

Table 1. Number of Precipitation (PR) stations and Snowpack (SN) by elevation range for the 1951-1985 period in the five-state Rocky Mountain Region.

ELEVATION (meters)	IDAHO PR	IDAHO SN	MONTANA PR	MONTANA SN	WYOMING PR	WYOMING SN	UTAH PR	UTAH SN	COLORADO PR	COLORADO SN	TOTAL PR	TOTAL SN
0-500	2	(0)	0	(0)	0	(0)	0	(0)	0	(0)	2	(0)
501-1000	11	(1)	46	(0)	0	(0)	0	(0)	0	(0)	57	(1)
1001-1500	11	(5)	36	(5)	10	(0)	9	(0)	18	(0)	84	(10)
1501-2000	12	(25)	11	(23)	14	(1)	21	(1)	22	(0)	80	(50)
2001-2500	0	(23)	2	(31)	7	(26)	3	(10)	20	(0)	32	(90)
2501-3000	0	(5)	0	(2)	0	(21)	0	(13)	9	(40)	9	(81)
3001-3500	0	(0)	0	(0)	0	(5)	0	(3)	2	(35)	2	(43)
TOTAL	36	(59)	95	(61)	31	(53)	33	(27)	71	(75)	266	(275)

A Comparison of elevations of PR stations and SN sites reveals that only 16% of the 266 PR sites are above 2000m elevation, while 78% of the 275 SN sites are above this level. The concentration of PR stations at elevations lower than SN sites confirms that PR and SN do not measure the same aspect of the total water supply. At the same time the two are not independent of each other either since they will capture information about similar storms.

Based on the previously discussed physical processes and data characteristics, the advantages of precipitation observations is that PR is measured all year rather than just during winter, it has a fuller areal extent of coverage and it identifies wet winters when the snowpack is located below the snow course sites. The disadvantages include PR's inaccurate measurements of snowfall, its inability to describe loss due to evaporation (Weiss and Wilson, 1957; Rasmussen, 1968), its variable point observations, its location bias in lower elevations and valleys, and the lack of stations located in the high-elevation snow zone.

The advantages of using snowpack observations include being located in the zone of maximum snow, and the integrated effects of several winter season weather elements such as precipitation, temperature, wind, and evaporation occurring through an entire winter. The disadvantages associated with SN observations are variable point observations, few sites are located below the high-elevation snow zone during wet winters, and the April 1 date is variable relative to the melting of the snowpack. Interestingly, SN data have not been used extensively in climatic studies of the West; this is surprising because SN data have been used routinely in operational water-supply monitoring and forecasting activities by the Soil Conservation Service and the National Weather Service in the West.

The advantages of using streamflow data are that they represent the measured output of the surface water supply and they integrate all hydrologic and geologic processes such as groundwater and soil types that are difficult to measure throughout a watershed. The disadvantages of using ST observations include diversions that alter the base virgin flow of the watershed, changes in water use over a period of years, variability not entirely caused by climate, and differing basin sizes (Meko and Stockton, 1984; Lins, 1985; Cayan and Peterson, 1990). The disadvantages of ST related to diversions and changes in water use cause trends that are not climate related and thus prevent ST from being the choice variable in climate studies. Also, there is no way to look only at streamflow derived from October-March moisture because summer precipitation events add to the spring and summer run-off. These disadvantages also alter the relationship between the snowpack or accumulated precipitation and total water-year

streamflow in non-virgin basins, and force those who manage and distribute water to use hydroclimatic indicators other than streamflow for designing reservoirs and predicting spring run-off. Further discussion of streamflow data in Rocky Mountain watersheds appears in greater detail in the basin selection criteria of Chapter 3.

A hydroclimatic database that includes PR, SN, and ST, was developed and will provide the foundation for analyses of hydroclimatic variability. Based on characteristics of the three hydroclimatic elements described in this chapter, all three elements were identified as being useful for aspects of a larger water resource issue. However, only PR and SN are useful to analyze large numbers of observational sites. Analyses in the next three chapters will assess how well the three elements are at representing the variability of the water source region located in the Rocky Mountains.

CHAPTER III

HYDROCLIMATIC VARIABILITY CHARACTERISTICS OF ROCKY MOUNTAIN WATERSHEDS

One way to understand the relationship between climatic and hydrologic elements in the western U.S. is by studying individual watersheds (Toy, 1981; Gleick, 1987; Cayan and Peterson, 1990). One of the major goals of this research was to describe the spatial and temporal hydroclimatic variability characteristics of watersheds and determine the factors that contribute to the variability in watersheds. This study analyzed three hydroclimatic elements, total water-year streamflow (ST), April 1 snowpack (SN), and accumulated winter (October 1 - March 31) precipitation (PR), within fourteen selected watersheds across a five-state area for the period 1951-1980.

The goals of this chapter are to: 1) describe the basin selection criteria, 2) define the magnitude of variability identified within watersheds and explain the differences in variability found between watersheds using surface physical variables, and 3) consider the relationships of elements within each watershed.

1. Basin Selection Criteria

The objective was to select a set of basins adequate to study the climate variability across a wide region. The procedures used to accomplish this task included selecting a number of candidate

watersheds, developing a basin selection criteria, and identifying the final set of watersheds that qualified for detailed study.

Over 600 basins of various sizes are located within the boundaries of the five-state region. It would have been informative to investigate streamflow variability for many, if not all, the basins. However, several characteristics of the region and of the basins within the region made thorough study an unproductive task. When selecting watersheds to study streamflow variability in the Rockies, Meko and Stockton (1984) identified man-made diversions as the most significant problem. Thirty-one watersheds that had less than 25% of their flow diverted were initially selected as candidate basins based on discussions with State Soil Conservation Service offices. These watersheds were subsequently judged based on criteria described below.

The intent of using a basin selection criteria was to develop a group of basins with similar physical characteristics. However, it was important that the criteria not be too restrictive; rather, it should be flexible because no one basin is exactly like another in the Rocky Mountain region (Pilgrim, 1983). Criteria were developed to: 1) determine watersheds with near-virgin flow, 2) identify geographical and climatological subregions within the five-state area, 3) consider elevational differences of watersheds across the Rockies, and 4) examine the availability, location, and quality of the data used in the study of a watershed.

The amount of water diverted from the virgin runoff was the first limiting factor examined in watershed selection. Meko and Stockton's study (1984) selected basins if less than 7% of the total flow was used for irrigation and less than 7% was used for reservoir capacity. In

this study watersheds were selected if less than 10% of the total flow was diverted for any reason such as transmountain diversion, reservoir storage and irrigation.

Initially, pairs of basins, one located up-wind (air ascending) and another down-wind (air descending) of a mountain barrier, along the mountain chain in the study region, were chosen to study the impact of large winter synoptic patterns on surface water supplies east and west of the Continental Divide (C.D.). However, because the mountain chain varies in width and topography, not all basins were selected in pairs. Basins that were geographically situated in locations where the up-wind flow was favorable for precipitation and was not impeded by other local mountain ranges would pass this selection criteria.

The third criteria, elevation, also limited basin selection. Selected watersheds were located at or above an elevation where snowmelt runoff was the most important contributor to the annual streamflow (Cayan and Peterson, 1990). This basin elevation varies with latitude and climate regime; consequently, no fixed elevation minimum was applied throughout the region. Thus, the farther south the basin, the higher its elevation.

Once the basin site and elevation were specified, questions regarding the data's quality were addressed (see Chapter 2 for detailed discusssion on evaluating the data quality of PR and SN sites). Snowpack, streamflow, and precipitation data were required for each basin because this study addressed climate and streamflow variability. However, because of the sparse network of National Weather Service cooperative stations, United States Geological Survey streamflow gauges, and Soil Conservation Service snow courses, only a limited

number of basins had all three data sets available. The more sites that could measure the data elements, the better the resolution through the basin. Length of recordkeeping also became a critical question regarding data. Most data sets for watershed analyses included records for the study period 1951 through 1980, and the minimum number of years accepted was 25. Therefore, some flexibility in the data quality selection criteria was critical, and data located just outside the watershed and in the same general climatic region was sometimes used.

The four major criteria, geographic location, elevation, amount of diverted water, and adequate data, eliminated 17 watersheds from further consideration, leaving 14 for detailed analyses. Some detailed information about the watershed's subregions such as slope and aspect, vegetation, and soil types were considered too complex for this study and were not used as criteria for selecting basins.

The group of 14 watersheds that met the basin selection criteria requirements and were chosen for detailed study are listed in Table 2 (below) by number and are located in Figure 4.

Table 2. Fourteen selected watersheds.

Number on Figure	Watershed	State
1	Swiftcurrent	MT
2	Coeur d'Alene	ID
3	Nevada	MT
4	Boulder	MT
5	Big Wood	ID
6	Wind	WY
7	Green	WY
8	Smith's Fork	WY
9	Bear	UT
10	West Fork Duchesne	UT
11	Muddy Creek	UT
12	North Fork Colorado	CO
13	St. Vrain	CO
14	San Juan	CO

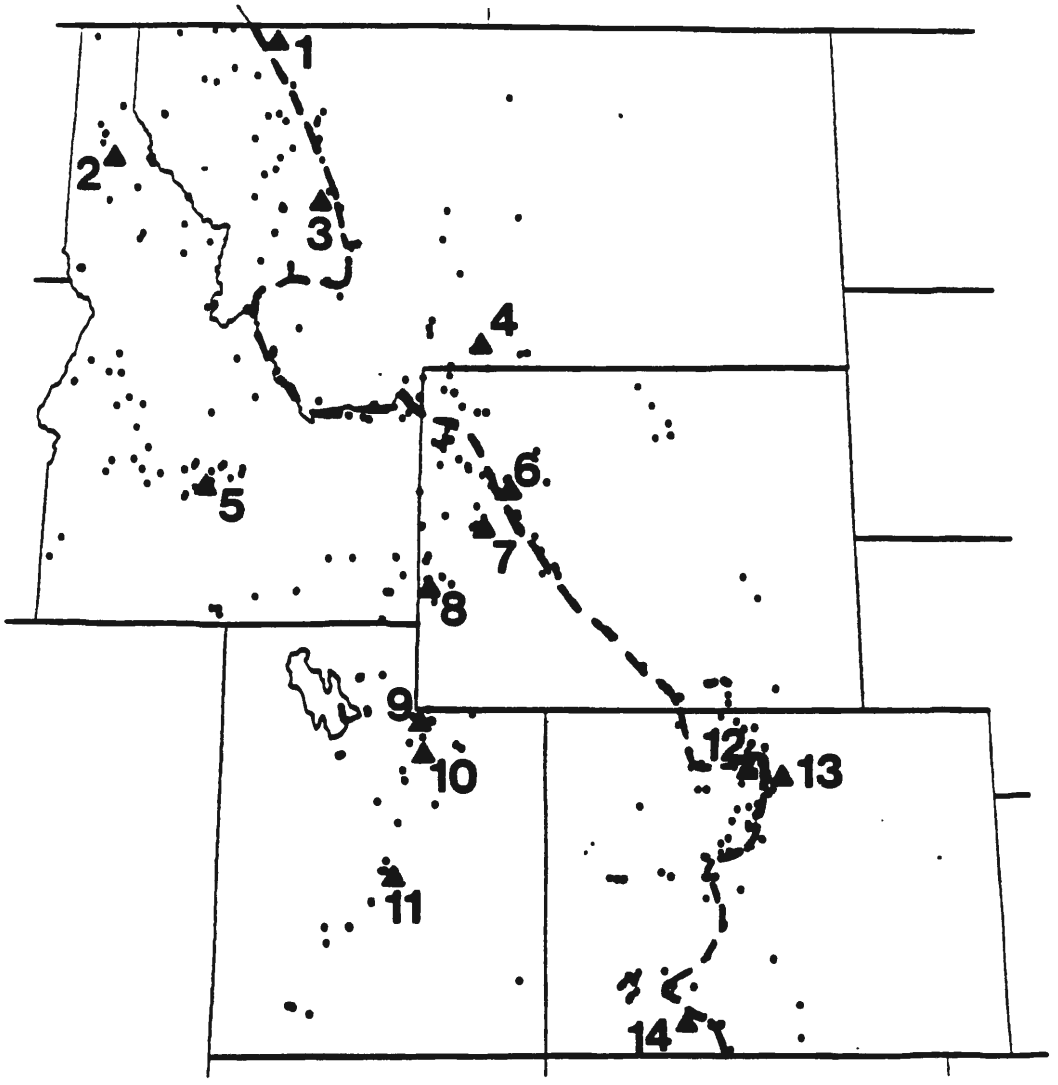

Figure 4. The locations of 14 selected watersheds used in the Rocky Mountain study region. Small dots indicate the position of the 275 SN sites. Dashed line represents the Continental Divide.

Of the 14 selected watersheds, 3 pairs were chosen that are located on opposite sides of a large mountain barrier. The three sets include: 1) the North Fork of the Colorado/St. Vrain, 2) the Bear/West Fork of the Duchense, and 3) the Smith's Fork/Wind. Figure 4 shows that four of the fourteen watersheds are located on the east side of the C.D.

A list of streamflow gauge sites, snow course sites, and precipitation stations analyzed in or near each watershed is found in Appendix III, along with physical characteristics of each station and site.

2. Determine the Magnitude of Variability and Explain Differences in Variability from one Watershed to another

Initial analysis involved preparing time series for each of the three hydroclimatic elements (ST, SN, and PR) for each of the 14 watersheds. Time series for two of the 14 watersheds, the San Juan basin in Colorado and the Coeur d'Alene basin in Idaho, appear in Figure 5. These were selected to reveal the differences in the variability of each watershed. Time series for the remaining 12 watersheds are located in Appendix III. The absolute values for each hydroclimatic element were normalized to the median so that the value of 1.0 represented the median for each of the elements in these plots. The median ($X_{50\%}$) was used rather than the mean because most hydroclimatic values were not normally distributed and often were skewed significantly by few very wet (more than twice the mean) or dry (less than half the mean) annual values. Figure 6 shows a dot diagram of average daily streamflow for each water-year above Lyons, CO, on the St. Vrain River during the 1951-1980 period. Each dot represents a

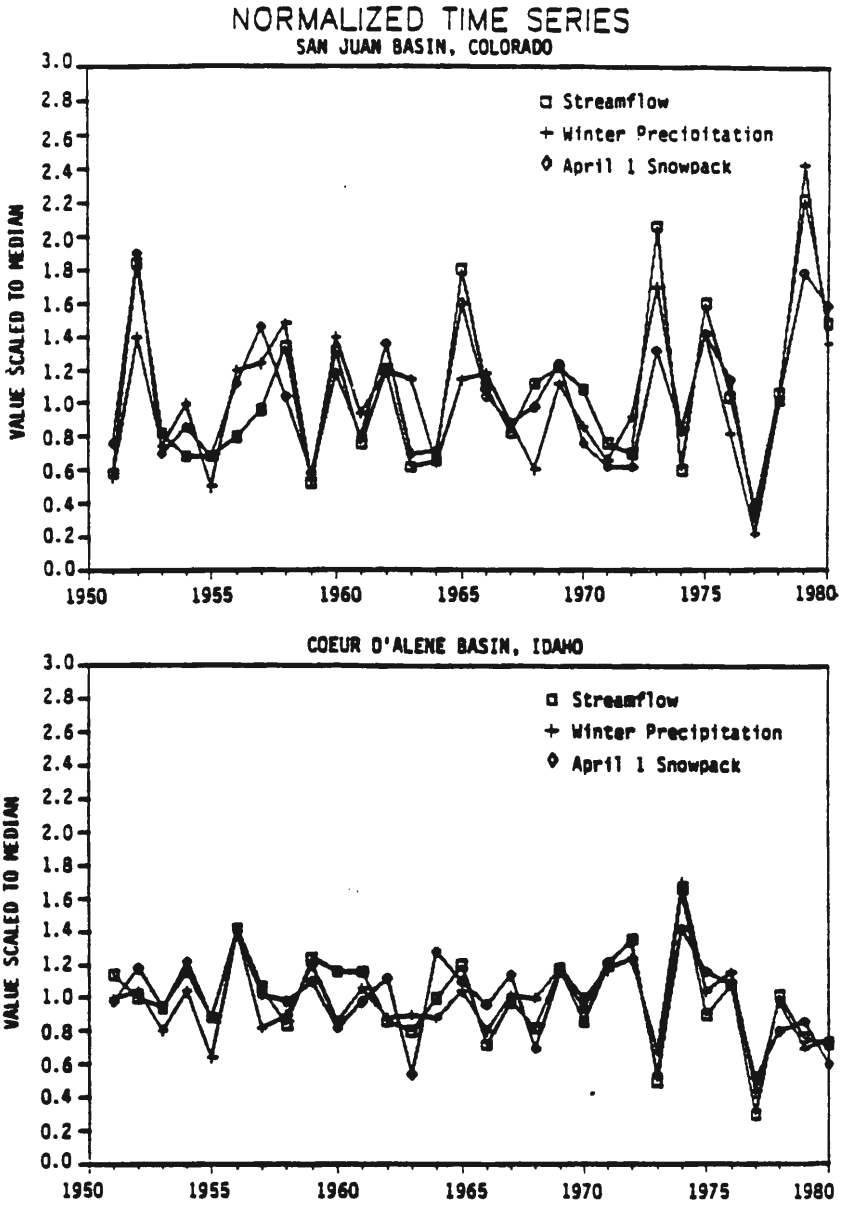

Figure 5. Coincident time series of normalized precipitation (October-March), April 1 snowpack, and total water-year streamflow for the San Juan watershed in Colorado and Coeur d'Alene in Idaho.

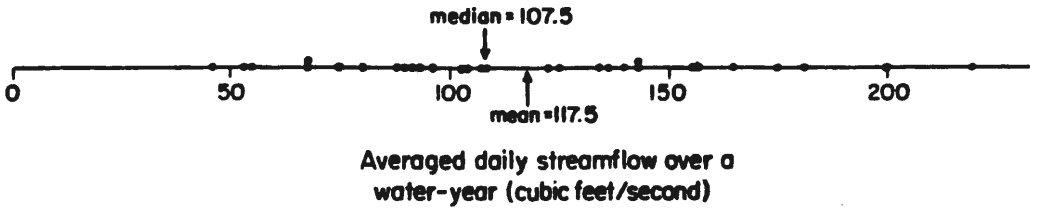

Figure 6. A dot diagram of average daily streamflow per water-year on the St. Vrain above Lyons, CO, for the years 1951-1980. The mean and median of the distribution are identified with arrows.

water-year value in cubic feet per second. Note that the mean and the median for this data set are different and the data is positively skewed by a few large values. These unusually distributed values often are found in the semi-arid West where annual values often can have a range from half to two times the mean value (Medina and Mielke, 1985; Faiers, 1988).

The time series plots (Figure 5) identify variability characteristics in the three hydroclimatic elements for each watershed. In both the San Juan and Coeur d'Alene watersheds the three hydroclimatic elements vary similarly through the 30-year period. The correlation of components to one another will be discussed in the next section. Differences between the two watersheds are identified by comparing the range in the values about the median (1.0). For example, Figure 5 shows that the conditions in the San Juan watershed are more variable than those in the Coeur d'Alene watershed for the 30 year period. In the San Juan watershed the normalized values ranged from 0.20 to 2.40, while the normalized values in the Coeur d'Alene watershed ranged from 0.30 to 1.70. Finally, when comparing the time series of the two watersheds, two primary types of years were identified. Years when the two watersheds had similar anomalies (both above 1.0 or both below 1.0) and years when the two watersheds had anomalies that were opposite (one basin below 1.0 and the other above 1.0). Annual patterns using SN and PR data from across the region will be discussed in Chapter 5.

A measure of variability was selected to compare basins and determine the magnitude of variability for the three hydroclimatic elements. For each data set all normalized to the median values were

ranked from lowest to highest and then assigned a non-exceedence probability that ranged from 0% to 100%. The measure of variability (MOV) was defined from the probability distribution of each data set as:

$$MOV = (X_{80\%} - X_{20\%})/X_{50\%} \quad (10)$$

where X represents the SN, PR, or ST value for each non-exceedence probability. This value is similar to the coefficient of variation (v_σ), which was defined in Chapter 1 as the standard deviation divided by the mean:

$$v_\sigma = \sigma/x \quad (11)$$

The v_σ has been used widely in hydroclimatic studies for regions in other parts of the world (Conrad, 1941; Longley, 1952; Hershfield, 1962). The MOV in this study contains the central 60% of observations while $2v_\sigma$ contains the central 68% of a normal distribution. Table 3 provides the SN values used in the equations for MOV and v_σ for the San Juan and Coeur d'Alene watersheds.

Table 3. SN values in inches used to compute the MOV and $2v_\sigma$ in the Coeur d'Alene and San Juan Watersheds.

Watershed	20% value	median value	mean value	80% value	standard deviation	MOV	$2v_\sigma$
Coeur d'Alene	25.6	32.1	31.9	38.9	7.9	0.41	0.50
San Juan	20.3	29.2	30.2	41.5	11.3	0.73	0.74

Both measures, the MOV and v_σ, have been normalized by dividing by the median or the mean respectively (in Table 3 both the mean and median for each watershed are similar) so there is a smaller dependence on the median or mean amount of precipitation at a given location. In Table 3 the MOV values increase by 78% from the Coeur d'Alene to the San Juan,

whereas the $2v_6$ values only increases about 50%. The decision to use the measure of variability was based on four issues. First, the MOV is essentially the typically-linear portion of the cumulative distribution curve between non-exceedence probabilities of 0.2 and 0.8. Second, the non-exceedence probabilities used in the MOV are not dependent on the distribution of the data (Medina and Mielke, 1985; Mielke, 1988; Faiers, 1989). Third, the median always represents the central point of a distribution. Fourth, extreme values, those with non-exceedence probabilities <20% and >80%, are not considered in the computation of MOV, where all values in a data set influence both the mean and the standard deviation.

Maps were prepared for each of the three hydroclimatic elements to show the measure of variability for the watersheds (Figures 7a-c). The range of variability for the 14 basins was: 1) PR from 0.38 to 0.90, 2) SN from 0.35 to 0.80, and 3) ST from 0.20 to 0.83. The mean values of variability for the 14 watersheds was 0.58 for PR, 0.56 for SN, and 0.53 for ST.

The small difference between the means and the ranges of the three interrelated hydroclimatic elements suggested that any of the three elements was a good indicator of the magnitude of variability for most basins. However, in seven basins one of the three hydroclimatic elements was considered anomalous. All MOV values were considered similar in a watershed if the range of the three MOV values did not exceed 0.15. The Swiftcurrent Creek's ST MOV value (0.20) was much smaller than the other two MOV values. The apparent reason for the low ST MOV value is because it is such a small watershed (80 km^2). The Boulder River's PR MOV value (0.68) is much greater than the other two

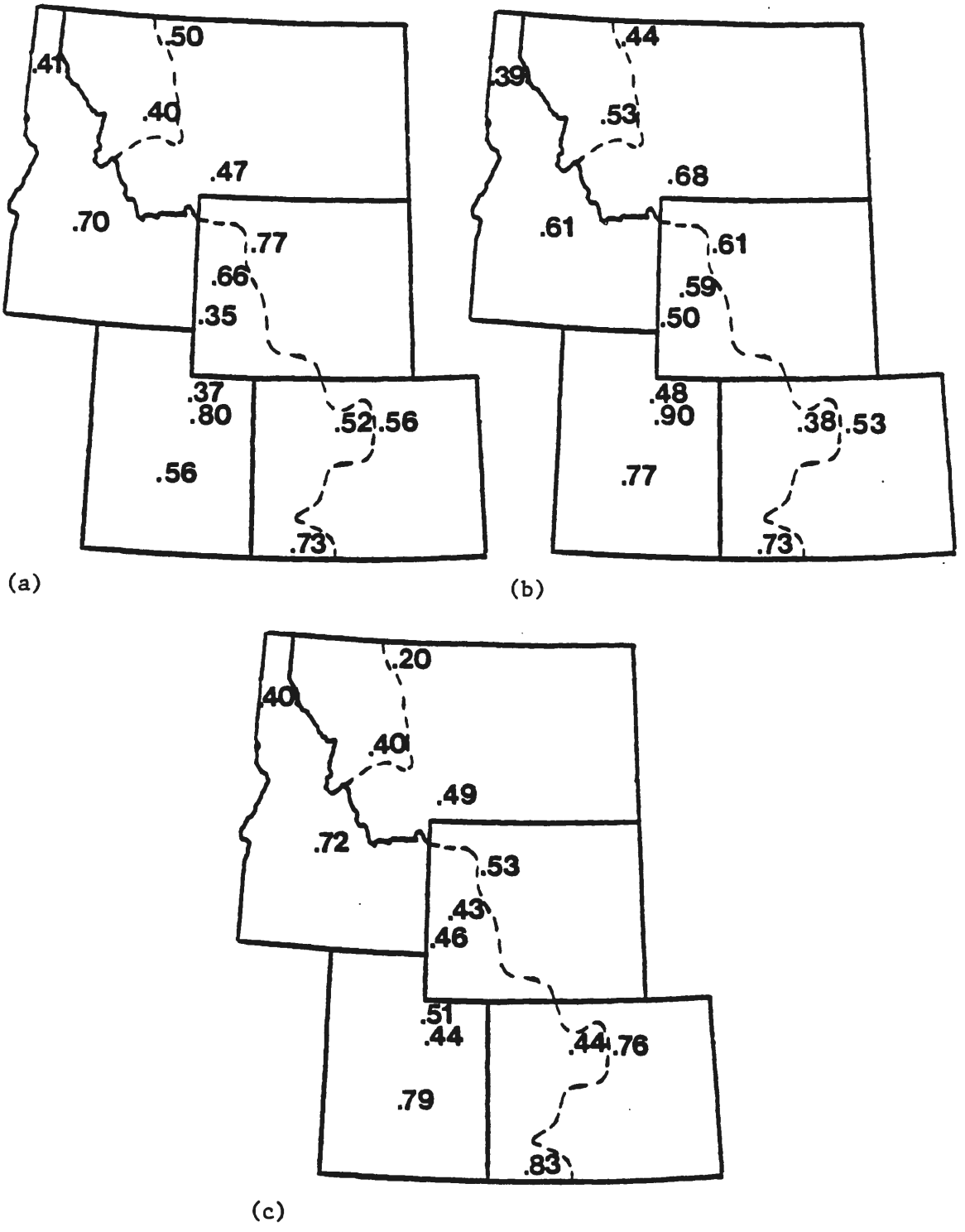

Figure 7. The measure of variability computed for a) April 1 snowpack, b) winter (October-March) precipitation, and c) total water-year streamflow in the 14 selected watersheds. The dashed line represents the Continental Divide.

MOV values and is due to the low elevation location of the PR station relative to the watershed. The Wind River's SN MOV value (0.77) is greater than the other two MOV values and there is no apparent reason why this should be. The Green River's ST MOV value (0.43) is less than the other two MOV values and this could be due to the large size of the watershed. The West fork of the Duchesne's ST MOV value (0.44) is less than the other two MOV values and it is uncertain to the reason why. The Muddy Creek's SN MOV value (0.56) is much less than the other two MOV values and the apparent reason for the low SN value is the high location of the SN site. The St. Vrain's ST MOV (0.76) is much greater than the other MOV values and implies that the precipitation after April 1 may be very important to the ST and also highly variable from year-to-year. These anomalous MOV values are not easily explained and suggest that there is some uncertainty in using any one of the three hydroclimatic elements individually when comparing differences in variability from one watershed to another. Because the three hydroclimatic elements were interrelated, the uncertainity associated with using just one of the hydoclimatic MOV values existed, and its easier to compare one MOV value for each watershed rather than three; thus the three MOV values for each watershed were averaged. These average variability values for the 14 watersheds appear in Table 4 with the watersheds ranked by their averaged measure of variability. Physical characteristics of each watershed are also shown.

Table 4. Characteristics of 14 watersheds.

Watershed	Location Relative to C.D.*	Average Measure of Variability	Aspect of Watershed	Watershed Size, km^2	Elevation of ST gauge, m
Swiftcurrent	East	0.38	North	80	1481
Coeur d'Alene	West	0.40	West	2310	640
Nevada	West	0.44	West	300	1420
Smith's Fork	West	0.44	West	427	2027
N.F. Colorado	West	0.45	West	137	2667
Bear	West	0.45	Northwest	445	2428
Boulder	East	0.55	Northeast	1378	1237
Green	West	0.56	South	1212	2276
St. Vrain	East	0.62	East	549	1613
Wind	East	0.64	Southeast	601	2191
Big Wood	West	0.68	South	1658	1614
Muddy Creek	West	0.71	Southeast	272	1951
W.F. Duchesne	West	0.71	South	161	2200
San Juan	West	0.76	Southwest	720	2149

*C.D. = Continental Divide

Analyzing the information in Table 4 helped to identify which surface physical variable is most important in explaining the differences in variability between watersheds. Six of the 14 watersheds with an average measure of variability less than 0.55 have a westerly or northerly aspect. The aspect reflects the exposure of each watershed to moist air flow. The other eight basins with larger average measures of variability have an easterly or southerly aspect, indicating that basin aspect influences hydroclimatic variability. Based on values given in Table 4, position relative to the C.D., basin size, or basin elevation, do not have similar relations to variability, indicating that the only apparent physical explanation of the spatial variability at the surface is the aspect. Aspect has been recognized for many years as an important climate control affecting the magnitude of precipitation in mountainous areas (Spreen, 1947; Peck and Brown, 1962); however, its role in influencing hydroclimatic variability has not been documented.

To further analyze the role of aspect in spatial variability, three pairs of watersheds located on opposite sides of a mountain barrier from each other were analyzed (Table 5). In each pair, the basin on the barrier's north or west side had a smaller average measure of variability than their opposites. Basins on the south or east side showed average measures of variability ranging from 0.17 to 0.26 larger than those on opposite sides. This analysis further indicated that of the surface physical variables described, the aspect of a watershed, or the location relative to a mountain barrier, provided the best explanation for the observed range of variability. Barry (1981) indicated that the rate of increase in precipitation with height was much lower on the windward side of large mountain barriers. On the lee slopes the increase of precipitation with height was found to be large, especially on the lower slopes, due to the frequent occurrence of descending air motions and the removal of moisture upwind. A majority of precipitation events which are associated with the predominant westerly or northerly airflow at 500 mb provide precipitation to watersheds on the west side of the C.D. with some spill-over to the high elevations on the east side of the C.D. These watersheds that experience the predominantly westerly or northerly flow are stable. Barry (1981) found that the general tendency for increased precipitation with height often to the highest elevations is modified considerably by a leeward slope location. He indicated that the winter maximum precipitation height east of the C.D. near Boulder, CO, is 3750 m, while on the western side of the C.D. in north central Colorado the precipitation maximum is at 3200 m. Only when there is airflow from the south or east, which is infrequent and variable from year-to-

year, do basins with exposure to the south or east experience precipitation over large areas especially at lower elevations. To compare the differences west and east of the C.D., daily precipitation events including those that produced a trace were analyzed for Grand Lake 1NW in the North Fork of the Colorado watershed and Estes Park used in the analysis of the St. Vrain. The median number of precipitation events per year at Grand Lake 1NW is 81.5, while at Estes Park the median number of precipitation events per year is 43.7. The median sized event at Grand Lake 1NW is 0.08 inches, while at Estes Park it is 0.02 inches. These differences east and west of the C.D. in these two watersheds are similar to those of the other pairs of watersheds and agree with the theory developed herein. Further discussion of the frequency of winter synoptic patterns and there relationship to variability identified in the watersheds will be discussed in Chapter 7.

Table 5. The measures of variability for pairs of watersheds located on opposite sides of a barrier.

Pair Number	Watershed	Location in Respect to Barrier	Measures of Variability PR	SN	ST	Average
1.	N.F. Colo.	West	0.38	0.52	0.44	0.45
	St. Vrain	East	0.53	0.56	0.76	0.62
2.	Bear	North	0.48	0.37	0.51	0.45
	W.F.Duchesne	South	0.90	0.80	0.44	0.71
3.	Smith's Fork	West	0.50	0.35	0.46	0.44
	Wind	East	0.61	0.77	0.53	0.64

Not all watersheds have three similar MOV values. Based on the uncertainty derived from these watershed analyses of spatial variability, the next chapter will analyze all PR and SN data located in the five-state study region. These analyses of PR and SN data will be used to test the results from the 14 basins that exposure to certain moist air flows is the primary physical variable explaining the range in the magnitude of the basins' hydroclimatic variability. It was not possible to analyze all ST data because of aforementioned problems that altered virgin flow.

3. Relationship of Hydroclimatic Elements

For each watershed the normalized time series of each hydroclimatic element was plotted (see Figure 5 and Appendix III). These plots show how each hydroclimatic element varies through the 30-year period from 1951-1980. To test how well each hydroclimatic element was related to one another within a watershed, correlations were made between PR and ST, SN and ST, and SN to PR in the 14 selected watersheds. The objective of this analysis was to describe the temporal variability characteristics of the three hydroclimatic elements within each watershed. Linear regressions provided correlation coefficients, or r-values.

simple linear regression model $Y = B_o + B_iX$ (12)

where B_o = the point where the line intercepts the y-axis

B_i = slope of the straight line

$$\text{Correlation Coefficent, } r = \frac{n\sum x_i y_i - (\sum x_i)(\sum y_i)}{\left[\sqrt{n\sum x_i^2 - (\sum x_i)^2}\right]\left[\sqrt{n\sum y_i^2 - (\sum y_i)^2}\right]} \quad (13)$$

where n = number of data points

(x_i, y_i) = data point location

R-values of +1.00 represented a perfect positive correlation, 0.00 represented no correlation, and -1.00 represented a perfect negative correlation.

Correlation coefficients between each set of time series of hydroclimatic elements are shown in Figure 8a-c. The range of r-values for PR to ST was +0.42 to +0.88, the range of r-values for SN to ST was +0.61 to +0.93, while the range in r-values for SN to PR was +0.36 to +0.90. The correlations further indicated how much the hydroclimatic elements are positively related to each other. R-values of +1.00 are not expected for SN to ST and PR to ST, because precipitation that occurs after April 1 contributes to ST differently each year. The correlation coefficients of SN to ST and PR to ST for the 14 watersheds should be considered very good because both SN and PR represent only half a years input (October-March) while ST is derived from an entire water-year of input. The watersheds were ranked by average measure of variability, as shown in Table 4, with the respective r-values given in Table 6.

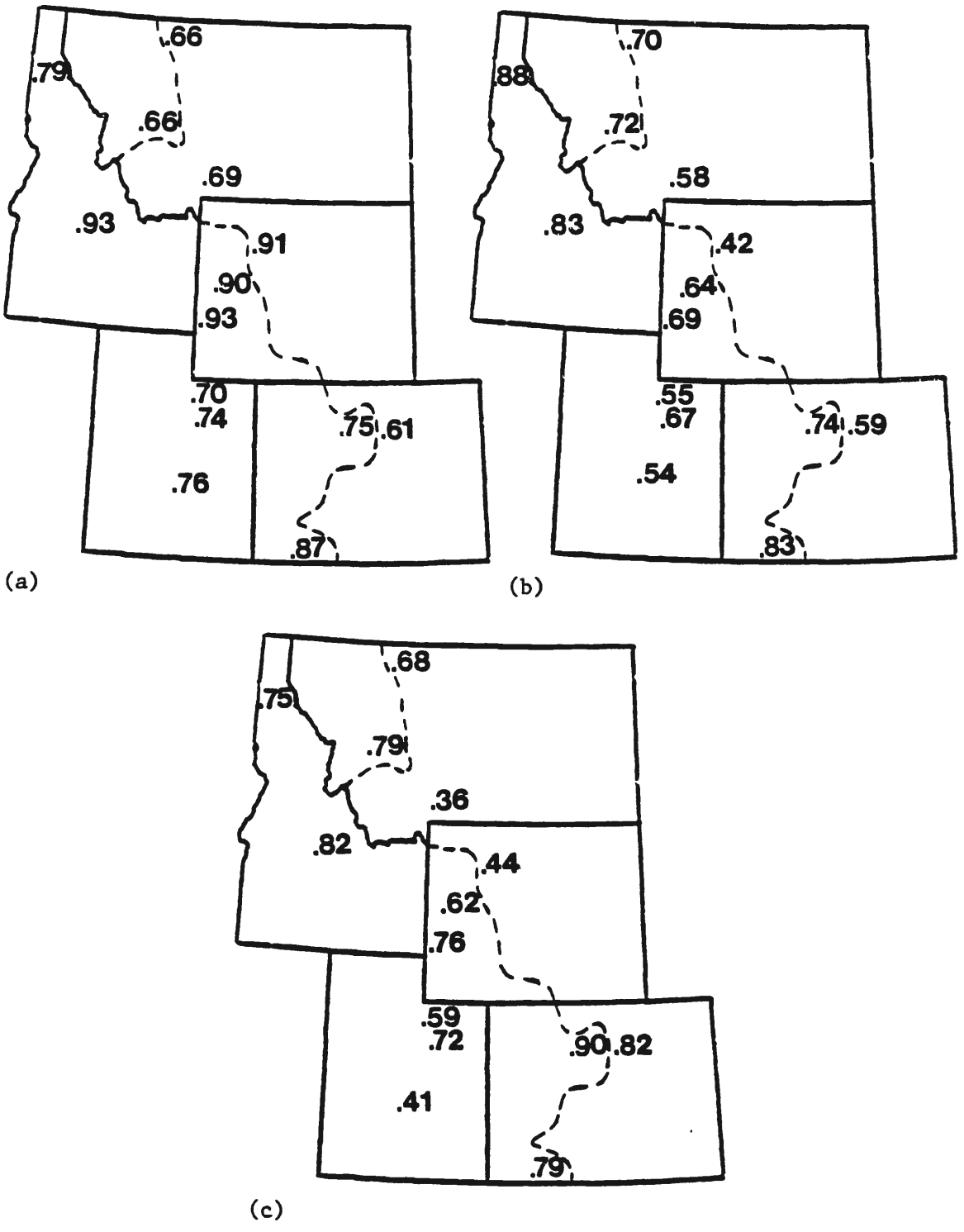

Figure 8. The correlation coefficients computed for a) SN to ST, b) PR to ST, and c) SN to PR in the 14 selected watersheds.

Table 6. Correlating SN to ST, PR to ST, and SN to PR for 14 watersheds. All r-values are positive (STA = stable, USTE = unstable easterly exposure, USTS = unstable southerly exposure).

Watersheds	Stability designator	SN vs. ST	PR vs. ST	SN vs. PR
Swiftcurrent	STA	0.66	0.70	0.68
Coeur d'Alene	STA	0.79	0.88	0.75
Nevada	STA	0.66	0.72	0.79
Smith's Fork	STA	0.93	0.69	0.76
N.F. Colorado	STA	0.75	0.74	0.90
Bear	STA	0.70	0.55	0.59
Boulder	USTE	0.69	0.58	0.36
Green	USTS	0.90	0.64	0.62
St. Vrain	USTE	0.61	0.59	0.82
Wind	USTE	0.91	0.42	0.44
Big Wood	USTS	0.93	0.83	0.82
Muddy Creek	USTE	0.76	0.54	0.41
W.F. Duchesne	USTS	0.74	0.67	0.72
San Juan	USTS	0.87	0.83	0.79
Average		0.78	0.67	0.68
Average for STA Watersheds		0.75	0.71	0.75
Average for USTS Watersheds		0.86	0.74	0.74
Average for USTE Watersheds		0.74	0.53	0.51

In 11 of the 14 watersheds, SN had a better relationship to ST than did PR. The overall average of the PR to ST r-values was +0.67, while the average of the SN to ST was +0.78. The average SN to ST r-values for stable watersheds (STA), unstable watersheds with easterly exposure (USTE) and unstable watersheds with southerly exposure (USTS) are all greater than those for PR to ST or SN to PR. For STA watersheds and USTS watersheds the SN to ST, PR to ST, and SN to PR r-values are similarly good suggesting that in both types of watersheds SN sites and PR stations are exposed to similar precipitation events from year-to-year. The predominant upper air flow during the winter is

westerly with long-wave troughs and ridges steering the winds into northerly or southerly directions. Both STA and USTS watersheds are exposed to these predominant winter flows that provide upslope precipitation throughout the watersheds. However, in USTE watersheds the SN to ST r-values are much better than the PR to ST r-values suggesting that two different types of precipitation events, one affecting high elevation SN sites associated with the predominant winter upper air flow and the other affecting low elevation PR sites associated with an easterly upslope flow. In USTE watersheds high elevation SN data represents ST data better than low elevation PR data from year-to-year. These theories will be tested in greater detail using all PR and SN data and the Rocky Mountain winter synoptic patterns in Chapter 6. Overall, in the 14 selected watersheds SN was identified as a better indicator of ST than PR, and SN appears to be the best monitor of winter climate in the Rocky Mountains.

The differences in r-values within each watershed of Table 6 could be explained by: 1) differences in small scale climate controls in each watershed, 2) the elevational siting of the instruments within the basin, and 3) the fact that the three elements do not sample precipitation the same in all watersheds. All of these differences were discussed in the data limitation section of Chapter 2. Because of the uncertainity associated with the limited watershed regression results, further investigation of the SN and PR relationships using all the SN and PR data across the five-state region is examined and discussed in Chapter 5.

Further assessment to determine whether extreme values of SN or PR effected their relationship with ST was done using results for the extremely high and low ST years. Values for the six high (wet) years and low (dry) years at each end of the ST distribution were correlated to SN or PR in each of the 14 watersheds. In 10 of the 14 watersheds, the SN to ST correlation was better than the PR to ST correlation. The average SN to ST, and PR to ST, r-values were high (+0.90 and +0.82 respectively). These r-values are affected because the data points are located on the ends of the distribution. The scatter plots of SN to ST and PR to ST for the 14 basins were compared and the absolute distance from each of the 30 points to the regression line was measured. The 12 (6 high and 6 low) data points were grouped and averaged, while the middle 18 (near average) points were grouped and averaged. The average absolute ST distance of the 12 extreme data points from the regression line was approximately 1.5 times greater than for that in the middle 18 years of the ST data distribution. Furthermore, when the 12 extreme ST points were considered, the average absolute ST distance, when relating SN to ST, was 6% smaller than that from relating PR to ST. Therefore, it is significant that during extreme wet and dry ST years, SN is a better indicator of water resources (ST) in most near-virgin watersheds than PR.

4. Summary

One way to describe and understand the spatial and temporal variability characteristics of hydroclimatic elements in the western U.S. is by studying individual watersheds. Based on the four primary

criteria, amount of water diverted, geographic location, elevation, and adequate data, 14 watersheds were selected for detailed analysis.

A measure of variability (MOV) defined from the probability distribution of each data set was developed for this study because a number of problems associated with non-normally distributed data sets discouraged the use of the coefficient of variation. The MOV is defined as:

$$MOV = (X_{80\%} - X_{20\%})/X_{50\%}$$

where X represents the SN, PR, or ST value. Six of the 14 watersheds with an average measure of variability less than 0.55 have a westerly or northerly aspect. The other eight basins with larger average measures of variability have a easterly or southerly aspect, indicating that basin aspect affects hydroclimatic variability. Position relative to the C.D., basin size, or basin elevation, do not have any similar relations to variability, indicating that the only apparent surface physical explanation of the spatial variability is the aspect. The aspect reflects the exposure of each watershed to moist air flow and has been recognized for many years as an important climate control affecting the magnitude of precipitation in mountainous areas (Peck and Brown, 1962). However, its role in influencing hydroclimatic variability, has not been documented. Based on the uncertainty derived from these watershed analyses of spatial variability, the next chapter will analyze all SN and PR data located in the five-state study region to further examine the physical reasons for differences in the range of variability. In Chapter 7 an analyses of Rocky Mountain winter synoptic patterns will examine reasons for the differences in spatial variability.

Linear regression analyses of SN to ST, PR to ST, and SN to PR for each watershed suggested that SN was a better overall indicator of ST than PR. This undoubtedly occurs because SN monitors the moisture in the elevational zone that provides the majority of available annual water resources (Grant and Kahan, 1974; Klazure et al., 1985; Day et al., 1989; Peck and Schaake, 1990). SN was better correlated with ST in 11 of the 14 watersheds with near-virgin flow. In stable watersheds and unstable watersheds with southerly exposures the average SN to ST, PR to ST, and SN to PR r-values were similar suggesting that both PR and SN sites are influenced by similar precipitation events in these watersheds. However, in unstable watersheds with easterly exposures the average SN to ST r-values were much greater than the PR to ST or SN to PR r-values indicating that high elevation SN sites monitor different precipitation events than do low elevation PR stations. The differences in r-values within each watershed could be explained by: 1) differences in small scale climate controls in each watershed, 2) the elevational siting of the instruments within the basin, and 3) the fact that the three elements do not sample precipitation the same in all watersheds. Of the three hydroclimatic elements SN appears to be the best monitor of winter climate in the Rocky Mountains. Because of the uncertainity associated with the limited watershed regression results, further investigation of the SN and PR relationships using all the SN and PR data across the five-state region is discussed in Chapter 5.

CHAPTER IV

SPATIAL PATTERNS OF WINTER PRECIPITATION AND APRIL 1 SNOWPACK VARIABILITY

Analyses of hydroclimatic variability in a small number of individual basins (described in the previous chapter) revealed that spatial variability appeared to be explained by exposure at the surface to air flows. To confirm this finding, and evaluate its significance, variability characteristics for all PR stations and SN sites were examined.

The objectives of this part of the study are: 1) to compute the measure of variability for all PR stations and SN sites and identify spatial patterns of variability; 2) to explain why these regions are located where they are using surface physical variables; and 3) to assess the value of developing a new hydroclimatic classification scheme for the Rocky Mountain region based on magnitude of variability.

1. Computing the Measure of Variability for all PR stations and SN sites and identifying spatial patterns of variability

The measure of variability (MOV), described in Chapter 3, was computed for the 275 SN sites and 266 PR stations in the five-state region (see Chapter 2) that had 35 years of data (1951-1985). The SN MOV ranged from 0.22 (low variability) to 1.19 (high variability). The PR MOV values ranged from 0.28 to 1.25. Although the elevation

distributions of SN and PR locations are very different (see Table 1, Chapter 2), both data sets showed a similar range in variability. The objective of this analysis was to identify spatial patterns of variability for SN and PR.

The analysis of hydroclimatic variability within the 14 watersheds indicated significant spatial differences. To establish the pattern of variability over the five-state region, the calculated MOV values of SN sites and PR stations were plotted on maps shown in Figure 9a and 9b. The analysis used to identify patterns of differing variability across the highly varied topographic regions within Rockies was selected to maintain geographical unity and coherence. On the SN map (Figure 9a) a contour line of 0.55 was drawn to separate regions of stable and unstable SN sites. This was done because, 1) the 0.55 value had divided stable (less variable, MOV < 0.55) and unstable (more variable, MOV > 0.55) watersheds, as defined in the previous chapter, and 2) the 0.55 value also represented the mean MOV value for the 275 SN sites. The 0.55 isoline identified eleven broad, homogeneous climatic regions for SN. Despite the differences in the location of SN sites and PR stations, the analysis of the PR variability values (Figure 9b) using the 0.55 isoline also identified the same eleven climatic regions. The similar location of the 0.55 isoline on these two maps strengthened the argument for using this type of analysis in studies where geographic coherence of regions must be maintained. An additional climate region was found for PR stations in the Black Hills of northeast Wyoming, an area where no SN sites existed. These results suggest there are differences in spatial variability even within large watersheds throughout the five-state region, such as the Colorado above Glen

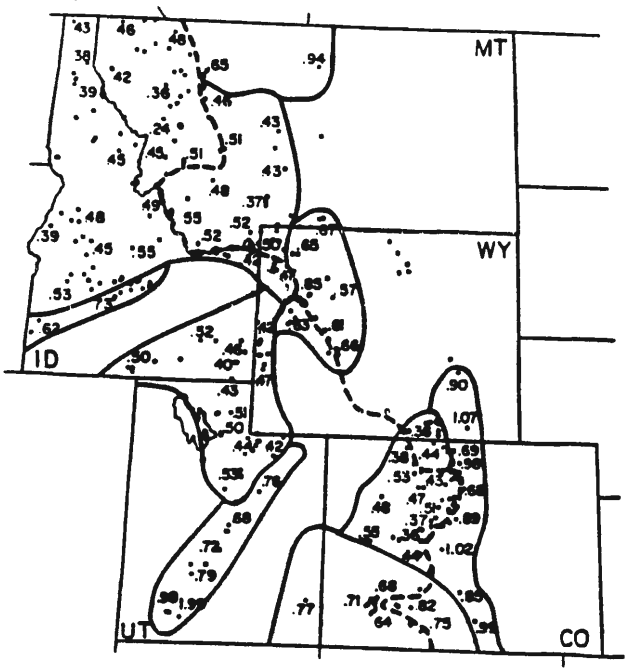

(a)

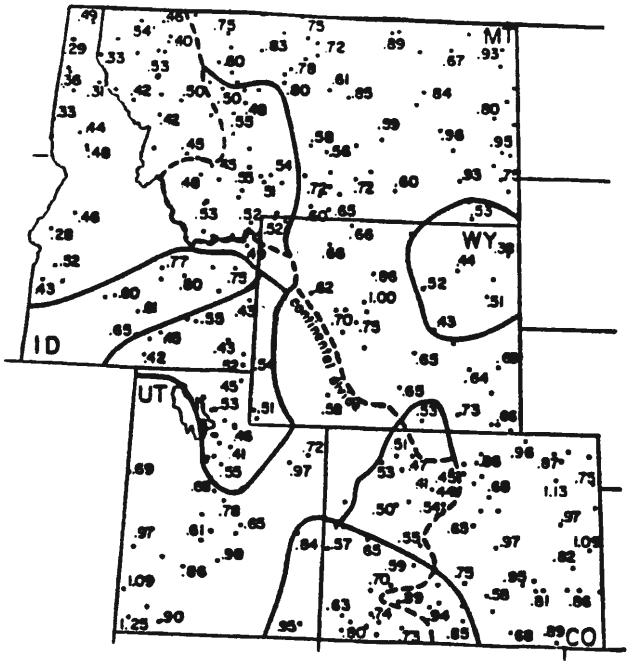

(b)

Figure 9. The measure of variability computed for a) SN sites and b) PR stations across the five-state region. The 0.55 measure of variability isoline separates areas of low variability (stable) and high variability (unstable).

Canyon Dam. The results from this analysis differ from the results of Peck and Schaake (1990), which indicate an average value of variability can be applied throughout large watersheds, such as the Colorado, in the Rockies. Appendix I and II show a detailed list of PR stations and SN sites respectively in each climatic region along with characteristics of the sites and stations such as elevation, the measure of variability, median value of PR (or SN), station number, and other information.

In each region identified in Figure 9a, a regionally average MOV value was computed by adding up the MOV values from all the sites in the region and then dividing by the number of sites.

$$\text{regionally averaged MOV} = \frac{\sum_{i=1}^{N_r} MOV_i}{N_r} \qquad (14)$$

where N_r = number of sites in a region

Regionally averaged MOV values were computed for SN and PR. Figures 10a and 10b show the regionally averaged variability values for SN and PR, and Figure 10c shows the regions numbered for future reference. SN and PR regionally averaged values are similar for each region. Five SN regions agree with six PR regions, all with average MOV values less than 0.55, indicating they are stable. Three of these stable regions lie along and west of the C.D., two lie just east of the C.D., and the remaining stable region (PR only) is located in the Black Hills of northeast Wyoming.

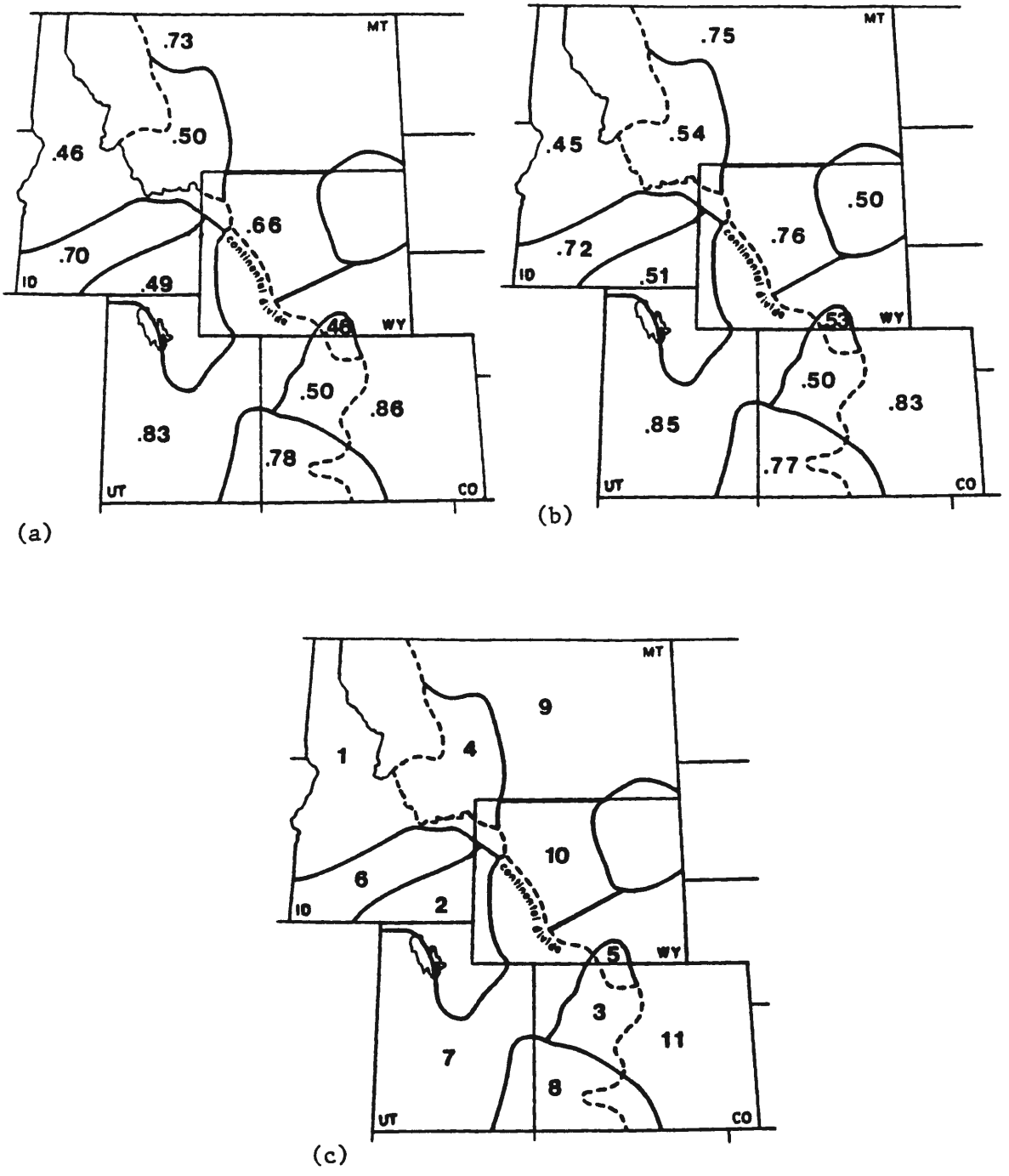

Figure 10. The regionally averaged measure of variability values for a) SN and b) PR in stable and unstable areas. The regions were numbered for future reference in c).

Six regions have average MOV values, both SN and PR, greater than 0.55. They are classified as unstable, and are, thus, much more variable precipitation areas. Three of these unstable regions are located west of the C.D., while three are located east of the C.D. The regions have similar average MOV for both SN and PR, indicating that although the measurements were taken within different elevational zones in a given region, they have the same magnitude of variability over the 35-year study period. Note also that the values in the unstable regions are nearly double those in the stable regions. Because the differences between the stable and unstable areas are so large, and because both SN and PR variability values agree within each region, these findings imply that spatial variability information is very important when attempting to understand the fluctuations over time in the available water resources in the Rocky Mountain region.

This information could be useful to those who manage water or are involved in development of new water storage facilities for the West's major rivers. For example, the available water supply of a large watershed in the West may be influenced by several unstable and stable regions. Understanding how these different regions exist and how they may influence the annual total flow differently can help identify what extremes might exist in the spring runoff period. The next section will try to explain the location of stable and unstable subregions.

2. Reasons for regional differences in variability

Several climate and topography characteristics can influence the spatial variability of the hydroclimatic elements analyzed in this study. The regional differences in variability are difficult to

explain because physical variables such as latitude, elevation, and exposure to different moisture flows vary widely for the SN sites and PR stations within the study region. One of the main objectives of this study was to identify the physical variables that would explain the differences in variability for geographically coherent regions within the five-state area.

Average precipitation in the Rocky Mountains generally increases with elevation (Peck and Brown, 1962; Marlatt and Riehl, 1963; Rhea, 1978); and variability of precipitation generally decreases with increasing average annual amounts of precipitation (Conrad, 1941; Longely, 1952; Hershfield, 1962). Thus, one would infer that precipitation variability in mountainous terrain should decrease with elevation in this data. However, the relationship of MOV to elevation for the 11 climatic regions does not demonstrate this feature. Examples are given in Figures 11a and 11b, where for two regions 1 (stable) and 6 (unstable) the scatter plots of MOV vs. elevation for SN and PR sites in each region are shown (plots for the other nine regions are in Appendix IV). For all regions the data points are clustered into groups rather than linear. The relationship of site MOV values to elevation in all regions explained between 5 and 30 percent of the variance. The slope of the regressional lines was nearly vertical. The regressional analysis implied that MOV and elevation were not correlated well and that there was no change of MOV with change in elevation.

The correlation of MOV to the median value of SN for sites in each region was poor. The slopes derived from the 11 regression equations ranged from +0.0016 to -0.0237, see Table 7.

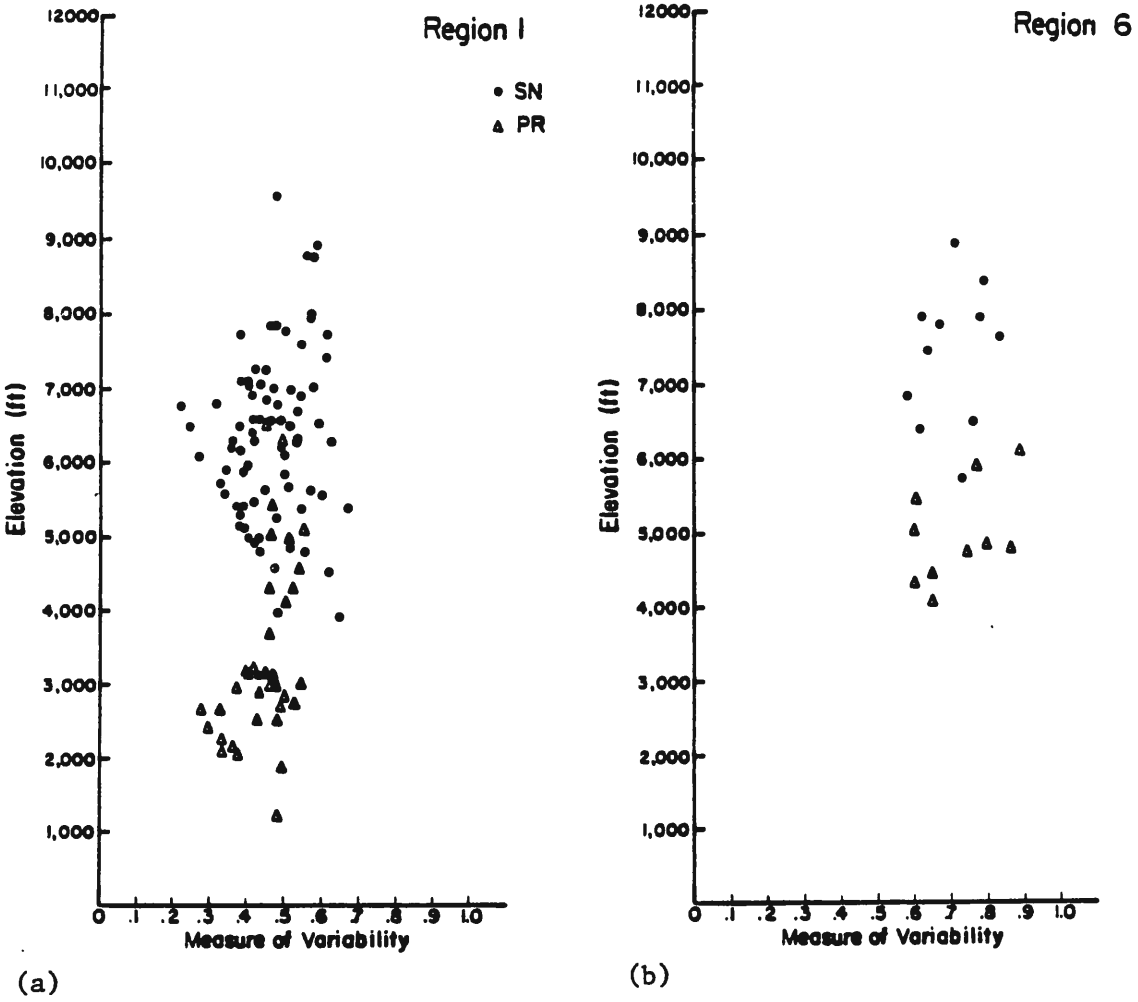

Figure 11. Scatterplot of measure of variability values versus the elevation of the SN sites and PR stations in a) Region 1 and b) Region 6. SN values are the dots, while the PR values are the triangles.

Table 7. The regression equation and explained variance for each region when considering median value of SN vs. MOV (inches, snow water equivalent).

Region	Regression Equation	Amount of Variance Explained, r^2
1	Y = 0.54 - 0.0032X	0.16
2	Y = 0.46 + 0.0016X	0.03
3	Y = 0.59 - 0.0062X	0.19
4	Y = 0.57 - 0.0060X	0.13
5	Y = 0.60 - 0.0073X	0.38
6	Y = 0.76 - 0.0032X	0.05
7	Y = 1.03 - 0.0152X	0.16
8	Y = 0.87 - 0.0062X	0.12
9	Y = 0.91 - 0.0237X	0.34
10	Y = 0.76 - 0.0107X	0.12
11	Y = 1.05 - 0.0237X	0.27

The regression equations in Table 7 show that 10 of the 11 regions have a small negative slope ranging from -0.0032 to -0.0237 indicating that as the median value of SN increases the MOV decreases, (Figure 12a-d). The small amount of variance explained in each region ($0.03 < r^2 < 0.38$) suggests that the relationships between median value of SN and MOV are not close and much less than the relationships between precipitation and elevation found in previous studies by Longely (1952) and Hershfield (1962). Note the smallest negative slopes (B_i) are associated with the stable regions (1 through 5) and unstable regions 6 and 8 west of the C.D., while the slopes (B_i) are generally greater in unstable regions (9 through 11) on the east side of the C.D. ($B_i < -0.0107$ and $B_i > -0.0237$). This indicates that as the median SN value decreases, variability in unstable regions on the east side of the C.D. increases more quickly than the variability on the west side of the C.D. The reason for the difference is because the unstable SN sites east of the C.D. are influenced by precipitation that 'blows-over' the top of the C.D. during storms, associated with the predominant winter

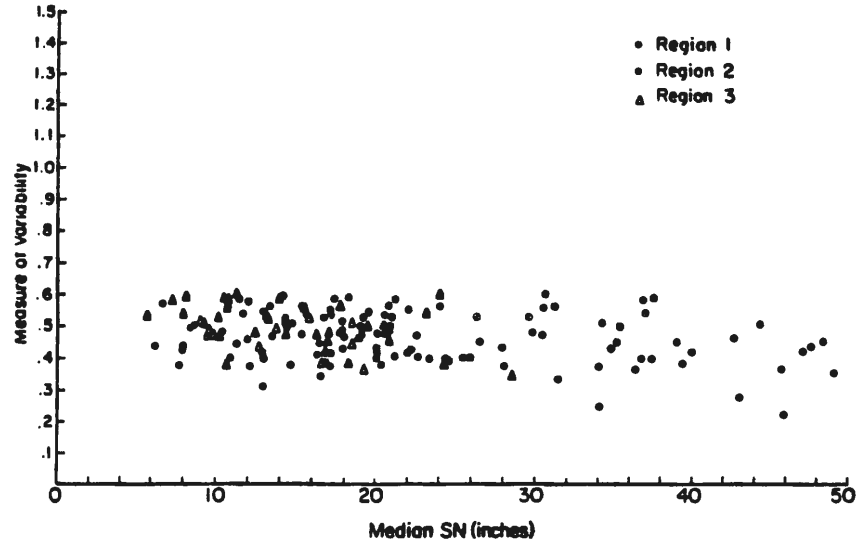

a)

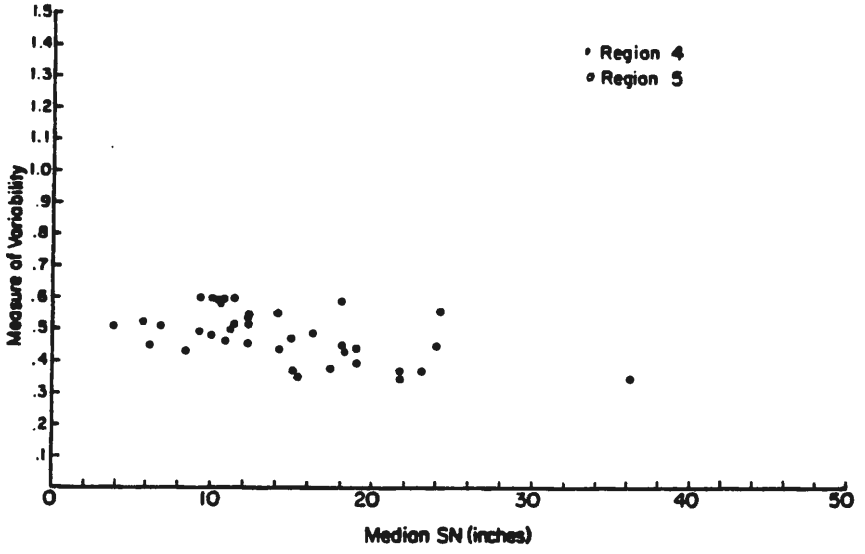

b)

Figure 12. Scatterplot of median SN value versus measure of variability value for sites in the different regions: a) stable regions 1, 2, and 3, west of the C.D. and b) stable regions 4 and 5 east of the C.D.

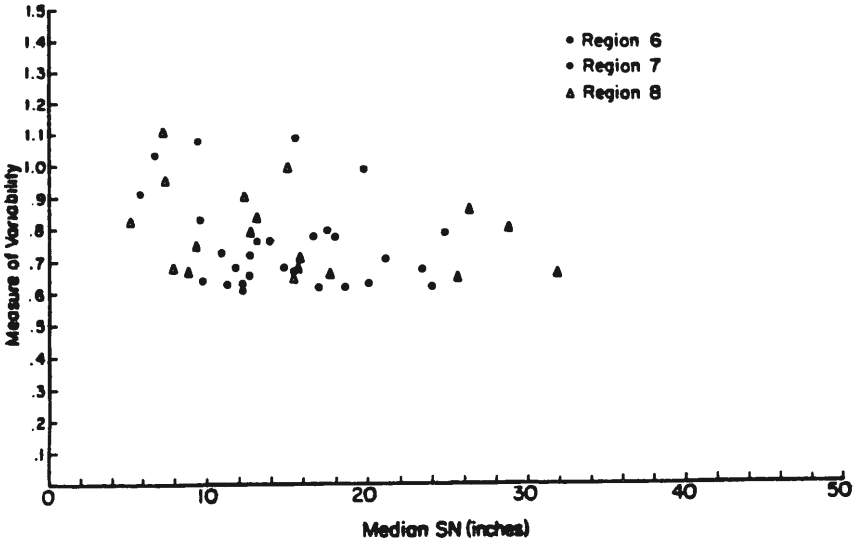

c)

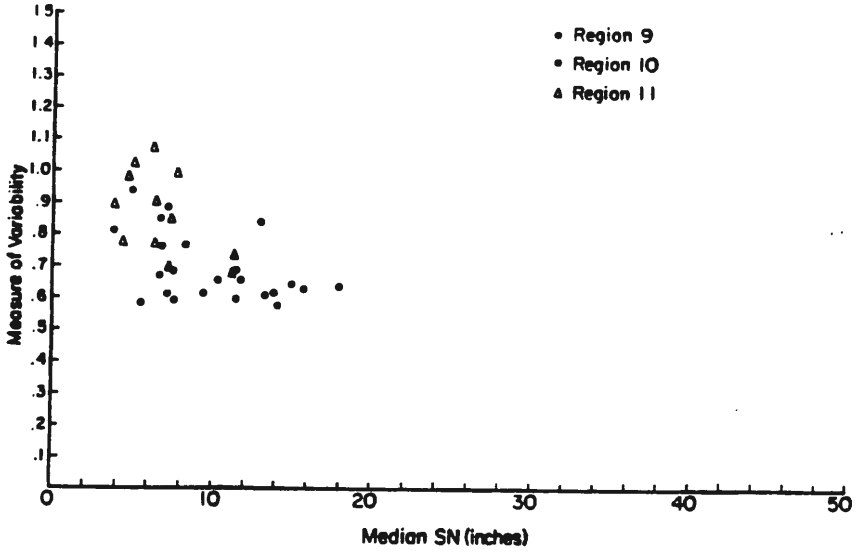

d)

Figure 12. Scatterplot of median SN value versus measure of variability value for sites in the different regions: c) unstable regions 6, 7, and 8, west of the C.D. and d) unstable regions 9, 10, and 11, east of the C.D.

upper air flow, that are affecting areas west of the C.D. Also, the relatively infrequent upslope events east of the C.D. do not always influence the SN sites east of the C.D. These regression analyses suggest that in all regions variability is influenced to some degree by changes in the median SN.

Stable and unstable regions west of the C.D. have similar regression equations (with slopes that only slightly decrease) that are different than the regression equations for regions east of the C.D., indicating that the relationship of median SN to MOV is dependent on location relative to the C.D. SN data analyzed at sites in stable (low variability) region 3 of Colorado were compared with SN data analyzed at sites in unstable (high variability) region 8 (also in Colorado). Both stable and unstable regions are located west of the C.D. and had SN sites that experienced a range in the median amount of winter precipitation from less than 5 inches to greater than 10 inches, yet the MOV values for SN sites in region 8 were twice that in region 3. The regressional analysis of median SN to MOV suggests that only a small part of the variability in the Rockies is a function of the median precipitation at a location.

The possible relationship of latitude differences and spatial patterns of hydroclimatic variability was examined, see Figures 10a and 10b. Although more unstable regions existed in the northern part of the study area, stable and unstable regions were found to exist in all parts of the five-state study area. No strong evidence of a latitudinal effect existed.

The investigation of 14 watersheds indicated that winter precipitation in basins with a surface exposure to moist air flow from

a westerly to northerly direction were stable (i.e. low variability), whereas those with exposure to southerly or easterly flow were more unstable. The relationship of variability to surface exposure was evident also in the 11 regions defined by the PR and SN data across the entire five-state region. The prevailing winter upper air flow over the study region is from the west and northwest (Trewartha and Horn, 1980). This prevailing flow provides upslope precipitation for regions with a northerly or westerly exposure and downslope dry winds for regions with an easterly exposure. During the winter infrequent periods of southerly or easterly upper air flow bring upslope precipitation events to those regions with southerly or easterly exposures. The precipitation in those regions with their highest mountain range exposed to northerly or westerly moist flow is less variable than in regions with their highest ranges exposed to moist air flow with a southerly or easterly direction. The geographically coherent regions defined by variability could increase the understanding of SN, PR, and ST for those basins that are not heavily instrumented. These results offer the potential for determining snowpack variability and hydrologic responses if there are strong ties between spatial patterns of variability and the frequency and patterns of winter large-scale atmospheric circulations. Further analyses in Chapters 6 and 7 will examine the relationship of SN patterns of variability to large-scale atmospheric/ oceanic circulations and the frequency of Rocky Mountain winter synoptic patterns.

3. Utility of a new hydroclimatic classification scheme based on magnitude of hydroclimatic variability for the Rocky Mountains

The information considered most important to those who manage and distribute water resources for the Western United States relates to the variability of the hydroclimatic system. Snowmelt runoff is the greatest contributor to the total water-year streamflow throughout the five-state region. However, dramatic differences in the variability of the primary hydroclimatic elements have been identified, first at the spatial level of the watershed, and then across the entire five-state region. These regions with differing variability can influence large watersheds, such as the Colorado River above Glen Canyon Dam, in very different ways. Further study (Chapters 6 and 7) indicates that unstable regions respond differently than stable regions in some years because of very different snowpack distributions associated with large-scale circulation patterns. Understanding how to use this information could potentially improve forecasts of spring water supplies. For example, some large rivers may be influenced by stable regions, as defined by SN or PR data, and may behave very differently than those heavily influenced by unstable regions. This situation indicates the need to develop a hydroclimatic classification system for the Rocky Mountains.

4. Summary

The computed SN MOV ranged from 0.22 to 1.19 for 275 SN sites, whereas the PR MOV values for 266 stations ranged from 0.28 to 1.25. Although the elevation distributions of SN and PR locations are very different, both data sets showed similar ranges in variability.

The calculated MOV values of all SN sites and PR stations were plotted on maps. The 0.55 isoline identified eleven homogeneous climatic regions for SN and PR, five stable and six unstable. The regions have similar MOV values for both SN and PR. The values in the unstable regions are nearly double those in the stable regions. Because the differences between the stable and unstable areas are so large, and because both SN and PR variability values agree within each region, these findings imply that spatial variability information is very important when attempting to understand the fluctuations over time in the available water resources in the Rocky Mountain region.

The relationship of elevation, median precipitation, and latitude to the MOV was poor. The precipitation in those regions with their highest mountain range exposed to northerly or westerly moist flow is less variable than those with their highest ranges exposed to moist air flow with a southerly or easterly direction. Thus, it appears that exposure/aspect is the surface physical variable that controls spatial patterns of SN and PR variability across the five-state region. Analyses examined in Chapter 7 will identify if the variability associated with winter synoptic patterns are linked to the spatial variability at the surface.

These results offer the potential for determining precipitation variability and predicting hydrologic responses if there is a strong tie to the frequency and patterns of winter large-scale atmospheric circulations. Analyses in the next chapter will examine the annual patterns of SN. The ties of the spatial patterns to large-scale atmospheric/oceanic circulations will be examined in Chapters 6 and 7.

CHAPTER V

SPATIAL PATTERNS OF ANNUAL APRIL 1 SNOWPACK AND WINTER PRECIPITATION

Several authors have identified the occurrence of uniform and recurrent seasonal or annual precipitation and streamflow patterns over large areas in the United States (Bradley, 1980; Bartlein, 1982; Lins, 1985; Redmond, 1989). One of this study's objectives was to understand the regions' annual spatial patterns based SN and PR, and examine the distribution of the annual patterns through the 1951-1985 period.

Possibly the greatest impact to regional water resources coming from temporal variations in precipitation results from long-term (decadal or longer) wet and dry periods in the West (Cayan and Peterson, 1990). Thus, another of this study's objectives was to identify characteristics of the interannual and long-term variability. This information would be valuable to those who plan and manage water supplies for the western United States.

This chapter: 1) defines how annual spatial patterns from SN and PR data were determined, 2) describes the relationship of annual SN to PR values, 3) delineates the changes in annual patterns of SN, and 4) describes the long-term variability of SN and PR and its link to north-to-south gradient patterns.

1. Delineation of annual patterns of SN and PR

The spatial distribution of April 1 snowpack values for each year (1951-1985) was investigated using data from each of the 275 long-term snowcourses in the study area. The objective of this analysis was to identify the types of annual patterns of SN and PR and describe the frequency of them through the 35-year period. Objectively analyzed non-exceedence probability maps were the most useful means to assess and present this large data array. Each map depicts the annual values divided into ten non-exceedence probability groups, each shaded differently (Figure 13). Assessing these patterns revealed three basic and oft-repeated patterns: 1) years with a consistent anomaly over the entire region, either wet (e.g. Figure 13) or dry (e.g. Figure 14); 2) years with a distinct north-to-south gradient (e.g. Figure 15); and 3) years with average amounts at many sites plus isolated areas of wet and dry throughout the region, labeled as "average" (e.g. Figure 16). The remaining 31 annual SN patterns are shown in Appendix V. Over the 35-year sample of SN data there were 14 consistent years (6 wet and 8 dry years), 12 years with a north-to-south gradient, and 9 average years.

A high frequency of north-to-south gradients in annual data also were observed by Doesken et al. (1981), Bartlein (1982), Meko and Stockton (1984), Lins (1985), and Redmond and Koch (1989) in their analyses of precipitation and streamflow data for several regions of the United States. Several of these studies, which have explored spatial patterns of hydroclimatic elements as a function of time, have integrated objective analyses of the data including Principal Component Analysis and Empirical Orthogonal Functions (Sellers, 1968; Diaz and Fulbright, 1981; Lins, 1985; Redmond and Koch, 1989).

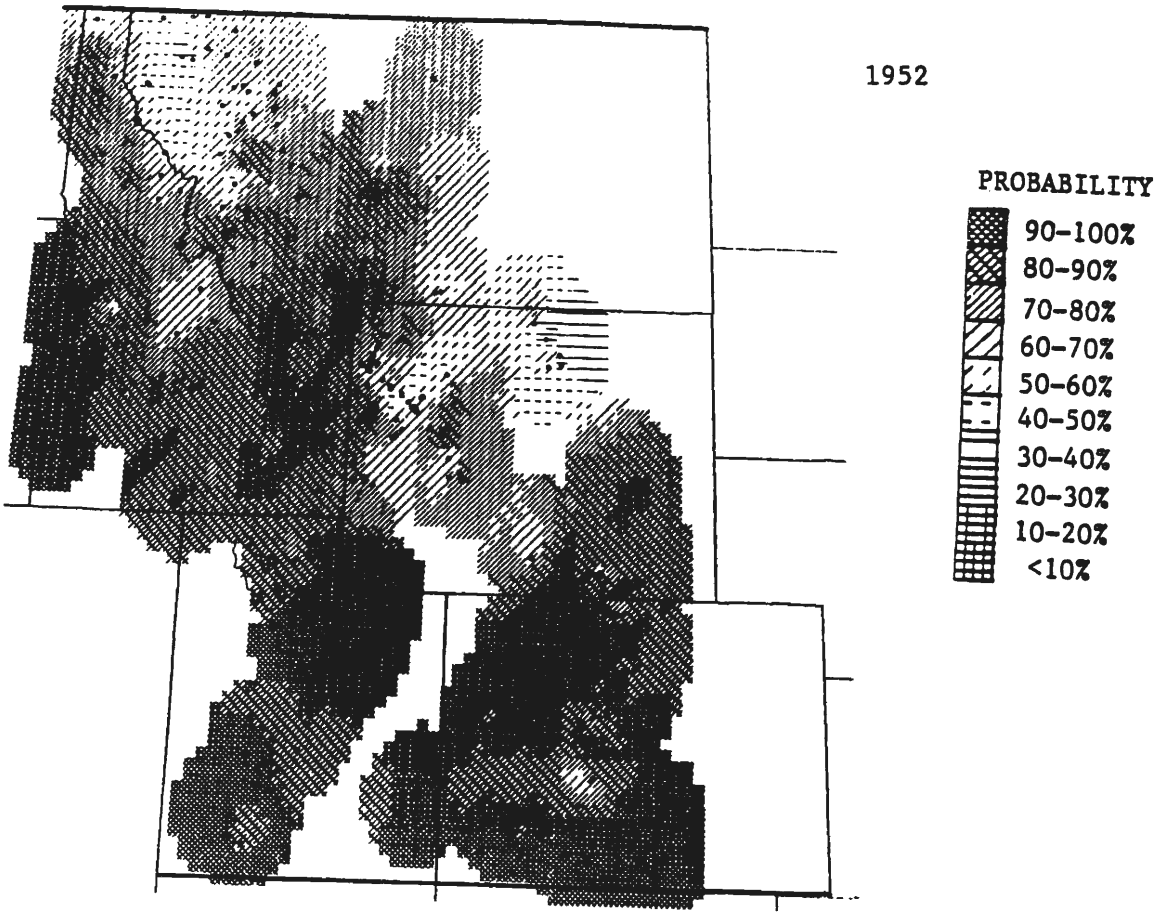

Figure 13. Objectively analyzed map showing the non-exceedence probabilities (based on 1951-1985 data) of April 1 snowpack for 1952. 1952 was a year with a wet pattern. Most regions experienced very wet conditions. Each of 10 non-exceedence probability ranges are shaded differently.

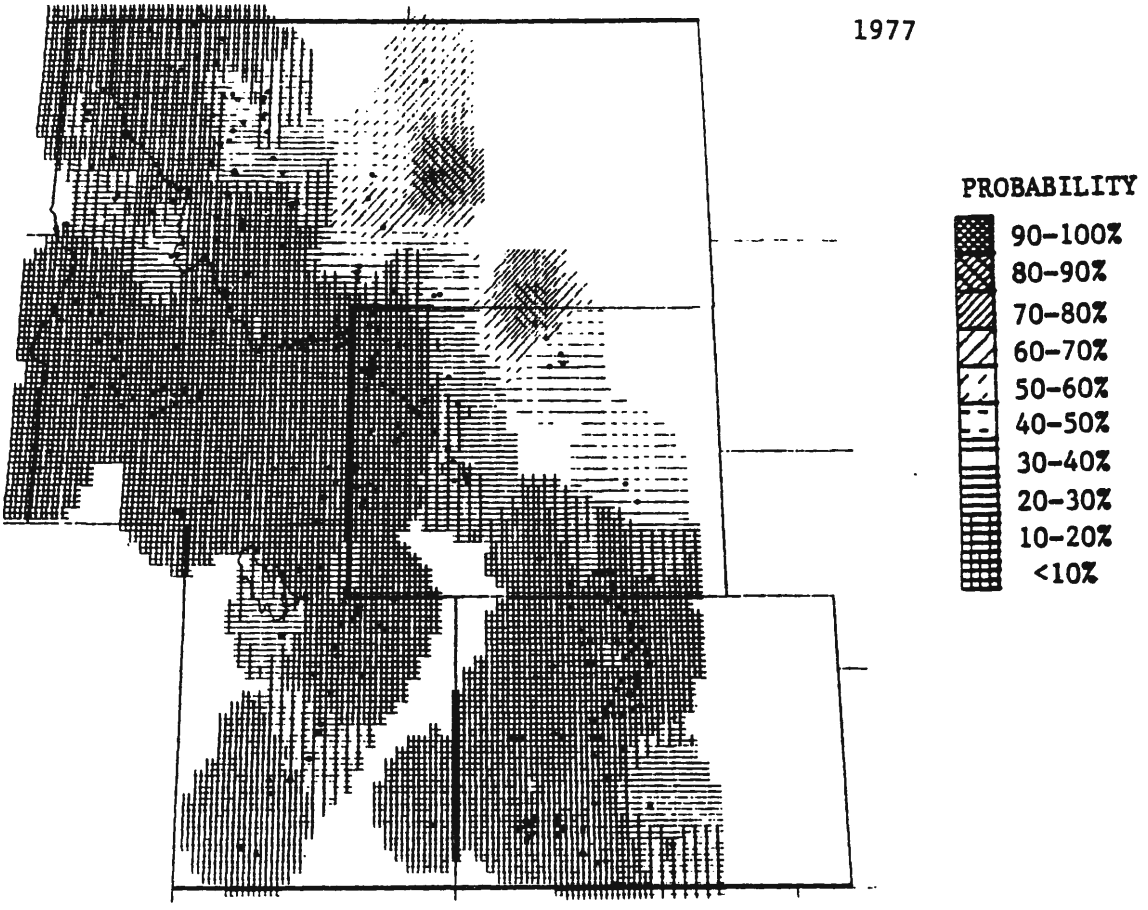

Figure 14. Objectively analyzed map showing the non-exceedence probabilities (based on 1951-1985 data) of April 1 snowpack for 1977. 1977 was a year with a dry pattern. Most regions experienced very dry conditions. Each of 10 non-exceedence probability ranges are shaded differently.

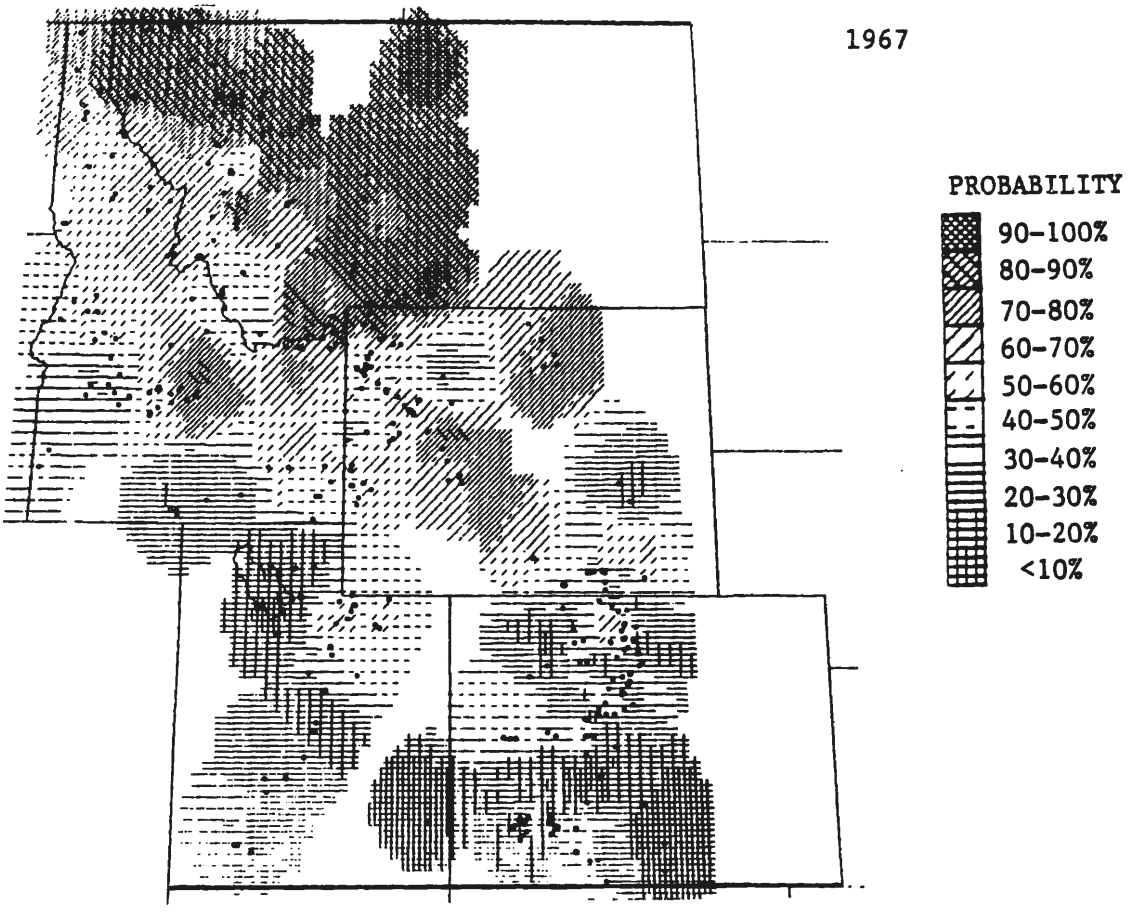

Figure 15. Objectively analyzed map showing the non-exceedence probabilities (based on 1951-1985 data) of April 1 snowpack for 1967. 1967 was a year with a north-to-south gradient pattern. Most northern regions experienced very wet conditions while southern areas were dry. Each of 10 non-exceedence probability ranges are shaded differently.

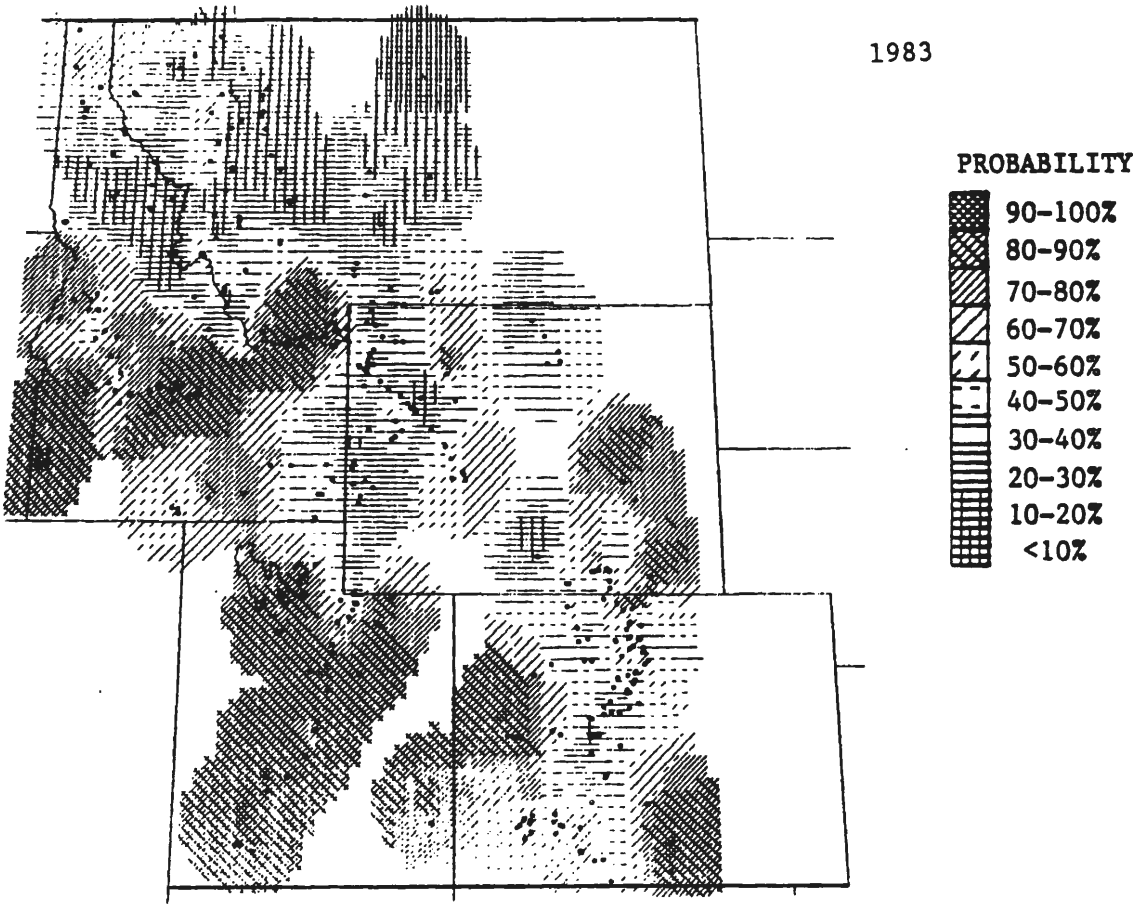

Figure 16. Objectively analyzed map showing the non-exceedence probabilities (based on 1951-1985 data) of April 1 snowpack for 1983. 1983 was a year with an average pattern. Most regions experienced near average amounts with isolated areas of wet and dry throughout the region. Each of 10 non-exceedence probability ranges are shaded differently.

The three basic spatial patterns identified in this study were examined further by plotting the annual number of snowcourses with snowpack in each of 10 non-exceedence probability ranges for 1952 (wet), 1977 (dry), 1967 (north-to-south gradient), and 1983 (average) in Figure 17. The years with all-wet and all-dry patterns had probability distributions skewed to opposite ends as shown in Figure 17. Six of 14 north-to-south gradient years have dual peaks on each end of the distribution, but most gradient and average/mixed years were characterized by flat distributions. One of the least common distributions is one in which most stations over the five-state region are near their median, like that of a bell-shaped curve. In most years, some areas experienced values within the wettest 20% of all years, while other areas were in the driest 20%. Again, wide spatial differences are common in SN data.

Averaging SN site data within the 11 regions (discussed in the previous chapter) allowed for easier comparison from region to region and permitted comparison of stable and unstable areas within the five-state region. The regionally-averaged SN data for the 11 regions were analyzed to develop non-exceedence probabilities for each year in each region. In each region, all normalized values of SN for each site (see Chapter 3) were averaged for each year (1951-1985). The 35 annual averages were ranked from 1 (largest) to 35 (smallest) and assigned a non-exceedence probability. Then, the 11 non-exceedence probabilities, one for each region, were plotted on 35 annual maps (1951-1985). SN patterns were identified and classed like those in the previous paragraph. The eleven regional non-exceedence values for each year revealed the regionally averaged SN maps were similar in all years to

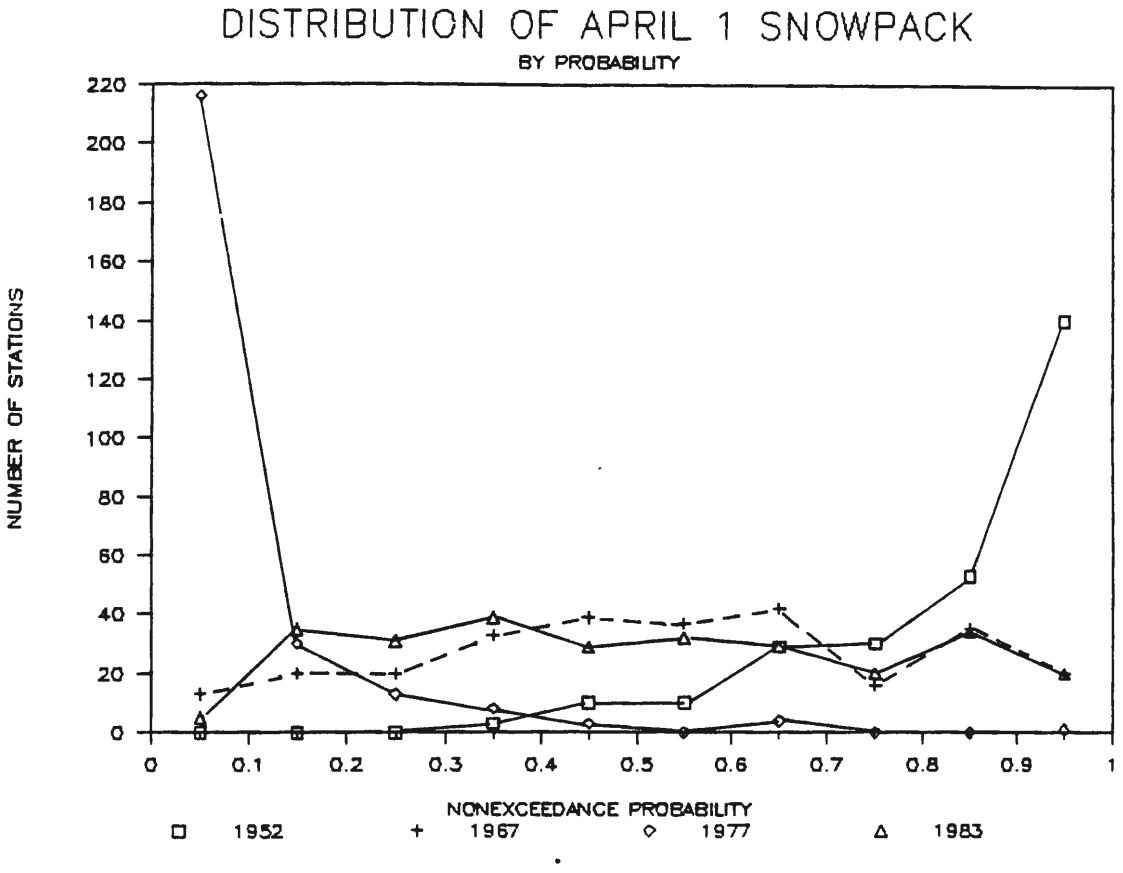

Figure 17. The distribution of SN stations, by 0.10 non-exceedence probability intervals of April 1 snowpack, over a five-state region for a wet year (1952), a dry year (1977), a north-to-south gradient year (1967) and a near average year (1983).

those when all sites were plotted. Figure 18a-d show the regional probabilities for the years, 1952 (wet), 1977 (dry), 1967 (north-to-south gradient pattern), and 1983 (average). These regional probability patterns are similar to the examples given in Figures 13-16 that used SN site data. Because of this similarity between site-analyzed patterns and regionally-averaged patterns, future analyses used the regional-averaged SN and PR data.

A similar analysis was performed using regionally averaged PR data (October 1 - March 31 accumulated precipitation). Because the types of winter precipitation events affecting the high-elevation SN sites differ from those affecting the low-elevation PR stations east of the C. D., the three unstable regions located in the eastern regions of the five-state regions were not used in the analyses. Regionally averaged PR non-exceedence probability patterns were similar to those of regionally averaged SN patterns in 26 of the 35 years. The other nine years showed a few PR regions experiencing differences in non-exceedence probability from that of SN greater than 25% but less than 40%. This is an important finding because the SN data represents small areas along a north-to-south line and only the highest monitored elevations, whereas the PR data represents the broader, low-elevation areas across the entire five-state region. Further analyses discussed in the next section focus on the relationship of SN to PR in each region.

2. Relationship of Annual SN to PR values

Regionally-averaged SN and PR annual values had similar patterns west of the C.D. However, areas east of the C.D. had dramatically

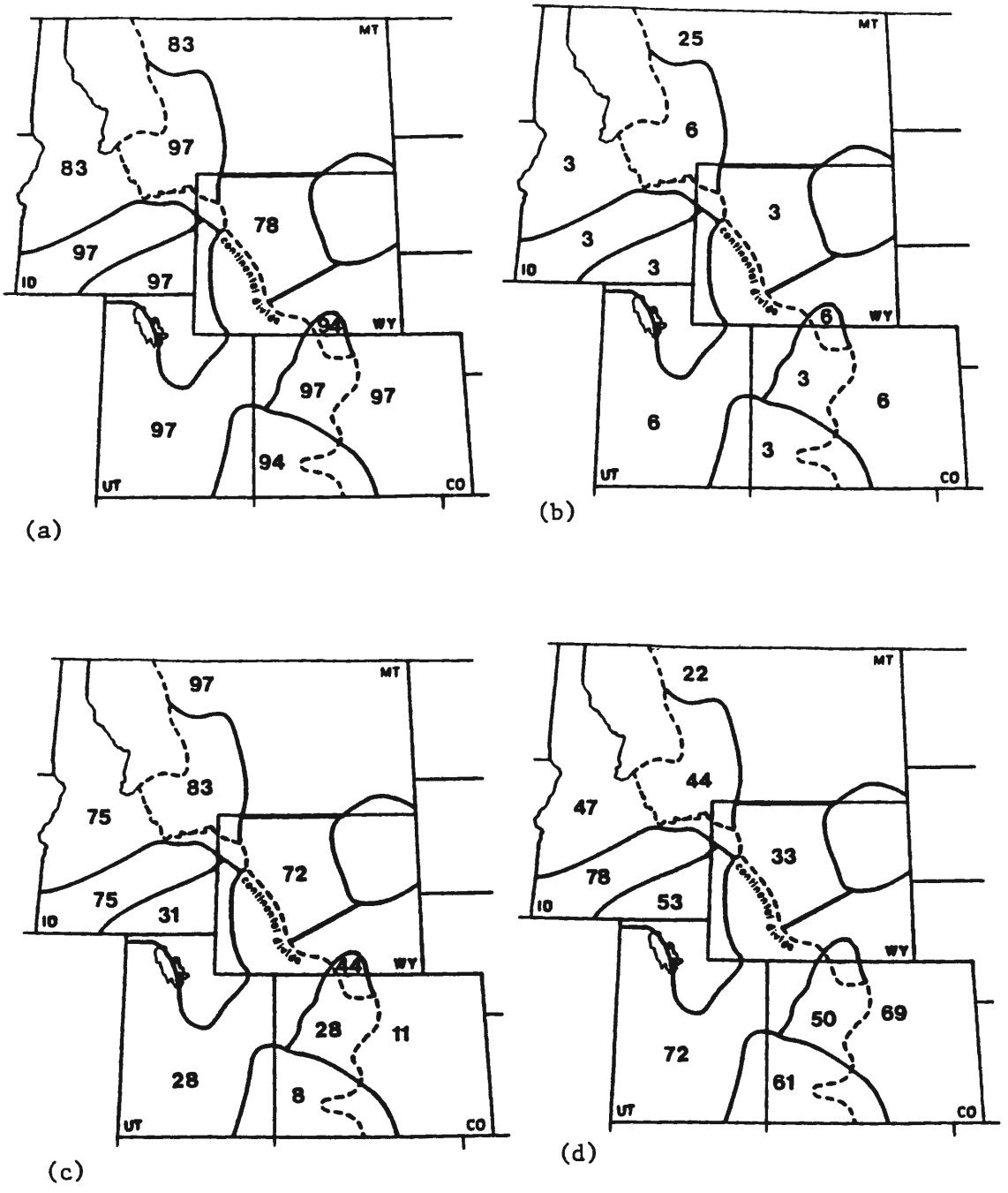

Figure 18. The regional SN non-exceedence probabilities for a) a wet year (1952), b) a dry year (1977), c) a north-to-south gradient year (1967), and d) a near average year (1983). Values are a percent of 100 (100 = wettest, 0 = driest).

different patterns of regionally-averaged SN and PR values. To test how well SN and PR were related during the 35-year period intraregional analysis using linear regression was employed. Based on the watershed analysis of PR to SN in Chapter 3 and the differences in annual patterns of SN and PR east of the C.D. the intraregional correlations of SN to PR were expected to be generally better west of the C.D.

In each of the eleven regions (Figure 19), regionally averaged SN values were correlated to regionally averaged PR values for the 1951-1985 period. Strong correlations (r-values > +0.71 and significant at 99% level) existed in the three stable regions and the three unstable regions located west of the C.D., and in region 4, located east of the C.D., a stable (low variability) zone with northerly exposure to moist air flow. Region 5, which is a stable northerly exposed region, was not considered in this analysis because only one PR station was located within the region. Unstable regions 9, 10, and 11, all located on the east side of the C.D., have poor (+0.25 to +0.41) correlation coefficients for their regionally-averaged PR and SN values. The strong SN to PR r-values apparently indicate that regions on the western side of the C.D., whether stable or unstable, are influenced by similar types of precipitation events at all elevations. The poor correlations on the east side of the C.D. result because higher-elevation areas (where SN sites are located) are influenced greatly by 'blow-over' precipitation from storms that influence regions west of the C.D., while low-elevation PR stations are largely influenced by another type of precipitation event, often referred to as the shallow upslope (Hjermstad, 1970). These areal differences were examined using Colorado values. The correlation of regionally-averaged SN values west

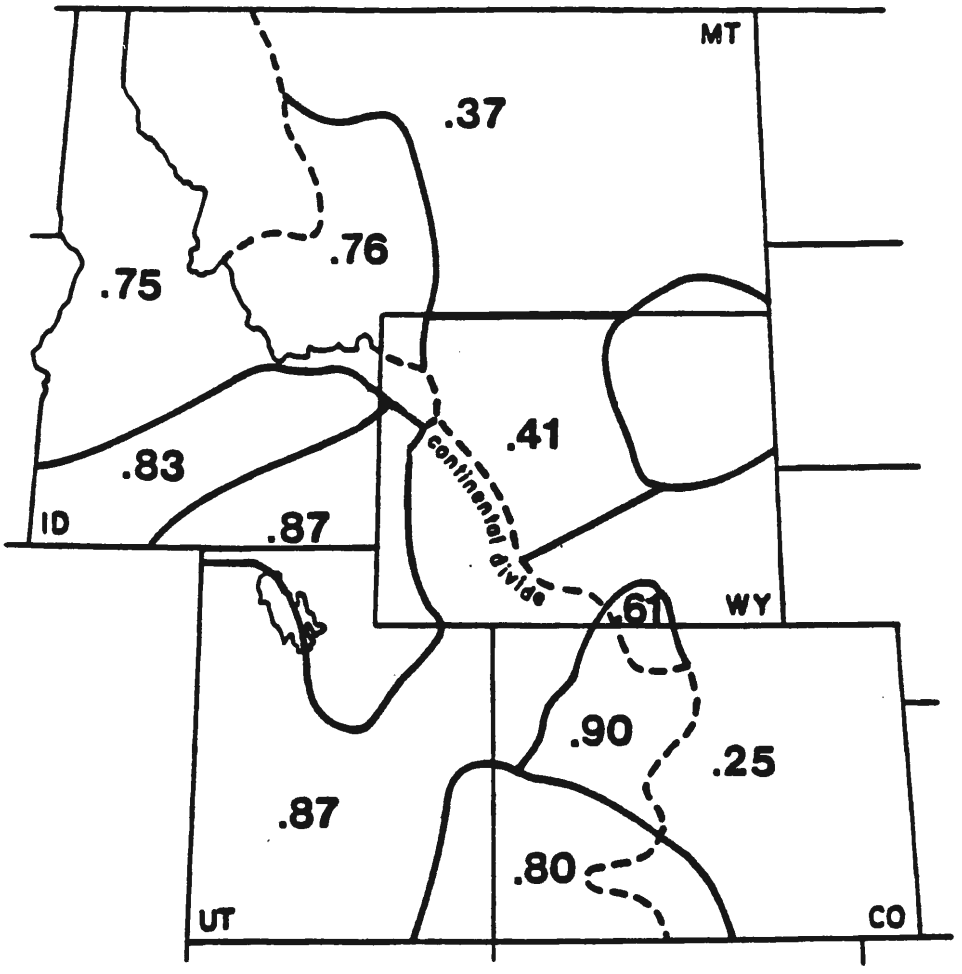

Figure 19. The correlation coefficients for regionally averaged SN to regionally averaged PR in the eleven regions.

of the C.D. in region 3 to regionally averaged SN values east of the C.D. in region 11 produced an r-value of +0.88. The correlations of regionally averaged SN or PR values west of the C.D. in region 3 to the PR values east of the C.D. in region 11 yielded r-values of +0.20 and +0.30 respectively.

The results based on regional correlations of SN to PR are similar to those identified in the watershed analysis of Chapter 3 (Table 6). In six watersheds that were considered stable (exposed to north or westerly flow) the average r-value for SN correlated to PR was 0.75. For the four watersheds located west of the C.D. with an exposure to southerly or southwesterly flow the average r-value was 0.74. For the four watersheds located east of the C.D. or on the eastern side of a large mountain barrier with an exposure to easterly flow, the average r-value was 0.51. Based on the watershed and regional correlations of SN to PR, streamflow and water supply forecasters should realize that both SN and PR data provide useful information about the source for ST in regions west of the C.D., while for areas east of the C.D. SN and PR data represent two different types of precipitation regimes and that SN data is better related to ST and is a best monitor of winter climate.

3. Interannual variability in annual patterns of SN

The magnitude of variability for regionally-averaged SN data identified 11 different regions in the five-state region and

ascertained the degree of interannual variability in these regions. In this analysis the objective was to identify spatial differences of annual SN patterns. Correlation coefficients were computed between regions of regionally-averaged annual SN values, and the greater the latitudinal distance between regions the poorer the r-value (Figure 20). For example, region 1 is moderately well correlated with other regions (r-values > +0.53, 99% significance level), both stable and unstable, in the northern half of the study region. However, the three southern unstable regions (7, 8, and 11) located the farthest away latitudinally from Region 1 show very weak correlations (r-values < +0.34, 95% significance level). The explanation for these differences in correlation for regions in Figure 20 is related to differences in latitude. In half the years northern and southern regions have SN anomalies that are opposite of one another causing the r-values to become smaller, near zero, like those of region 1 to regions 7 or 8. These latitudinal differences are apparently related to the mean location of the upper level jet stream/storm track that varies annually (Weaver, 1968; Cayan and Peterson, 1990). Further discussion of the relationship of SN variations in space to large-scale circulations and Rocky Mountain winter synoptic patterns is in Chapters 6 and 7.

As discussed in the first section, each year had an identifiable pattern based on the objectively analyzed non-exceedence probability maps based on data from all SN sites. Another objective of this study was to examine the distribution of the annual patterns through the 1951-1985 period. Their temporal distribution appears in Table 8.

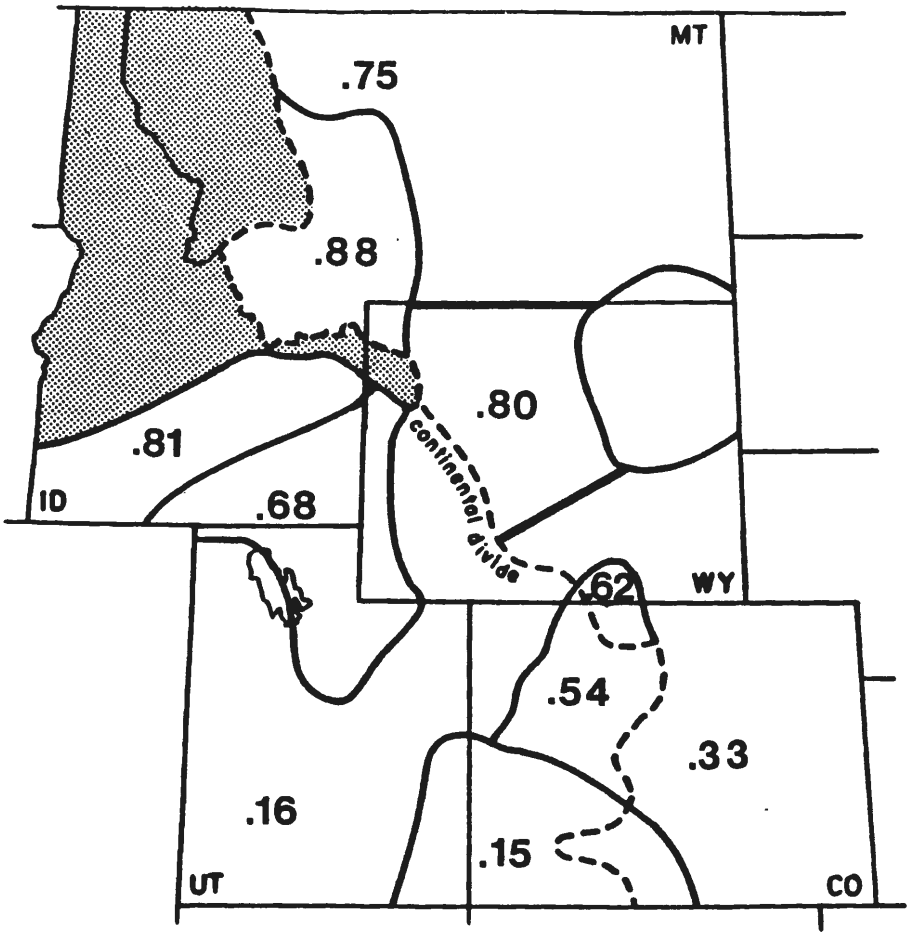

Figure 20. The correlation coefficients computed between region 1 and all other regions using regionally averaged annual SN values. Region 1 is stipled.

Table 8. Annual patterns of SN data from 275 sites for 1951-1985.

YEAR	WET	DRY	WET NORTH/DRY SOUTH	DRY NORTH/WET SOUTH	AVERAGE
1951			X		
1952	X				
1953		X			
1954			X		
1955		X			
1956			X		
1957					X
1958					X
1959					X
1960		X			
1961		X			
1962	X				
1963		X			
1964			X		
1965	X				
1966		X			
1967			X		
1968					X
1969	X				
1970					X
1971			X		
1972			X		
1973				X	
1974			X		
1975	X				
1976					X
1977		X			
1978					X
1979				X	
1980				X	
1981		X			
1982	X				
1983					X
1984				X	
1985					X
TOTAL	6	8	8	4	9 = 35

Table 8 identifies several interesting features. First, wet, dry, and average years occurred frequently throughout the 35-year period. Second, wet-north/dry-south gradient years occurred only between 1951-1974, and dry-north/wet-south gradient years occurred only between 1973-1985. Furthermore, three periods were identified based on north-to-south gradient patterns: 1) 1951-1972, when only wet-north/dry-south

gradient patterns occurred, 2) 1973-1974, a transition period from one gradient pattern type to the other, and 3) 1975-1985, when only dry north/wet-south gradient patterns occurred (see Table 9).

Table 9. Frequency of patterns during each period.

PERIOD	WET	DRY	WET-NORTH/DRY-SOUTH	DRY-NORTH/WET-SOUTH	AVERAGE
1951-1972	4	6	7	0	5
1973-1974	0	0	1	1	0
1975-1985	2	2	0	5	4

From the 1951-1972 period to the 1975-1985 period the only change in frequency of patterns occurs in the north-to-south gradient patterns. Wet, dry and average patterns occur in both the earlier and later periods shown in Table 9. These analyses of the temporal distribution of annual SN patterns indicates two important results. First, the occurrence of certain types of gradient patterns changed abruptly in the mid 1970s. Second, both types of gradient patterns did not occur at the same time, except during the transition period (1973-1974), throughout the 35-year period. These results appear linked to some type of change in large-scale atmospheric/oceanic circulations. Chapters 6 and 7 discuss the relationship of SN annual patterns to large-scale circulations and Rocky Mountain winter synoptic patterns.

4. Relationship between long-term changes in SN and PR and north-to-south gradient patterns

The influence of a multi-year period when only one type of gradient pattern occurs is very important in water management. A major objective of this work was to identify long-term variability in SN and PR and see if interannual variability influenced the long-term variability. To investigate this issue further, annual normalized data (see Chapter 3) were regionally averaged (see last section) to form a single snowpack time series for each of the 11 regions. These time series were developed to examine possible north and south differences. Ten-year running means, computed for each region and shown in Figure 21, were selected because they: 1) eliminated much of the interannual "noise" found in the variability data, 2) smoothed out the large anomalies that occur due to large-scale atmospheric/oceanic circulation events such as El Nino/Southern Oscillation (ENSO) or the Pacific/North American (PNA) Index, and 3) depicted the long-term variation of SN.

Distinct and regionally consistent temporal differences emerged between the northern and southern parts of the five-state region as shown in Figure 21. Based on the t-test statistic, described below, a widespread downturn (significant at the 0.01 level) in SN magnitudes began in the mid 1970s across the northern Rockies. Meanwhile, the southern Rockies, at least until 1985, have experienced a steady and significant (at 0.01 level) increase of nearly 20%. The one-sample t-test is shown below.

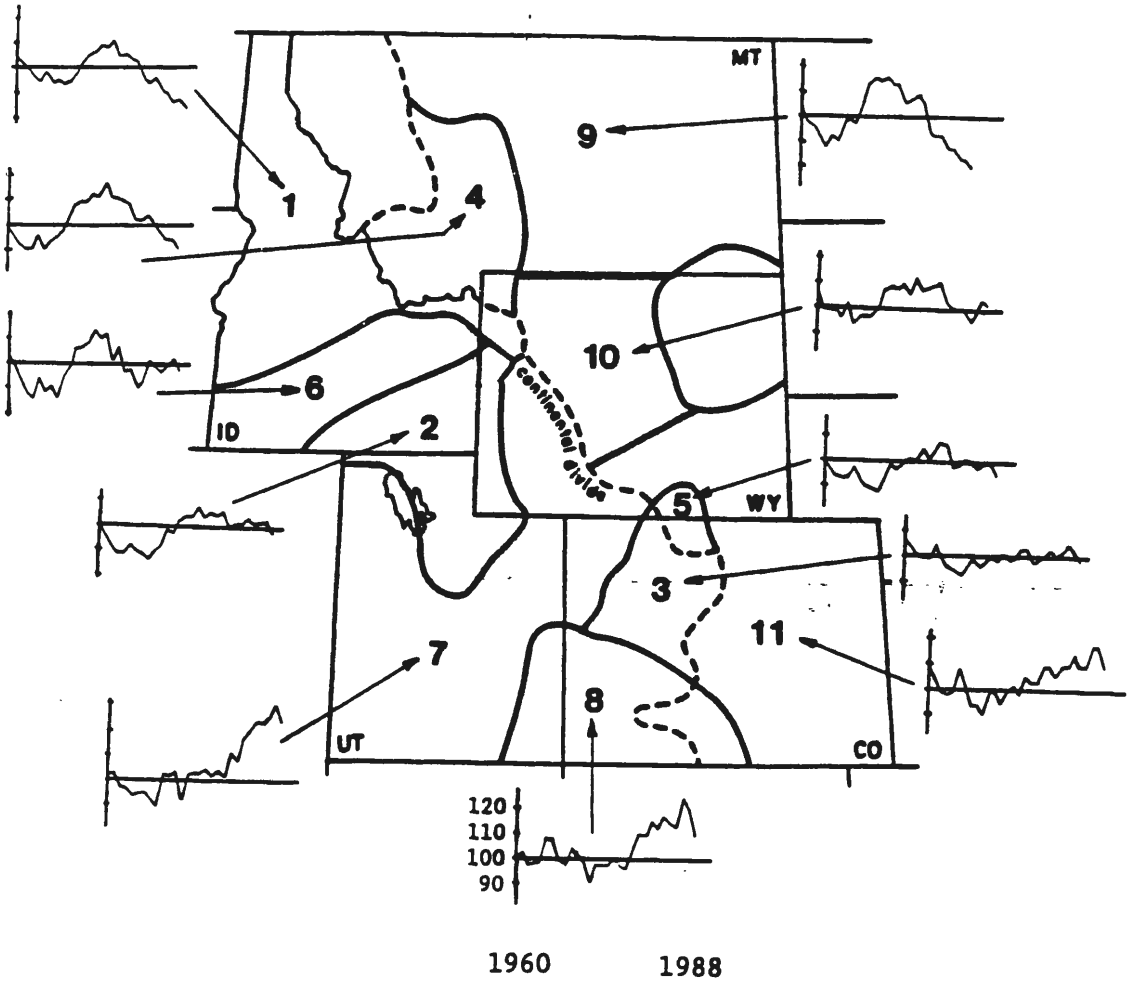

Figure 21. Smoothed time series (10-year running means 1951-1988) of regionally averaged normalized SN for the 11 regions identified in Figure 10c. The horizontal line on each graph is the 1951-1985 median. The Y-axis is the percentage above or below the median for each region. Each tick mark on the Y-axis is 10%.

The one-sample t-test

The Null hypothesis: $H_o : M = M_o$

Test statistic value:

$$t = \frac{\bar{x} - M_o}{6/\sqrt{n}} \qquad (15)$$

where M_o = tested mean
$\bar{x}$ = mean of sample
6 = standard deviation
n = number in sample

Alternative hypothesis	Rejection region for a level @ test
$H_@: M > M_o$	$t > t_{@,n-1}$
$H_@: M < M_o$	$t < -t_{@,n-1}$
$H_@: M = M_o$	$t > t_{@/2,n-1}$ or $t < -t_{@/2,n-1}$

Recent studies have identified long-term significant changes in climatic elements (Angell et al., 1984; Diaz, 1990; Gray, 1990; Hastenrath, 1990; Rasmusson and Arkin, 1990) similar to those found in this study. The center of the Upper Colorado watershed in northern Colorado appears to be the division point where no significant trend was detected. Note that this region also is the southernmost region in the five-state region characterized by low variability. This region is influenced not only by what happens in other stable regions exposed to northerly and westerly moist flow, but also by the types of events that affect the two southern unstable subregions (regions 7 and 8). Thus, this region never experienced interdecadal wet or dry periods during the 1951-1985 period.

Figure 22 illustrates these large north-south long-term differences. This annual time series shows the north-south differences in SN between region 9 (mountains of central Montana) and region 7 (southern Wasatch Range in Utah). In 25 of the past 38 years the relative differences in SN were at least +/-30% and 11 years showed

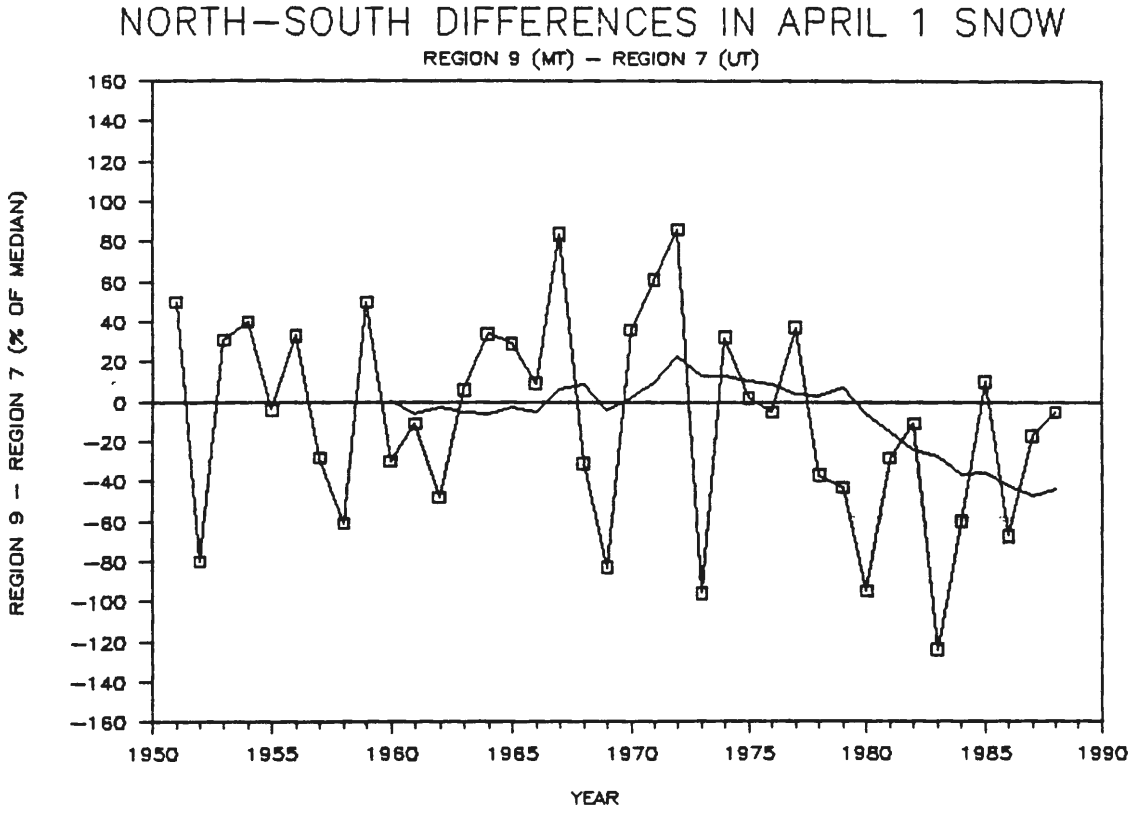

Figure 22. Time series, 1951-1988 and the 10-year running mean, of the differences of SN between region 9 (Montana) and region 7 (Utah). Differences are computed relative to the 1951-1985 median value for each region.

differences of more than 60%. Since 1951, SN in Montana's region 9 exceeded SN in Utah's region 7 (relative to median values) 21 times, and was less than Utah's SN in 17 years. However, beginning in 1978, 10 of the last 11 years were relatively drier in Montana. During this period, regionally averaged SN in region 9 was as much as 47% drier than that in Utah. Next, the causes for the north-south differences will be discussed.

A mean liquid content of SN, based on April 1 values annually averaged from sites within each region, was computed for each region during two periods, 1951-1972 and 1975-1985 (see Table 10). These periods were chosen because they represent the two periods when different types of gradient patterns were occurring as discussed in the previous section. The years 1973-1974 were not used because they were transition years. The regions are listed in a north-to-south order.

Table 10. Mean SN values in each region for two periods and changes from earlier period to later period.

Region	1951-1972 Mean (inches)	1975-1985 Mean (inches)	Change (inches)	Change from 1951-1972 (percent)
1	29.37	25.74	-3.63	-12.4**
4	11.36	10.86	-0.50	- 4.4*
9	12.99	10.04	-2.95	-22.7**
10	9.76	8.92	-0.84	- 8.6*
6	16.84	16.46	-0.38	- 2.3
2	17.76	18.28	+0.52	+ 2.9
5	16.02	15.98	-0.04	- 0.3
3	14.66	14.85	+0.19	+ 1.3
7	13.95	16.36	+2.41	+17.3**
8	16.12	19.47	+3.35	+20.8**
11	6.65	7.62	+0.97	+14.6**

** = significant at the 1% level
* = significant at the 5% level

In the later period, 1975-1985, SN in northern regions decreased while SN in southern regions increased as shown in Table 10. Region 1

decreased 12.4% from the earlier period while region 8 increased 20.8% from the earlier period indicating there was a change north to south of up to 33.2% from the earlier period. This change in the average SN values parallels the period when the years with dry-north/wet-south patterns prevailed. These long-term differences in SN in the northern and southern regions are due to the north-to-south gradient patterns. The north-to-south anomalies are actually controlling the dry or wet conditions that are measured in terms of ten to twenty years. Long-term drought conditions are likely to be due to the persistence of these patterns.

It is impossible to totally interpret these time series, and they offer little predictive skill. The 1951-1985 record length is considered too short to draw significant conclusions. Nevertheless, because the two types of north-to-south gradient years occurred in two different periods helps reveal the involvement of gradient patterns in the long-term (decadal or longer) wet and dry periods for different areas of the study region.

Long-term SN data do not exist for periods before 1935. To test the results based on 35 years a much longer data set was necessary to see if north-to-south gradient patterns and long-term dry and wet periods have persisted before. Several PR stations were considered, however only two stations, Durango, Colorado, located in unstable region 8 of southwestern Colorado, and Coeur d'Alene, Idaho, located in stable region 1 of northern Idaho, were identified as having high-quality data back to the 1910s. The time series of each was plotted on the same graph to identify out-of-phase years that were considered north-to-south gradient patterns (Figure 23). To classify as a north-

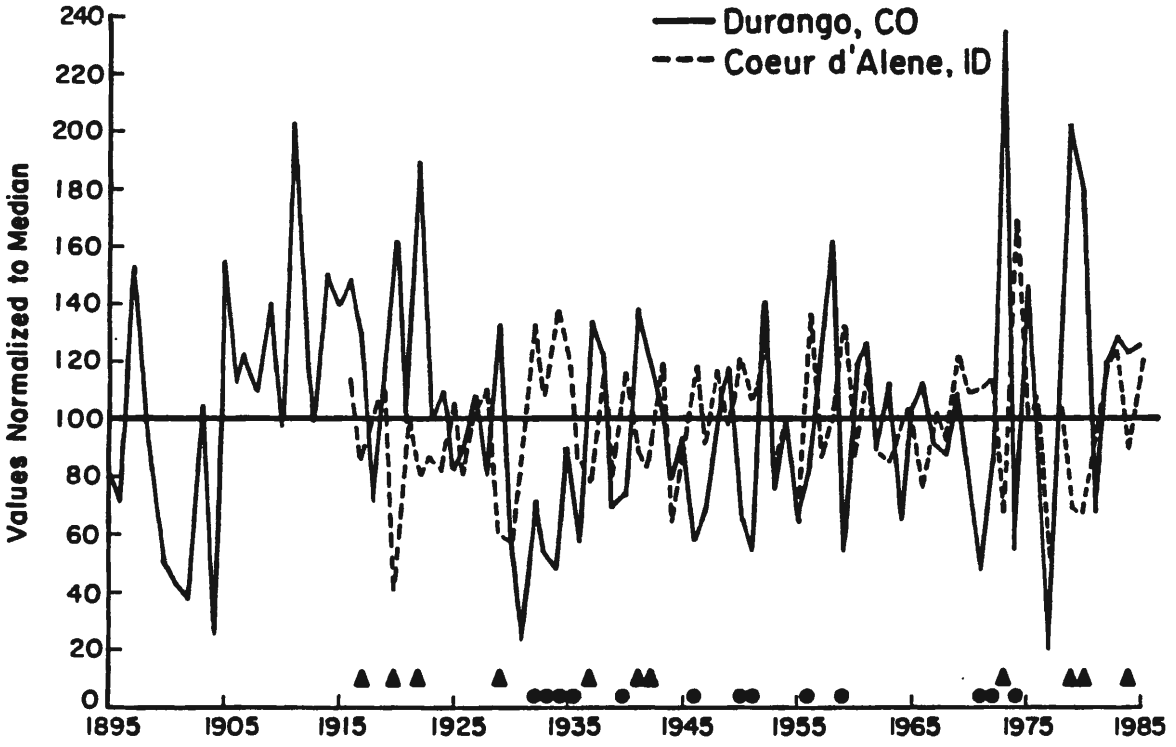

Figure 23. The 1895-1985 time series of two PR stations, Durango, Colorado (dark line) and Coeur d'Alene, Idaho (dashed line). The PR values are normalized to the median for each station (100 equals the median). The dots represent years with a north-wet/south-dry gradient pattern while triangles represent years with a north-dry/south-wet pattern.

to-south gradient pattern the yearly values, normalized to the median, had to be located on opposite sides of the 1.00 line (1.00 represented the median value for each station) and had to have an absolute difference in values of 0.30. North-wet/south-dry patterns existed exclusively in two periods, 1931-1936, and 1946-1972, and are identified with a dot below the years they occurred. North-dry/south-wet patterns occurred from 1916-1924, 1937-1943, and 1975-1985, and are identified with a triangle below the years they occurred. When examining the 10-year running means of the two stations, four distinct long-term periods are identified (Figure 24). For two periods Durango was wetter than Coeur d'Alene, 1916-1930 and 1977-1985 (areas between curves during these periods are stipled). Also, for two periods 1932-1943 and 1947-1960, Coeur d'Alene was wetter than Durango, (areas between curves during these periods are dotted). Other periods did not exhibit long-term, out-of-phase differences. The analysis of the two PR time series and 10-year running means, indicated two things: 1) that long-term wet and dry periods did exist before the 1951-1985 study period, and 2) north-to-south gradient years played a role in making these wet and dry periods for the two stations behave out-of-phase.

These long-term changes in SN and PR may be associated with detectable and potentially predictable large-scale atmospheric and oceanic circulations. It would be very useful for those planning large water projects to have some knowledge regarding the timing and location of these long-term wet and dry periods. Investigation into possible links to large-scale atmospheric/oceanic indices and winter synoptic patterns is continued in Chapters 6 and 7.

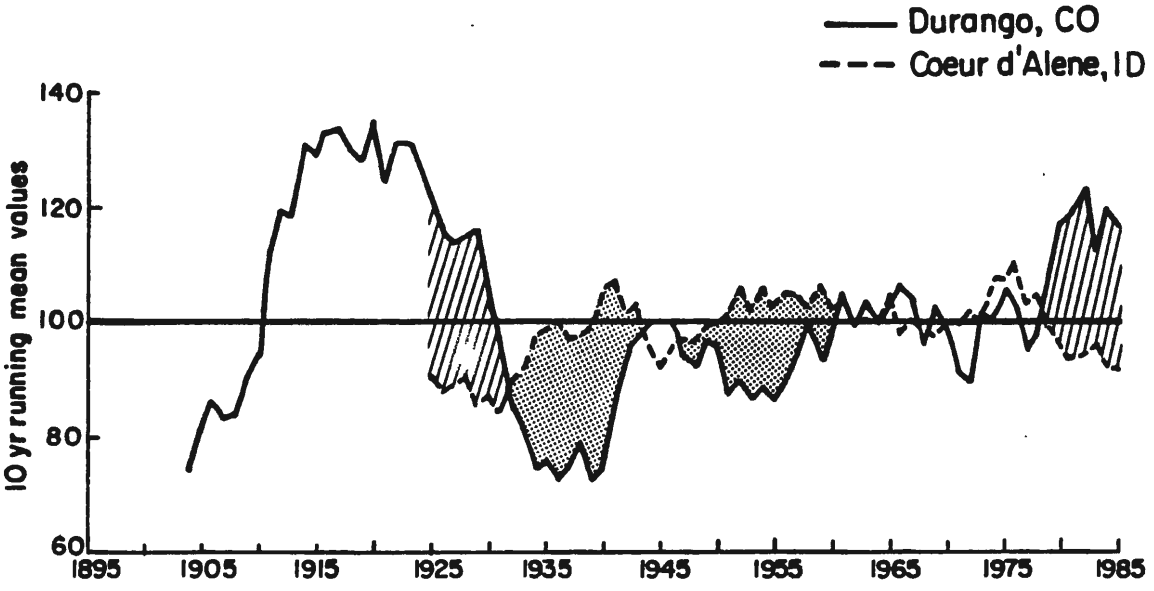

Figure 24. Smoothed time series (10-year running means 1895-1985) of PR for Durango, CO (dark line) and Coeur d'Alene, ID (dashed line). Long periods of years when the Durango is much wetter than Coeur d'Alene are stipled while long periods of years when Coeur d'Alene is much wetter than Durango are colored in with dots.

5. Summary

Assessing objectively analyzed non-exceedence probability SN patterns revealed three basic and oft-repeated patterns: 1) years with a consistent anomaly over the entire region, either wet or dry, 2) years with a distinct north-to-south gradient, and 3) years with average amounts at many sites plus isolated areas of wet and dry throughout the region, labeled as "average". Over the 35-year sample of SN data there were 14 consistent years (6 wet years, 8 dry years), 12 years with a north-to-south gradient, and 9 average years. The relationship of these years to large-scale circulations and winter synoptic patterns is examined in Chapters 6 and 7.

In each of the eleven regions, regionally-averaged SN values were correlated to regionally-averaged PR values for the 1951-1985 period. Strong correlations (r-values $\geq$ +0.71 and significant at 99% level) existed in the three stable regions and the three unstable regions located west of the C.D. and in region 4, located east of the C.D. but located in a stable (low variability) zone with northerly exposure to moist air flow. Unstable regions 9, 10, and 11, all located on the east side of the C.D., have poor (+0.25 to +0.41) correlation coefficients for their regionally-averaged PR and SN values. These results indicate that in areas west of the C.D. both SN and PR data are influenced by the similar precipitation events from year to year, while areas east of the C.D. are influenced by two types of precipitation events that provide 'blow over' precipitation at high elevations and 'upslope' precipitation at low elevations.

The physical explanation for differences in SN variability from one region to another is related to differences in latitude. Based on

the distribution of SN annual patterns from 1951-1985, several features were identified. First, wet, dry, and average/mixed years occurred frequently throughout the 35-year period. Second, wet-north/dry-south gradient years only occurred between 1951-1974, and dry-north/wet-south gradient years occurred only between 1973-1985. The relationship of gradient years to large-scale circulations and winter synoptic patterns is discussed in the next two chapters.

When analyzing ten-year running means of regional SN data, distinct and regionally consistent temporal differences emerged between the northern and southern parts of the five-state region. Based on the t-test statistic, a widespread downturn (significant at the 0.01 level) in SN magnitudes began in the mid 1970s across the northern Rockies. Meanwhile, the southern Rockies, at least until 1985, have experienced a steady and significant (at 0.01 level) increase of nearly 20%. These long-term differences in SN in the northern and southern regions are due to the north-to-south gradient SN patterns. The north-to-south anomalies are actually controlling the dry or wet conditions that are measured in terms of ten or twenty years. An analysis using two PR stations with records dating back to the 1910's identified two things: 1) that long-term (decadal or longer) wet and dry periods did exist before the 1951-1985 study period, and 2) that north-to-south gradient years make these wet and dry periods for the two stations behave out of phase. The relationship of long-term changes in SN to long-term changes in large-scale circulations and winter synoptic patterns is examined in Chapters 6 and 7.

CHAPTER VI

TELECONNECTIONS OF LARGE-SCALE CIRCULATIONS TO SN IN THE ROCKY MOUNTAINS

Long-term records of SN and PR imply that out-of-phase, long-term (decade or longer) wet and dry periods occur in the northern and southern sections of the study region and are due to north-to-south gradient patterns. These long-term changes suggest that shifts in large-scale atmospheric/oceanic patterns exist for several years, and then reverse. Different authors have compared the relationship of temperature, precipitation, and streamflow data in North America to large-scale atmospheric and oceanic circulation patterns (Diaz and Namias, 1983; Meko and Stockton, 1984; Yarnal and Diaz, 1986, Ropelewski and Halpert, 1986 and 1990; Trenberth, 1990). The objective of this research was to discern the physical explanations for the spatial and temporal variability of SN as described in previous chapters and understand the relationship of SN to several large-scale indicators.

The goals of this part of the study are to: 1) describe certain large-scale atmospheric/oceanic circulations that have potential teleconnections to winter hydroclimatic patterns in North America, 2) discuss the association of ENSO and to spatial patterns of SN variability 3) discuss the relationship of seasonal averaged indices of large-scale circulations to SN, 4) identify the annual patterns of SN

using seasonal and monthly averaged indices of large-scale circulations and, 5) compare long-term changes in large-scale atmospheric/oceanic circulations to those in SN and north-to-south gradient patterns.

1. Large-scale atmospheric/oceanic circulations with potential teleconnections to the winter hydroclimatic patterns in North America

Several studies have considered the relationships between large-scale atmospheric/oceanic circulations and hydroclimatic patterns in North America, including those of Namias (1978, 1988), Wallace and Gutzler (1981), Horel and Wallace (1981), Yarnal and Diaz (1986), Ropelewski and Halpert (1986 and 1990), Angell and Korshover (1987), Trenberth (1988, 1990), Lussky (1989), Cayan and Peterson (1990), and Gray (1990). Most studies have concentrated on the relationships of winter indices to winter hydroclimatic anomalies of temperature, precipitation, and/or streamflow in the mid-latitude regions of North America, because these indices are usually more marked and more persistent than summer indices. The objective in past studies was to detect a predictive signal that could be used several months before a forecast period. The indices considered for in-depth analysis in this study included the El Nino-Southern Oscillation (ENSO), the Pacific-North American (PNA) Index, the Summer Monsoon Rainfall in India (SMRI), and the Quasi-Biennial Oscillation (QBO). Because these indices usually develop over an ocean (sometimes thousands of miles away from the area of interest), the potential relationship is called a teleconnection.

The ENSO atmospheric/oceanic phenomena has been well described by many authors (Rasmusson and Carpenter, 1982; Cane, 1983; Rasmusson and Wallace, 1983; Wallace, 1990). The Southern Oscillation Index (SOI), which represents the Tahiti minus Darwin sea-level pressure (SLP), has been strongly correlated ($r > +0.80$) to warm (El Nino) ENSO and cold (La Nina) Non-ENSO water periods in the equatorial Pacific. A negative SOI occurs during an El Nino and is referred to as an ENSO event. On the average, ENSOs occur once every two to four years and generally last approximately 18 to 24 months (Trenberth, 1976; Rasmusson and Carpenter, 1982; Rasmusson and Wallace, 1983). Theories speculate that during these large warm water periods, positive sea-surface temperatures cover a great deal of the equatorial eastern Pacific Ocean. The ocean emits great amounts of heat to the atmosphere. This increased heat is associated with increased cloudiness and rainfall north of the equator in the winter seasons (Figure 25). This increase in local convection as shown in Figure 25 forces Rossby Waves near the equator and sets up a wavetrain of disturbances and teleconnections downstream (Chen and Trenberth, 1988; Trenberth, 1990). Possible teleconnections were studied between the long-term, well-documented SOI, and the equatorial Pacific sea-surface temperature (EQPSST) anomalies, to the subregional SN values in the Rocky Mountains.

The PNA is another winter atmospheric phenomena related to tropical Pacific sea-surface temperature and enhanced convective activity anomalies (Trenberth, 1990; Nitta and Yamada, 1989). A study by Douglas et al. (1982) also considered the relationship of changes in the Northern Pacific to weather patterns in the United States. When a PNA or a non-PNA pattern develops there are four pressure centers, that

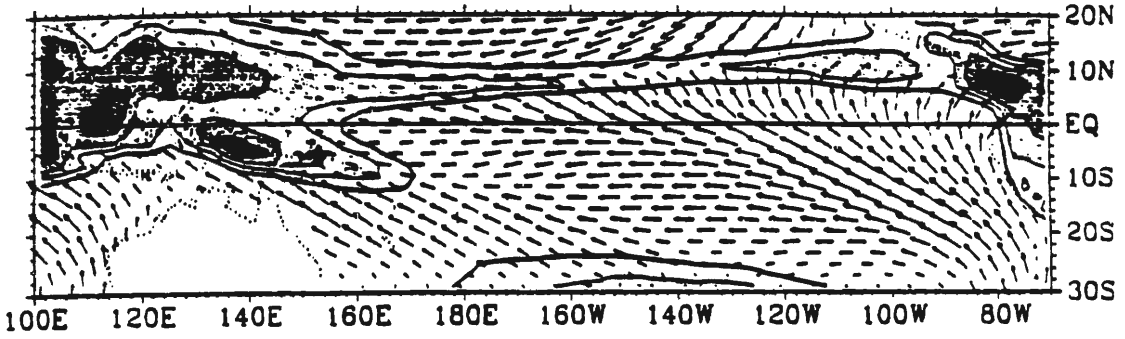

(a)

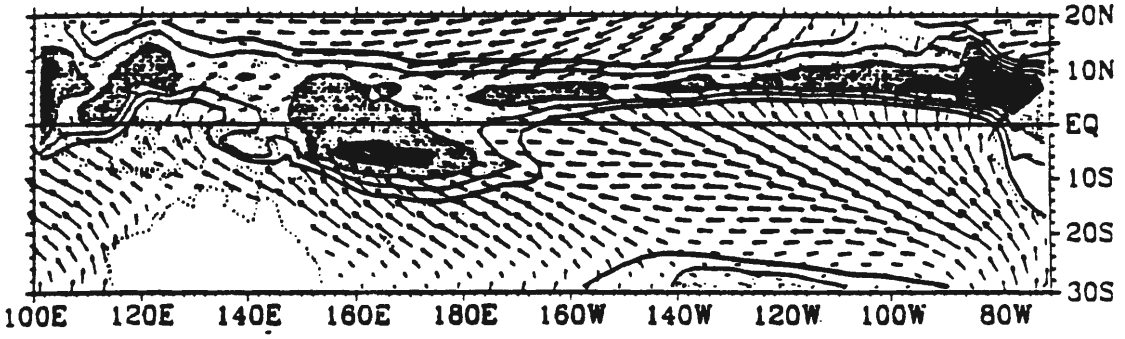

(b)

Figure 25. Outgoing longwave radiation indicated by the contours and shading and surface winds (arrows) during July-November of a a) typical cold year (Non-ENSO) and b) typical warm year (ENSO) in the equatorial Pacific, as deduced from regression analysis of gridded fields from the COADS (a compilation of surface observations from ships of opportunity) upon an SST index defined as July-November SST averaged from the dateline to the South American coast and from 6'N-6'S. Shading indicates areas of heavy cloudiness and precipitation. Figures from Deser and Wallace (1990).

are connected by the dark line with arrows at each end in Figure 26, (one near Hawaii, and one along the west coast of North America of one sign (positive or negative); and two of the opposite sign, one over the North Pacific and one over the southeast United States) that can be identified by sea level pressure (SLP), 700 mb pressure and 500 mb pressure anomalies (Blaising and Lofgren, 1980; Trenberth, 1990). Figure 26 shows the four connected upper air pressure centers that form an arc across the eastern Pacific and North America. The North Pacific sea-level pressure (SLP) represents a PNA index. The North Pacific SLP is highly correlated ($r = +0.92$) with the four teleconnected PNA centers and to the strength and location of the Aleutian Low (Trenberth, 1988 and 1990). Because of the strong correlation of the PNA to the North Pacific SLP index, the SLP index was used to analyze the relationship of PNA to surface SN data in our study.

Summmer Indian monsoon rainfall anomalies were related to the ENSO cycle (Parthasarathy and Pant, 1985; Rasmusson and Arkin, 1990). Furthermore, the combined influence of the Indian monsoon and circulation changes near the Himalayan-Tibetan Plateau complex are seen through teleconnections with the Aleutian Low and North American hydroclimatic elements (Trenberth, 1990). In this study, the rainfall anomalies in the summer Indian Monsoon are considered a predictive index and will be used to consider teleconnections to fall and winter hydroclimatic patterns in North America.

The quasi-biennial oscillation, QBO, is the large-scale circulation phenomenon that comes closest to exhibiting periodic behavior. The oscillation occurs in the mean zonal winds of the equatorial stratosphere (Holton, 1979). Zonally symmetric easterly

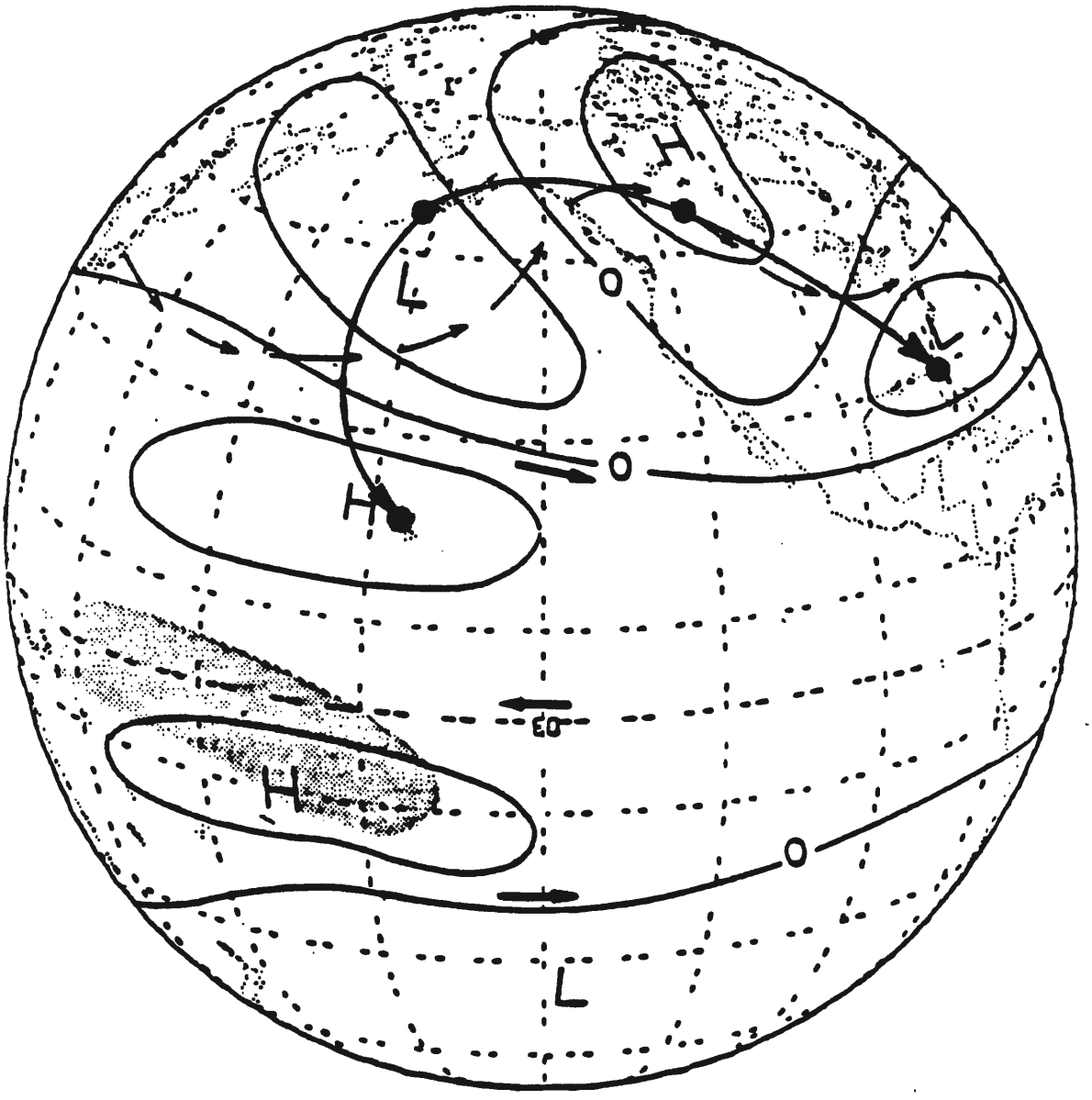

Figure 26. Schematic illustration of middle- and upper-troposphere pressure anomalies during a Northern Hemisphere winter with a PNA pattern occurring. Figure from Horel and Wallace (1981).

and westerly wind regimes located between 20 and 70 mb alternate regularly with a period varying from 24 to 30 months. The oscillation is located symmetrically over the equator. The QBO has been found to influence the summer hurricane season in the Atlantic Ocean (Gray, 1990). Whether or not it will be related to winter mid-latitude snowpack patterns is determined. In this study the QBO is represented as the October - March average wind speed at 50 mb.

Note that these large scale atmospheric/oceanic phenomena are apparently related to changes that are initiated in the tropics (Trenberth, 1988). Persistent oceanic anomalies are slow to change here from month to month, and they are strongly related to atmospheric pressure and temperature anomalies. Because these oceanic anomalies are persistent over a long period makes them good potential indicators of the future weather. How well these seasonally averaged large-scale indices correlate to SN is analyzed in the next section.

2. Association of ENSO to spatial patterns of variability

Based on the results of Chapter 4 spatial patterns of SN variability (stable and unstable) were identified across the five-state region. In the analysis that follows the objective was to determine what association ENSO events have with the spatial variability of SN. Eleven warm ENSO events, based on seasonally averaged SOI's, occurred during the 1951-1985 period (Quinn et al., 1978). The eleven ENSO events ranged in strength (based on size of the average SOI anomaly) from: 1) very weak in 1963/64 and 1975/76, 2) weak in 1951/52 and 1969/70, 3) moderate in 1953/54, 1965/66, 1976/77, and 1983/84, and 4) strong in 1957/58, 1972/73, and 1982/83. To understand the

relationship of the ENSO years to SN values at 275 SN sites, the SN values that occurred during the 24 non-ENSO years were averaged at the 275 SN sites.

$$\text{Non-ENSO Average Value} = NEN_{ave} = \frac{\sum Y_{\text{Non-El Nino}}}{24} \qquad (16)$$

where Y = annual SN value

Then the 11 ENSO years were averaged at the 275 SN sites.

$$\text{ENSO Average Value} = EN_{ave} = \frac{\sum Y_{\text{El Nino}}}{11} \qquad (17)$$

At each site the Non-ENSO average value based on 24 years would be divided by the ENSO average value based on 11 years to form the 'ENSO SN ratio'.

$$\text{ENSO SN ratio} = EN_{SN} \text{ ratio} = \frac{NEN_{ave}}{EN_{ave}} \qquad (18)$$

The values of the EN_{SN} ratio were plotted for each site across the five-state region and EN_{SN} ratio isolines drawn (Figure 27). Ratios below 1.00 indicated that, on the average, ENSO years were wetter than non-ENSO years at these sites, while values larger than 1.00 implied that, on the average, ENSO years were drier than non-ENSO years. The range in the EN_{SN} ratios for the sites was 0.79 to 1.33 across the region. A few important features can be noted from Figure 27. Areas in southwest Idaho, southwest Utah and southwest Colorado had EN_{SN} ratios smaller than 1.00 indicating that they were wetter than average during ENSO years. A broad region from northwestern Idaho through

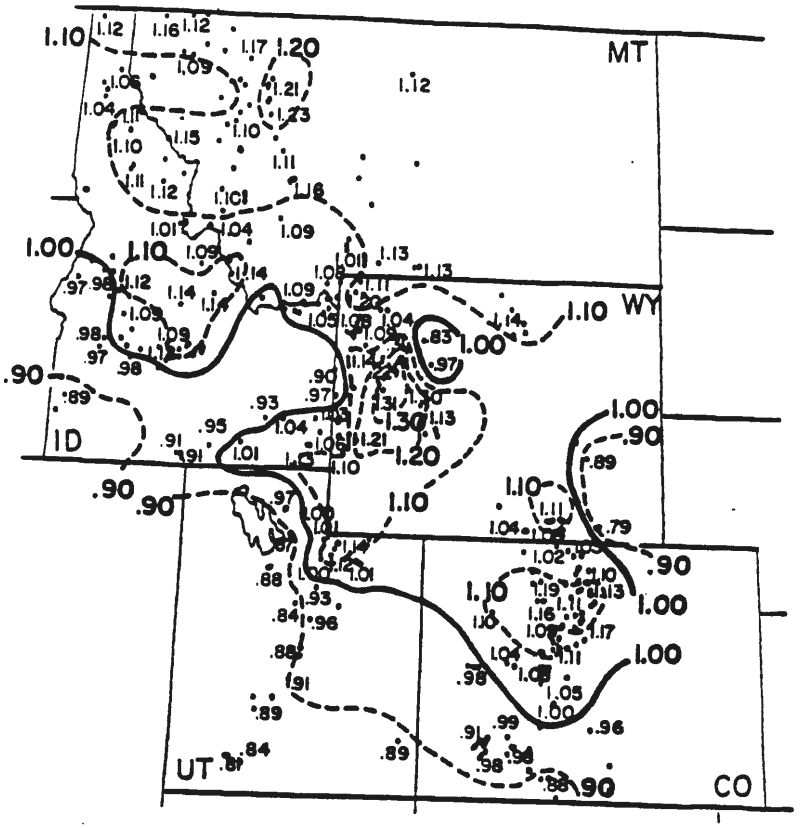

Figure 27. EN_{SN} ratios are plotted for SN sites in the five state region. EN_{SN} is defined as NEN_{ave} (24 years) divided by EN_{ave} (11 years). Ratio isolines are drawn. A EN_{SN} ratio of 1.00 indicates that SN in ENSO years equals SN in non-ENSO years. A EN_{SN} ratio greater than 1.00 indicates areas where the SN is greater during non-ENSO years.

western Wyoming into the north and central parts of Colorado had EN_{SN} ratios above 1.00 indicating that they were drier on average during ENSO years. The pattern of EN_{SN} ratios is similar to the pattern of ratios Redmond and Koch (1988) identified using October through March precipitation data averaged from a number of climatic districts in the Western United States.

The significant new findings based on the pattern of EN_{SN} ratios shown in Figure 27 is that areas of <1.00 and >1.00 are associated with the spatial patterns of SN variability described in Chapter 4. Based on the measure of variability regions of stable (low variability) and unstable (high variability) were identified (Figure 10a, Chapter 4). From Figure 27 the SN sites located in unstable regions 6,7, and 8 west of the C.D., exposed to southwesterly air flow were generally wetter during ENSO years (EN_{SN} ratios below 1.00). The SN sites located in the five stable regions, 1 through 5, exposed to westerly to northerly air flow were generally drier (EN_{SN} ratios greater than 1.00). The sites located in unstable regions 9, 10, and 11, east of the C.D., exposed to easterly air flow were generally drier during ENSO years in regions 9 and 10, while region 11 in Colorado had ratios that were both above and below 1.00. These differences in EN_{SN} ratios across the five-state area, especially west of the C.D., suggest that different regions characterized by different magnitudes of variability can perhaps be explained by atmospheric circulation patterns, such as those associated with ENSO events. During ENSO events the mean upper air wind flow patterns are altered (providing more potential precipitation opportunities associated with southwesterly flow aloft) so that during many precipitation events greater precipitation occurs in regions

exposed to south or southwesterly flow. Descriptions of similar upper air flow characteristics that occur during ENSO events are discussed in a study by Cayan and Peterson (1990), see Figure 28, whose work identified streamflow anomalies associated with the different air flow during ENSO events. During ENSO years, areas in the southwestern U.S. experienced positive (high) streamflow anomalies associated with southwesterly flow aloft, while areas in the northern part of the Rockies experienced negative (low) anomalies associated with being located south of the Polar Jet in a large ridge. Cayan and Peterson did not consider how the air flows affected the magnitude of variability across the Rockies.

To confirm the results based on site data, a similar analysis that averaged the SN site data each year, within each of the 11 regions (described in Chapter 4). As with the SN sites a NEN_{ave} was calculated using the regionally averaged data from 24 non-ENSO years. Also, a EN_{ave} was calculated using the regionally averaged data from the 11 ENSO years. A regional EN_{SN} ratio was then computed by dividing NEN_{ave} with EN_{ave}, see Table 11 and Figure 29.

Table 11. Regionally averaged NEN_{ave}, EN_{ave}, and EN_{SN} ratios. Regions are listed from north to south through five states.

Region	NEN_{ave} (inches)	EN_{ave} (inches)	EN_{SN} Ratio
1	29.02	26.59	1.09
4	11.43	10.73	1.07
9	12.51	10.55	1.19
6	16.80	16.97	0.99
2	18.82	17.89	1.05
10	9.74	8.90	1.09
5	16.34	15.56	1.05
3	15.26	14.22	1.07
7	13.93	15.70	0.89
8	17.02	17.86	0.95
11	6.90	7.25	0.95

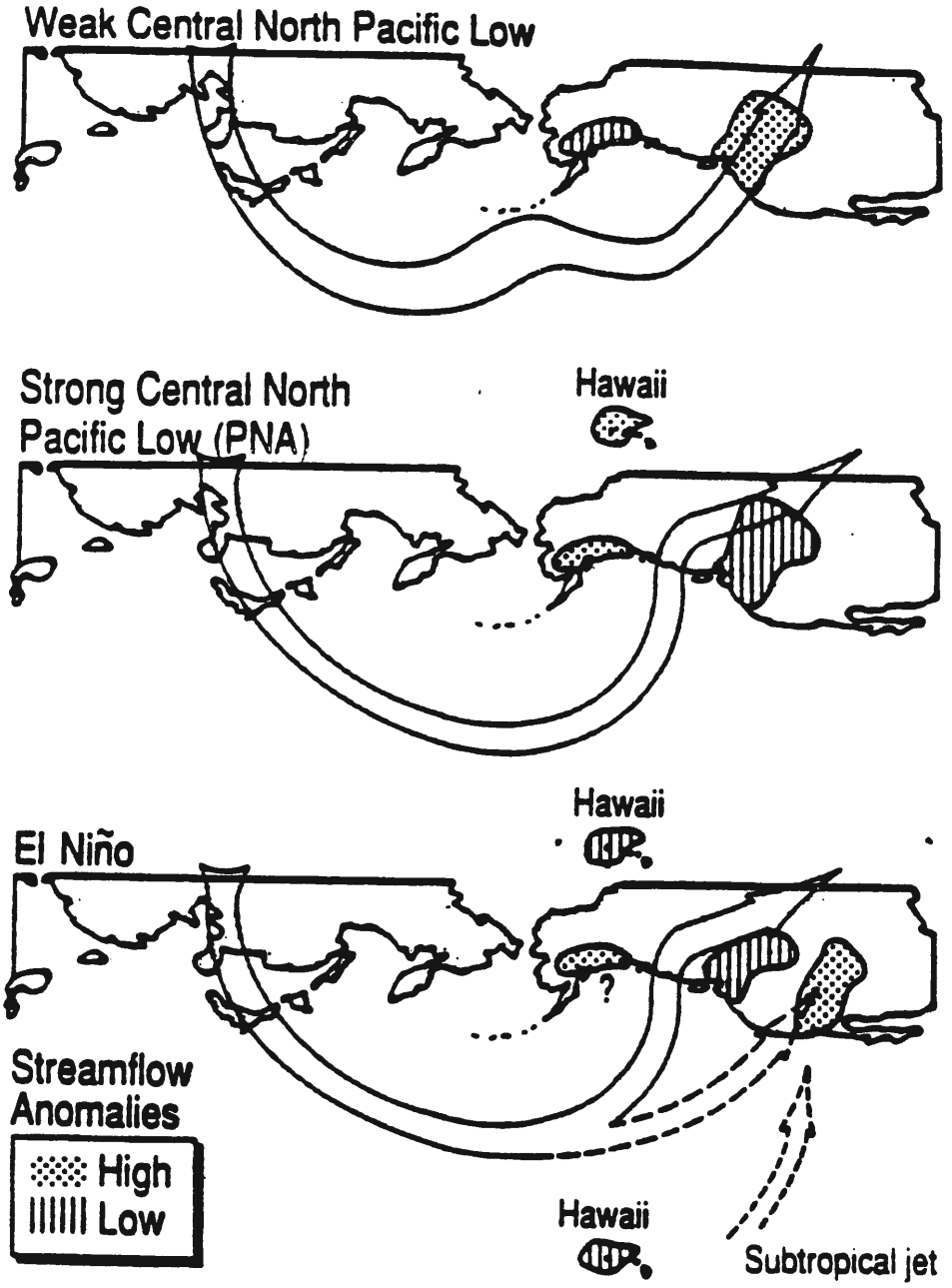

Figure 28. Location of the Polar and Subtropical Jets across the Pacific Ocean and western United States and streamflow anomalies in the western U.S. during a) a winter with a non-PNA pattern, b) a winter with a PNA pattern, and c) a winter with an ENSO event. Figure from Cayan and Peterson (1990).

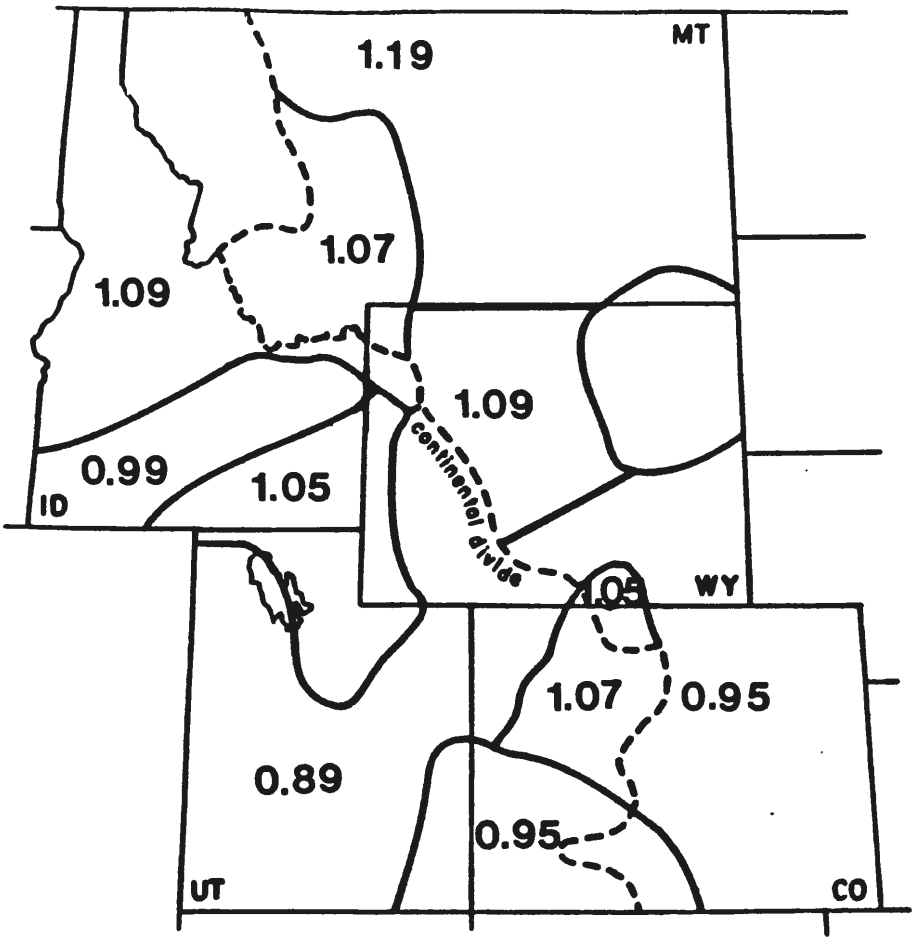

Figure 29. Regionally averaged EN_{SN} ratios. A EN_{SN} ratio greater than 1.00 indicates areas where the SN is greater during non-ENSO years (see also Table 11).

Figure 29 shows that regionally averaged data in unstable regions 6, 7, and 8 have EN_{SN} ratios that are below 1.00 indicating these regions are wetter on average during ENSO years. The opposite is true in the five stable regions. The regionally averaged data in unstable regions 9, 10, and 11 have EN_{SN} ratios that range from above 1.00 in region 9 to below 1.00 in region 11. This analysis indicates, as did the site analysis, that regions exposed to south or southwesterly flow (unstable regions west of the C.D.) have greater precipitation during ENSO years, while regions exposed to westerly to northerly flow (stable regions) have less precipitation during ENSO years. The possible explanation for the ratios that increase from south-to-north in the three unstable regions east of the C.D. is appearantly associated with how near each region is to the location of the southwesterly flow aloft associated with the Subtropical Jet (Figure 28) during ENSO events. Eastern unstable regions that are south and are closer to the upper-level airflow during ENSO events are apparently wetter, while those that are north and farther away from the influence of the upper-level airflow during ENSO events are drier. The association between ENSO events and spatial patterns of SN variability are possibly identified through these analyses. Understanding that stable and unstable regions, especially those that are west of the C.D. which have the greatest impact on the water resources of the West, are affected differently by large-scale circulation patterns such as ENSO represents an important predictive tool for water managers of large reservoir systems.

3. Relationship of seasonal averaged indices of large-scale circulations to SN

Several studies have examined the relationship of large-scale atmospheric/oceanic circulations to temperature, precipitation, and streamflow data in North America. However, no studies have analyzed the relationship of these anomalous circulations to snowpack data. The SN sites are located in an elevation zone of the Rocky Mountains that produces 85% (Grant and Kahan, 1974) of the total runoff for streamflow each year. Because this study's interests focus on the hydroclimatic variability of this region, it's logical that any relationships to large-scale circulations be compared with SN data.

Seasonally averaged indices of large-scale atmospheric circulations influenced by persistent oceanic anomalies generally show little variability in monthly data (Rasmusson and Carpenter, 1982; Rasmusson and Wallace, 1983). Therefore, averaged seasonal indices computed for different periods before and/or during the winter season could be correlated with SN to identify which period was the best related to SN. Initially, the SOI was related to SN for the period 1951-1985.

Historic monthly Southern Oscillation Index (SOI) values were available (written communication with Roy Koch, 1989) for our study. Six different averaged SOI periods were then related to regionally averaged SN data for each of the 11 subregions. These 11 subregions were identified by differences in the magnitude of variability (see previous chapters for details). Months that preceded the winter period (October - March) were designated with a (-1) and those during the period of interest a (0). The six SOI averaged periods were:

1. Jan.(-1) to Dec.(0)
2. Apr.(-1) to Sep.(-1)
3. Apr.(-1) to Mar.(0)
4. Jul.(-1) to Sep.(-1)
5. Jul.(-1) to Dec.(0)
6. Oct.(0) to Mar.(0)

The results of the regressional analysis are shown in Figures 30a-f. The correlation coefficient equation described in Chapter 3 was used to compute r-values. Averaged periods 3, 4, and 6 had the best correlations with the April 1 snowpack. Only region 10 had moderate correlations (+0.5 < r-value < +0.8) between the averaged SOI and SN, and the highest correlation explained only 30% of the variance. All other regions had weak (-0.5 < r-values < +0.5) correlations. Nevertheless, r-values greater than +0.29 or less than -0.29 were significant to the 5% level, while r-values greater than +0.40 or less than -0.40 were significant to 1% based on 35 years of data.

The pronounced shift from positive correlations in the northern regions to negative correlations in the southern regions indicates that SN distribution in northern and southern regions are influenced in different ways by ENSO events. The results of the correlation of Oct.(0) to Mar.(0) averaged SOI period to regional SN indicate that unstable regions on the west side of the C.D. were negatively correlated with the SOI (wetter during winters with ENSO events than winters with non-ENSO events), while the five stable regions were positively correlated with the SOI (drier during winters with ENSO events than winters with non-ENSO events). The results of the correlations discussed here agree with discussions from the previous

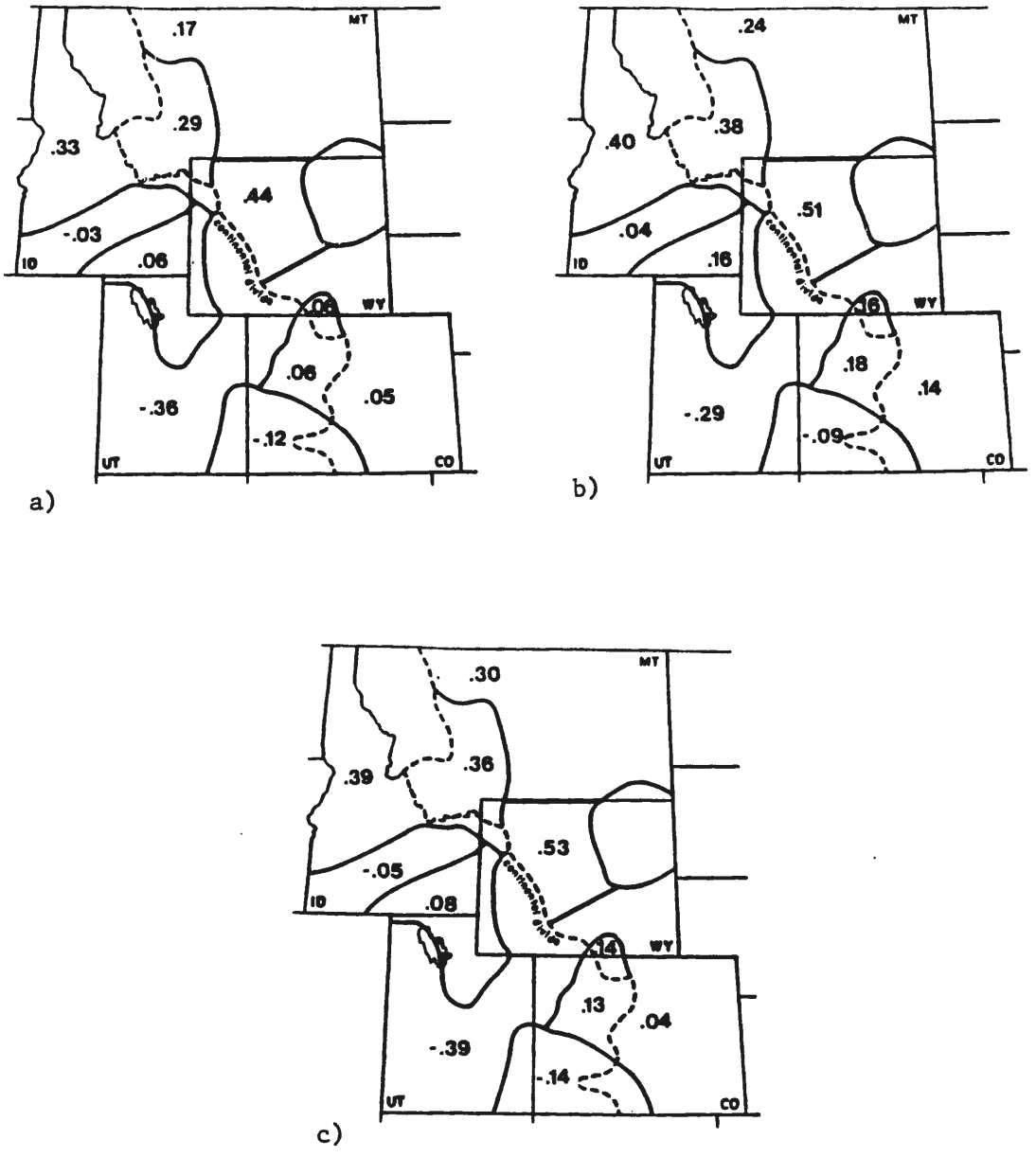

Figure 30. Correlation coefficients for regionally averaged normalized SN data to averaged SOI periods: a) Jan.(-1) to Dec.(0), b) Apr.(-1) to Sep.(-1), and c) Apr.(-1) to Mar.(0). Correlation coefficients are based on data from 1951-1985.

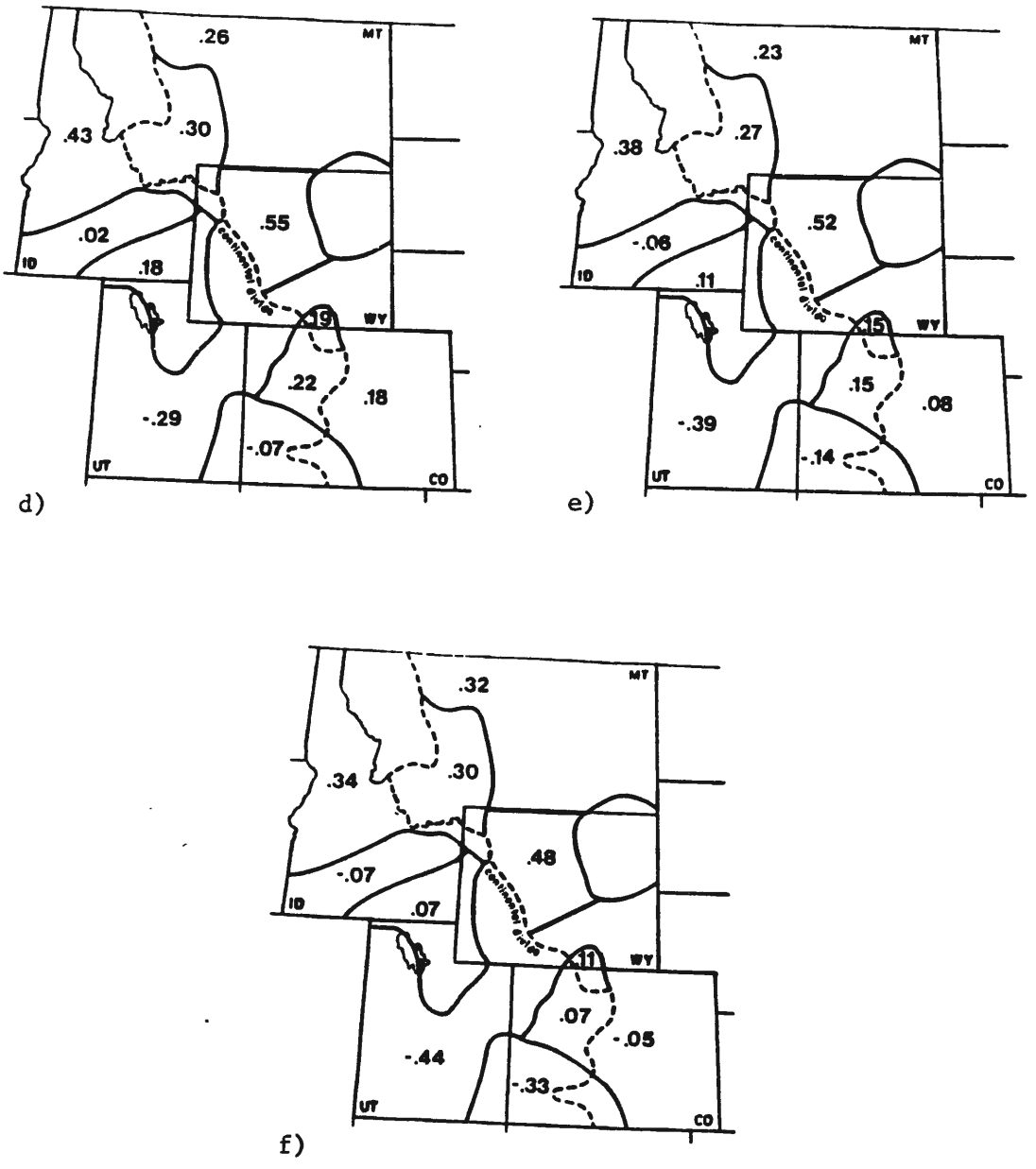

Figure 30. Correlation coefficients for regionally averaged normalized SN data to averaged SOI periods: d) Jul.(-1) to Sep.(-1), e) Jul.(-1) to Dec.(0), and f) Oct.(0) to Mar.(0). Correlation coefficients are based on data from 1951-1985.

section. Stable and unstable regions (described in Chapter 4) located west of the C.D. are influenced differently by the presence or non-presence of an ENSO event. This implies that although there is low skill large-scale circulation patterns that occur over North America are altered during years when ENSO events occur and this suggests that ENSO should be used to predict SN anomalies in the Rockies. Descriptions of air flow changes that occur during ENSO events are discussed in a study by Cayan and Peterson (1990). Figure 28 shows how the Polar jet stream splits over the eastern Pacific and combines with the Subtropical jet stream to produce high streamflow anomalies over the southwestern U.S., while the northern Rockies, located under a ridge, experience below average streamflows.

The correlation of the seasonally averaged EQPSST [July(-1) to Nov(0)] to regionally averaged SN indicated results similar to those when comparing the SOI to SN. The r-values were generally poor (+0.5 > r-values > -0.5) for all regions but region 10 (r = -0.53). However, the r-values in the northern regions were negative while those in the southern region were positive. The r-value signs were opposite of the SOI to SN correlations because during ENSO events the SOI is negative and the EQPSST index is positive. Furthermore, it is not surprising that the absolute values of the correlations using the two indices were similar, since the SOI and EQPSST are highly correlated (Wallace,1990).

The correlation of the seasonally averaged (November-March) North Pacific SLP (an index of the PNA) to the regionally averaged SN also had values similar to those of the SOI and EQPSST index as correlated to SN (Figure 31). Figure 31 shows that the r-values of SLP to SN were more positive (r = +0.51) than the SOI in the northern region, numbered

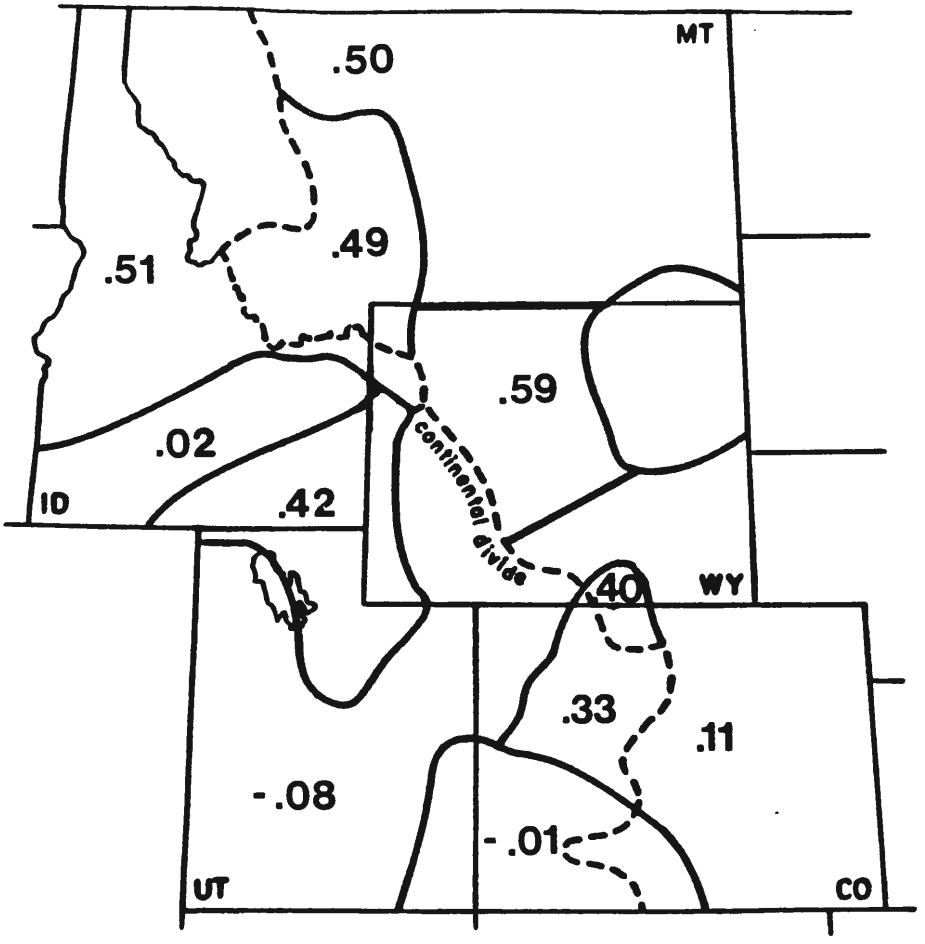

Figure 31. Correlation coefficients for regionally averaged normalized SN data to averaged November-March North Pacific sea-level pressure (an index of PNA). Correlation coefficients are based on data from 1951-1985.

1, and less negative (r = -0.08) in region 7, located in southern Utah. Similar to the SOI pattern of correlations, the r-values are positive in the northern subregions while they are negative in the south. This suggests major shifts in the average large-scale circulations affecting different subregions during PNA and non-PNA years. Descriptions of upper air flow characteristics associated with PNA and non-PNA years are discussed in Cayan and Peterson (1990). Figure 28 shows that during PNA years, when a strong central North Pacific Low exists, the northern regions of the five-state study area are under a strong upper level ridge producing below-average streamflow anomalies. This upper air pattern is similar to when ENSO events occur except the Polar jet does not split over the eastern Pacific and the Subtropical jet does not influence the southwestern U.S. During non-PNA years, when a weak central North Pacific Low exists, a long-wave trough exists over the eastern Pacific and the northwestern U.S. producing above-average streamflow anomalies over the northern regions of the five-state study region. In the next section, seasonal averaged indices of ENSO, EQPSST, and PNA will be used to identify annual SN patterns.

The QBO has been identified as having an association with hurricane forecasts in the Atlantic Ocean (Gray, 1990). In this study the QBO, defined as the October - March average 50 mb winds were related to regionally averaged SN in the five-state region. Westerly zonal 50 mb winds were positive while easterly zonal 50 mb winds were negative. The relationship of QBO to SN was identified as weaker than the relationships of ENSO and PNA to SN, see Figure 32. The r-values range from -0.17 to 0.24 across the five-state region. These poor correlations apparently indicate that the QBO is not well related to

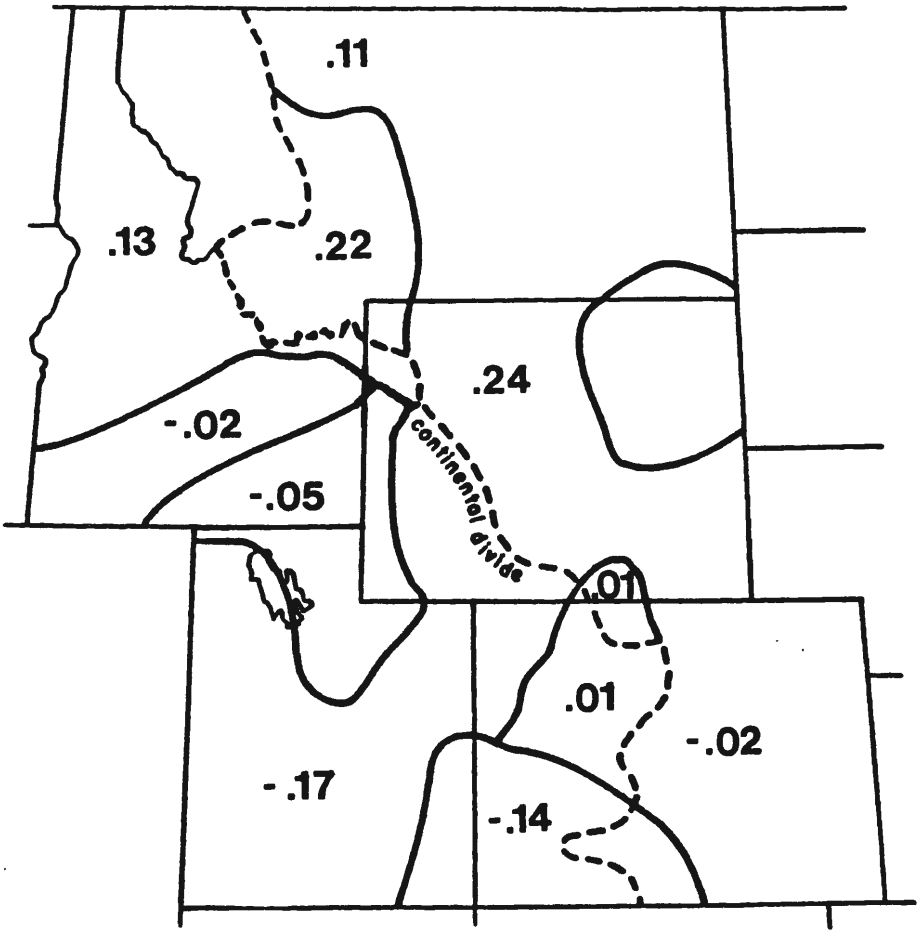

Figure 32. Correlation coefficients for regionally averaged normalized SN data to averaged October-March 50 mb zonal equatorial winds associated with the Quasi-Biennial Oscillation. Correlation coefficients are based on data from 1951-1985.

midlatitude winter SN anomalies in North America. Because of its poor relationship to SN, further analysis of QBO was not pursued.

The least promising indicator of SN is the summer monsoon rainfall for India (SMRI) anomalies. The correlation coefficients between SMRI and regional SN were all weak (-0.10 to +0.15), and no north-to-south change in sign was identified. Because of its poor correlations to SN, further analysis of the SMRI was not pursued.

The weak to moderate correlations based on the relationship of the seasonal averaged indicies of ENSO, EQPSST, PNA, and SMRI with SN may result because a single-area average of the mean seasonal circulation is too simplistic to identify interannual variations in time or space (Cayan and Peterson, 1990). Although the correlation coefficients were not high, they still provide useful information for those making streamflow forecasts. The correlation coefficients suggests that there is a relationship between large-scale circulations and spatial patterns of SN variability. Other variables associated with the larger global ocean/climate system must explain more of the interannual variance.

4. Identification of annual patterns of SN using seasonal and monthly averaged indices of large-scale circulations

The time series of SOI, EQPSST, PNA's Northern Pacific SLP index were used to identify which of three annual SN patterns, as described in the previous chapter, were easily detected (Figure 33). This analysis was undertaken to see if large-scale indices could identify the temporal variability of SN in northern and southern regions during years with pronounced SN anomalies. The large-scale index data used for comparison of large-scale indices to SN patterns came from three

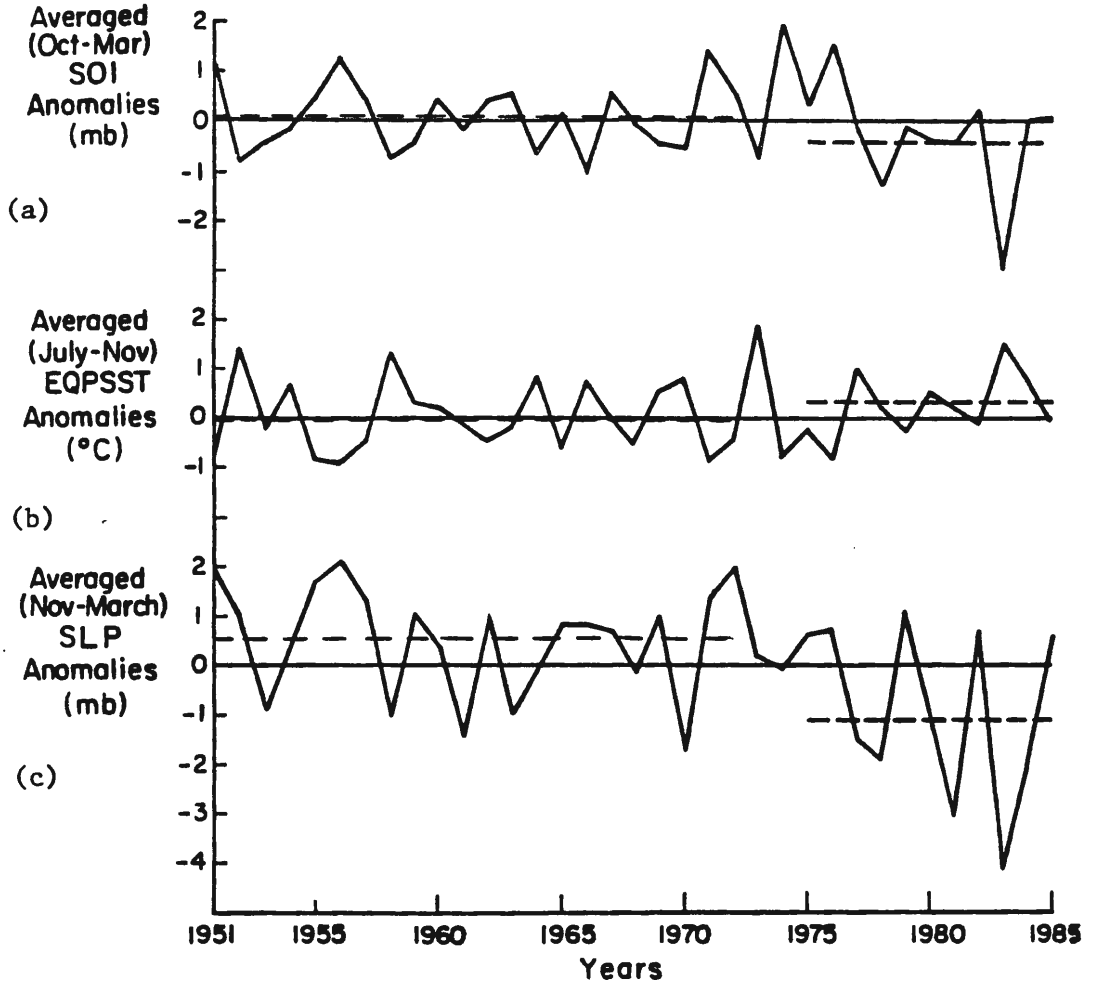

Figure 33. Time series for a) the averaged October-March SOI anomalies (mb), b) the averaged July-November EQPSST anomalies (^{o}C), and c) the averaged November-March North Pacific SLP anomalies (mb) from 1951-1985. Each zero line represents the 35-year average for each large-scale index. The dashed lines for each time series represent two periods when anomalies were averaged, 1951-1972 (period with only north-wet/south-dry gradient patterns) and 1975-1985 (period with only north-dry/south-wet gradient patterns).

sources. The SOI data was presented in a table of monthly values by Redmond and Koch (1988). The EQPSST values were taken from a time series graph of SST anomalies drawn by Deser shown in a paper by Wallace (1990). The North Pacific SLP values were also taken from a time series graph shown in a paper by Trenberth (1990). Figure 33 shows large interannual variations for the three large-scale indices similar to the interannual variations shown for SN, PR, and ST in Figure 5 of Chapter 3.

By ignoring the nine years having average SN patterns (described earlier in the study) 26 years were used to judge how accurately the seasonally averaged large-scale indices predicted annual wet, dry, and north-to-south gradient anomalies in the northern and southern parts of the study region. A correctly predicted annual pattern occurred when the index for that year was identified as either above or below the long-term (1951-1985) index average depending on what type of anomaly the SN pattern represented. For example, in the case of the SOI, wet everywhere and north-wet/south-dry patterns for region 1, in the northern part of the five-state region, should have the index above the long-term average, whereas dry everywhere and north-dry/south-wet patterns for region 1 should have the index below the long-term average. The seasonally averaged [Oct.(0) to Mar.(0)] SOI predicted 18 of the 26 (69%) SN patterns, based on SN anomalies in regions 1 and 7 correctly; the seasonally averaged [July(-1) to Nov.(0)] EQPSST index predicted 16 of the 26 (62%) SN patterns correctly; and the seasonally averaged [Nov.(0) to Mar.(0)] SLP index predicted 20 of the 26 (77%) SN patterns correctly (Table 12).

Table 12. Identifying annual SN patterns, except years with average patterns, using averaged large-scale indices. Y = SN pattern identified by index, N = SN pattern not identified by index.

Year	SN Pattern	Seasonally Averaged SOI	Seasonally Averaged EQPSST	Seasonally Averaged PNA	Seasonally Averaged 700mb	Monthly Averaged 700mb
1951	NW/SD	Y	Y	Y	-	-
1952	WET	N	N	Y	-	-
1953	DRY	Y	N	Y	-	-
1954	NW/SD	N	N	Y	-	-
1955	DRY	N	N	N	-	-
1956	NW/SD	Y	Y	Y	-	-
1960	DRY	N	Y	N	N	N
1961	DRY	Y	N	Y	Y	Y
1962	WET	Y	Y	Y	Y	Y
1963	DRY	N	N	Y	Y	Y
1964	NW/SD	N	N	Y	Y	Y
1965	WET	Y	Y	Y	N	N
1966	DRY	Y	Y	N	Y	Y
1967	NW/SD	Y	N	Y	Y	Y
1969	WET	N	N	Y	N	Y
1971	NW/SD	Y	Y	Y	N	N
1972	NW/SD	Y	Y	Y	Y	Y
1973	ND/SW	Y	Y	N	N	Y
1974	NW/SD	Y	Y	N	N	Y
1975	WET	Y	Y	Y	N	N
1977	DRY	Y	Y	Y	Y	Y
1979	ND/SW	Y	N	N	Y	Y
1980	ND/SW	Y	Y	Y	Y	Y
1981	DRY	Y	Y	Y	Y	Y
1982	WET	Y	Y	Y	Y	Y
1984	ND/SW	N	Y	Y	Y	Y
PART OF TOTAL -		18/26	16/26	20/26	13/20	16/20
PERCENT -		69%	62%	77%	65%	80%

NW/SD = North-wet/south-dry gradient pattern
ND/SW = North-dry/south-wet gradient pattern

Data from three National Weather Service rawinsonde stations located in or near the study region were analyzed to identify direct ties between winter seasonally-averaged upper air data, during the winter of interest, to that of SN patterns (Diaz and Namias, 1983; Cayan and Roads, 1984; Klein and Kline, 1984; Yarnal, 1985). If a

relationship existed it would not offer a predictive index for SN, but instead help explain the SN pattern.

Published averaged monthly data for the months of October through March were averaged over the six months to form a seasonal index for the three sites: Spokane, WA (1964-1985); Boise, ID, and Grand Junction, CO (1958-1985). The monthly averaged data chosen for analyses included geopotential heights, dew-point depression, and wind direction and speed from both the 700 mb and 500 mb levels. The monthly and seasonally averaged 700 mb zonal wind data identified only wet and dry years, because the zonal wind anomalies for each year from 1958-1985 were the same, either all positive or all negative, for the three rawinsonde stations. In the second analysis, the median of the 700 mb height and 700 mb dew-point depression values were identified; then the anomaly was computed for each month and the six anomalies averaged for each winter (Oct.-March) season. After excluding the average years from the 1958-1985 period, seasonally averaged 700 mb height and dew-point depression anomalies from the three sites identified 13 of the 20 patterns (65%) (Table 12). As seen in Table 12 this percent is located at the lower end of the range of percents when compared to the other seasonally averaged large-scale indices.

In the next analysis, 28 years (1958-1985) of monthly 700 mb height and dew-point depression values for each month from October through March were ranked. The lowest monthly value was ranked 1 and the highest monthly value was ranked 28. Each monthly height and dew-point depression value for the 28 years were given a probability based on its rank. For each winter season the six monthly probabilities were averaged to produce a seasonal probability value for the height and

dew-point depression data sets. Also, because the correlation of seasonally averaged height to dew-point depression was strong (r = +0.81) through 28 years, the two seasonal probabilities were averaged for each site. Sixteen of 20 patterns (80%) were identified based on the seasonally averaged monthly probability values at the three sites (Table 12). This percent implies that monthly 700 mb height and dew point depression data identify annual SN patterns better than do seasonally averaged 700 mb indices.

The important finding from the comparisons of annual SN patterns (not including years with average patterns) with seasonal averaged large-scale circulation indices is that the seasonally averaged North Pacific SLP index identifies 20 of 26 (77%) of the annual SN patterns. Based on monthly data from three rawinsonde sites located in the five-state region, monthly probabilities of 700 mb height and dew-point depression were computed and averaged into a seasonal probability that identified 16 of the 20 (80%) annual SN patterns or 15% more patterns than did the seasonally averaged 700 mb anomalies during a period from 1958-1985. The monthly probabilities of 700 mb height and dew-point depression only identified 3% more annual SN patterns than did the seasonally averaged North Pacific SLP index, indicating that bringing the averaging period down to the month improves forecasting of SN patterns in the Rockies by a small amount. Based on these results seasonal and monthly averaged indices should be used in identifying SN patterns across the northern Rockies. A daily analysis of 700 mb height and dew-point depression data may identify a greater number of annual SN patterns than monthly averaged data. A paper by Esbensen (1988) suggested that the spatial patterns of interannual fluctuations

were identified in upper air data only when tropical signals such as the SOI have been correlated with mid-latitude monthly anomalies (Horel and Wallace, 1981), or when extreme events having an interannual frequency of occurrence have been used as an index (Rasmussen, 1968; van Loon and Rogers, 1978). Two dynamic mechanisms control the annual SN patterns across the region, one seasonal (ENSO and PNA) and the other on the scale of events to months (700 mb height and dew-point depression anomalies). Because the seasonally averaged North Pacific SLP index identified 77% of the annual (non-average) SN patterns, further investigation and analyses using the monthly PNA-related SLP index values could improve the understanding and predicting of interannual hydroclimatic variability in the Rockies.

5. Comparison of long-term changes in large scale atmospheric/oceanic circulations to those in SN and north-to-south gradient patterns

The importance of long-term (decadal or longer) dry and wet periods to the water resources of the Western United States creates a need to understand the interannual variations in the hydroclimatic elements during these periods. Drought conditions in northern Idaho and western Montana that have persisted for most of the last 10 to 15 years have created critical water supply problems. Conversely, areas in Colorado and Utah experienced late spring river flooding, near catastrophic dam collapse, and all time high levels of the Great Salt Lake as a result of several above-average snowpack years. SN and PR data analyzed in the previous chapter indicated that interdecadal wet and dry periods existed back to the 1910s and were largely out-of-phase with one another in the northern and southern regions of study area.

These periods when the northern and southern regions were out-of-phase are due to north-to-south gradient patterns. As large scale atmospheric/oceanic circulations have become better documented, the capability of understanding what causes these regional extreme periods has increased (Gray, 1990; Hastenrath, 1990). The objective of this analysis was to distinguish long-term ties between the identified long-term SN characteristics and features of large-scale atmospheric/oceanic circulations.

Three long-term, large-scale atmospheric/oceanic circulation indices, the SOI, the EQPSST index, and the PNA North Pacific SLP index, were investigated to identify possible relationships with the long-term changes in SN and north-to-south gradient patterns across the five-state region. The data used to generate Table 13 came from three sources described in the previous section. The two periods, 1951-1972 and 1975-1985, were chosen because they represent the two periods when different types of north-to-south gradient patterns occurred (see Chapter 5).

Table 13. Changes in the average value of large-scale indices from an earlier period to a later one.

Index	Mean/Standard Deviation 1951-1972	Mean/Standard Deviation 1975-1985	Change in Mean
Oct.-March SOI	0 mb/ 0.68 mb	-0.4 mb/ 1.10 mb	-0.4 mb*
July-Nov. EQPSST	0°C/ 0.70 C	+0.3°C/ 0.68 C	+0.3 °C*
North Pacific SLP	1012.8 mb/ 1.13 mb	1011.2 mb/ 1.78 mb	-1.6 mb**

** = significant at the 1% level, * = significant at the 5% level

Because the seasonal PNA North Pacific SLP index identified more annual SN patterns (20 of 26) than the SOI or the EQPSST index, the

long-term trends of the SLP index were analyzed first, shown in Figure 32 (Trenberth, 1990). A long-term change in the average value of the SLP index occurred in the mid 1970s, as shown in Table 13 and Figure 32 (dashed lines). The change in the means was statistically significant at the 1% level. Trenberth (1990) reported that the average sea level pressure in the Northern Pacific associated with the Aleutian Low decreased from the early (1947-1976) period to the later (1977-1988) period by 2 mb and that the Aleutian Low was generally located farther east during the later period. This change in the PNA occurred at the time when significant changes in regional SN occurred across the region. Average SN values decreased in northern regions and increased in southern regions during the period from 1975-1985, (Table 10, Chapter 5). Also the type of north-to-south gradient pattern occurring switched.

Similarly, the time series of SOI and EQPSST index, both used to indicate ENSO events, show distinct changes (significant at 5% level) in their mean values starting in the mid 1970s, see Table 13 and Figure 32 (dashed lines). These changes in mean large-scale indices occurred at the same time that changes in SN means and north-to-south gradients patterns were identified. The average anomaly value of the October-March SOI changed 0.4 mb from near zero to negative. The negative average SOI anomaly indicates a period of warmer than normal equatorial Pacific sea-surface temperatures. Table 13 shows that the average EQPSST anomaly also changed in the mid 1970s by +0.3 C. During the period from 1976-1987, the seasonal EQPSST index did not dip much below the 1947-1988 average, suggesting that no cold water 'La Nina' events occurred during the most recent period (Trenberth, 1990).

Similar long-term changes occurring for SOI, EQPSST index, and the SLP index, have occurred at approximately the same time, suggesting that the three seasonal indices are connected (Yarnal and Diaz, 1986). When the long-term SOI was negative, the long-term EQPSST index was positive, and the long-term SLP index in the North Pacific was negative, long-term SN anomalies in northern regions of the Rockies were negative while those in the southern regions were positive and dry-north/wet-south gradient patterns occurred. These changes in long-term averages of large-scale indices that occurred in the mid 1970s coincide with the change in the type of gradient SN pattern that occurred in the period from 1972-1975.

The change in the mid 1970s in both the SN and the seasonal indices, SOI, EQPSST, and North Pacific SLP, suggest that they are all dependent on some other physical phenomena. Various other studies have identified multidecadal climatic trends in different regions of the world (Rodgers, 1981; Whitacker and Horn, 1981; Sheaffer and Reiter, 1985; Kay and Dias, 1985; Mysak and Manak, 1989; and Gray, 1990). Multidecadal climatic trends are apparently part of larger global-scale climate variations that are controlled by global-scale oceanic trends and processes (Gray, 1990). Understanding the global oceanic trends and processes may increase the knowledge about the regional multidecadal climatic trends. As has been identified in this part of the study, apparent teleconnections such as ENSO and PNA to SN in North America indicate that 1) long-term changes in sea surface temperatures over the equatorial Pacific Ocean have an effect on atmospheric and oceanic patterns that develop over the north central Pacific and western North America and 2) these large-scale patterns apparently

influence the SN distribution at the surface across the Rocky Mountains. Multidecadal periods with above average SN in the southern regions and below average SN in the northern regions of the Rocky Mountains were favored by: 1) above average SST's across the eastern equatorial Pacific Ocean, 2) lower sea surface pressure in the eastern Pacific, 3) increased convective activity along the northern boundary of the ITCZ, 4) a stronger Aleutian Low located farther east forming strong north meridional flow over the east central Pacific, 5) a large ridge apparently develops over the northern Rockies, and 6) the Sub-tropical Jet more frequently influences the southern Rockies. The exact location and strength of the Aleutian Low from year to year has a great deal to do with the atmospheric circulations that effect Rocky Mountain precipitation and snowpack (Trenberth, 1990; and Cayan and Peterson, 1990). Research has shown that in individual years not always does a stronger Aleutian Low develop when there are above average SST temperatures in the equatorial eastern Pacific. However, during most strong and moderate ENSO events (6 of 7) the stronger Aleutian Low associated with PNA did exist.

6. Summary

Several indices of large scale atmospheric/oceanic circulations are teleconnected to the interannual and long-term variability found in SN in the Rocky Mountains. This study considered five well-known and documented indices, the Southern Oscillation Index, the Equatorial Pacific Sea Surface Temperature Index, the Pacific-North American Index through the Sea Level Pressure Index for the Northern Pacific, the Summer Monsoon Rainfall for India Index, and the Quasi-Biennial

Oscillation, all which can be used as possible predictive indices. Also, 700 mb data from three rawinsonde sites located near or in the study region were analyzed to see what relationship existed between upper air data measured during the winter months of October through March and April 1 snowpack.

The results of analyses that considered the association of ENSO to SN pattern variability indicated that the three unstable regions located west of the C.D. experience greater average SN during ENSO years than in non-ENSO years, while the five stable regions experience greater average SN during non-ENSO years than in the ENSO years. The SN in stable region 1 (northern Idaho/Montana) averaged 9% less in ENSO years, while the SN in unstable region 7 (southern Utah) averaged 11% more in ENSO years. The 20% difference shows that the large-scale circulations associated with ENSO events provide more SN to southern unstable sites with a south or southwesterly exposure to air flow, while northern stable regions with exposures to northerly or westerly air flow are drier during ENSO events. The association of ENSO with patterns of SN variability is potentially an important predictive tool for those that manage the water resources of the West.

The correlation of regional SN values to seasonally averaged large-scale atmospheric/oceanic indices was weak to moderate ($|r|<0.60$) for the period from 1951-1985. Northern regions tend to have r-values that are opposite in sign to southern regions. West of the Continental Divide the correlations in stable regions were generally of opposite sign to the correlations in the unstable regions indicating (as in the previous section) that large-scale circulations such as ENSO and PNA influence snowpack distribution across the Rockies differently from

year-to-year and that large-scale indices can potentially assist in predictions of SN anomalies in regions with different variability.

Of the seasonally averaged large-scale indices, the PNA index was best at identifying wet, dry, and north-to-south gradient patterns (20/26, 77%) for northern and southern regions of the study area. Monthly-averaged 700 mb height and dew point depression probabilities identified 80% (16 of 20) of the annual (non-average) SN patterns or 15% more than the seasonally-averaged 700 mb anomalies identified during a period from 1958-1985. These results imply that at least two mechanisms; 1) seasonally averaged large-scale circulation patterns such as ENSO or PNA, and 2) regional anomalous precipitation events that occur in periods of a month or less, are involved in producing annual SN patterns.

Long-term changes found in regional SN data that occurred in the mid 1970s also emerged in large-scale circulation indices. Long-term changes in the type of north-to-south gradient pattern that occurred are related to long-term changes in large-scale indices. Therefore, the long-term periods when certain types of north-to-south gradient patterns (dry-north/wet-south) occur are apparently linked to: 1) long-term periods of anomalous SN (below average in northern Rockies) and 2) long-term large-scale circulation patterns (below average North Pacific SLP). The multidecadal change in the mid 1970s in both the SN and the seasonal indices suggest that they are all dependent on some other physical phenomena that is a part of the global ocean-climate system.

CHAPTER VII

THE ASSOCIATION OF ROCKY MOUNTAIN WINTER SYNOPTIC PATTERN FREQUENCY TO SPATIAL AND TEMPORAL VARIABILITY IN SN

The results from the previous studies in this report indicate that spatial and temporal variability of hydroclimatic elements are apparently associated with surface exposure and large-scale atmospheric/oceanic circulations, respectively. To confirm these results a new set of hypotheses were developed that integrated a set of winter synoptic patterns associated with different precipitation distributions across the Rockies. First, each annual pattern -- wet, dry, north wet/south dry, north dry/south wet, and average -- is identified by an above average number of a specific synoptic pattern or group of patterns occurring in a year. Second, the multidecadal changes that occurred in the mid 1970s are identified in frequency changes of certain synoptic types. Third, these synoptic patterns that change during the mid 1970s should be associated with the north-to-south gradient patterns that also changed in the mid 1970s. Fourth, the spatial variability of SN across the five-state region is related to the variability in the number of certain daily synoptic patterns that provide the opportunity for precipitation to areas with different exposures each year. For example, synoptic patterns that have a low variability (stable from year-to-year) provide a stable number of precipitation opportunities and are associated with low variability SN

regions. Fifth, large-scale indices such as ENSO and PNA events can be identified when certain synoptic patterns occur.

This chapter: 1) defines and characterizes the predominant Rocky Mountain winter synoptic patterns, 2) identifies the annual frequency of each synoptic pattern, 3) determines the number of annual patterns that can be identified by the frequency of certain winter synoptic patterns, 4) identifies ties between certain synoptic patterns and north-to-south gradient SN patterns as well as multidecadal changes in SN across the five-state region, and 5) discusses the potential association between winter synoptic patterns and other issues.

1. Predominant Rocky Mountain winter synoptic patterns

Questions had to be answered about what the synoptic patterns represent and why they were chosen to develop a set of winter synoptic patterns for examining the new set of hypotheses. The research described in previous chapters examined aspects of hydroclimatic variability across the Rocky Mountains, through the use of SN, PR, and ST data. Throughout the 35-year period the SN and PR distribution across the five-state region varied greatly and was best explained by exposure, a surface physical variable. To prove that spatial and temporal variability of SN and PR was linked to a surface's exposure to airflow, a group of 500 mb winter synoptic patterns over the eastern Pacific and western United States was considered appropriate for determining airflow patterns over the Rocky Mountains. Because the study is located in the midlatitudes, most 500 mb airflow goes from west to east in the "westerlies". In this study, each winter synoptic pattern was chosen because it represented an opportunity for

precipitation associated with a given airflow into different parts of the five-state region. This set of synoptic patterns was identified primarily to assist in a climate analysis that explained the differences in winter precipitation distribution across the Rockies. The group of winter synoptic patterns had to be carefully defined and classified for this synoptic climatology study to successfully consider the new hypotheses.

A California Institute of Technology (CIT) technical paper (1943) identified synoptic weather types for the eastern Pacific Ocean and North America. Sixteen 500 mb winter synoptic types and their associated surface features were identified in this paper. These synoptic weather types were developed to help improve one-to-five day weather forecasts across the United States. A later paper by Elliott (1950) redefined the synoptic weather types detailed in the CIT technical paper and described ten basic winter types. These ten types identified most if not all 500 mb winter weather types associated with making long-range forecasts. The Elliott paper also described surface pressure, temperature and precipitation features for each of the ten weather types. Each weather type focused on airflows into the western United States associated with different directions and latitudes. Five of the 500 mb weather types were associated with meridional flows, five with more zonal flows. These early papers helped to identify the basic winter synoptic patterns that could be used for forecasting.

Based on the winter precipitation distributions associated with the four primary annual SN patterns described earlier (wet, dry, north-wet/south-dry, and north-dry/south-wet), seven 500 mb Rocky Mountain winter synoptic patterns were identified for climate analysis in this study. Each synoptic pattern was chosen because it represented a different airflow that provided precipitation opportunities for certain areas across the five-state region. The set of seven synoptic patterns for climate analyses include -- ridge, meridional NW, WNW, zonal, trough (long wave or short wave), split-flow, and cut-off -- are listed in Table 14 with their characteristics. This group of synoptic patterns represents a close cousin to the group of synoptic patterns described by CIT (1943) and Elliott (1950). However, the group of synoptic patterns used in this study was derived from precipitation distributions associatied with annnual SN patterns across the five-state region, while the group of synoptic patterns developed in earlier papers were used for forecasting weather across the United States. In Table 14, the synoptic patterns are listed in order by type of potential precipitation distribution they are associated with: 1) dry anomalies associated with ridge (D_R) patterns, 2) west to north wet anomalies associated with meridional NW (NW_M), WNW (NW_W), and zonal (NW_Z) patterns, and 3) west to south wet anomalies associated with trough (SW_T), split-flow (SW_S), and cut-off (SW_C) patterns.

Table 14. List of seven 500 mb Rocky Mountain winter synoptic patterns and their characteristics.

Potential Precipitation Distribution	Synoptic Pattern	Airflow Direction	Latitude Constraints	Longitude Constraints	Meridional or zonal Feature
DRY	D_R	weak NW 310′-360′	main flow north of 50′N	ridge crest 110′W-125′W	flow is meridional
WEST TO NORTH WET	NW_M	strong NW to N 310′-360′	main flow between 40′-50′N	ridge crest 117′W-135′W	flow is meridional
	NW_W	strong WNW 290′-320′	main flow between 35′-50′N	small ridge crest if any 115′W-135′W	flow is zonal
	NW_Z	weak or strong W 260′-280′	No constraints	No constraints	flow is zonal
WEST TO SOUTH WET	SW_T	strong SW 200′-260′	main flow between 35′-47′N	bottom of trough (NW-SW flow) between 115′W-127′W	flow is meridional
	SW_S	weak NW north 300′-340′ weak WSW south 210′-260′	flow divided north of 50′N and south of 40′N	largest split in flows 115′W-125′W	flow is meridional
	SW_C	strong N-turns SW; flow around Low - south to east	Cut-off low between 45′N and 32′N	Cut-off low between 105′W-125′W	flow is meridional

In Table 14, any area that is identified as having an above-average precipitation anomaly due to a specific synoptic pattern depends on two key factors: 1) if there is moisture available in the general flow, and 2) if there are synoptic disturbances, or waves, in the flow. These synoptic patterns provide precipitation opportunities to areas based on their exposure to the airflow associated with the winter synoptic

pattern. The WNW, meridional NW, and zonal synoptic patterns provide potential precipitation to areas exposed to W to NW flow while trough, cut-off and split-flow patterns provide precipitation opportunities to areas exposed to SW airflow. Figures 34 through 40 include maps showing each Rocky Mountain winter synoptic pattern. On each map the heavy dark lines represent the main 500 mb upper airflow associated with the synoptic pattern. The dashed line box represent the longitude and latitude constraints of each synoptic pattern discussed in Table 14. Areas of cross hatched lines are areas in the five-state region where opportunities for precipitation exist, while shaded areas represent locations of little or no opportunity for precipitation in the five-state region. The tilt of the ridges and troughs may vary by a few degrees from the patterns shown.

These seven 500 mb Rocky Mountain winter synoptic patterns will be used to test the new set of hypotheses described earlier. In the next section, the 500 mb maps for each winter day through the 35-year period will be carefully analyzed and classified into one of the seven Rocky Mountain winter synoptic patterns.

2. Annual frequency of each winter synoptic pattern

To identify which of the seven Rocky Mountain winter synoptic patterns occurred each winter day (October 1 - March 31), the morning 12Z 500 mb map was carefully analyzed. These daily 500 mb maps are published by the National Weather Service (NWS) and are available for the period of interest, October 1950 through March 1985. Also published daily by the NWS were the surface pressure maps (1950-1985) and the maps that showed precipitation amounts at first order weather

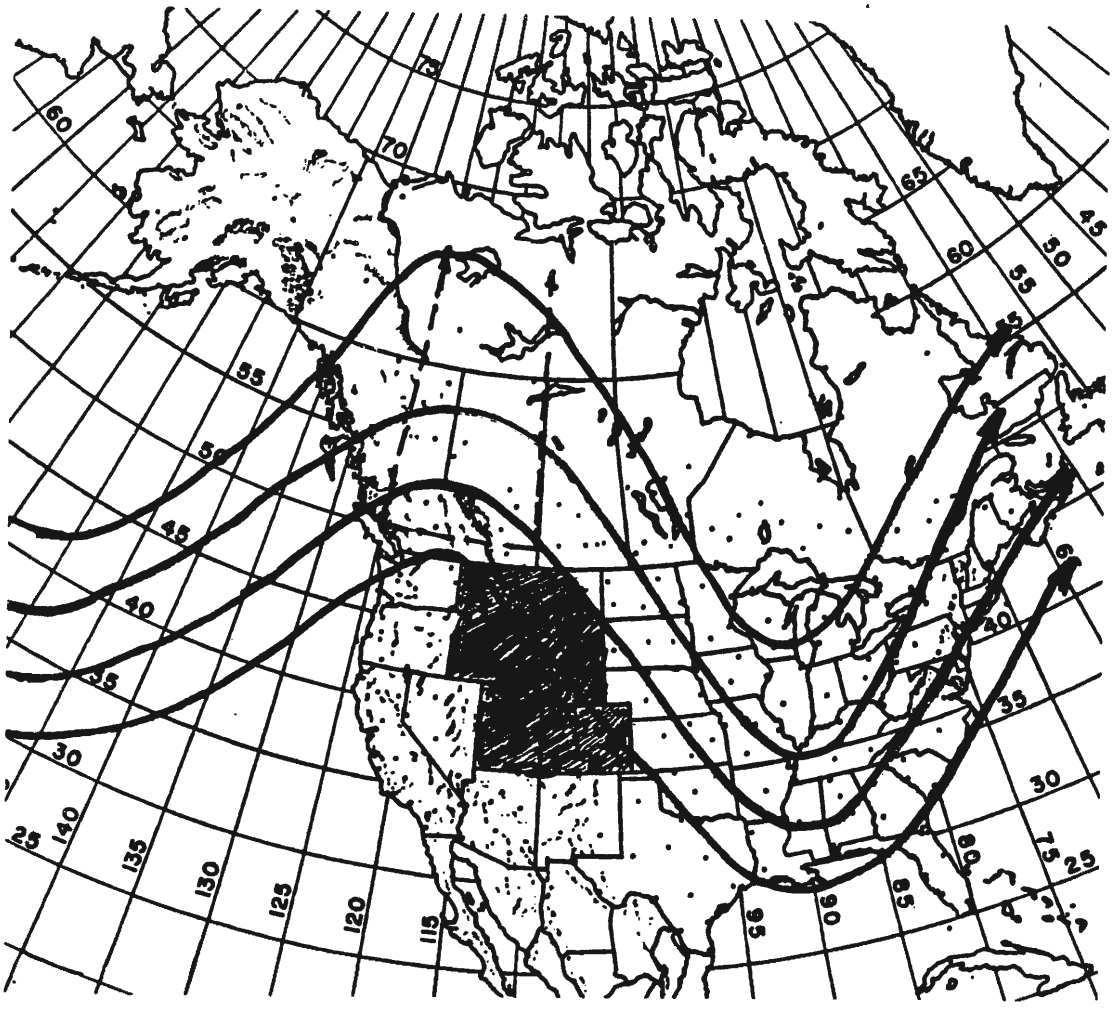

Figure 34. The ridge (D_R) winter synoptic pattern located on map that includes the eastern Pacific Ocean and western North America. The heavy dark lines represent the main 500 mb upper airflow associated with the synoptic pattern. The dashed lines represent the longitude and latitude constraints of the main synoptic feature (the ridge crest in this case) associated with the synoptic pattern. In the five-state region cross hatched area represent areas where there are precipitation opportunities, while shaded areas represent little or no opportunity for precipitation.

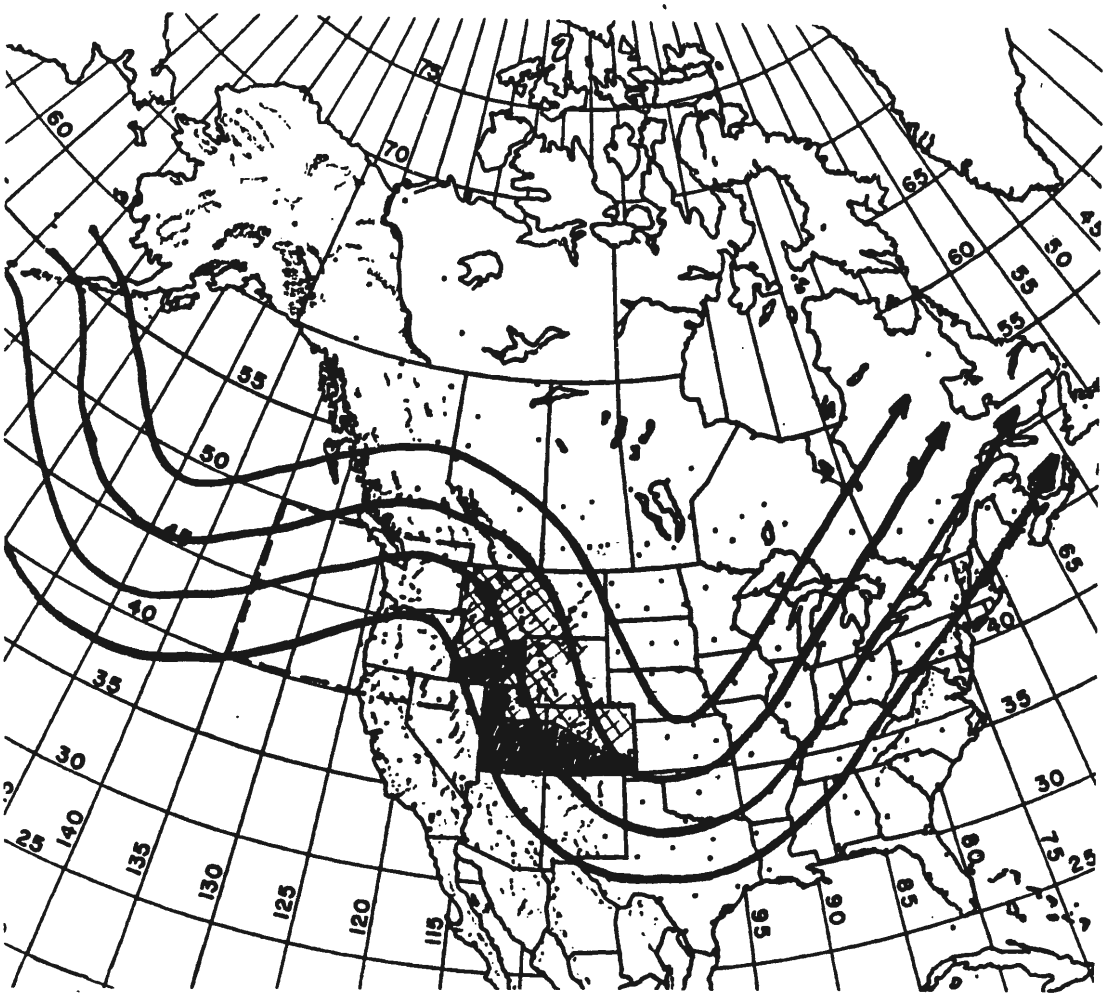

Figure 35. Same as Figure 34 except for the meridional NW (NW_M) winter synoptic pattern.

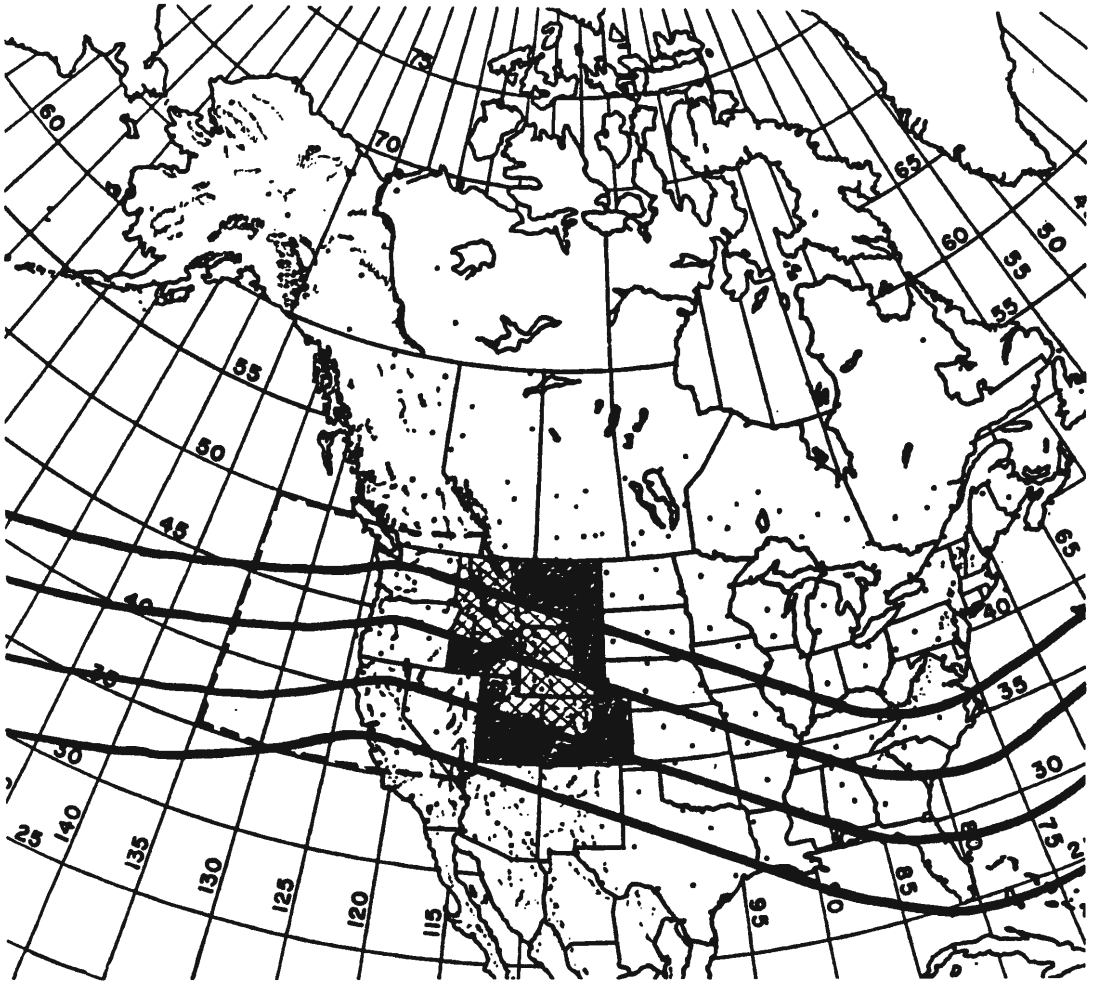

Figure 36. Same as Figure 34 except for the WNW (NW_W) winter synoptic pattern.

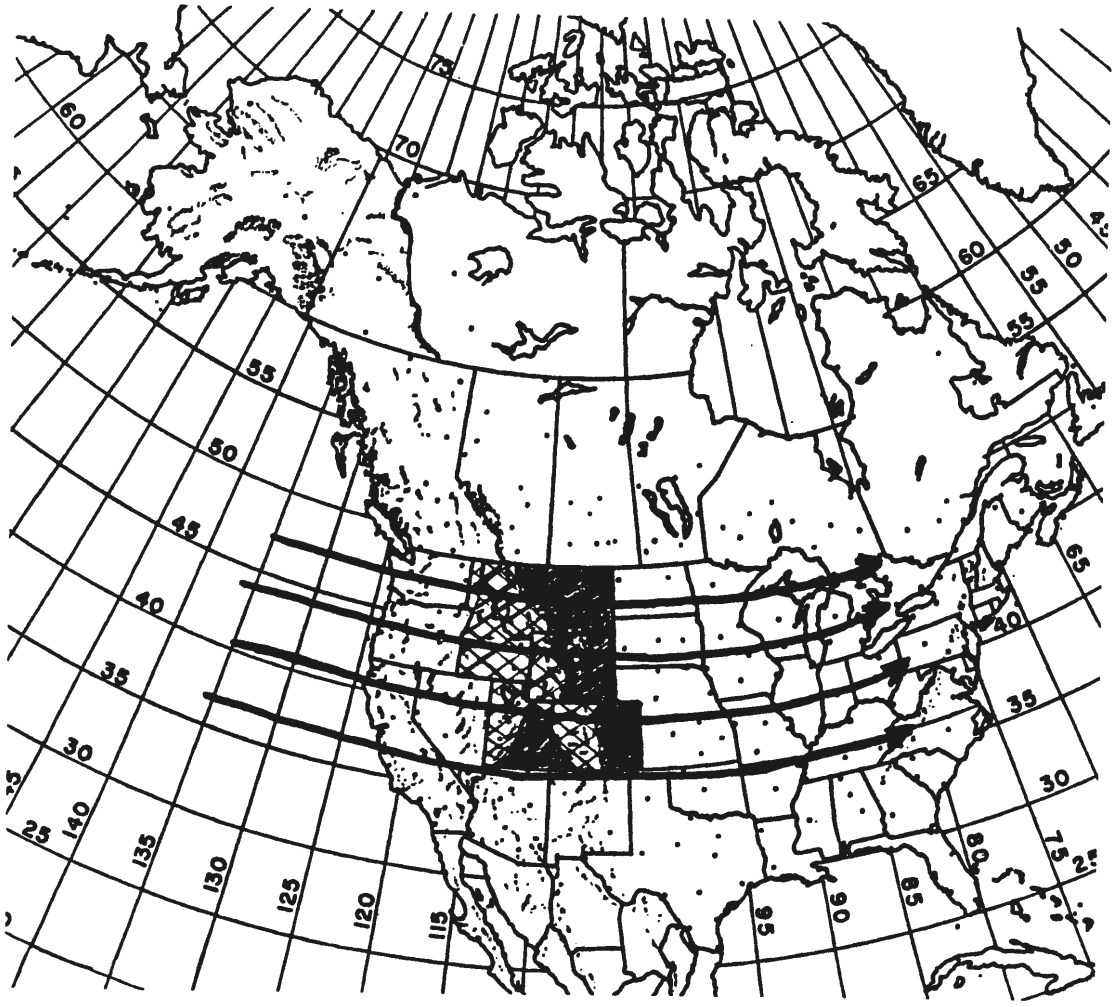

Figure 37. Same as Figure 34 except for the zonal (NW_Z) winter synoptic pattern.

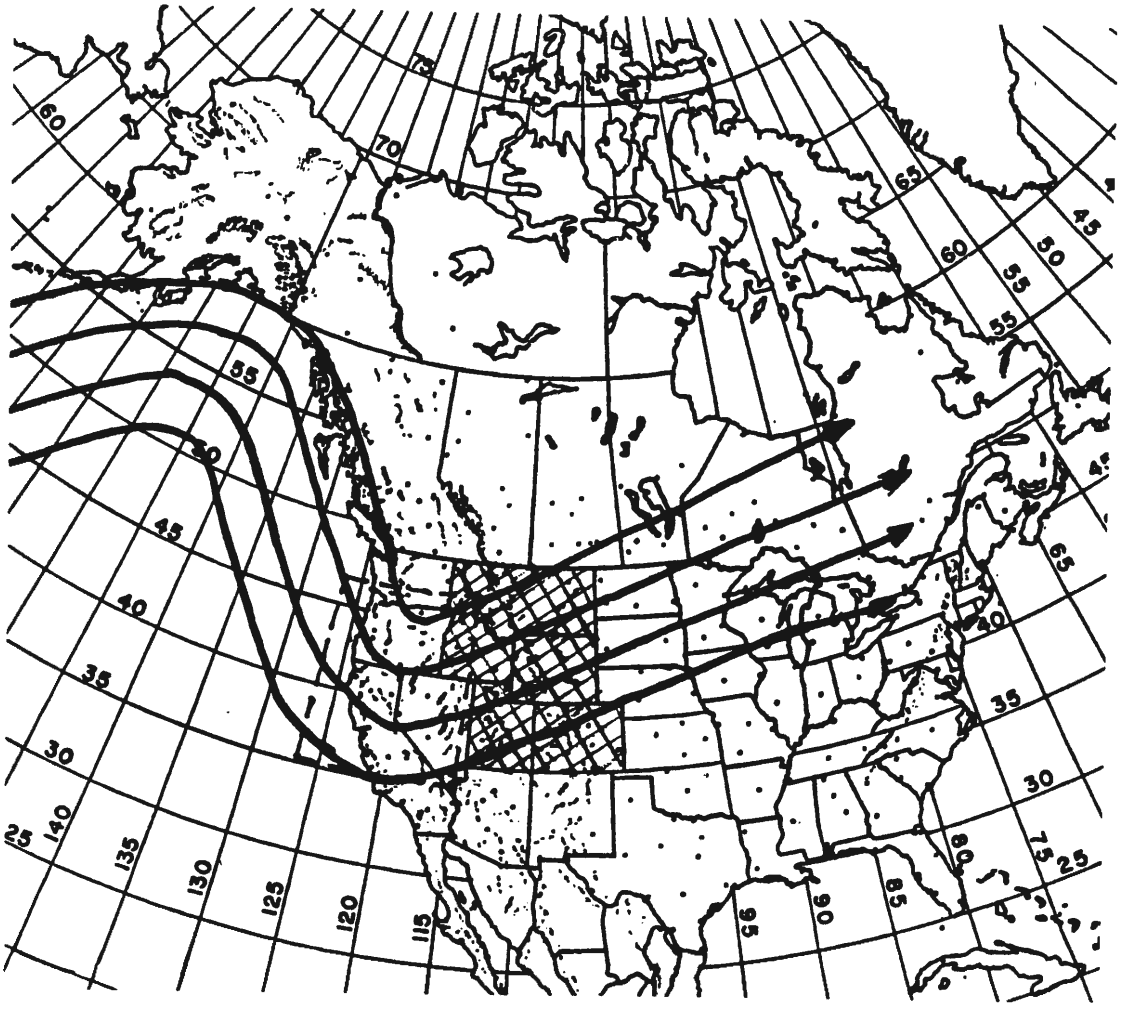

Figure 38. Same as Figure 34 except for the trough (SW_T) winter synoptic pattern.

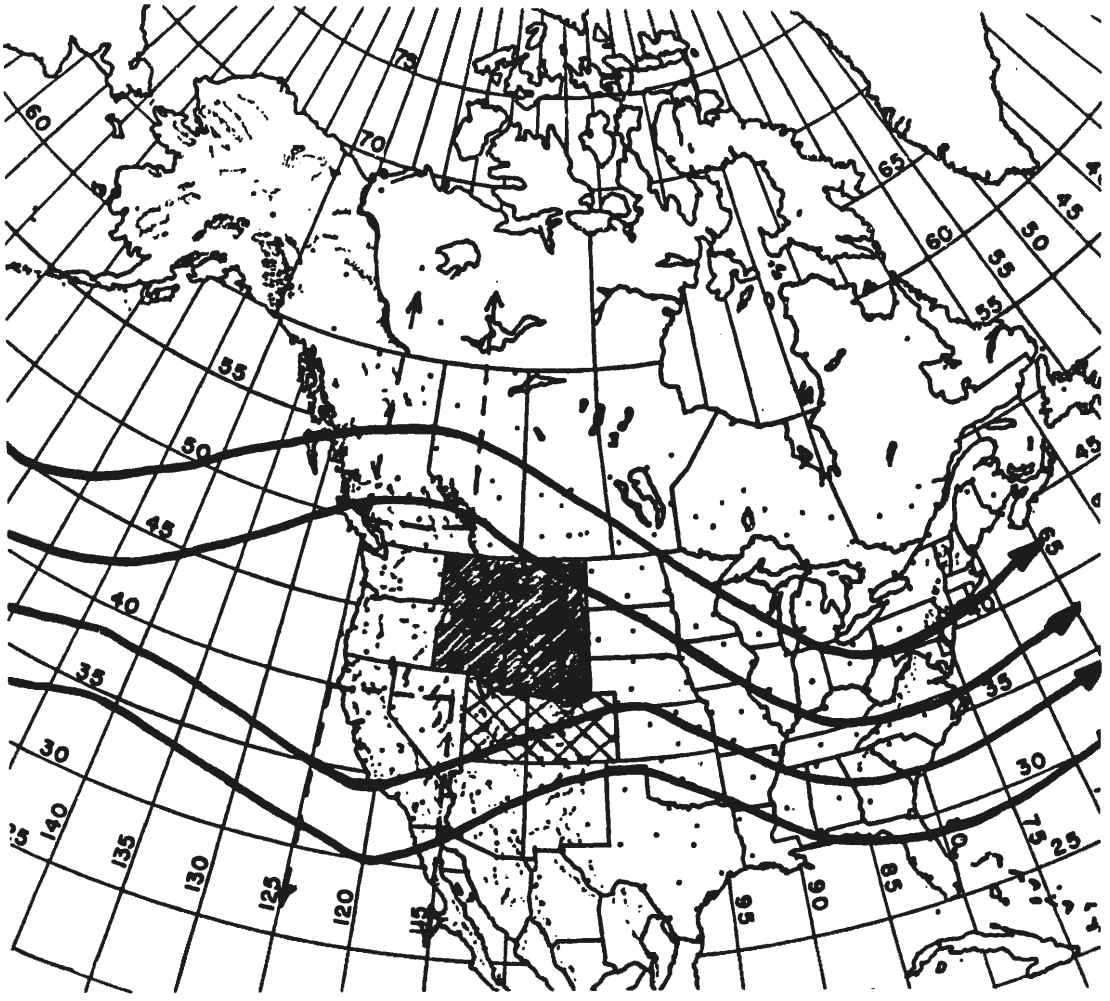

Figure 39. Same as Figure 34 except for the split-flow (SW_S) winter synoptic pattern.

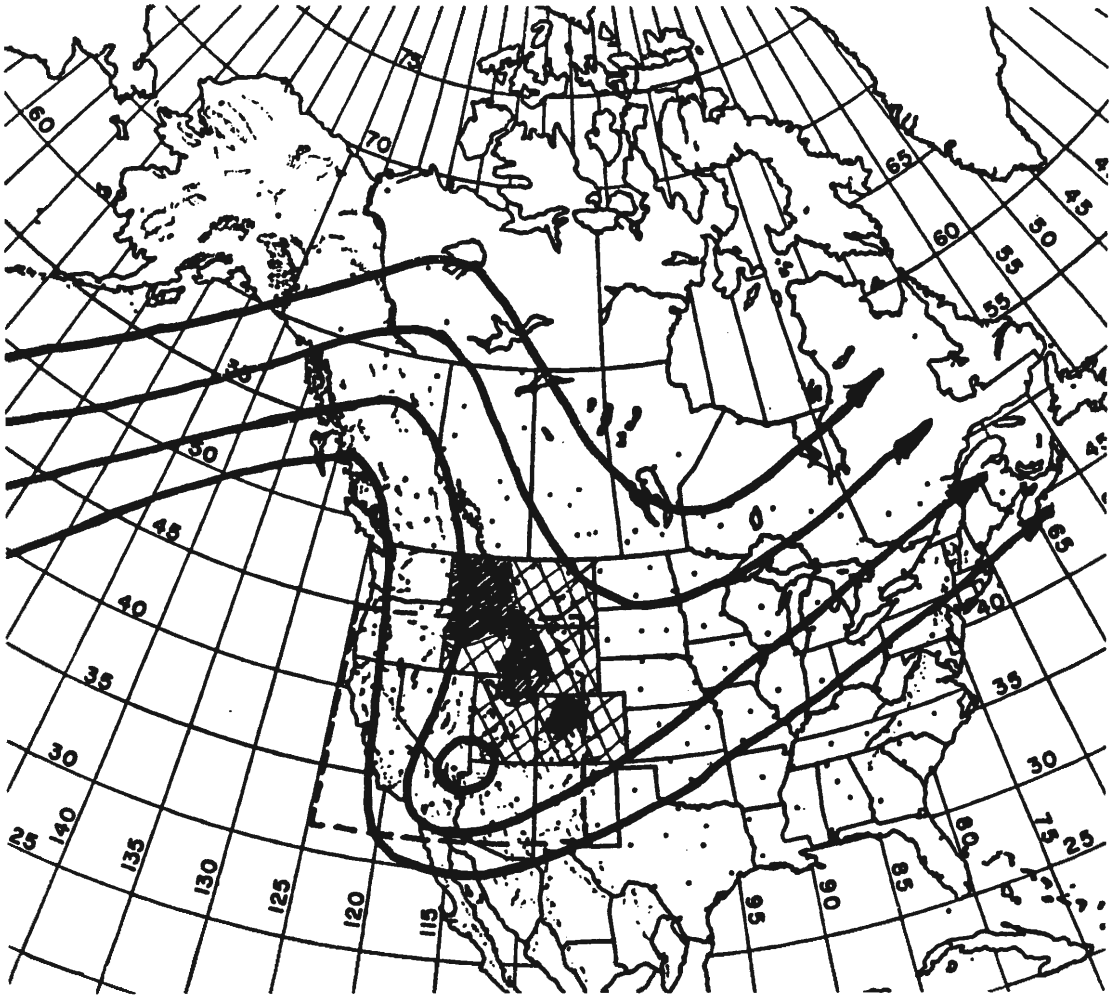

Figure 40. Same as Figure 34 except for the cut-off (SW_C) winter synoptic pattern.

stations (1969-1985). Once all the daily winter maps were analyzed and classified into synoptic patterns, totals for each synoptic pattern were computed for each winter and then the number of each synoptic pattern identified was divided by the total number of winter days (period from October 1 - March 31 equals 182 or 183 days depending on whether there is a February 29 on the calendar) to determine a percent for each synoptic pattern. Table 15, shown on the next page, gives the percents for each synoptic pattern for the 35-year period. Days that do not fit any of the seven synoptic patterns will be classified as not identified. The mean and median values were similar for the synoptic patterns suggesting normally distributed data.

The average annual frequency of the ridge (D_R) synoptic pattern, which is related to dry precipitation anomalies, is 10.7%. The synoptic patterns producing west to north wet precipitation anomalies, meridional NW (NW_M), WNW (NW_W), and zonal (NW_Z), have an average annual frequency of 40.4%. The synoptic patterns producing west to south wet precipitation anomalies, trough (SW_T), split-flow (SW_S), and cut-off (SW_C), have an average annual frequency of 46.6%.

The frequency of synoptic patterns each year as a percent of the total number of winter days is presented in the form of time series (see Figures 41-44). The solid line in each graph represents the 35-year mean, while the dashed lines represent the means for two separate periods, 1951 to 1972 and 1975 to 1985. The time series for trough and ridge synoptic patterns are shown in Figure 41a and 41b. The trough synoptic pattern varies very little about the 35-year mean and shows no temporal trend, while the ridge synoptic pattern shows great variability about its long-term mean. Neither change in the mean from

earlier to later period is significant. The time series for WNW and Meridional NW synoptic patterns are shown in Figure 42a and 42b. The

Table 15. Frequency of synoptic patterns each year as a percent of the total number of winter days.

Year	NW_Z	NW_W	D_R	SW_S	SW_C	SW_T	NW_M	Not Identified
1951	4	31	3	2	9	25	24	2
1952	2	20	3	5	15	31	21	3
1953	2	18	19	4	12	17	26	2
1954	2	30	5	1	12	21	27	2
1955	2	17	21	2	12	24	20	2
1956	1	35	3	3	9	24	23	2
1957	5	24	12	5	9	22	16	3
1958	0	26	14	5	22	22	11	0
1959	3	26	7	3	12	26	20	3
1960	1	25	13	4	14	22	20	1
1961	1	18	24	7	13	22	14	1
1962	0	22	13	2	22	31	10	0
1963	1	19	23	3	14	25	14	1
1964	2	22	6	1	14	33	20	2
1965	2	22	8	3	16	35	12	2
1966	5	24	18	2	12	25	12	2
1967	3	28	2	0	15	31	20	1
1968	3	19	6	7	13	26	24	2
1969	1	18	8	5	16	34	15	3
1970	6	24	9	12	16	20	11	2
1971	3	34	10	4	17	22	8	2
1972	3	35	10	5	20	21	4	2
1973	2	10	1	12	34	28	7	6
1974	9	29	2	2	10	38	10	0
1975	2	23	4	5	25	28	10	3
1976	11	19	12	1	18	28	8	3
1977	2	10	38	5	14	19	9	3
1978	8	27	9	8	10	23	12	3
1979	5	16	5	5	29	29	8	3
1980	5	15	15	3	27	21	13	1
1981	3	16	25	4	15	19	15	3
1982	7	22	6	3	18	26	16	2
1983	4	15	8	7	21	24	16	5
1984	3	17	8	3	24	23	20	2
1985	3	9	5	14	23	29	15	2
Mean	3.3	21.9	10.7	4.5	16.6	25.5	15.2	2.3
Median	3	22	8	4	15	25	15	2
σ	2.5	6.7	8.1	3.2	6.1	5.0	5.9	1.2

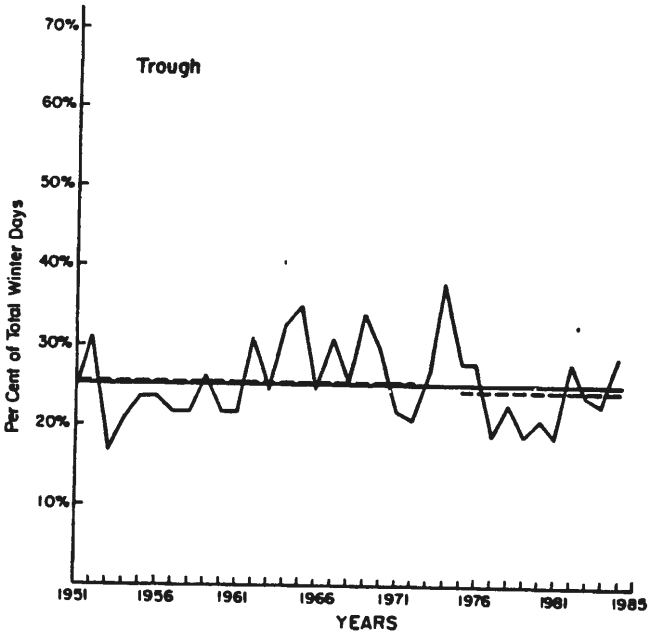

a)

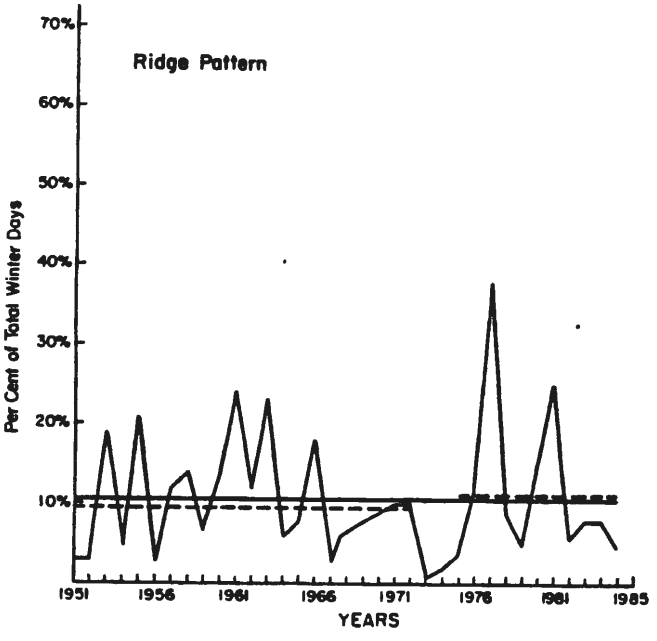

b)

Figure 41. Time series representing the frequency of synoptic patterns each year as a percent of the total number of winter days for the a) trough (SW_T) synoptic patterns and b) ridge (D_R) synoptic patterns. The solid line represents the 35-year mean, while the dashed lines represent the means for two separate periods, 1951-1972 and 1975-1985.

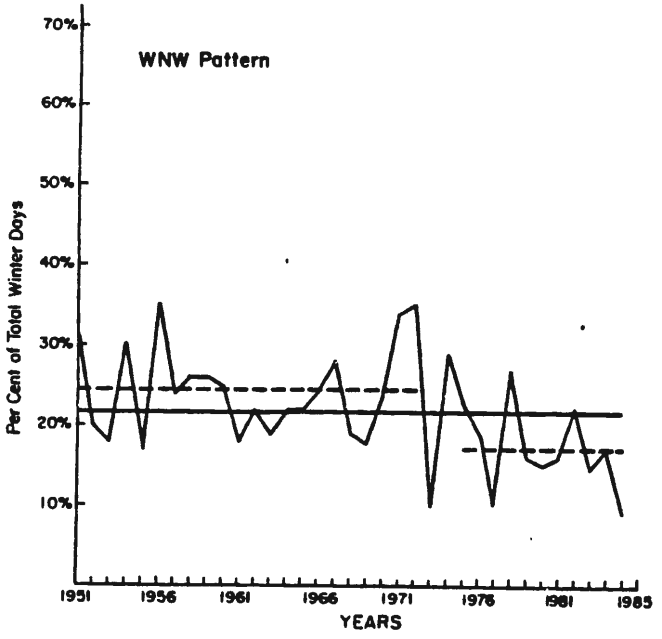

a)

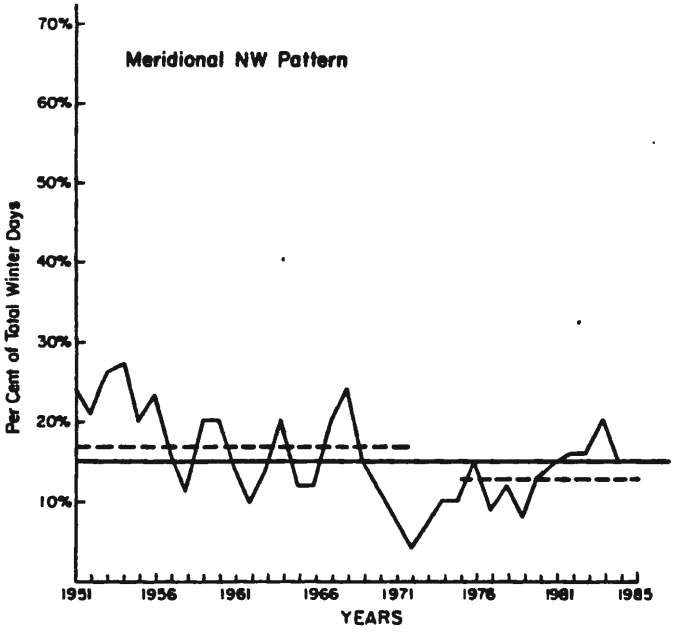

b)

Figure 42. Same as Figure 41 except for a) WNW (NW_W) synoptic patterns and b) meridional NW (NW_M) synoptic patterns.

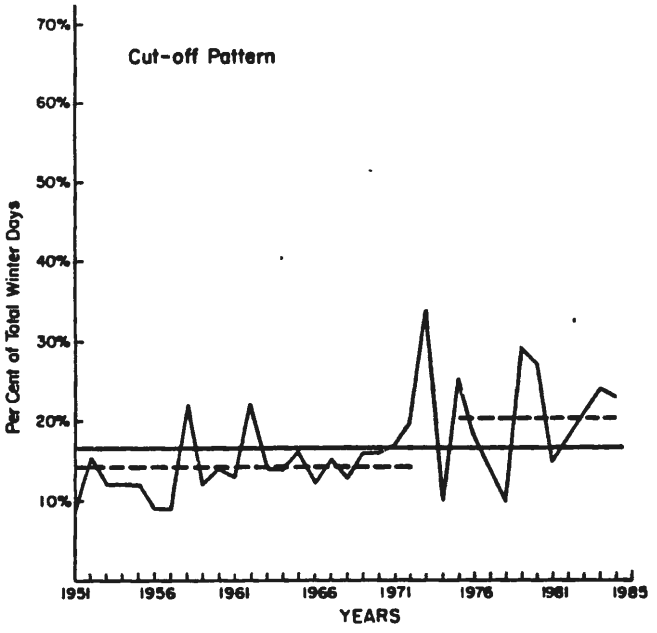

a)

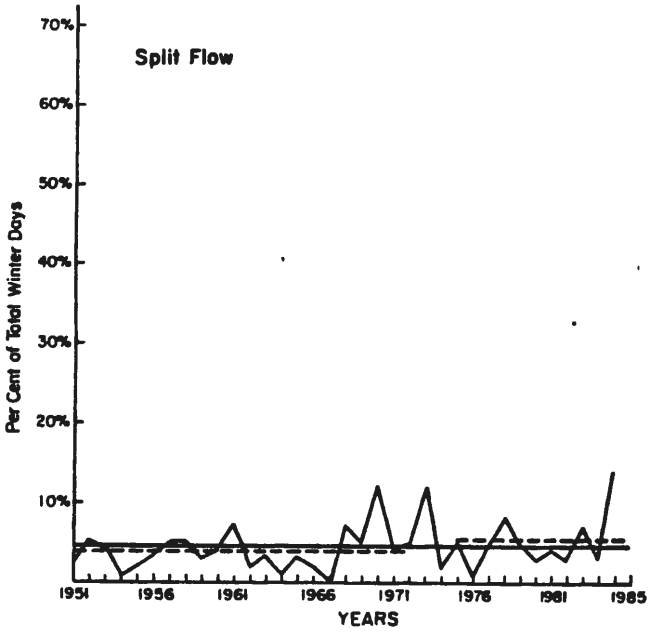

b)

Figure 43. Same as Figure 41 except for a) cut-off (SW_C) synoptic patterns and b) split-flow (SW_S) synoptic patterns.

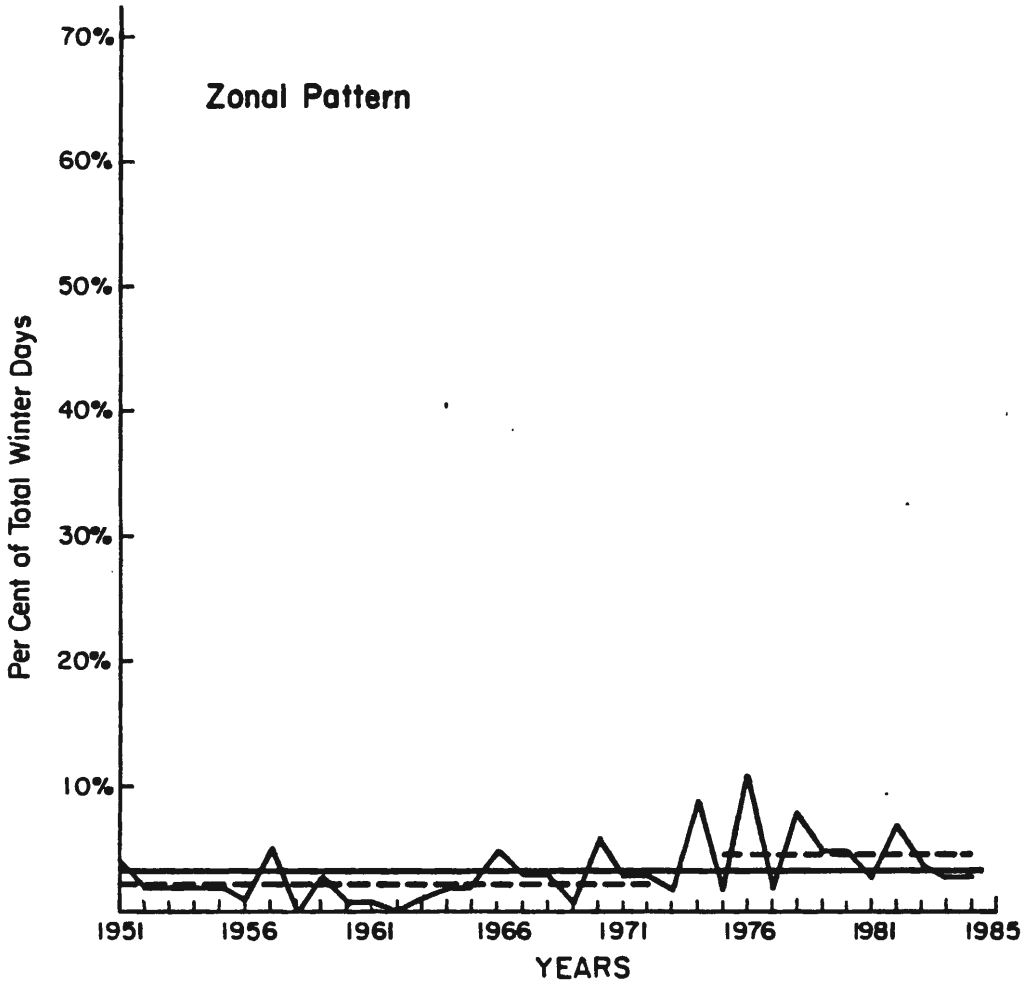

Figure 44. Same as Figure 41 except for zonal (NW_Z) synoptic patterns.

WNW synoptic pattern exhibits a decreasing trend beginning in the early 1970s, while the meridional NW synoptic pattern shows a decreasing trend to the late 1970s and then a slight increase until 1985. The change in the means from the earlier to later periods were statistically significant for the WNW synoptic pattern at the 1% level and at the 10% level for the meridional NW pattern. Because both these synoptic patterns exhibit similar decreasing temporal trends and provide precipitation opportunities to similar locations their annual percentages will often be combined for future analyses. Figure 43a and 43b shows the time series for cut-off and split-flow synoptic patterns. The cut-off synoptic pattern shows an increase during the entire period with greater interannual variability occurring during the 1970s and 1980s. The change in the means from the earlier to the later period was significant at the 1% level for the cut-off synoptic pattern. The split-flow synoptic pattern exhibits little variability around its long-term mean and a small non significant increases in the 1980s. Because both these synoptic patterns exhibit similar increasing temporal trends and provide precipitation opportunities to similar locations their annual percentages will often be combined for future analyses. The time series for the zonal synoptic pattern shown in Figure 44, exhibits more interannual variability after 1970 than before. Also, the change in the means from the earlier to later period was significant at the 1% level.

3. Relationships between annual SN patterns and synoptic patterns

The five annual SN patterns -- wet, dry, north wet/south dry, north dry/south wet, and average -- were identified and described in

Chapter 5. In Chapter 6 seasonally averaged large-scale atmospheric/oceanic indices were used to identify non-average SN patterns in the 35-year period. They identified between 62% and 77% of all the non-average SN patterns. This section will define the average number of synoptic patterns for the 35-year period as well as for each type of SN pattern. Also, synoptic patterns will be used to identify the non-average SN patterns.

Initially, the average frequency, in percent of total winter days (October 1 - March 31) days, of each synoptic pattern was computed for the 35-year period (see Table 16). The synoptic patterns were then averaged as a percent of the total number of winter days for each SN pattern.

Table 16. Synoptic pattern frequency average for 1951-1985 period and deviation from average for each SN pattern in percent.

Synoptic Pattern	35-year mean	Wet	Dry	N. wet/s. dry	N. dry/s. wet	Ave.
D_R	10.7%	-3.7%	+11.9%**	-5.6%*	-3.5%	-1.6%
NW_M	15.2%	-1.2%	+1.1%	+1.8%	-3.2%	-0.4%
NW_W	21.9%	-0.7%	-2.7%	+8.6%**	-7.4%*	-0.9%
NW_Z	3.3%	-1.0%	-1.2%	+0.1%	+0.4%	+1.5%
SW_T	25.5%	+5.3%**	-3.9%**	+1.3%	-0.3%	-1.1%
SW_C	16.6%	+2.0%	-3.4%	-3.4%	+11.9%**	-0.6%
SW_S	4.5%	-0.7%	-0.6%	-2.2%*	+1.3%	+2.4%*
Not Identif.	2.3%	-0.1%	-0.1%	-0.6%	+0.8%	+0.3%
TOTAL	100.0%					

** = difference from 35-year mean significant at the 1% level
* = difference from 35-year mean significant at the 5% level

Table 16 indicates that the five most frequent synoptic patterns -- ridge (D_R), meridional NW (NW_M), WNW (NW_W), trough (SW_T), and cut-off (SW_C) --account for approximately 90% of all winter days. Wet SN patterns show a large increase in the average number of trough and cut-

off patterns with a decrease in the number of ridge patterns. Dry SN patterns show the reverse with an increased number of ridges and a decrease in the number of troughs and cut-offs. The north wet/south dry SN patterns exhibit increases in WNW and meridional NW synoptic patterns with decreases in ridge, split-flow, and cut-off synoptic patterns. The north dry/south wet SN patterns indicate increases in the frequency of cut-off and split-flow synoptic patterns while the number of ridge, WNW, and meridional NW synoptic patterns decrease. The average SN patterns are characterized by small (less than 2.4%) increases or decreases in all synoptic patterns.

As discussed earlier in this chapter, Rocky Mountain winter synoptic patterns provide airflows from different directions into the C.D. Synoptic patterns that provide a northwesterly airflow include the WNW, the meridional, and the ridge; these patterns account for 47.8% of all winter days on average. The zonal synoptic pattern provides a westerly airflow into the C.D. The synoptic patterns that provide a southwesterly airflow include the cut-off, the split-flow, and the trough; these patterns account for 46.7% of all winter days on average.

Table 16 implies that each SN pattern except the average should have some synoptic patterns more frequent and others that are less frequent. For each winter the deviation from the 1951 to 1985 average for each synoptic pattern was computed. Years having an above average number in trough and/or cut-off synoptic patterns and a below average number in ridges were considered wet years. Five of six wet SN pattern years -- 1952, 1962, 1965, 1969, and 1975 -- were identified with these characteristics. Only 1982 did not show a large increase in trough or

cut-off patterns. Seven of eight dry SN pattern years showed large increases (>7.5%) in the number of ridge patterns, with 1960 the only dry SN pattern year not showing a dramatic increase in ridges. Seven of eight north wet/south dry SN pattern years were identified as having large increases (>6.0%) in the number of WNW or meridional NW synoptic patterns. Only 1964, with an increase of 4.8% in meridional NW patterns, did not meet the requirements. Finally, all four north dry/south wet SN pattern years were identified as having large increases (>7.0%) in the number of cut-off or split-flow synoptic patterns and large decreases (>5.0%) in the number of WNW patterns. The frequency of synoptic patterns during the winter (October 1 - March 31) identified 23 of 26 (89%) non-average SN patterns. This value is clearly higher than any of the seasonal large-scale indices and indicates that annual SN patterns can be identified easily when the frequency of Rocky Mountain winter synoptic patterns is known. This result is important because it focuses on the fact that the synoptic patterns explain how the annual SN patterns are formed.

4. <u>The association of multidecadal changes in SN and north-to-south gradient patterns to changes in frequency of synoptic patterns</u>

Chapter 5 indicated that the type of north-to-south gradient SN patterns changed in the mid 1970s. This change occurred at the same time when the SN in the northern Rockies decreased, while in the southern Rockies it increased. The large-scale indices analyzed in Chapter 6 indicated that changes in ENSO and PNA also occurred in the mid 1970s. The objective in this section is to identify changes in the frequency of daily winter synoptic patterns that could explain why the

change in type of north-to-south gradient years is the reason for the dramatic changes in the SN across the five-state area.

Section 2 of this chapter showed the time series of each synoptic pattern. The time series for trough, ridge, and zonal synoptic patterns showed no significant increasing or decreasing trends during the 35-year period, while the cut-off, split-flow, WNW, and meridional NW showed dramatic changes. Section 3 identified the annual SN patterns by the different winter synoptic patterns. The north wet/south dry SN pattern showed an above average number of WNW and meridional NW synoptic patterns and below average number of ridge, cut-off and split-flow synoptic patterns, while years with north dry/south wet SN patterns showed above average cut-off and split-flow synoptic patterns and below average ridge, WNW, and meridional NW synoptic patterns. Because the frequency of ridges decreased in both types of gradient SN patterns they were not considered important in separating the two gradient types and not used for further study. Figure 45a shows the combined time series of cut-off and split-synoptic patterns, while Figure 45b presents the combined time series of WNW and meridional NW synoptic patterns. The line drawn through each graph represents the 35-year average, while the dashed lines represent the 1951-1972 average (period of north wet/south dry SN patterns) and the 1975-1985 average (period of north dry/south wet SN patterns). In both combined time series the change in means from the earlier to later period were significant at the 1% level see Table 17. The combined number of cut-off and split-flow patterns increases throughout the 35-year period while the combined number of WNW and meridional NW patterns decreases. The decreases in WNW and meridional NW synoptic

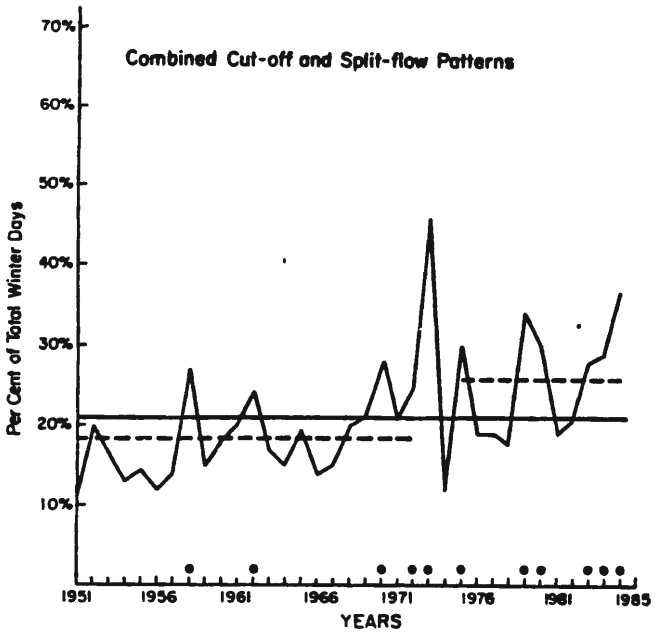

a)

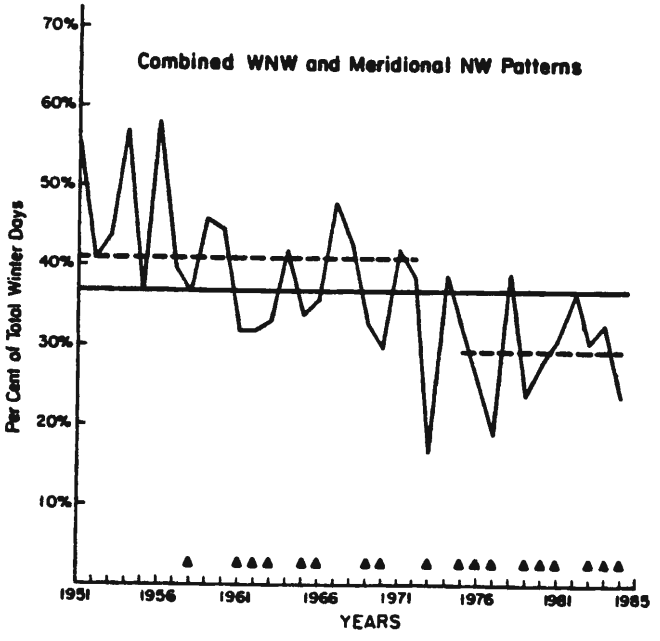

b)

Figure 45. Combined time series representing the frequency of two synoptic patterns each year as a percent of the total number of winter days for the a) cut-off (SW_C) and split-flow (SW_S) synoptic patterns and b) WNW (NW_W) and meridional NW (NW_M) synoptic patterns. The solid line represents the 35-year mean, while the dashed lines represent the means for two separate periods, 1951-1972 and 1975-1985.

patterns occurred during the period when the northern Rockies became drier (after 1970), while the increases in the cut-off and split-flow synoptic patterns occurred during this same period when the southern Rockies got wetter. These time series clearly indicate that the frequency of the two combinations of synoptic patterns are related to the type of north-to-south gradient pattern experienced. Futhermore, changes in SN that occurred across the five-state region in the mid 1970s is associated with the long-term changes in the frequency of these two combinations of synoptic patterns. The long-term changes in frequency of certain synoptic patterns represents the physical explanation for the multidecadal changes identified in SN across the five-state Rocky Mountain region. Table 17 shows the changes that occurred from the 1951-1972 period to the 1975-1985 period.

Table 17. Changes in average value of synoptic patterns from an earlier period to a later one.

Combined synoptic patterns	Mean/Standard Deviation 1951-1972	Mean/Standard Deviation 1975-1985	Change in Mean
SW_S and SW_C	18.5%/ (4.8%)	25.8%/ (6.8%)	+7.3%**
NW_M and NW_W	41.1%/ (7.8%)	29.6%/ (6.4%)	-11.5%**

** = change in mean significant at the 1% level

Table 17 shows that the split-flow and cut-off (SW_S and SW_C) synoptic patterns increased by 7.3 percent (13.3 days during the period from October 1 - March 31), while the meridional NW and WNW (NW_M and NW_W) synoptic patterns decreased 11.5 percent (20.9 days during the period from October 1 - March 31). The mean value of WNW and meridional NW patterns is still greater than that for cut-off and split-flow patterns

in the period from 1975-1985. This analysis suggests that precipitation occurring in precipitation events associated with cut-off and split-flow patterns in the southern regions is apparently heavier than the precipitation occurring during precipitation events associated with WNW and meridional NW patterns in the northern regions. Further research using daily precipitation data would prove or disprove this point.

The analyses in this section clearly indicates the change in type of north-to-south gradient patterns is caused by: 1) increases in cut-off and split-flow synoptic patterns and 2) decreases in WNW and meridional NW synoptic patterns. Because changes in north-to-south gradient SN patterns were identified as the cause for changes in SN across the five-state region, the changes in cut-off, split-flow, WNW, and meridional NW synoptic patterns through time must also be associated with the multidecadal changes in SN across the region.

5. <u>The potential association between synoptic patterns and other issues</u>

Two other areas of interest were considered: 1) to consider the relationship of winter synoptic pattern variability to spatial variability of SN and 2) to identify the potential association of different synoptic patterns to large-scale indices. These two issues were analyzed and the results are described below.

In section 2, Table 15 listed the seven Rocky Mountain winter synoptic patterns and the percentange of winter (October 1 - March) days in each synoptic pattern for each winter. For each of those synoptic patterns the MOV, $(X_{80\%} - X_{20\%})/X_{50\%}$, was computed over the

35-year period. Table 18 shows the MOV values for each synoptic pattern as well as two combinations.

Table 18. Measure of Variability values for each synoptic pattern and two combinations of synoptic patterns.

Synoptic Pattern	Direction of airflow	Measure of Variability
D_R	Northwest	1.75
NW_M	Northwest	0.65
NW_W	Westnorthwest	0.53
NW_Z	West	1.33
SW_T	Southwest	0.40
SW_S	Southwest	1.25
SW_C	Southwest - East	0.67
NW_M and NW_W	West NW - North	0.35
SW_S and SW_C	Southwest - East	0.74

In Table 18, only the trough, the WNW, and the combined WNW and meridional NW have MOV values less than 0.55. This 0.55 MOV value was used to separate stable and unstable watersheds and regions (see Chapter 3 and 4). This analysis suggests that unstable (MOV > 0.55) watersheds and regions, identified as having surface exposure to southerly or easterly airflow, apparently have its SN or PR variability derived from combined cut-off and split-flow patterns. The combined cut-off and split-flow synoptic pattern MOV is 0.74. Other synoptic patterns with MOV > 0.55 are associated with flows from the west to north that produce little or no precipitation to unstable watersheds or SN regions with exposures to the south or east. Stable (MOV < 0.55) watersheds and regions with surface exposure to westerly or northerly airflow apparently have its SN or PR variability derived from combined WNW and meridional NW synoptic patterns. The combined WNW and meridional NW synoptic pattern MOV is 0.35. The trough synoptic pattern has an MOV equal to 0.40, however it is associated with airflow

from the southwest that would not produce as much precipitation in stable watersheds or N regions with surface exposures to the northwest. These results provide some indication about the association of synoptic patterns to spatial variability of SN and PR across the five-state region; however, these results are not conclusive. Further research may improve the significance of these results.

As discussed in the previous chapter, 11 ENSO events and 12 PNA events occurred during the 1951-1985 period. The regionally averaged SN was greater in southern regions and less in northern regions during the average ENSO and PNA event. A hypothesis based on these results indicated that during ENSO and PNA events the predominant large-scale atmospheric circulation pattern over the western U.S. consisted of a ridge over the northern Rockies with the Subtropical Jet affecting the the southern Rockies more frequently than average. Based on this hypothesis, a greater frequency of ridge, cut-off, and split-flow patterns were expected during ENSO and PNA events. Table 19 shows the average non-ENSO annual percent (NEN_{ave}), the average ENSO annual percent (EN_{ave}), the average non-PNA annual percent ($NPNA_{ave}$), the average PNA annual percent (PNA_{ave}), the average annual percent for years when both ENSO and PNA did not occur ($NENPNA_{ave}$), and the average annual percent for years when both ENSO and PNA did occur ($ENPNA_{ave}$), for each daily synoptic type. The average annual percent is computed by taking the number of occurrences of a synoptic pattern during a winter (October 1 - March 31) and dividing it by the total number of winter days. These winter average percents are then averaged for all NEN, EN, NPNA, PNA, NENPNA, and ENPNA years. Table 19 also shows the differences between each set of values.

Table 19. Average NEN_{ave}, EN_{ave}, $NPNA_{ave}$, PNA_{ave}, $NENPNA_{ave}$, and $ENPNA_{ave}$ annual percents and differences for each daily synoptic type.

Synoptic pattern	EN_{ave}	NEN_{ave}	Diff	PNA_{ave}	$NPNA_{ave}$	Diff	$ENPNA_{ave}$	$NENPNA_{ave}$	Diff
D_R	11.1	10.6	-0.6	15.3	8.3	-7.0*	13.0	10.2	-2.8
NW_M	14.7	15.4	+0.7	14.9	15.3	+0.4	12.3	15.8	+3.5
NW_W	19.7	22.8	+3.1	18.2	23.7	+5.5*	17.0	22.9	+5.9*
NW_Z	3.2	3.5	+0.3	2.9	3.5	+0.6	2.8	3.4	+0.6
SW_T	24.9	25.8	+0.9	23.1	26.8	+3.7**	24.2	25.8	+1.6
SW_S	4.9	4.3	-0.6	6.4	3.5	-2.9**	7.3	3.9	-3.4**
SW_C	18.4	15.8	-2.6	17.3	16.3	-1.0	21.8	15.6	-6.2*

** = difference in means is significant at the 1% level
* = difference in means is significant at the 5% level

The difference values with a positive sign indicated that fewer patterns occurred during ENSO, PNA, or events with both ENSO and PNA. As hypothesized, during average ENSO or PNA years the frequency of ridges, cut-offs and split-flow patterns increased, while other patterns such as WNW, trough and meridional NW decreased. Table 19 shows that the average differences for years when both ENSO and PNA occurred were the largest. Thus, together the PNA and ENSO phenomena act to change the average frequency of Rocky Mountain winter synoptic patterns. This suggests that only during years with both PNA and ENSO occurring together is there a significant change in the average number of certain winter synoptic patterns.

Although when averaging the frequency of synoptic patterns the differences between ENSO and non-ENSO, PNA and non-PNA, and ENPNA and non-ENPNA appear large, few of the individual years experiencing ENSO or PNA events can be identified by anomalous frequencies of the seven winter synoptic patterns. Because large increases in the average number of split-flow and cut-off patterns as well as large decreases in

the average number of meridional NW and WNW were identified (see Table 19) these four synoptic patterns were chosen to identify ENSO and PNA events in the 35-year period. The number of cut-off and split-flow patterns were combined for one time series and the number of WNW and meridional NW synoptic patterns were combined for another time series (see Figures 45a and 45b). In Figure 45a a dot appears at the bottom of the graph when the number of cut-off and split-flow patterns was above the 35-year average. In Figure 45b a triangle appears at the bottom of the graph when the number of WNW and meridional NW patterns was below the 35-year average. Those years when both the triangle and dot occur together are years with the type of anomalous patterns expected in the ENSO or PNA events. The years with the dot and triangle both occurring include 1958, 1962, 1970, 1973, 1975, 1979, 1980, 1983, 1984, and 1985. Of this group only 1958, 1970, 1973, 1983, and 1984 represent years when both ENSO or PNA events occurred. Because half of the 10 years did not include PNA or ENSO events indicates that not all ENSO or PNA years are identified by similar numbers of synoptic patterns. The reasons why greater or fewer numbers of certain synoptic patterns do not occur during all ENSO or PNA events is apparently because the ENSO and PNA phenomenon do not always set up identical anomalous atmospheric/oceanic patterns during each event. The differences between the development of ridge, meridional NW and cut-off synoptic patterns is small, implying that if the large-scale atmospheric/ oceanic circulation patterns are shifted in some ENSO or PNA events by 300 to 500 miles latitudinally or longitudinally, these patterns can produce a very different distribution of winter synoptic patterns than what is expected in averaged ENSO and PNA events. These

interesting results indicate that the association between large-scale indices and winter synoptic patterns is not conclusive. Further research is needed to identify if there is any significant link between large-scale indices and SN across the the five-state region.

6. Summary

Based on precipitation and snowpack distributions identified in earlier chapters, seven 500 mb Rocky Mountain winter synoptic patterns were identified as the climatological group that explained almost 98% of the daily winter (October 1 - March 31) synoptic maps for the period from October 1950 through March of 1985. Each daily winter synoptic pattern was characterized as providing opportunities for precipitation to different regions of the five-state study area. The seven patterns included: 1) ridge, which is associated with dry precipitation anomalies across the five-state region, 2) meridional NW, WNW, and zonal, which are associated with potential wet precipitation anomalies across the northern regions, and 3) trough, split flow, and cut-off, which are associated with potential wet precipitation anomalies across the southern regions. Whether each synoptic pattern produced precipitation depended on whether a disturbance and/or appropriate moisture was available in the airflow that accompanied the synoptic pattern. The number of occurrences of each synoptic pattern was determined for each year.

Chapter 5 identified five annual SN patterns -- wet, dry, north wet/south dry, north dry/south wet, and average. This study averaged the synoptic patterns that occurred in each of the five annual SN pattern years. From the averages, wet years were identified as having

an increased amount of troughs (+5.3%) and cut-offs (+2%) with a decrease in the frequency of ridges (-3.7%). Dry years had 12% more ridge patterns with decreases in cut-offs (-3.4%) and troughs (-3.9%). North wet/south dry years had increased WNW (+8%) and meridional NW (+1.8%) patterns showed decreases in ridges (-5.6%) and cut-offs (-3.4%). North dry/south wet years had increases in cut-offs (+11.9%) and split-flow (+1.3%) patterns while decreases occurred in WNW (-6.8%) and meridional NW (-3.2%) patterns. Average years showed no synoptic patterns increasing or decreasing by more than 2%. Individual years were determined by their annual anomalies in each synoptic pattern. Excluding the nine average SN pattern years, the synoptic patterns identified 23 of 26 (89%) SN patterns which is a higher percentage than any of the previously tested large-scale indices. These important results clearly indicated that the frequency of winter synoptic patterns can best represent the physical explanation for the annual SN patterns across the five-state region.

Also in Chapter 5 the time series of SN patterns identified that three periods existed: 1951 to 1972 when only north wet/south dry gradient SN patterns existed, 1973 to 1974 when there was a transition from one north-to-south gradient pattern to the other, and 1975 to 1985 when only north dry/south wet gradient SN patterns existed. This study identified that the number of WNW and meridional NW synoptic patterns in a year identified 7 of 8 north wet/south dry SN patterns and that these patterns decreased by 12% from the earlier (1951-1972) period to the later (1975-1985) period. At the same time, the number of cut-off and split-flow synoptic patterns in a year identified all four north dry/south wet SN patterns and these patterns increased by 7% from the

earlier period to the later period. These results clearly confirm the hypotheses that the north-to-south gradient patterns are associated with different synoptic patterns and that the multidecadal changes in SN across the region during the mid 1970s are tied to the change in north-to-south gradient patterns resulting from the change in frequency of different winter synoptic patterns. The long-term changes in frequency of certain synoptic patterns represents the physical explanation for the multidecadal changes identified in SN across the five-state Rocky Mountain region.

Chapters 3 and 4 explained differences in spatial variability at the surface by the physical variable, aspect. Stable sites or watersheds were exposed to upper airflows from the west or north (270′ to 360′), while unstable sites or watersheds were exposed to upper airflows from the south or east (30′ to 260′). In this study synoptic patterns that provided west to north upper airflows (including WNW and meridional NW patterns), had low variability, while synoptic patterns that provided south to east upper airflows (including the split-flow and the cut-off patterns), had high variability. These results provide some indication about the association of synoptic patterns to spatial variability of SN and PR across the five-state region; however, these results are not conclusive. Further research may improve the significance of these results.

Rocky Mountain winter synoptic patterns averaged over the 11 ENSO events indicated that during ENSO events, WNW and meridional NW synoptic patterns combined decreased 5% while combined cut-off and split-flow synoptic patterns increased 3.5%. Similar increases and decreases were identified when synoptic patterns were averaged over the

12 PNA events. During the six years when both the PNA and ENSO occurred concurrently, the WNW and meridional NW synoptic patterns decreased an average 11% while the cut-off and split-flow synoptic patterns increased an average 10%. However, when considering anomalies for individual years, only five of 11 ENSO events and five of 12 PNA events show a concurrent increase in cut-off and split-flow synoptic patterns and decrease in WNW and meridional NW synoptic patterns. This suggests that ENSO or PNA events are associated with anomalous large-scale patterns that can differ in location by 300 to 500 hundred miles from one event to another. Small changes in the large-scale circulations can alter the frequency of some synoptic patterns. These interesting results indicate that the association between large-scale indices and winter synoptic patterns is not conclusive. Further research is needed to identify if there is any significant physical link between large-scale indices and SN across the the five-state region.

CHAPTER VIII

CONCLUSIONS AND SUGGESTIONS FOR FUTURE RESEARCH

Water stored in the winter snowpack of the Rocky Mountains is a variable resource for the West. Interrelated hydroclimatic elements were investigated to 1) determine how variable the elements are in the water source region, 2) identify spatial and temporal variability characteristics and patterns, and 3) detect what the physical explanations are for the variability located in a five-state region of the Rocky Mountains. The study covered a 35-year period from 1951-1985. The study included: 1) developing an interrelated hydroclimatic database, 2) analyzing 14 carefully selected watersheds, 3) analyzing complete and consistent snowpack and precipitation measurement sites in the five-state region, and 4) describing the association of large-scale circulation indices and patterns to hydroclimatic variability in the Rocky Mountains.

A database was developed that incorporated interrelated processes involved with hydroclimate. The three primary hydroclimatic elements that were chosen for analysis include total water-year streamflow (ST), winter (October 1-March 31) accumulated precipitation (PR), and April 1 snowpack (SN-snow water equivalent).

The results from the watershed analyses show that the range in variability values for 14 watersheds can be explained largely by

exposure or aspect to moist air flows. The measure of variability used in this study is

$$MOV = (X_{80\%} - X_{20\%})/X_{50\%}$$

where X represents SN, PR, or ST non-exceedence probability values. Stable basins (low variability) have measure of variability values less than 0.55 and are exposed to prevailing flows from the north and west, while more variable or unstable basins are exposed to infrequent flows from the south or east. Correlation analysis between hydroclimatic elements within basins identified SN as the best indicator of ST in 11 of 14 watersheds in the Rocky Mountains. Overall SN was determined to be the best monitor of winter climate in the Rockies. ST data in the West is so affected by man-made diversions that in most areas it is difficult to use as a representative measure of the hydroclimate.

Areal variability patterns were determined using 275 snow course sites and 266 cooperative weather stations in the region. Using both data sets, stable and unstable regions were separated by the 0.55 measure of variability isoline. The average variability differed by a factor of two from stable to unstable regions. Large mountain barriers in stable regions were exposed to northerly or westerly air flow, while large mountain barriers in unstable regions were exposed to southerly or easterly air flow. These regions identified by PR and SN variability differences represent a new hydroclimatic classification system for the West.

Based on objectively analyzed, non-exceedence April 1 snowpack and winter precipitation patterns, three basic and repeatable annual patterns emerged: 1) years with a consistent anomaly over the entire region, either wet or dry, 2) years with a distinct north-to-south

gradient, and 3) mixed years with average amounts as well as isolated areas of wet and dry located throughout the study region. The first two types of patterns occurred in 26 of the 35 years (74%). The correlation of regionally averaged SN to PR explained more than 50% of the variance west of the Continental Divide (C.D.), while correlations of regionally averaged SN to PR explained less than 20% of the variance east of the C.D. The distribution of SN patterns over 35 years showed that wet, dry, and average patterns were evenly distributed throughout the period. However, wet-north/dry-south gradient patterns did not occur after 1974, and dry-south/wet-north gradient patterns did not occur before 1973. Furthermore, ten-year running means of regionally averaged April 1 snowpack indicated that the northern regions have endured a statisically significant decrease in snowpack since the mid 1970s, while the southern regions have experienced a significant increase (20%) during the same period. These long-term wet and dry periods are due to north-to-south gradient patterns. Longer precipitation records also indicate that these long-term wet and dry periods exist back to the 1910s and are due to north-to-south gradient patterns.

Large-scale circulations associated with ENSO events provide more SN to unstable sites with a south or southwesterly exposure to moist air flow, while stable regions with exposures to northerly or westerly moist air flow are generally drier during ENSO events. Large-scale atmospheric/oceanic circulations are not well correlated ($|r| < +0.60$) to regionally averaged SN over the 35-year period, but r-values with opposite signs (+/-) in the northern stable and southern unstable regions indicates that the hydroclimatic interannual spatial

variability is apparently tied to large scale circulations. For the 26 years with marked patterns (all wet, all dry, or gradients), seasonally averaged indices such as the Southern Oscillation, the Pacific/North American, the Equatorial Pacific sea-surface temperature, and the local 700 mb height and dew-point depression anomalies identified between 62% to 77% of the snowpack patterns. The seasonally averaged PNA index identified 20 of 26 (77%) annual SN patterns, while monthly averaged 700 mb height and dew-point depression probabilities explained 80% of the annual SN patterns. These two high percentages illustrated that at least two mechanisms are involved in producing annual SN patterns: 1) seasonally averaged large-scale circulation patterns such as ENSO or PNA, and 2) regional anomalous precipitation events that occur in periods of a month or less. These seasonal and monthly large-scale indices should be used to identify annual SN patterns and identify whether or not they improve water supply forecasts. Long-term changes in the seasonally averaged values of large-scale indices occurred in the mid 1970s and are related to long-term changes in regionally averaged April 1 snowpack and the type of north-to-south gradient pattern experienced. The change in the mid 1970s in both the SN and the seasonal indices suggests that they are all dependent on some other physical phenomena that is a part of the global ocean-climate system. Since the economic and social impacts from the persistent wet and dry periods are sizable, further research should focus on identifying long-term variability characteristics and understanding the global ocean/climate system.

Finally, based on PR and SN distributions identified in Chapters 3 and 4, seven 500 mb Rocky Mountain winter synoptic patterns were

identified as the climatological group that explained almost 98% of the daily winter (October 1 - March 31) synoptic maps for the period from October 1950 through March of 1985. Each synoptic pattern was chosen because it represented a different airflow that provided precipitation opportunities for certain areas across the five-state region. The seven patterns included: 1) ridge, which is associated with dry precipitation anomalies across the five-state region, 2) meridional NW, WNW, and zonal, whihc are associated with potential wet precipitation anomalies across the northern regions, and 3) trough, split-flow, and cut-off, which are associated with potential wet anomalies across the southern regions. The five annual SN patterns described in earlier work were cleary identified by above average frequency of certain synoptic pattern(s): 1) wet SN years, increases in troughs (+5.3%) and cut-offs (+2.0%), 2) dry SN years, increases in ridges (+11.9%), 3) north-wet/south-dry SN years, increases in WNW (+8.6%) and meridional NW (+1.8%), 4) north-dry/south-wet SN years, increases in cut-offs (+11.9%) and split-flow (+1.3%), and 5) average SN years showing no increases greater than 2% in any synoptic pattern. The synoptic patterns identified 89% of the non-average SN years which is better than any of the large-scale indices. These important results clearly indicated that the frequency of winter synoptic patterns can best represent the physical explanation for the annual SN patterns across the five-state region. This study identified that the combination of WNW and meridional synoptic patterns (associated with north-wet/south-dry SN patterns) decreased by 12% from the earlier (1951-1972) period to the later (1975-1985) period. At the same time, the combination of cut-off and split-flow synoptic patterns (associated with north-

dry/south-wet SN patterns) increased 7% from the earlier period to the later period. These results clearly confirm the hypotheses that the north-to-south gradient patterns are associated with different synoptic patterns and that the multidecadal changes in regionally averaged SN across the five-state region during the mid 1970s are tied to the change in north-to-south gradient patterns resulting from the change in frequency of certain synoptic patterns. Furthermore, the long-term changes in the frequency of certain synoptic patterns represents the physical explanation for 1) the change in north-to-south gradient years and 2) the multidecadal changes identified in regionally averaged SN across the Rockies. Analyses that considered the association of variability in winter synoptic patterns to the spatial variability of SN identified some potentially interesting but inconclusive results: 1) the less variable synoptic patterns that influenced the stable SN regions were the WNW and the meridional NW (associated with west to north airflow) and 2) the more variable synoptic patterns that influenced the unstable SN regions were the cut-off and the split-flow (associated with west to south airflow). The analyses of large-scale indices such as ENSO and PNA to winter synoptic patterns found that when all ENSO or PNA years were averaged, positive or negative anomalies occurred in certain synoptic patterns. However, when trying to identify individual ENSO or PNA years by anomalies in certain synoptic pattern frequencies, less than half of the large-scale events were detected. This implies that during large-scale events the anomalous large-scale patterns are often shifted enough to apparently provide for somewhat different distributions in winter synoptic patterns. These results indicated that the association between large-

scale indices and winter synoptic patterns is not conclusive and further research is needed.

REFERENCES

Abramopoulus, F., C. Rosenzweig, and B. Choudhury, 1988: Improved ground hydrology calculations for Global Climate Models (GCMs): Soil water movement and evapotranspiration. J. Climate, 1, pp. 921-941.

Angell, J. K., J. Korshover, and G. F. Cotton, 1984: Variation in United States cloudiness and sunshine, 1950-1982. J. Climate Appl. Meteor., 23, pp. 752-761.

Angell, J. K. and J. Korshover, 1987: Variability in United States cloudiness and relation to El Nino. J. Climate Appl. Meteor., 26, pp. 580-584.

Aston, A. R., 1984: The effect of doubling atmospheric CO2 on streamflow: A simulation. J. Hydrology, 67, pp. 273-280.

Barry, R. G., 1973: A climatological transect along the east slope of the Front Range, Colorado. Arct. Alp. Res., 5, pp. 89-110.

Barry, R. G., 1981: Mountain weather and climate. New York, Methuen, Inc., 313 p.

Bartlein, P. J., 1982: Streamflow anomaly patterns in the United States and southern Canada 1951-1970. J. Hydrology, 57, pp. 49-63.

Blaising, T. J. and G. R. Lofgren, 1980: Seasonal climatic anomaly types for the northern Pacific sector and western North America. Mon. Wea. Rev., 108, pp. 700-719.

Bradley, R. S., 1980: Secular fluctuations of temperature in the Rocky Mountain states and a comparison with precipitation fluctuations. Mon. Wea. Rev., 108, pp. 873-885.

California Institute of Technology, 1943: Synoptic weather types of North America. Technical paper from Meteorology Department. Pasadena, CA, Dec. 1950, 161 pp.

Caine, N., 1975: An elevation control of peak snowpack variability. Water Res. Bull., 11, pp. 613-621.

Cane, M. A., 1983: Oceanographic events during El Nino. Science, 222, pp. 1189-1195.

Cayan, D. R. and J. O. Roads, 1984: Local Relationships between United States west coast precipitation and monthly mean circulation parameters. Mon. Wea. Rev., 112, pp. 1276-1282.

Cayan, D. R. and D. H. Peterson, 1990: The influence of north Pacific atmospheric circulations on streamflow in the West. Geophysical Monograph No. 55, pp. 375-397.

Changnon, D., T. B. McKee, N. J. Doesken, 1989: Hydroclimatic variability in selected watersheds located in the Rocky Mountains. Preprints, Sixth Conference on Applied Climatology, 7-10 March 1989, Charleston, SC, pp. 55-59.

Chen, S-C and K. E. Trenberth, 1988: Forced planetary waves in the northern hemispheric winter: Wave-coupled orographic and thermal forcings. J. Atmos. Sci., 45, pp. 682-704.

Chen, W. Y., 1982: Fluctuations in northern hemispheric 700 mb height fields associated with the Southern Oscillation. Mon. Wea. Rev., 110, pp. 808-823.

Conrad, V., 1941: The variability of precipitation. Mon. Wea. Rev., 69, pp. 5-11.

Cowie, J. R. and T. B. McKee, 1986: Colorado precipitation event and variability analysies. Climatology Report No. 86-3, Dept. Atmospheric Sciences, Colorado State University, 102 p.

Day, G. N., J. C. Schaake, and J. H. Ellis, 1989: A direction toward improved streamflow forecasting in the Western mountatins. Preprints, 57th Western Snow Conference, 18-20 April 1989, Ft. Collins, CO, pp. 79-89.

Diaz, H. F. and D. C. Fulbright, 1981: Eigenvector analysis of seasonal temperature, precipitation and synoptic scale system frequency over the contiguous United States. Part 1: Winter. Mon. Wea. Rev., 109, pp. 1267-1284.

Diaz, H. F. and J. Namias, 1983: Association between anomalies of temperature and precipitation in the United States and western northern hemispheric 700 mb height profiles. J. Climate Appl. Meteor., 22, pp. 352-363.

Diaz, H. F., 1990: Large-scale differences in atmospheric circulation patterns associated with wet and dry regions in the United States. Preprints, AMS Symposium on Global Change Systems - Special Session on Climate Variations and Hydrology, 5-9 February 1990, Anaheim, CA, pp. 184-188.

Doesken, N. J., B. A. Shafer, and T. B. McKee, 1981: Winter drought in the Colorado mountains. Preprints, Second Conf. on Mountain Meteor., Ft. Collins, CO, pp. 57-58.

Doesken, N. J., D. Changnon, and T. B. McKee, 1989: Interannual variations in snowpack in the Rocky Mountain region. Preprints, 57th Western Snow Conference, 18-20 April 1989, Ft. Collins, CO, 10 p.

Douglas, A. V., D. R. Cayan, and J. Namias, 1982: Large-scale changes in north Pacific and North American weather patterns in recent decades. Mon. Wea. Rev., 110, pp. 1851-1862.

Esbensen, S. K., 1984: A comparison of intermonthly and interannual teleconnections in 700 mb geopotential height fields during the northern hemispheric winter. Mon. Wea. Rev., 112, pp. 2016-2023.

Elliott, R. D., 1950: Extended-range forecasting by weather types. Published in the Compendium of Meteorology, New York, NY, 1950, pp. 834-840.

Faiers, G. E., 1988: Defining normal precipitation. Nat. Wea. Dig., 13, pp 20-22.

Faiers, G. E., 1989: Normality and variability of seasonal snowfall in the eastern two-thirds of the United States. Nat. Wea. Dig., 14, pp. 23-25.

Gleick, P., 1986: Methods for evaluating the regional hydrologic impacts of global climatic changes. J. Hydrology, 88, pp. 97-116.

Gleick, P., 1987: The development and testing of a water balance model for climate impact assessment: Modeling the Sacramento Basin. Wat. Resourc. Research, 23, pp. 1049-1061.

Grant, L. O. and A. M. Kahan, 1974: Weather modification for augmenting orographic precipitation. Weather and Climate Modification, W. N. Hess, Ed., John Wiley and Sons, pp. 282-317.

Gray, W. M, 1990: Strong association between West African rainfall and U.S. landfall of intense hurricances. Science, 249, pp. 1251-1256.

Hastenrath, S., 1990: Decadal-scale changes of the circulation in the tropical Atlantic sector associated with Sahel drought. Inter. J. Climatology, 10, pp. 459-472.

Hershfield, D. M., 1962: A note on the variability of annual precipitation. J. Appl. Meteor., 1, pp. 575-578.

Hjermstad, L. M., 1970: The influence of meteorological parameters on the distribution of precipitation across central Colorado mountains. M. S. Thesis, Colorado State University, Ft. Collins, CO, 87 p.

Hindman, E. E., 1986: An atmospheric water balance over a mountain barrier. J. Climate Appl. Meteor., 25, pp. 180-183.

Horel, J. D. and J. M. Wallace, 1981: Planetary-scale atmospheric phenomena associated with the Southern Oscillation. Mon. Wea. Rev., 109, pp. 813-829.

Kiladis, G. N. and H. F. Diaz, 1989: Global climatic anomalies associated with extremes in the Southern Oscillation. J. Climate, 2, pp. 1069-1090.

Klazure, G. E., 1983: Description of winter precipitation characteristics in the upper Colorado river basin. Preprints, 16th Conference on Agriculture and Forest Meteorology, Ft. Collins, CO, pp. 167-172.

Klazure, G. E., A. B. Super, and J. G. Medina, 1985: Precipitation gauge siting for evaluation of an orographic cloud seeding demonstration project in the central Rocky's. Preprints, 4th WMO Scientific Conf. Weather Modification, Honolulu, HA, pp. 75-80.

Klein, W. H. and J. M. Kline, 1984: The synoptic climatology of monthly mean surface temperature in the United States during winter relative to surronding 700 mb height field. Mon. Wea. Rev., 112, pp. 433-448.

Lins, H. F., 1985: Streamflow variability in the United States: 1931-1978. J. Climate Appl. Meteor., 24, pp. 463-471.

Longley, R. W., 1952: Measures of the variability of precipitation. Mon. Wea. Rev., 80, pp. 111-117.

Lussky, G. R., 1989: Current issues relating to the El Nino/Southern Oscillation. Nat. Wea. Dig., 14, pp. 26-31.

Manabe, S. and R. T. Weatherald, 1975: The effects of doubling the CO_2 concentration on the climate of a GCM. J. Atmos. Sci., 32, No. 1, pp. 3-15.

Marlatt, W. and H. Riehl, 1963: Precipitation regimes over the upper Colorado River. J. Geoph. Res., 68, pp. 6447-6458.

McKee, T. B., D. Changnon, and N. J. Doesken, 1989: Data for hydroclimatic research in the Rocky Mountain region. Preprints, Sixth AMS Conference on Applied Climatology, 7-10 March 1989, Charleston, SC, pp. 162-163.

Medina, J. G. and P. W. Mielke Jr., 1985: A comparison of permutation procedure results between mean, median, and individual station winter precipitation employed to estimate treatment differences from cloud seeding. Preprints, 4th WMO Scientific Conf. Weather Modification, Honolulu, HA, pp. 307-316.

Meko, D. M. and C. W. Stockton, 1984: Secular variations in streamflow in the western United States. J. Climate Appl. Meteor., 23, pp. 889-897.

Namias, J., 1978: Multiple causes of the North American abnormal winter 1976-77. Mon. Wea. Rev., 106, pp. 279-295.

Namias, J., 1986: Persistence of flow patterns over North America and adjacent ocean sectors. Mon. Wea. Rev., 114, pp. 1368-1383.

Namias, J., X. Yuan, and D. R. Cayan, 1988: Persistence of north Pacific sea surface temperature and atmospheric flow patterns. J. Climate, 1, pp.682-703.

Nicholson, S. E., 1986: The spatial coherence of African rainfall anomalies: Interhemispheric teleconnections. J. Climate Appl. Meteor., 25, pp. 1365-1381.

Nitta, T. and S. Yamada, 1989: Recent warming of the tropical sea surface temperature and its relationship to the northern hemispheric circulation. J. Meteor. Soc. Japan, 67, pp. 375-383.

Parthasarathy, B. and G. B. Pant, 1985: Seasonal relationships between Indian summer monsoon rainfall and the Southern Oscillation. J. Climatology, 5, pp. 369-378.

Peck, E. L., 1972: Relation of orographic precipitation patterns to meteorological parameters. In Distribution of Precipitation in Mountainous Areas, vol. II. Geneva, World Meteorological Organization No. 326, pp. 234-242.

Peck, E. L. and M. J. Brown, 1962: An approach to the development of isohyetal maps for mountainous areas. J. Geoph. Res., 67, pp. 681-694.

Peck, E. L. and J. C. Schaake, 1990: Network design for water supply forcasting in the West. Water Resour. Res. Bull., 26, pp. 87-99.

Peterson, D. H., D. R. Cayan, J. Dileo-Stevens, and T. G. Ross, 1987: Some effects of climate variability on hydrology in western North America. Preprints, The Influence of Climate Change and Climate Variability on the Hydrologic Regime and Water Resources, August 1987, Vancouver, Canada, pp. 45-61.

Pilgrim, D. H., 1983: Some problems in transferring hydrologic relationships between small and large drainage basins and between regions. J. Hydrology, 65, pp. 49-72.

Quinn, W. H., D. O. Zopf, K. S. Short, and R. T. W. Kuo-Yang, 1978: Historical trends and statistics of the Southern Oscillation, El Nino and Indonesian droughts, Fishery Bull., 76, pp. 663-691.

Rasmussen, J. L., 1968: Atmospheric water balance of the upper Colorado River basin. Dissertation Colorado State University, Department of Atmospheric Sciences, Ft. Collins, CO, 112 p.

Rasmusson, E. M. and T. H. Carpenter, 1982: Variations in tropical SST and surface wind fields associated with Southern Oscillation/El Nino. Mon. Wea. Rev., 110, pp. 354-384.

Rasmusson, E. M. and J. M. Wallace, 1983: Meteorological aspects of El Nino/ Southern Oscillation. Science, 222, pp. 1195-1202.

Rasmusson, E. M. and P. A. Arkin, 1990: Measuring and understanding global precipitation variability. Preprints, Symposium on Global Change Systems Special Session on Climate Variations and Hydrology, 5-9 February 1990, Anaheim, CA, pp. 37-44.

Redmond, K. T. and R. W. Koch, 1990: Western surface climate and streamflow and the El Nino/Southern Oscillation. International Symposium on the hydraulics/hydrology of arid lands. American Society of Civil Engineers. July 30 to August 3, 1990, San Diego, CA, pp. 567-572.

Rhea, J. O., 1978: Orographic precipitation model for hydrometeorological use. Ph.D. thesis, Colorado State University, Ft. Collins, CO, 221 p.

Rhea, J. O. and L. O. Grant, 1974: Topographic influences on snowfall patterns in mountainous terrain. In Advanced Concepts and Techniques in the Study of Snow and Ice Resources. Washington, D.C., National Academy of Science, pp. 182-192.

Rind, D., 1988: The doubled CO2 climate and the sensitivity of the modeled hydrologic cycle. J. Geoph. Res., 93, D5, 5385-5412.

Ropelewski, C. F. and M. S. Halpert, 1986: North American precipitation and temperature patterns associated with El Nino/Southern Oscillation (ENSO). Mon. Wea. Rev., 114, pp. 2352-2362.

Ropelewski, C. F. and M. S. Halpert, 1990: Interannual variability and the detection of climatic trends. Preprints, Symposium on Global Change Systems - Special Session on Climate Variations and Hydrology. 5-9 February 1990, Anaheim, CA, pp. 96-99.

Sellers, W. D., 1968: Climatology of monthly precipitation patterns in the western United States , 1931-1966. Mon. Wea. Rev., 96, pp.585-595.

Spreen, W. C., 1947: Determination of the effect of topography on precipitation. Trans. Am. Geophys., 28, pp. 285-290.

Toy, T. J., 1981: Precipitation variability and surface-mine reclamation in the Green, Powder and San Juan River basins. J. Appl. Meteor., 20, pp. 756-764.

Trenberth, K. E., 1976: Spatial and temporal variations of the Southern Oscillation. Quart. J. Roy. Meteor. Soc., 102, pp. 639-653.

Trenberth, K. E., G. W. Branstator, and P. A. Arkin, 1988: Origins of the 1988 North American drought. Science, 242, pp. 1640-1645.

Trenberth, K. E., 1990: Recent observed interdecadal climate changes. Preprints, Symposium on Global Change Systems - Special Sessions on Climate Variations and Hydrology, 5-9 February, 1990, Anahiem, CA, pp. 91-95.

van Loon, H. and J. C. Rogers, 1978: The seesaw in winter temperatures between Greenland and Northern Europe. Part 1: General description. Mon. Wea. Rev., 106, pp.296-310.

Wallace, J. M. and D. S. Gutzler, 1981: Teleconnections in geopotential height fields during the northern hemisphere winter. Mon. Wea. Rev., 109, pp. 784-812.

Wallace, J. M., 1990: Mechanisms of atmosphere-ocean interaction in ENSO. Preprints, Symposium on Global Change Systems - Special Session on Climate Variations and Hydrology, 5-9 February, 1990, Anaheim, CA, pp. 4-10.

Weaver, R. L., 1968: Meteorology of major storms in western Colorado and Eastern Utah. Weather Bureau Technical Memorandum HYDRO-7, Office of Hydrology. Washington D.C., 75p.

Weiss, E. B., 1982: Value of seasonal forecasts in managing energy resources. J. Appl. Meteor., 21, pp. 510-517.

Weiss, L. L. and W. T. Wilson, 1958: Precipitation gauge shields. Transactions, International Association of Scientific Hydrology, Toronto, 1957, Vol. 1, pp. 462-484.

Yarnal, B., 1985: A 500 mb synoptic climatology of Pacific north-west coast winters in relation to climatic variability, 1948-1949 to 1977-1978. J. Climatology, 5, pp. 237-251.

Yarnal, B, and H. F. Diaz, 1986: Relationship between extremes of the Southern Oscillation and winter climate of the Anglo-American Pacific Coast. J. Climatology, 6, pp. 197-219.

Yeh, T. C., R. T. Wetherald, and S. Manabe, 1984: The effects of soil moisture on short-term climate and hydrology change - A numerical experiment. Mon. Wea. Rev., 112, pp. 474-490.

APPENDIX I

PR SITES AND THEIR CHARACTERISTICS FOR EACH REGION

In Chapter II, 266 cooperative weather stations were chosen to analyze hydroclimatic variability in the five-state region. Separated into the the 12 PR regions discussed in Chapter IV, information is provided about each of the 266 PR stations in Table I.1. The site characteristics include, station name and number, median value of PR, measure of variability value, elevation, latitude and longitude. Figure I.1 shows the median PR value plotted for a selected number of NWS cooperative weather stations.

Table I.1 For each region, PR sites and their characteristics are listed.

Region number and type / Name	Station Number	Median Value	Measure of Variability	Elevation (feet)	Lat.	Long.
1. stable						
Bonners Ferry	101079	15.73	0.49	1860′	48 41′	116 19′
Priest River Exp. St.	107386	21.03	0.29	2380′	48 21′	116 50′
Coeur d'Alene	101956	17.57	0.36	2158′	47 41′	116 45′
Wallace Woodland Park	109498	25.11	0.37	2935′	47 30′	115 53′
Moscow U. of I.	106152	15.85	0.33	2660′	46 44′	116 58′
Lewiston WSO AP	105241	6.85	0.60	1413′	46 23′	117 01′
Nezperce	106424	11.01	0.45	3145′	46 15′	116 15′
Kamaih	104793	12.46	0.48	1212′	46 14′	116 01′
McCall	105708	18.82	0.46	5025′	44 54′	116 07′
Cambridge	101408	14.64	0.28	2650′	44 34′	116 41′
Centerville Arb. Rch.	101636	19.79	0.52	4300′	43 54′	115 51′
Emmitt 2E	102942	9.17	0.48	2500′	43 52′	116 28′
Boise WSFO	101022	7.71	0.50	2838′	43 34′	116 13′
Hill City	104268	10.42	0.55	5090′	43 18′	115 03′
Sand Point Exp. St.	108137	22.33	0.34	2100′	48 18′	116 33′
Island Park Dam	104598	18.12	0.49	6300′	44 25′	111 24′
St. Anthony 1WNW	108022	7.42	0.51	4950′	43 58′	111 43′
Deer Flat Dam	102444	6.27	0.43	2510′	43 35′	116 45′
Lincoln R.S.	245040	9.49	0.54	4540′	46 57′	112 39′
Babb	240392	5.02	0.46	4300′	48 56′	113 22′

Fortine 1N	243139	7.15	0.54	3000′ 48 47′ 114 54′
Polebridge	246615	12.46	0.46	3690′ 48 47′ 114 16′
West Glacier	248809	16.57	0.41	3154′ 48 30′ 113 59′
Hungry Horse Dam	244328	17.87	0.40	3160′ 48 21′ 114 00′
Kalispell WSO AP	244558	7.35	0.46	2965′ 48 14′ 114 16′
Creston	242104	8.48	0.48	2940′ 48 11′ 114 08′
Libby 1NE	245015	12.06	0.38	2080′ 48 24′ 115 32′
Heron 3NW	244084	22.51	0.33	2240′ 48 05′ 116 00′
Polson Kerr Dam	246640	6.03	0.53	2730′ 47 41′ 114 14′
Haugen 3E	243984	20.14	0.47	3100′ 47 23′ 115 21′
Superior	248043	9.09	0.49	2710′ 47 12′ 114 53′
St. Ignatius	247286	6.34	0.43	2900′ 47 19′ 114 06′
Seely Lake R.S.	247448	12.88	0.50	4100′ 47 13′ 113 31′
Missoula	245745	5.95	0.42	3190′ 46 55′ 114 05′
Divide 2NW	242421	3.66	0.47	5406′ 45 46′ 112 47′
Silver Lake	247605	6.93	0.45	2510′ 46 10′ 113 13′
2, stable				
Oakley	106542	4.87	0.42	4600′ 42 14′ 113 53′
Burley FAA	101303	5.37	0.45	4146′ 42 32′ 113 46′
Minidoka Dam	105980	5.02	0.53	4210′ 42 40′ 113 29′
Pocatella	107211	5.58	0.56	4444′ 42 55′ 112 36′
Palisades Dam	106764	10.19	0.43	5385′ 43 21′ 111 13′
Grace	103732	6.96	0.43	5550′ 42 35′ 111 44′
Montpieler	106053	7.30	0.37	5960′ 42 19′ 111 18′
Lifton Pumping St.	105275	4.12	0.52	5926′ 42 07′ 111 18′
Border 3N	480915	6.51	0.54	6120′ 42 15′ 111 02′
Evanston 1E	483100	4.69	0.51	6810′ 41 16′ 110 57′
Bear River Refuge	420506	6.32	0.59	4208′ 41 28′ 112 16′
Ogden Sugar Fac.	426414	8.02	0.59	4280′ 41 14′ 112 02′
Ogden Pioneer	426404	11.69	0.53	4350′ 41 15′ 111 57′
Laketown	424856	5.85	0.45	5980′ 41 49′ 111 19′
Morgan	425826	10.89	0.57	5060′ 41 02′ 111 41′
Salt Lake City WSO	427598	8.24	0.55	4222′ 40 46′ 111 58′
Garfield	423097	8.28	0.59	4310′ 40 43′ 112 12′
Utah Lake Lehi	428973	5.69	0.55	4497′ 40 22′ 111 54′
Elberta	422418	5.48	0.52	4690′ 39 57′ 111 57′
Snake Creek PH	427909	14.30	0.41	5950′ 40 33′ 111 30′
Cottonwood Wier	421759	13.34	0.45	4960′ 40 37′ 111 47′
Echo Dam	422385	6.97	0.59	5470′ 40 58′ 111 26′
Coalville	421588	8.02	0.46	5550′ 40 55′ 111 24′
3, stable				
Little Hills	055048	5.65	0.53	6140′ 40 00′ 108 12′
Hamilton	053738	8.99	0.46	6230′ 40 22′ 107 37′
Hayden	053897	8.97	0.51	6375′ 40 29′ 107 15′
Pyramid	056797	11.11	0.59	8009′ 40 14′ 107 05′
Steamboat Springs	057936	13.32	0.47	6770′ 40 30′ 106 50′
Yampa	059265	6.72	0.42	7892′ 40 09′ 106 54′
Grand Lake 1NW	053496	8.96	0.47	8680′ 40 16′ 105 50′
Grand Lake 6SSW	053500	5.55	0.45	8288′ 40 11′ 105 52′
Winter Park	059175	13.12	0.44	9058′ 39 54′ 105 46′
Green Mtn. Dam	053592	6.58	0.41	7740′ 39 53′ 106 20′

Dillon 1E	052281	6.17	0.58	9065' 39 38' 106 02'
Breckenridge	050909	7.80	0.54	9580' 39 29' 106 02'
Climax	051660	10.82	0.54	11350' 39 22' 106 11'
Taylor Park	058184	7.35	0.56	9206' 38 49' 106 37'
Grand Junction WSO	053488	4.14	0.55	4849' 39 07' 108 32'
Colorado Nat. Mon.	051772	5.42	0.52	5780' 39 06' 108 44'
Shoshone	057618	10.12	0.50	5933' 39 34' 107 14'
Eagle	052454	4.49	0.55	6497' 39 39' 106 55'
Berthoud Pass	050674	19.22	0.40	11314' 39 48' 105 47'
4. stable				
Lima	245030	2.43	0.60	6270' 44 39' 112 35'
Lakeview	244820	8.08	0.59	6710' 44 36' 111 48'
West Yellowstone	248857	11.67	0.55	6662' 44 39' 111 06'
Hebgen Dam	244038	16.24	0.52	6489' 44 52' 111 20'
Dillon WMCE	242409	2.91	0.53	5228' 45 12' 112 38'
Dillon Airport	242404	2.34	0.55	5218' 45 15' 112 33'
Virginia City	248597	4.92	0.46	5776' 45 18' 111 57'
Trident	248363	2.74	0.60	4036' 45 57' 111 29'
Townsend	248324	2.99	0.60	3833' 46 19' 111 31'
Bozeman 12NE	241050	14.80	0.52	5950' 45 49' 110 53'
Livingston	245086	4.39	0.54	4653' 45 42' 110 27'
Belgrade	240622	4.40	0.59	4451' 45 47' 111 09'
Bozeman Univ.	241044	6.46	0.51	4856' 45 40' 111 03'
Norris Madison	246157	5.55	0.52	4745' 45 29' 111 38'
Wisdom	249067	4.21	0.48	6060' 45 37' 113 27'
Ennis	242793	3.30	0.61	4953' 45 21' 111 43'
Gibson Dam	243489	6.09	0.47	4590' 47 36' 112 46'
Augusta	240364	3.46	0.50	4070' 47 29' 112 23'
Sun River	248021	2.88	0.58	3560' 47 29' 111 44'
Great Falls WSFO	243751	5.04	0.29	3662' 47 29' 111 22'
Ft. Benton	243113	4.18	0.48	2636' 47 49' 110 40'
Cascade 5S	241552	3.91	0.50	2290' 47 13' 111 43'
Holter Dam	244241	2.68	0.56	3487' 47 00' 112 01'
Helena WSFO	244055	3.55	0.55	3828' 46 36' 112 01'
Tower Falls	489025	6.72	0.52	6266' 44 55' 110 25'
Yellowstone Park	489905	6.20	0.55	6200' 44 58' 110 42'
Lake Yellowstone	485345	9.25	0.57	7762' 44 33' 110 24'
5. stable				
Encampment 10ESE	483045	6.14	0.53	7387' 41 11' 106 37'
6. unstable				
Fairfield R.S.	103108	10.70	0.62	5065' 43 21' 114 47'
Mackay R.S.	105462	3.82	0.77	5897' 43 55' 113 37'
Grouse	103882	5.88	0.89	6100' 43 42' 113 37'
Howe	104384	3.66	0.80	4820' 43 47' 113 00'
Dubois Exp. St.	102707	4.65	0.61	5452' 44 15' 112 12'
Hamer 4NW	103964	3.49	0.87	4791' 43 58' 112 16'
Idaho Falls AP	104457	4.44	0.75	4730' 43 31' 112 04'
Aberdeen Exp. St.	100010	4.23	0.65	4405' 42 57' 112 50'
Hazelton	104140	6.20	0.65	4060' 42 36' 114 08'
Richfield	107673	7.60	0.61	4306' 43 04' 114 09'

7, unstable				
Ibapah	424175	3.34	0.69	5280' 40 02' 113 59'
Desert Exp. Range	422116	2.15	0.97	5252' 38 36' 113 45'
Milford WSO	425654	4.38	0.64	5028' 38 26' 113 01'
Modena	425752	3.88	1.09	5460' 37 48' 113 55'
Gunlock Powerhouse	423506	5.71	1.25	4060' 37 17' 113 43'
New Harmony	426181	9.45	1.25	5290' 37 29' 113 18'
Zion Nat. Park	429717	7.56	0.90	4050' 37 13' 112 59'
Beaver Canyon PH	420527	9.41	0.86	7275' 38 16' 112 29'
Loa	425148	2.37	0.98	7080' 38 24' 111 39'
Richfield Radio KSVC	427260	3.94	0.63	5270' 38 46' 112 05'
Salina	427557	4.80	0.65	5190' 38 57' 111 52'
Ferron	422798	3.66	0.96	5930' 39 05' 111 08'
Scipio	427714	6.80	0.93	5306' 39 15' 112 06'
Morini	425837	5.17	0.78	5525' 39 32' 111 35'
Nephi	426135	7.33	0.68	5130' 39 42' 111 50'
Scofield Dam	427724	7.60	1.06	7630' 39 47' 111 07'
Roosevelt	427395	3.01	0.97	5104' 40 18' 109 59'
Vernal Airport	429111	3.41	0.72	5280' 40 27' 109 31'
Rock Springs	487845	3.60	0.58	6741' 41 36' 109 04'
Fruita	053146	4.09	0.76	4510' 39 10' 108 44'
Alterbern	050214	7.76	0.63	5690' 39 30' 108 23'
8, unstable				
Thompson	428705	4.36	0.84	5150' 38 58' 109 43'
Bluff	420788	4.27	0.95	4315' 37 17' 109 33'
Gateway	053246	5.34	0.59	4560' 38 40' 108 59'
Cedaredge	051440	5.78	0.65	6244' 38 54' 107 56'
Cochetopa Creek	051713	4.54	0.59	8000' 38 26' 106 46'
Lake City	054734	5.74	0.70	8670' 38 03' 107 19'
Saguache	057337	2.26	1.02	7697' 38 05' 106 09'
Great Sand Dunes	053541	2.69	0.80	8120' 37 43' 105 32'
Blanca	050776	2.11	0.85	7750' 37 26' 105 31'
Center	051458	1.97	0.92	7683' 37 44' 106 08'
Del Norte	052184	3.13	0.94	7884' 37 40' 106 21'
Hermit	053951	5.90	0.89	9000' 37 46' 107 08'
Telluride	058204	10.21	0.62	8800' 37 57' 107 49'
Tacoma	058154	10.28	0.72	7300' 37 31' 107 47'
Vallecito Dam	058582	14.27	0.74	7650' 37 22' 107 35'
Ignacio	054250	7.07	0.80	6460' 37 08' 107 38'
Durango	052432	9.63	0.72	6600' 37 17' 107 53'
Mancos	055327	8.10	0.80	6975' 37 21' 108 18'
Mesa Verde Nat. Park	055531	9.27	0.81	7070' 37 12' 108 29'
Dolores	052326	9.89	0.63	6950' 37 28' 108 30'
9, unstable				
Cut Bank	242173	2.22	0.75	3838' 48 36' 112 22'
East Glacier	242629	16.44	0.61	4806' 48 27' 113 13'
Valier	248501	2.18	0.68	3805' 48 19' 112 15'

Blackleaf	240877	3.70	0.60	4323′	48	01′	112	26′
Galata	243346	2.63	0.83	3100′	48	15′	111	25′
Joplin	244512	1.76	0.97	3360′	48	35′	110	47′
Simpson	247620	2.06	0.75	2740′	48	59′	110	19′
Big Sandy	240770	3.06	0.78	2700′	48	10′	110	07′
Choteau Airport	241737	1.86	0.81	3945′	47	49′	112	10′
Fairfield	242857	2.49	0.70	3983′	47	37′	111	59′
Rocky Boy	247148	4.48	0.66	3690′	48	15′	109	47′
Ft. Assinniboine	243110	2.89	0.72	2613′	48	30′	109	48′
White Water	248939	1.89	0.87	2355′	48	46′	107	38′
Forks 4NNE	243089	2.40	0.65	2600′	48	47′	107	28′
Glasgow WSO AP	243558	2.15	0.74	2280′	48	13′	106	37′
Lustre 4NNW	245285	2.00	0.67	2920′	48	27′	105	56′
Scobey	247424	3.02	0.83	2458′	48	47′	105	25′
Redstone	246927	2.06	0.83	2107′	48	50′	104	57′
Medicine Lake 3SE	245572	2.41	0.93	1952′	48	29′	104	27′
Culbertson	242122	2.54	0.89	1920′	48	09′	104	30′
Sidney	247560	2.59	0.75	1920′	47	44′	104	09′
Savage	247382	2.40	0.71	1985′	47	27′	104	21′
Glendive	243581	2.58	0.80	2076′	47	06′	104	43′
Jordan	244522	2.75	0.96	2590′	47	19′	106	54′
Haxby 18SW	244007	2.70	0.84	2650′	47	34′	106	42′
Roy 8NE	247228	2.99	0.85	3445′	47	26′	108	50′
Winifred	249033	4.00	0.64	3243′	47	33′	109	23′
Loma 1WNW	245153	3.40	0.76	2580′	47	56′	110	31′
Geraldine	243445	4.31	0.60	3130′	47	36′	110	16′
Harlowtown	243939	3.07	0.58	4160′	46	26′	109	50′
Barber	240466	3.20	0.59	3730′	46	19′	109	22′
Roundup	247214	2.64	0.69	3227′	46	27′	108	32′
Melstone	245596	3.82	0.59	2890′	46	36′	107	52′
Rock Springs	247136	2.21	0.96	3024′	46	49′	106	14′
Miles City FAA	245690	3.20	0.77	2629′	46	26′	105	52′
Wibaux	248957	2.48	0.95	2670′	46	59′	104	09′
Plevna	246601	2.58	0.95	2765′	46	25′	104	30′
Baker	240412	2.92	0.83	2929′	46	22′	104	16′
Mac Kenzie	245303	3.00	0.86	2810′	46	09′	104	44′
Ekalaka	242689	3.49	0.75	3425′	45	53′	104	32′
Belltower	240636	3.41	0.89	3300′	45	39′	104	23′
Volberg	248607	2.93	0.93	3030′	45	50′	105	40′
Crow Agency	242112	5.02	0.61	3030′	45	36′	107	27′
Ballantine	240432	3.90	0.60	3000′	45	57′	108	08′
Billings WSO	240807	4.97	0.58	3567′	45	48′	108	32′
Joliet	244506	4.89	0.58	3700′	45	29′	108	58′
Red Lodge	246918	9.39	0.65	5575′	45	11′	109	15′
Mystic Lake	245961	8.89	0.62	6558′	45	14′	109	45′
Columbus	241938	3.67	0.72	3585′	45	38′	109	14′
Rapelje 4S	246862	4.22	0.59	4125′	45	55′	109	15′
Big Timber	240780	4.10	0.66	4100′	45	50′	109	57′

10. unstable

Deaver	482415	1.01	0.66	4105' 44 53' 108 36'
Buffalo Bill Dam	481175	2.76	0.66	5156' 44 30' 109 11'
Worland	489770	1.53	0.86	4060' 44 01' 107 58'
Dubois	482715	2.09	0.62	6917' 43 33' 109 37'
Diversion Dam	482595	1.71	0.70	5575' 43 14' 108 56'
Pavillion	487115	1.52	0.86	5440' 43 15' 108 41'
Boysen Dam	481000	2.17	1.01	4642' 43 25' 108 11'
Sheridan	488155	1.47	0.73	3964' 44 46' 106 58'
Riverton	487760	1.99	0.75	4950' 43 01' 108 23'

11. unstable

Pathfinder Dam	487105	2.96	0.65	5930' 42 28' 106 51'
Rawlins FAA	487533	3.53	0.65	6736' 41 48' 107 12'
Larimee FAA	485415	3.08	0.73	7226' 41 19' 105 41'
Double Four Ranch	482680	3.71	0.64	6200' 42 11' 105 24'
Whalen Dam	489604	2.66	0.69	4294' 42 15' 104 38'
Cheyenne WSO	481675	3.13	0.66	6126' 41 09' 104 49'
Archer	480270	3.20	0.73	6010' 41 09' 104 39'
Carpenter	481547	2.30	1.01	5390' 41 03' 104 19'
Kauffman	054460	2.16	0.96	5250' 40 50' 103 56'
Fleming	052944	3.60	0.78	4248' 40 40' 102 50'
Leroy 5W	054945	3.75	1.05	4470' 40 29' 103 01'
Holyoke	054082	3.72	0.75	3730' 40 35' 102 18'
Akron FAA	050114	2.99	1.13	4663' 40 10' 103 13'
Wray 1E	059243	3.33	0.86	3560' 40 04' 102 13'
Bonny Lake	050834	2.91	1.14	3748' 39 38' 102 11'
Flagler	052932	3.05	0.97	4975' 39 19' 103 05'
Cheyenne Wells	051546	2.58	1.09	4250' 38 49' 102 21'
Eads	052446	3.09	0.82	4215' 38 29' 102 47'
Ordway	056131	2.26	0.85	4315' 38 13' 103 45'
Fowler	053079	2.06	0.95	4328' 38 07' 104 02'
Rocky Ford	057167	2.53	0.81	4170' 38 02' 103 42'
La Junta	054720	2.38	1.07	4190' 38 03' 103 31'
John Martin Dam	054388	1.97	1.19	3814' 38 04' 102 56'
Lamar	054770	2.87	0.86	3620' 38 07' 102 36'
Holly	054076	2.75	1.07	3390' 38 03' 102 07'
Troy	058568	2.70	0.89	5610' 37 08' 103 19'
Trinidad	058434	3.34	0.68	5746' 37 15' 104 20'
Walsenburg	058781	5.51	0.59	6150' 37 37' 104 48'
Rye	057315	7.59	0.58	6790' 37 55' 104 56'
Westcliffe	058931	4.43	0.75	7860' 38 08' 105 29'
Colorado Springs	051778	2.77	0.97	6090' 38 49' 104 43'
Cheesman	051528	4.64	0.65	6875' 39 13' 105 17'
Kassler	054452	5.82	0.70	5495' 39 30' 105 06'
Parker	056326	2.60	1.09	6310' 39 31' 104 39'
Denver	052220	4.72	0.68	5283' 39 45' 104 52'
Boulder	050848	5.78	0.64	5420' 40 00' 105 16'
Longmont 2N	055116	3.51	0.88	4950' 40 10' 105 04'
Estes Park	052759	3.26	0.68	7525' 40 23' 105 31'
Waterdale	058839	3.87	0.86	5230' 40 25' 105 12'
Ft. Collins	053005	3.90	0.70	5004' 40 35' 105 05'

12. stable

Broadus	241127	3.56	0.53	3030′ 45 26′ 105 24′
Biddle	240739	2.60	0.58	3339′ 45 06′ 105 20′
Shoshoni	488209	4.59	0.56	4830′ 43 14′ 108 07′
Kaycee	485055	3.37	0.52	4660′ 43 43′ 106 38′
Casper WSO	481570	4.14	0.43	5338′ 42 55′ 106 28′
Glenrock	483960	4.84	0.50	6430′ 42 40′ 105 49′
Rochelle	487810	2.93	0.51	4496′ 43 36′ 104 54′
Sundance	488705	4.39	0.38	4750′ 44 24′ 104 21′
Gillette 2E	483855	4.75	0.44	4556′ 44 17′ 105 28′

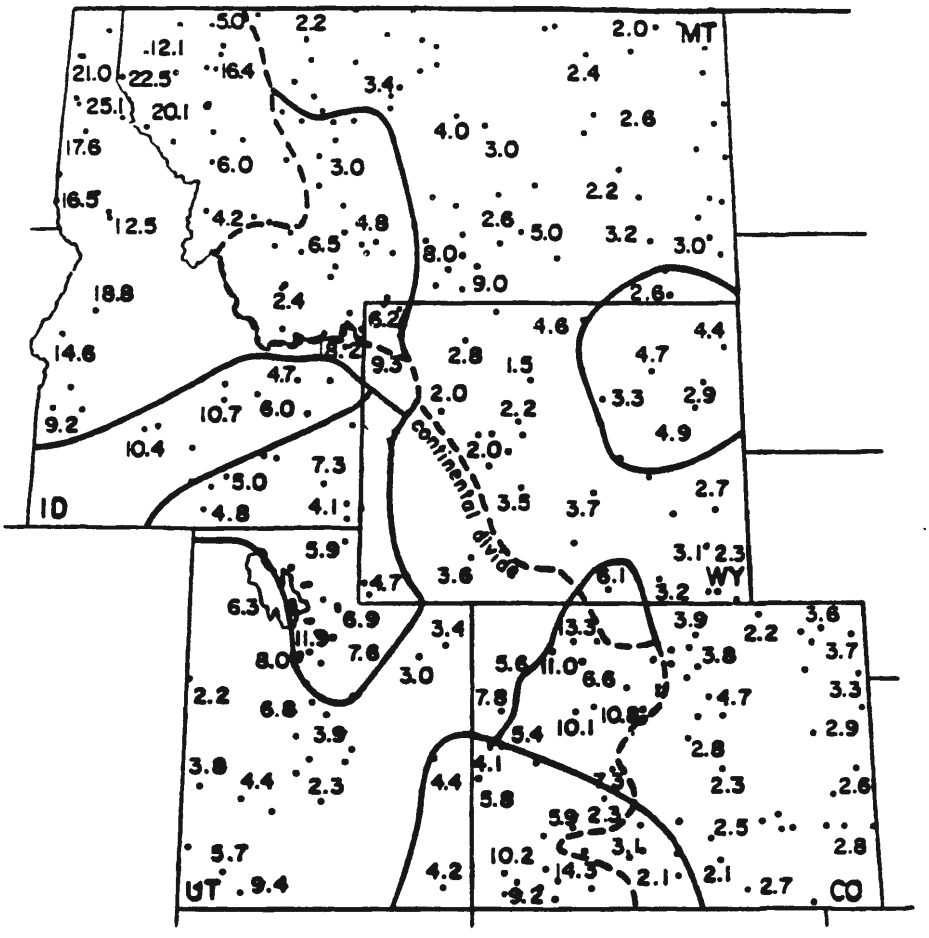

Figure I.1 Median winter (October-March) precipitation value plotted for a selected number of NWS cooperative weather stations.

APPENDIX II

SN SITES AND THEIR CHARACTERISTICS FOR EACH REGION

In Chapter II, 275 snowcourses were chosen to analyze hydroclimatic variability in the five-state region. Separated into the the 11 SN regions discussed in Chapter IV, information is provided about each of the 275 SN sites in Table II.1. The site characteristics include, station name and number, median value of SN, measure of variability value, elevation, latitude and longitude. Figure II.1 shows the median SN value plotted for a selected number of SCS snowcourse sites.

Table II.1 For each region, SN sites and their characteristics are listed. Median value is in inches snow water equivalent.

Region number and type	Station Name	Station Number	Median Value	Measure of Variability	Elevation (feet)	Lat.	Long.
1. stable							
	Upper Holland Lake	13B05	36.3	0.36	6200′	47 28′	113 31′
	Holbrook	13B13	10.6	0.55	4530′	47 35′	113 19′
	Big Creek	13B03	45.8	0.22	6750′	47 41′	113 57′
	Mineral Creek	13A16	20.0	0.48	4000′	48 46′	113 49′
	Kishenehn	14A06	8.9	0.59	3890′	48 58′	114 25′
	Logan Creek	14A05	8.4	0.50	4300′	48 20′	114 39′
	Hell Roaring Divide	14A03	31.4	0.33	5770′	48 30′	114 21′
	Brush Creek Timber	14A13	10.8	0.40	5000′	48 22′	114 52′
	Trinkus Lake	13B01	43.0	0.27	6100′	47 57′	113 45′
	Spotted Bear Mtn.	13B02	14.6	0.51	7000′	47 54′	113 27′
	Baree Creek	15B11	47.1	0.42	5500′	47 58′	115 32′
	Red Mtn.	15A01	20.0	0.40	6000′	48 55′	115 21′
	Desert Mtn.	13A02	16.4	0.34	5600′	48 25′	113 57′
	Stemple Pass	12C01	11.8	0.46	6600′	46 53′	112 29′
	Nez Perce Camp	14D02	15.2	0.55	5650′	45 44′	114 29′
	Nez Perce Pass	14D01	17.4	0.57	6570′	45 43′	114 30′
	Slide Rock Mtn.	13C02	17.0	0.38	7100′	46 35′	113 34′
	Stuart Mtn.	13C01	34.0	0.24	7400′	47 00′	113 55′
	Hoodoo Creek	15C01	49.0	0.35	5900′	46 59′	115 01′
	North Fork Jocko	13B07	45.8	0.36	6330′	47 16′	113 46′

Skalkaho Summit	13C03	26.5	0.45	7250' 46 15' 113 46'
Storm Lake	13C07	14.6	0.38	7780' 46 05' 113 16'
Stuart Mill	13C06	7.6	0.38	6500' 46 10' 113 16'
Ten Mile Lower	12C02	7.9	0.43	6600' 46 27' 112 17'
Ten Mile Middle	12C03	12.8	0.31	6800' 46 26' 112 18'
Lookout	15B02	36.7	0.39	5140' 47 27' 115 42'
Savage Pass	14C04	28.0	0.38	6170' 46 28' 114 38'
Shanghai Summit	15C04	30.4	0.47	4570' 46 34' 115 45'
Fishlake Airstrip	15C02	39.0	0.45	5650' 46 20' 115 04'
Lower Sands Creek	16B01	22.1	0.43	3120' 47 44' 116 29'
Forty Nine Meadows	15B03	34.2	0.51	4830' 47 06' 115 53'
Moores Creek Summit	15F01	35.6	0.50	6100' 43 55' 115 40'
Moose Creek	13D16	17.8	0.49	6200' 45 40' 113 57'
Placer Creek	16E02	18.9	0.50	5860' 44 49' 116 42'
Rock Flat Summit	16E01	20.2	0.38	5310' 44 56' 116 09'
Cozy Cove	15E08	17.1	0.54	5380' 44 17' 115 39'
Deadman Gulch	16F01	18.2	0.60	5600' 43 55' 116 01'
Deadman Summit	15E04	48.3	0.45	6860' 44 33' 115 34'
Squaw Meadow	15D02	37.4	0.39	5900' 45 09' 116 00'
Jackson Peak	15E09	34.8	0.43	7070' 44 03' 115 27'
Lake Fork	15E01	17.7	0.48	5290' 44 55' 115 57'
Graham Ranch	14F05	14.2	0.53	6270' 43 47' 114 25'
Bogus Basin	16F02	26.3	0.53	6340' 43 46' 116 06'
Big Creek Summit	15E02	40.0	0.42	6580' 44 38' 115 48'
Boulder Creek	16D01	24.4	0.39	5440' 45 04' 116 27'
Glade Creek	10E13	23.3	0.40	7040' 44 06' 110 44'
Huckleberry Divide	10E14	22.0	0.42	7300' 44 05' 110 41'
Coulter Creek	10E10	22.5	0.47	7020' 44 10' 110 34'
Grassy Lake	10E15	35.1	0.45	7265' 44 08' 110 50'
Lewis Lake Divide	10E09	42.7	0.46	7850' 44 12' 110 40'
Aster Creek	10E08	30.6	0.59	7750' 44 17' 110 38'
Thumb Divide	10E07	20.8	0.57	7980' 44 22' 110 34'
Big Springs	11E09	22.6	0.41	6400' 44 29' 111 16'
Island Park	11E10	17.1	0.42	6290' 44 25' 111 23'
Valley View	11E08	16.7	0.53	6680' 44 38' 111 19'
Kilgore	11E12	11.0	0.61	6320' 44 24' 111 54'
Blue Ledge Mine	11E11	15.6	0.54	6900' 44 26' 112 00'
Camp Creek	12E03	10.4	0.49	6580' 44 27' 112 14'
Trinity Mtn.	15F05	44.4	0.50	7770' 43 38' 115 26'
Vienna Mine	14F04	36.9	0.58	8960' 43 48' 114 51'
Williams Creek Summit	14D04	13.3	0.57	7990' 45 06' 114 05'
Benton Spring	16A03	20.0	0.42	4920' 48 21' 116 46'
Mosquito Ridge	16A04	39.4	0.38	5200' 48 03' 116 14'
Copper Ridge	16B02	30.4	0.55	4820' 47 43' 116 30'
Mill Creek Summit	14E01	22.0	0.56	8800' 44 28' 114 28'
Smith Creek	16A01	47.6	0.43	4800' 48 52' 116 45'
Atlanta Summit	15F04	37.0	0.54	7580' 43 45' 115 14'
Galena Summit	14F12	24.0	0.57	8780' 43 51' 114 43'
Galena	14F01	19.5	0.61	7440' 43 53' 114 40'
East Fork R.S.	13D01	6.6	0.67	5400' 45 55' 113 43'
Weasel Divide	14A07	33.9	0.37	5450' 48 57' 114 44'
Wrong Creek	12B04	14.3	0.51	5700' 47 53' 112 56'
Wrong Ridge	12B03	20.4	0.48	6800' 47 56' 112 55'

Intergaard	13C04	8.6	0.51	6540' 46 13' 113 17'
Gibbons Pass	13D02	24.3	0.40	7100' 45 42' 113 57'
Snake River Station	10E12	21.1	0.41	6920' 44 08' 110 40'
Base Camp	10F02	20.3	0.58	7030' 43 56' 110 26'
Four Mile Meadows	10F06	13.4	0.47	7860' 43 49' 110 16'
Togwotee Pass	10F09	29.8	0.48	9580' 43 45' 110 03'
2, stable				
Beaver Cr.-Skunk Cr.	11H14	13.0	0.57	7150' 41 24' 111 35'
Ben Lomond Peak	11H08	37.6	0.59	8000' 41 22' 111 52'
Bevan's Cabin	12J02	12.0	0.37	6458' 40 28' 112 15'
Hayden Fork	10J07	16.2	0.42	9400' 40 44' 110 50'
Burts Miller Ranch	10J06	6.1	0.44	7900' 40 47' 110 50'
Lakefork #1	10J10	11.6	0.54	10700' 40 36' 110 26'
Mammoth Cottonwood	11K03	21.1	0.59	8800' 39 41' 111 19'
Middle Canyon	12J03	14.3	0.50	7000' 40 29' 112 12'
Chalk Creek #3	11J03	7.9	0.44	7500' 40 55' 111 06'
Daniels Strawberry	11J23	15.3	0.48	8000' 40 18' 111 15'
Farmington Canyon	11J11	31.2	0.56	8000' 40 58' 111 48'
Payson R.S.	11K01	19.2	0.53	8050' 39 56' 111 38'
Strawberry Divide	11J08	19.9	0.43	8400' 40 11' 111 13'
Trial Lake	10J08	25.9	0.40	9960' 40 41' 110 57'
Kelley R.S.	10G12	17.9	0.47	8180' 42 15' 110 48'
CCC Camp	10G07	12.8	0.42	7500' 42 31' 110 53'
Big Park	10G11	20.6	0.48	8620' 42 21' 110 46'
Salt River Summit	10G08	16.4	0.45	7700' 42 31' 110 55'
Grey's Boundary	10F18	12.0	0.58	5720' 43 09' 110 00'
Grover Park Divide	10G03	12.8	0.42	7000' 42 48' 110 54'
Poison Meadows	10G06	29.6	0.53	8500' 42 33' 110 41'
Snider Basin	10G13	17.1	0.55	8060' 42 28' 110 32'
Emigrant Summit	11G06	25.5	0.40	7390' 42 22' 111 34'
Emigration Canyon	11G07	11.3	0.45	6500' 42 22' 111 30'
Franklin Basin	11G08	27.9	0.43	8040' 42 03' 111 37'
Mink Creek	12G01	17.8	0.52	6410' 42 46' 112 29'
Austin Bros. Ranch	11G03	9.3	0.46	6400' 42 47' 111 26'
Badger Gulch	14G03	14.1	0.61	6660' 42 06' 114 10'
Bostetter R.S.	14G01	20.8	0.50	7500' 42 10' 114 11'
Magic Mtn.	14G02	21.0	0.53	6880' 42 11' 114 18'
Slug Creek Divide	11G05	17.8	0.43	7225' 42 34' 111 18'
Pebble Creek	12G02	16.7	0.39	6400' 42 46' 112 06'
Sublett	12G08	11.3	0.61	5950' 42 23' 112 58'
3, stable				
Twin Lakes Tunnel	06K03	10.7	0.60	10450' 39 04' 106 32'
Independence Pass	06K04	15.7	0.53	10600' 39 04' 106 36'
Fremont Pass	06K08	16.9	0.45	11400' 39 22' 106 12'
Shrine Pass	06K09	18.8	0.46	10700' 39 31' 106 31'
Ivanhoe	06K10	19.2	0.36	10400' 39 17' 106 33'
Alexander Lake	07K03	23.2	0.54	10160' 39 02' 107 58'
Mesa Lakes	08K04	17.6	0.55	10000' 39 03' 108 05'
Two Mile	05J26	14.2	0.47	10500' 40 23' 105 40'
University Camp	05J08	19.3	0.50	10300' 40 02' 105 34'
Loveland Pass	05K05	16.2	0.47	10800' 39 41' 105 54'
Jefferson Creek	05K08	9.9	0.47	10280' 39 26' 105 52'

Grizzly Peak	05K09	18.4	0.51	11100' 39 39' 105 52'
Hoosier Pass	06K01	13.0	0.55	11400' 39 22' 106 03'
Tennessee Pass	06K02	10.6	0.55	10200' 39 21' 106 20'
N. Inlet Grand Lake	05J09	9.0	0.51	9000' 40 17' 105 46'
Grandby	05J16	7.3	0.58	8600' 40 09' 105 59'
Dry Lake	06J01	20.8	0.45	8400' 40 32' 106 47'
Lynx Lake	06J06	12.4	0.48	8880' 40 05' 106 40'
Yampa View	06J10	15.5	0.55	8200' 40 21' 106 46'
Glen Mar Ranch	06K20	9.1	0.51	8750' 39 51' 106 04'
Rio Blanca	07J01	16.5	0.38	8500' 40 02' 107 17'
Cameron Pass	05J01	28.5	0.34	10285' 40 31' 105 53'
Park View	06J02	9.5	0.48	9160' 40 22' 106 06'
Columbine Lodge	06J03	24.2	0.39	9400' 40 23' 106 36'
Willow Creek	06J05	12.6	0.43	9540' 40 21' 106 05'
Gore Pass	06J11	10.3	0.47	9400' 40 05' 106 32'
Summit Ranch	06K14	8.1	0.59	9400' 39 43' 106 09'
Pando	06K19	10.6	0.37	9500' 39 27' 106 20'
Burro Mtn.	07K02	19.0	0.48	9400' 39 53' 107 36'
Park Reservoir	07K06	24.0	0.60	9960' 39 02' 107 52'
Milner Pass	05J24	13.2	0.52	9750' 40 24' 105 50'
Phantom Valley	05J04	11.2	0.60	9030' 40 24' 105 51'
Lake Irene	05J10	20.4	0.50	10700' 40 25' 105 49'
Berthoud Pass	05K03	17.0	0.48	9700' 39 49' 105 45'
Arrow	05K06	13.9	0.58	9680' 39 55' 105 45'
Lapland	05K07	10.8	0.59	9300' 39 53' 105 53'
Berthoud Falls	05K13	13.7	0.49	10500' 39 47' 105 47'
Hidden Valley	05J13	10.1	0.52	9480' 40 23' 105 39'
Porphyry Creek	06L03	18.4	0.44	10760' 38 29' 106 20'
Monarch Pass	06L04	17.7	0.42	10500' 38 31' 106 19'
Empire	05K10	7.9	0.54	9600' 39 46' 105 47'
Elk River #2	06J15	18.1	0.38	8700' 40 50' 106 58'
Park Cone	06L02	10.4	0.59	9600' 38 49' 106 35'
Chochetopa Pass	06L06	5.7	0.53	10000' 38 09' 106 35'
4. stable				
Grasshopper	10C02	6.7	0.51	7000' 46 31' 110 46'
West Yellowstone	11E07	12.1	0.46	6700' 44 40' 110 06'
Lakeview Ridge	11E02	10.5	0.58	7400' 44 35' 110 50'
Independence	10D06	18.9	0.40	7850' 45 13' 110 51'
Twentyone Mile	11E06	17.9	0.61	7150' 44 54' 110 03'
King's Hill	10C01	14.1	0.43	7500' 46 51' 110 42'
Devils Slide	10D04	23.0	0.37	8100' 45 24' 110 57'
Elk Horn Springs	13D15	9.8	0.48	7800' 45 28' 113 06'
Pipestone Pass	12D01	6.0	0.45	7200' 45 51' 112 27'
Ten Mile Upper	12C04	15.2	0.35	8000' 46 25' 112 17'
Trail Creek	13E02	9.0	0.49	7090' 44 58' 113 26'
White Pine Ridge	12E01	5.6	0.52	8850' 44 37' 112 44'
Bloody Dick	13D10	14.0	0.55	7600' 45 10' 113 30'
Cheeseman Res.	12C05	3.7	0.51	6200' 46 28' 112 11'
Crevice Mtn.	10D05	10.7	0.60	8400' 45 02' 110 36'
Hebgen Dam	11E05	12.2	0.52	6550' 44 52' 111 20'
Lakeview Canyon	11E04	11.3	0.60	6930' 44 35' 111 49'
Hood Meadow	10D03	10.7	0.46	6600' 45 29' 110 58'

New World	10D01	14.9	0.37	6900′ 45 34′ 110 55′
Porcupine	10C03	8.2	0.43	6500′ 46 07′ 110 28′
Gold Stone	13D09	18.0	0.45	8100′ 45 09′ 113 32′
Lake Camp	10E04	9.2	0.61	7780′ 44 34′ 110 24′
Canyon	10E02	16.1	0.49	7940′ 44 44′ 110 30′
Norris Basin	10E02	11.1	0.50	7500′ 44 44′ 110 42′
Lupine Creek	10E01	10.2	0.59	7380′ 44 54′ 110 37′
5. stable				
Albany	06H11	14.8	0.47	9120′ 41 11′ 106 10′
Brooklyn Lake	06H13	23.9	0.45	10220′ 41 22′ 106 14′
N. Barrett Creek	06H05	21.6	0.35	9430′ 41 19′ 106 26′
N. French Creek	06H20	24.2	0.55	10130′ 41 20′ 106 22′
Old Battle	06H10	36.2	0.35	9920′ 41 09′ 107 58′
Webber Springs	06H09	21.6	0.37	9250′ 41 10′ 106 56′
Hairpin Turn	06H02	18.1	0.43	9460′ 41 20′ 106 12′
Roach	06J12	18.9	0.44	9700′ 40 52′ 106 03′
Ryan Park	06H06	12.2	0.52	8350′ 41 19′ 106 30′
Libby Lodge	06H03	12.2	0.54	8750′ 41 19′ 106 11′
Deadman Hill	05J06	17.2	0.37	10220′ 40 48′ 105 46′
McIntyre	05J15	11.3	0.52	9100′ 40 47′ 105 56′
Chambers Lake	05J02	9.9	0.60	9000′ 40 36′ 105 50′
6. unstable				
South Mtn.	16G01	14.0	0.76	6500′ 42 46′ 116 54′
Silver City	16F03	17.0	0.63	6400′ 43 00′ 116 44′
Dollarhide Summit	14F08	25.0	0.79	8420′ 43 36′ 114 40′
Mt. Baldy	14F09	21.2	0.71	8920′ 43 40′ 114 24′
Copper Basin	13F02	9.6	0.83	7640′ 43 49′ 113 55′
Couch Summit	14F10	20.2	0.59	6840′ 43 31′ 114 48′
Soldier R.S.	14F11	10.5	0.73	5740′ 43 29′ 114 49′
Mascot Mine	14F07	15.6	0.67	7780′ 43 42′ 114 06′
Stickney Mill	14F02	9.8	0.65	7430′ 43 52′ 114 13′
Bear Canyon	13F03	18.2	0.78	7900′ 43 45′ 113 56′
Lost Wood Divide	14F03	24.2	0.63	7900′ 43 50′ 114 16′
7. unstable				
Gooseberry R.S.	11L02	12.7	0.66	8400′ 38 47′ 111 41′
Harris Flat	12M05	7.3	1.19	7800′ 37 29′ 112 35′
Indian Canyon	10K01	13.1	0.76	9100′ 39 45′ 110 45′
Midway Valley	12M02	19.9	0.98	9800′ 37 34′ 112 50′
Mt. Baldy R.S.	11K12	23.6	0.68	9500′ 39 08′ 111 30′
Squaw Springs	12L05	6.7	1.04	9300′ 38 29′ 112 00′
Webster Flat	12M03	15.7	1.09	9200′ 37 35′ 112 54′
Beavers Dam	11K13	12.3	0.61	9500′ 39 06′ 111 32′
Big Flat	12L07	17.6	0.79	10290′ 38 18′ 112 21′
Box Creek	12L04	12.8	0.72	9800′ 38 30′ 112 01′
Lakefork Mtn #3	10J12	5.8	0.91	8400′ 40 33′ 110 21′
Kimberly Mine	12L06	16.7	0.56	9300′ 38 29′ 112 23′
Loomis Park	10F16	18.6	0.62	8240′ 43 10′ 110 08′
East Rim Divide	10F17	14.4	0.58	7930′ 43 08′ 110 12′
Gros Ventre Summit	10F19	11.8	0.68	8750′ 43 23′ 110 08′
Kendall R.S.	10F15	12.3	0.63	7740′ 43 15′ 110 01′
Larsen Creek	09G06	11.4	0.63	9020′ 42 36′ 109 05′

8, unstable				
Trout Lake	07M09	14.9	0.71	9780' 37 50' 107 53'
Upper Rio Grande	07M16	7.1	1.11	9400' 37 43' 107 15'
Culebra	05M03	9.3	0.75	10500' 37 12' 105 12'
Lizard Head	07M03	17.8	0.66	10200' 37 48' 107 56'
Lake City	07M08	7.9	0.68	10160' 37 59' 107 15'
Spud Mtn.	07M11	25.7	0.64	10660' 37 42' 107 46'
Molas Lake	07M12	12.6	0.84	10500' 37 45' 107 41'
Mineral Creek	07M14	15.8	0.57	10040' 37 51' 107 43'
Platora	06M09	15.0	0.99	9950' 37 21' 106 33'
Pool Table Mtn.	06M14	5.1	0.82	9840' 37 48' 106 48'
Telluride	07M02	7.4	0.95	8800' 37 56' 107 48'
Cascade	07M05	12.4	0.90	8880' 37 39' 107 48'
Ironton Park	07M06	15.6	0.64	9600' 37 58' 107 39'
Wolf Creek Summit	06M17	29.0	0.75	11000' 37 28' 106 48'
Wolf Creek Pass	06M01	26.3	0.86	10320' 37 28' 106 47'
Upper San Juan	06M03	32.1	0.66	10200' 37 29' 106 49'
Porcupine	07M20	8.8	0.67	10200' 37 50' 107 10'
Buckboard Flat	09M01	12.9	0.77	9000' 37 52' 109 27'
9, unstable				
Goat Mtn.	12B07	11.3	0.69	7000' 47 39' 112 55'
Fivebull	12B09	7.2	0.88	5700' 47 27' 112 49'
Cabin Creek	12B06	6.7	0.76	5200' 47 42' 112 53'
Freight Creek	12A01	15.0	0.65	6000' 48 01' 112 50'
Rocky Boy	09A01	4.9	0.94	4700' 48 11' 109 39'
Crystal Lake	09C01	13.8	0.59	6050' 46 48' 109 30'
Marias Pass	13A05	18.0	0.64	5250' 48 19' 113 21'
10, unstable				
Sylvan Pass	10E05	14.0	0.56	7100' 44 29' 110 02'
Dunoir	09F06	8.2	0.77	8760' 43 34' 109 48'
Geyser Creek	09F07	7.4	0.68	8500' 43 32' 109 45'
Little Warm	09F08	15.6	0.58	9620' 43 30' 109 45'
Timber Creek	09E03	3.6	0.81	7950' 44 02' 109 11'
Blue Ridge	08G02	11.6	0.66	9620' 42 39' 108 52'
Hobbs Park	09G03	13.1	0.56	10100' 42 52' 109 06'
St. Lawrence	09F11	7.0	0.61	8960' 43 02' 109 12'
Dinwoody	09F10	11.3	0.59	10160' 43 16' 109 28'
Owl Creek	08F01	5.4	0.57	8975' 43 40' 109 01'
T-Cross Ranch	09F03	6.5	0.85	7900' 43 43' 109 38'
Burroughs Creek	09F04	12.9	0.84	8750' 43 42' 109 40'
Sheridan	09F14	7.6	0.55	7720' 43 38' 109 55'
East Entrance	09E05	10.2	0.65	6960' 44 29' 110 00'
Camp Senia	09D01	6.6	0.67	7890' 45 10' 109 28'
Northeast Entrance	10D07	9.4	0.61	7350' 45 00' 110 00'

11. unstable

Copeland Lake	05J18	4.3	0.77	8600′ 40 12′ 105 34′
Ward	05J21	6.4	0.77	9500′ 40 05′ 105 30′
Wild Basin	05J05	11.4	0.73	9600′ 40 12′ 105 36′
Long's Peak	05J22	11.1	0.68	10500′ 40 16′ 105 35′
Geneva Park	05K11	3.6	0.89	9750′ 39 30′ 105 42′
Hourglass Lake	05J11	7.2	0.69	9360′ 40 34′ 105 37′
Deer Ridge	05J17	4.6	0.98	9000′ 40 23′ 105 38′
Westcliffe	05L02	7.3	0.85	9400′ 38 07′ 105 35′
Laveta Pass	05M01	7.7	0.99	9440′ 37 35′ 105 12′
Fourmile Park	06K07	5.0	1.02	9700′ 39 04′ 106 26′
Labonte	05G02	6.3	0.90	7750′ 42 18′ 105 39′
Pole Mtn.	05H01	6.1	1.07	8360′ 41 15′ 105 25′

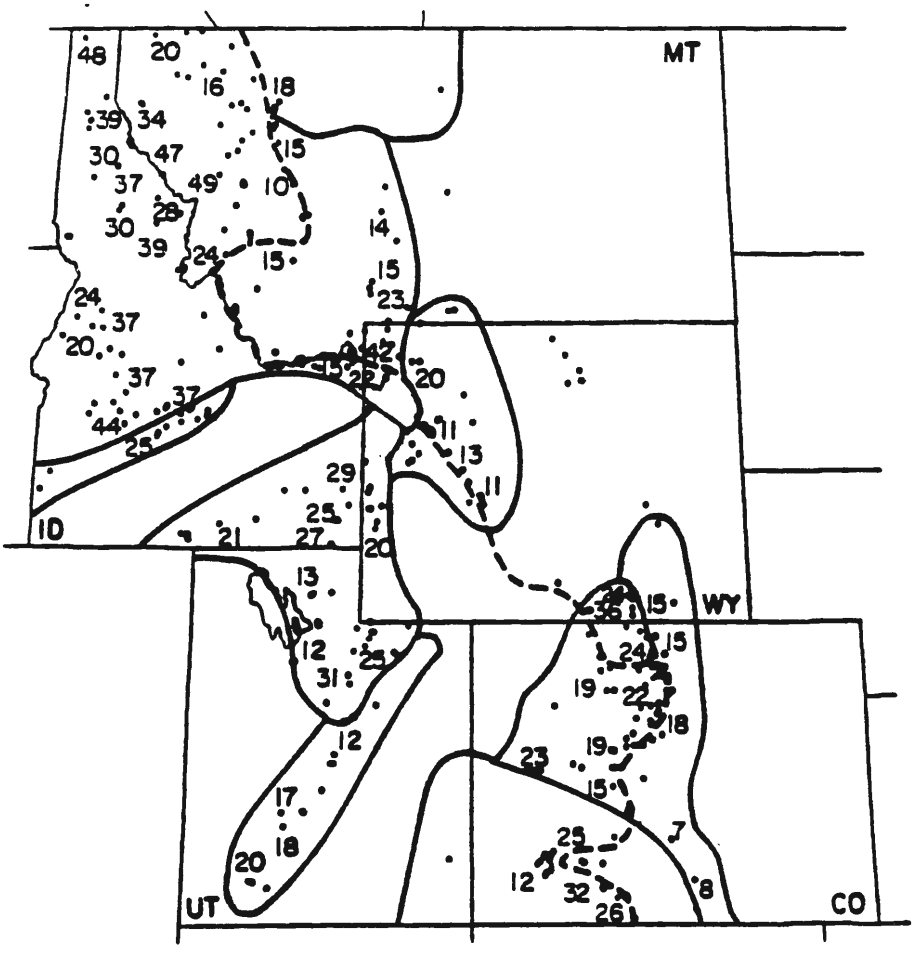

Figure II.1 Median April 1 snowpack value plotted for a selected number of SCS snowcourse sites.

APPENDIX III

DATA CHARACTERISTICS OF THE 14 SELECTED WATERSHEDS

In addition to the information pertaining to the 14 selected watersheds described in Chapter 3, Table III.1 is provided. In Table III.1 station type and number, elevation, latitude, longitude, and median annual value are given for all gauges, sites and stations used in each watershed analysis. In Figure 5 of Chapter 3, the coincident time series of normalized SN, PR, and ST are plotted for the San Juan watershed in Colorado and the Coeur d'Alene watershed in Idaho. In Figures III.1-III.6, the coincident time series of normalized SN, PR, and ST are plotted for the other 12 selected watersheds.

Table III.1 The data characteristics of the 14 selected watersheds.

Name of Watershed	Station Type/ Number	Elevation	Latitude	Longitude	Median Annual Value
North Fork Colorado					
	ST/09010500	8750′	40 20′	105 51′	170.6 cfs*
	SN/05J24	9750′	40 24′	105 30′	13.7 inches**
	SN/05J04	9030′	40 24′	105 51′	11.2 inches
	SN/05J19	8600′	40 15′	105 50′	8.7 inches
	SN/05J10	10700′	40 25′	105 49′	20.4 inches
	PR/53496	8720′	40 16′	105 50′	19.9 inches
	PR/53500	8290′	40 11′	105 52′	12.9 inches
San Juan					
	ST/09342500	7052′	37 16′	107 01′	310.0 cfs
	SN/06M03	10200′	37 29′	106 49′	31.0 inches
	SN/06M01	10320′	37 28′	106 47′	26.2 inches
	SN/06M17	11000′	37 28′	106 48′	27.9 inches
	PR/56258	7240′	37 16′	107 01′	9.7 inches

St. Vrain					
	ST/06724000	5292′	40 13′	105 16′	107.5 cfs
	SN/05J22	10500′	40 16′	105 35′	11.5 inches
	SN/05J05	9600′	40 12′	105 36′	12.0 inches
	SN/05J18	8600′	40 12′	105 34′	4.3 inches
	PR/50183	8500′	40 32′	105 32′	7.2 inches
	PR/52759	7530′	40 23′	105 31′	3.3 inches
Muddy Creek					
	ST/09330500	6400′	39 00′	111 15′	34.0 cfs
	SN/11K13	8000′	39 06′	111 32′	11.9 inches
	PR/422484	6350′	38 55′	111 15′	2.9 inches
West Fork Duchesne					
	ST/09275500	7200′	40 27′	110 53′	47.0 cfs
	SN/10J18	7900′	40 31′	110 43′	6.1 inches
	PR/423624	6750′	40 24′	110 46′	5.4 inches
Bear					
	ST/10011500	7965′	40 58′	110 51′	188.0 cfs
	SN/10J06	7900′	40 47′	110 50′	6.4 inches
	SN/10J17	8550′	40 46′	110 52′	11.4 inches
	SN/10J07	9400′	40 44′	110 50′	16.2 inches
	PR/483100	6780′	41 16′	110 57′	4.7 inches
Smith's Fork					
	ST/10032000	6650′	42 17′	110 52′	200.0 cfs
	SN/10G07	7500′	42 31′	110 53′	12.9 inches
	SN/10G11	8620′	42 21′	110 46′	21.3 inches
	SN/10G08	7700′	42 31′	110 55′	17.1 inches
	SN/10G12	8180′	42 15′	110 48′	18.4 inches
	PR/480915	6120′	42 15′	111 02′	6.5 inches
Green					
	ST/09188500	7468′	43 01′	110 07′	541.0 cfs
	SN/10F19	8750′	43 23′	110 08′	11.8 inches
	SN/10F15	7740′	43 15′	110 01′	13.1 inches
	PR/485115	7645′	43 10′	109 59′	6.2 inches
Wind					
	ST/06218500	7189′	43 35′	109 46′	170.0 cfs
	SN/09F06	8760′	43 34′	109 48′	8.5 inches
	SN/09F14	7720′	43 38′	109 55′	8.0 inches
	SN/09F04	8750′	43 42′	109 40′	14.5 inches
	PR/482715	6917′	43 33′	109 37′	2.1 inches
Boulder					
	ST/06200000	4060′	45 50′	109 56′	598.0 cfs
	SN/10D06	7850′	45 13′	110 15′	19.5 inches
	PR/240780	4100′	45 50′	109 57′	3.9 inches

Nevada					
	ST/12335500	4660′	46 47′	112 45′	42.0 cfs
	SN/12C01	6600′	46 53′	112 29′	11.8 inches
	PR/245040	4540′	46 57′	112 39′	9.5 inches
Swiftcurrent Creek					
	ST/05014500	4860′	48 48′	113 39′	149.0 cfs
	SN/13A16	5000′	48 46′	113 49′	20.0 inches
	PR/240392	4300′	48 56′	113 22′	5.0 inches
Coeur d'Alene					
	ST/12413000	2100′	47 34′	116 15′	1967.0 cfs
	SN/15B02	5140′	47 27′	115 42′	36.8 inches
	SN/16B01	3120′	47 44′	116 29′	22.8 inches
	SN/16A04	5200′	48 03′	116 14′	39.5 inches
	SN/16B02	4820′	47 43′	116 30′	32.0 inches
	PR/101956	2160′	47 41′	116 45′	21.9 inches
	PR/109498	2940′	47 30′	115 53′	25.0 inches
Big Wood					
	ST/13139500	7620′	43 31′	114 20′	162.0 cfs
	SN/14F09	8920′	43 40′	114 24′	20.9 inches
	SN/14F05	6270′	43 47′	114 25′	14.2 inches
	SN/14F03	7900′	43 50′	114 16′	24.3 inches
	SN/14F01	7440′	43 53′	114 40′	19.8 inches
	SN/14F12	8780′	43 51′	114 43′	24.2 inches
	PR/103942	5310′	43 31′	114 18′	9.6 inches

* cfs = cubic feet per second
** inches = inches snow water equivalent

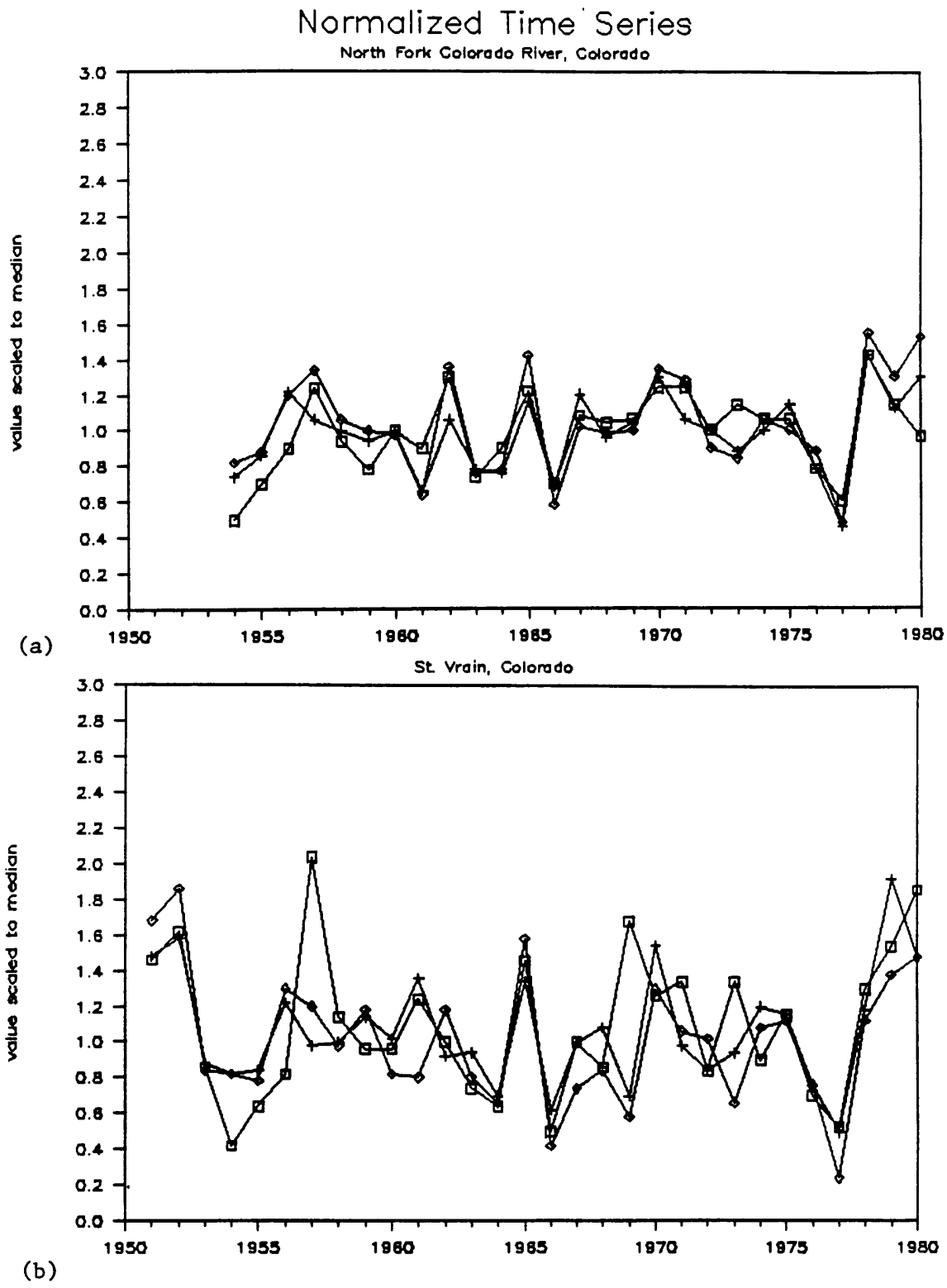

Figure III.1 Coincident time series of normalized (October-March) Precipitation (+), April 1 snowpack (□), and total water-year streamflow (◇) for a) North Fork of the Colorado River and b) the St. Vrain, both in Colorado.

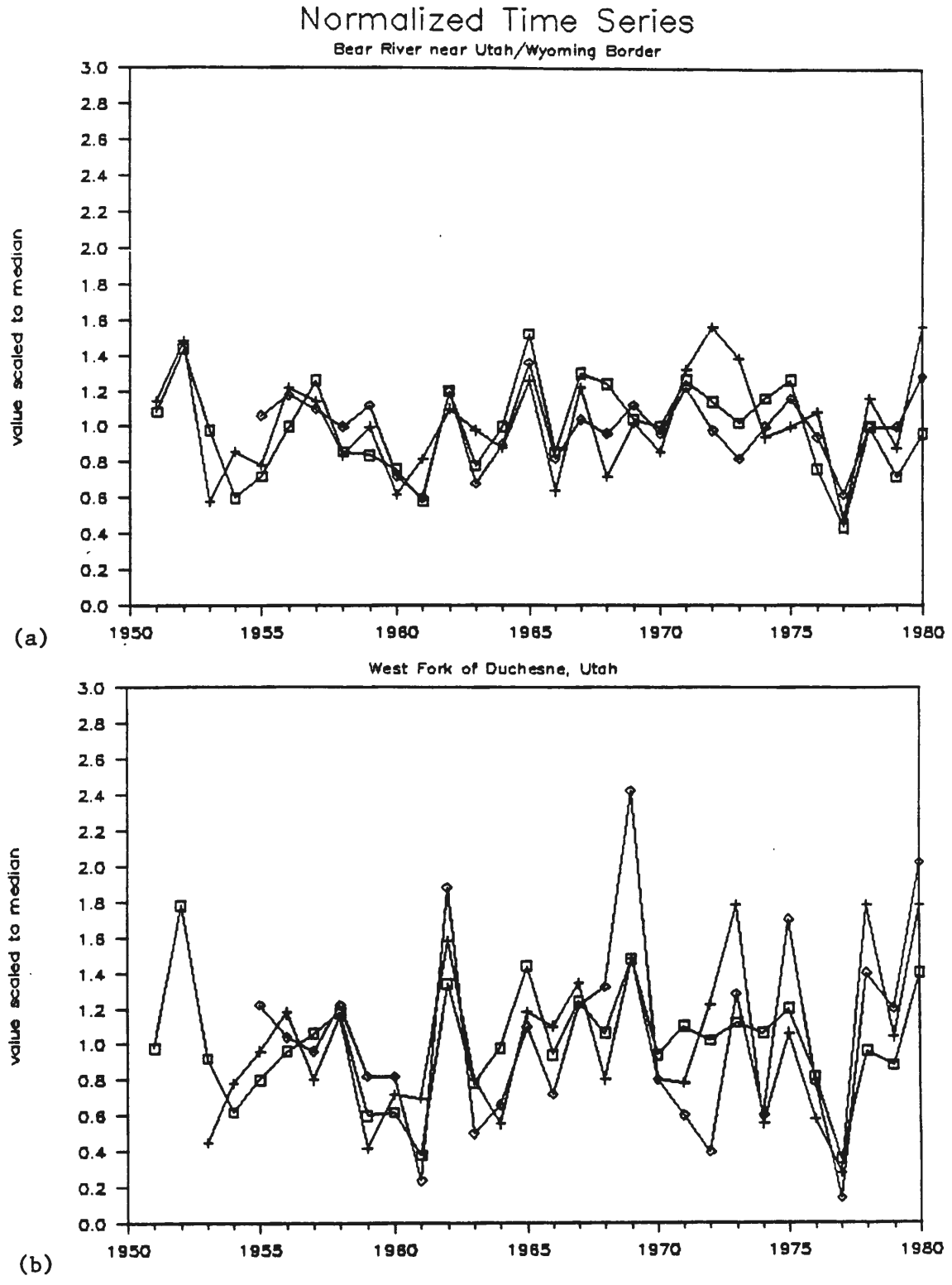

Figure III.2 Same as Figure III.1 except for a) the Bear River near the Utah/Wyoming border and b) the West Fork of the Duchesne in Utah.

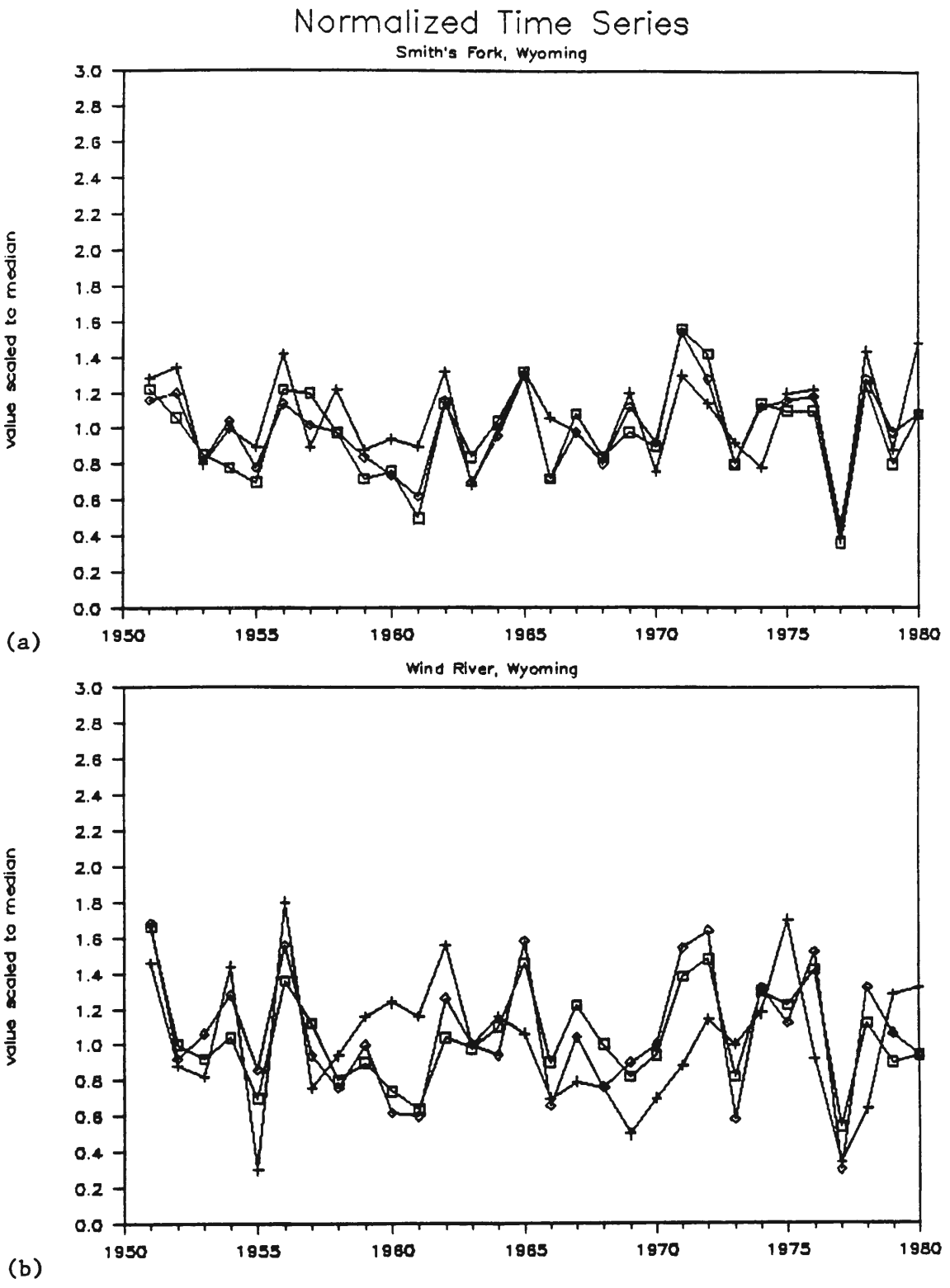

Figure III.3 Same as Figure III.1 except for a) Smith's Fork and b) the Wind River, both in Wyoming.

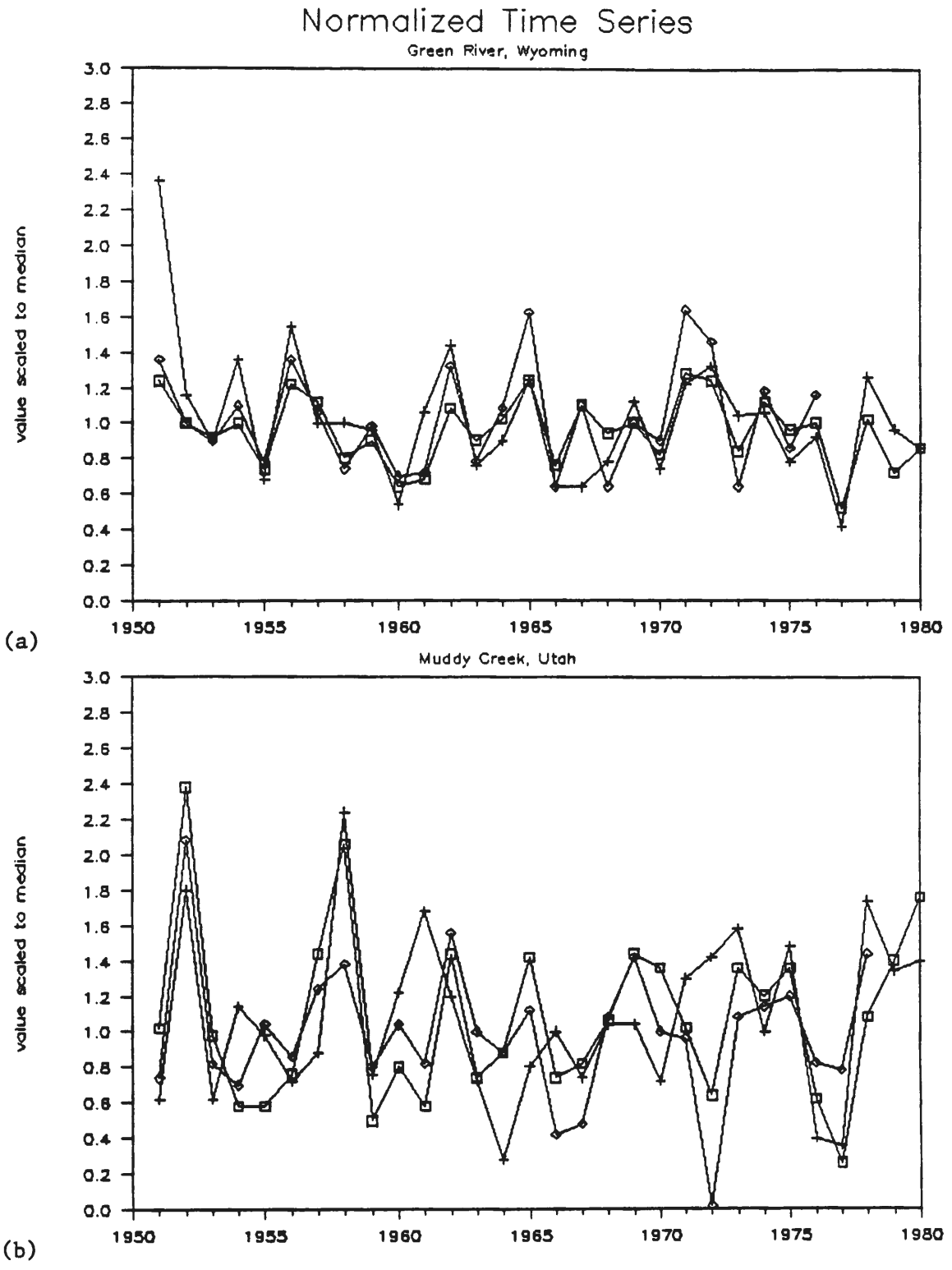

Figure III.4 Same as Figure III.1 except for a) the Green River in Wyoming and b) the Muddy Creek in Utah.

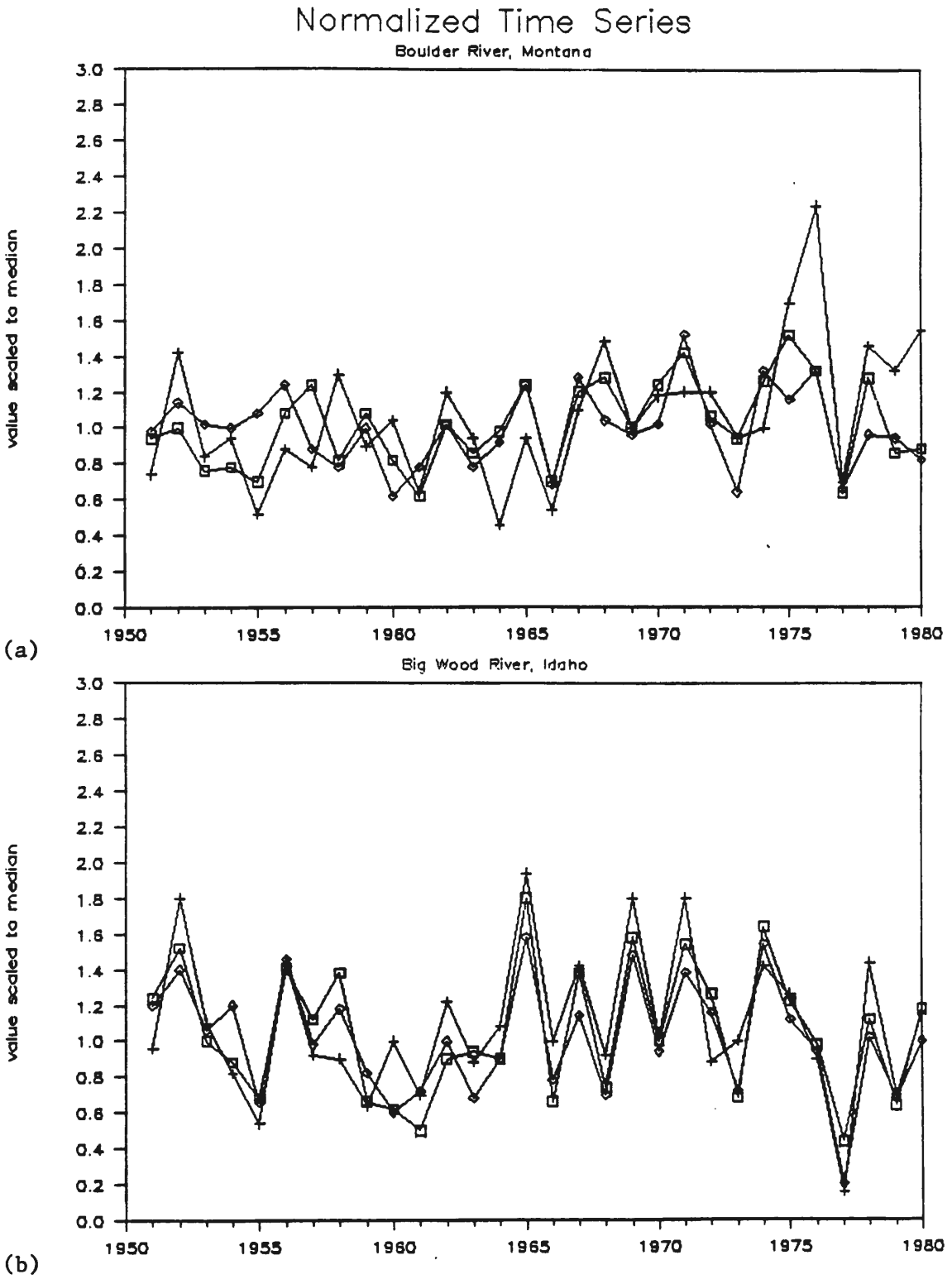

Figure III.5 Same as Figure III.1 except for a) the Boulder River in Montana and b) the Big Wood River in Idaho.

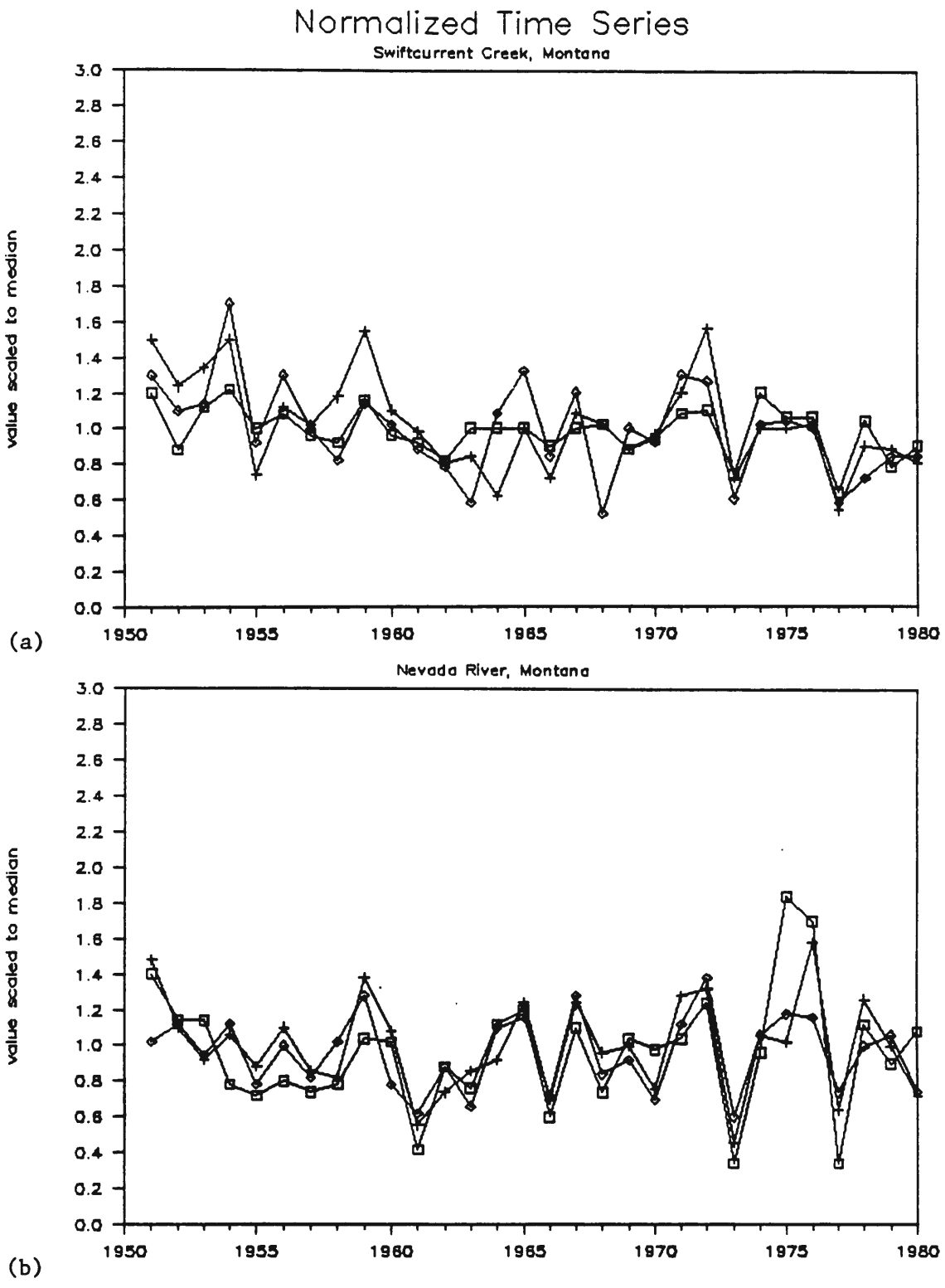

Figure III.6 Same as Figure III.1 except for a) Swiftcurrent Creek and b) the Nevada River, both in Montana.

APPENDIX IV

MEASURE OF VARIATION VERSUS ELEVATION FOR SN AND PR SITES

Figure 11 shown in Chapter IV provides scatterplots of measure of variability versus elevation for SN and PR sites in regions 1 and 6. In this appendix scatterplots of measure of variability versus elevation for the SN and PR sites in the other nine regions (described in Chapter IV) are shown. In Figures IV.1 - IV.5, SN values are represented by dots, while the PR values are represented by triangles. In all figures the vertical slope of the points indicates that SN and PR variability is not explained by elevation.

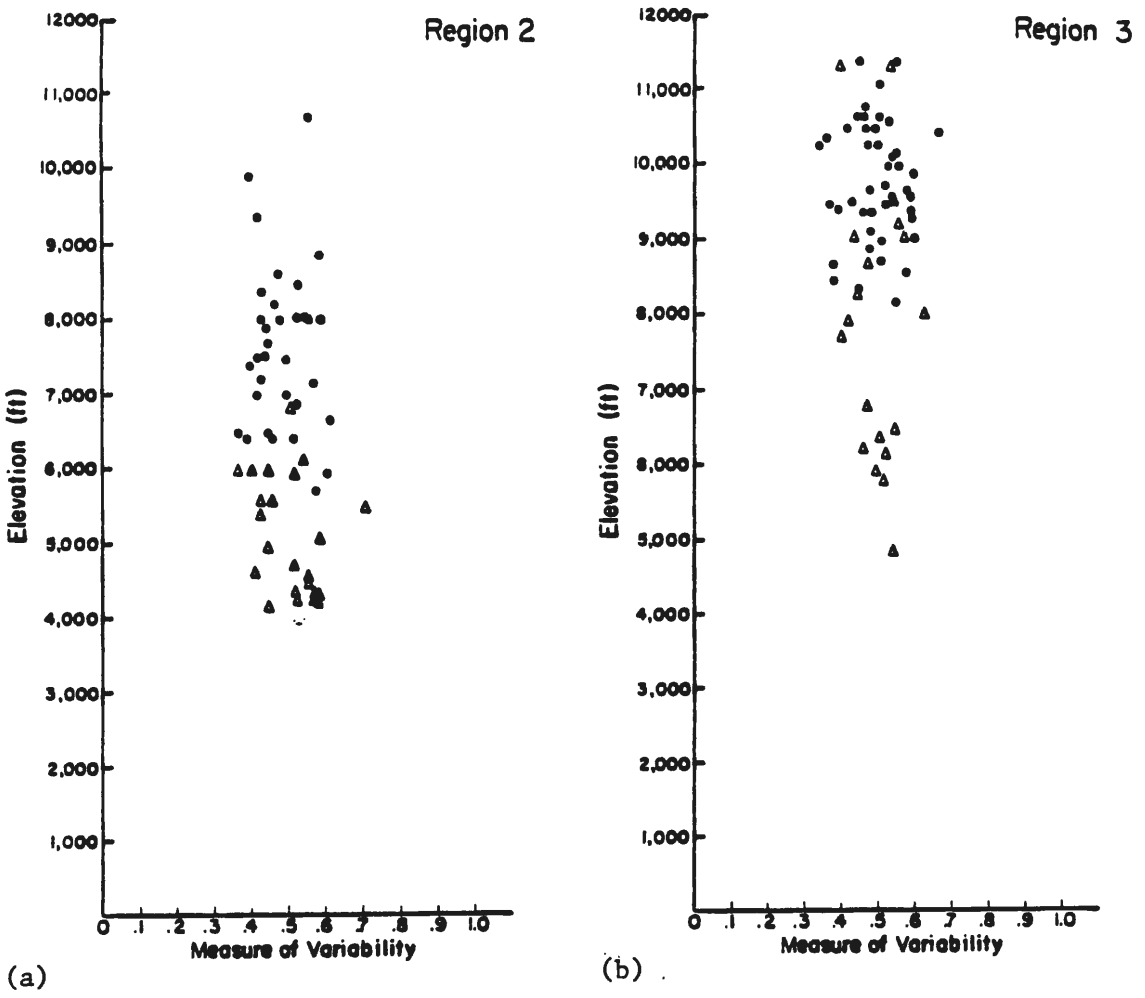

Figure IV.1 Scatterplot of measure of variability values versus the elevation of the SN sites and PR stations in a) region 2 and b) region 3. SN values are the dots, while the PR values are the triangles. SN values are in inches of snow water equivalent.

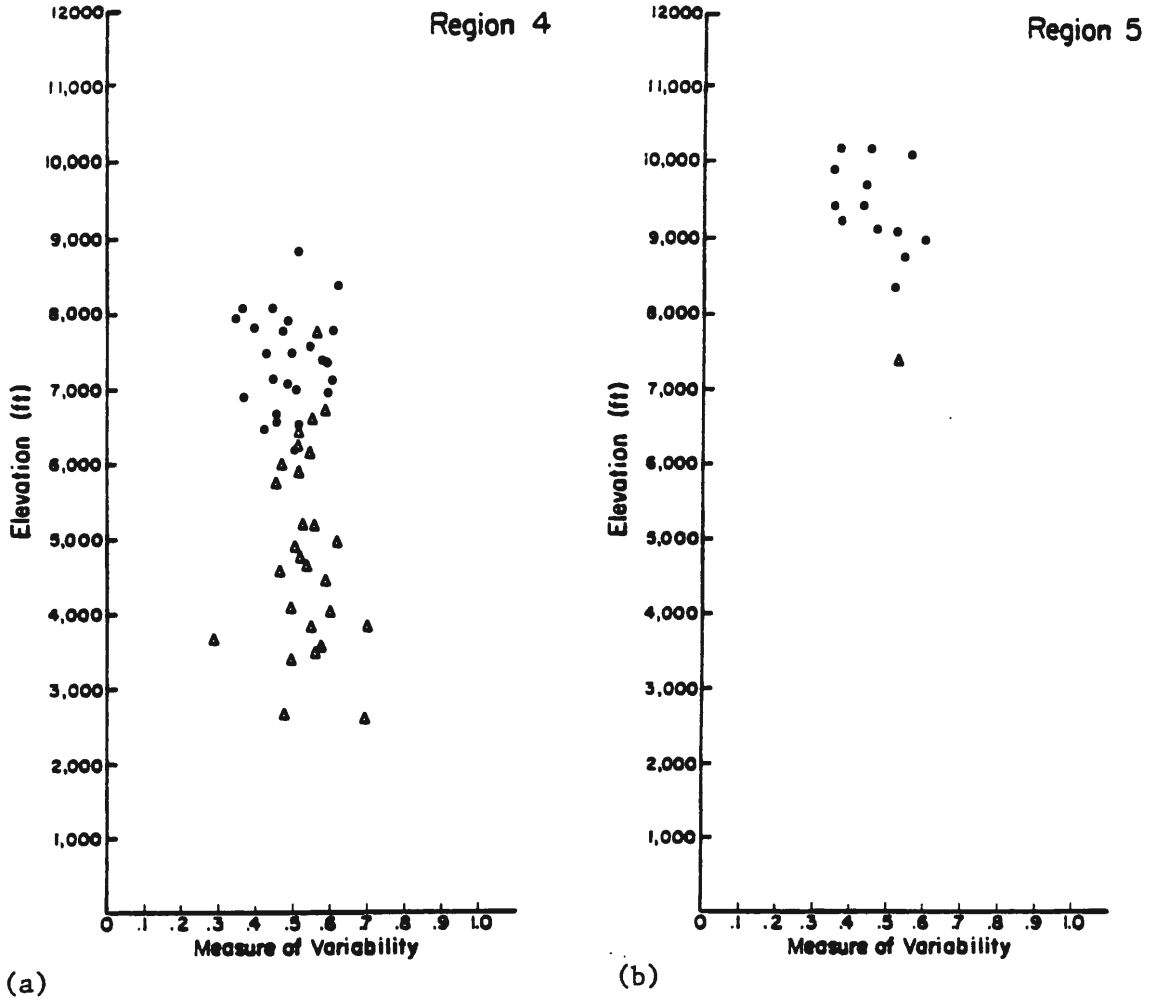

Figure IV.2 Same as Figure IV.1 except for a) region 4 and b) region 5.

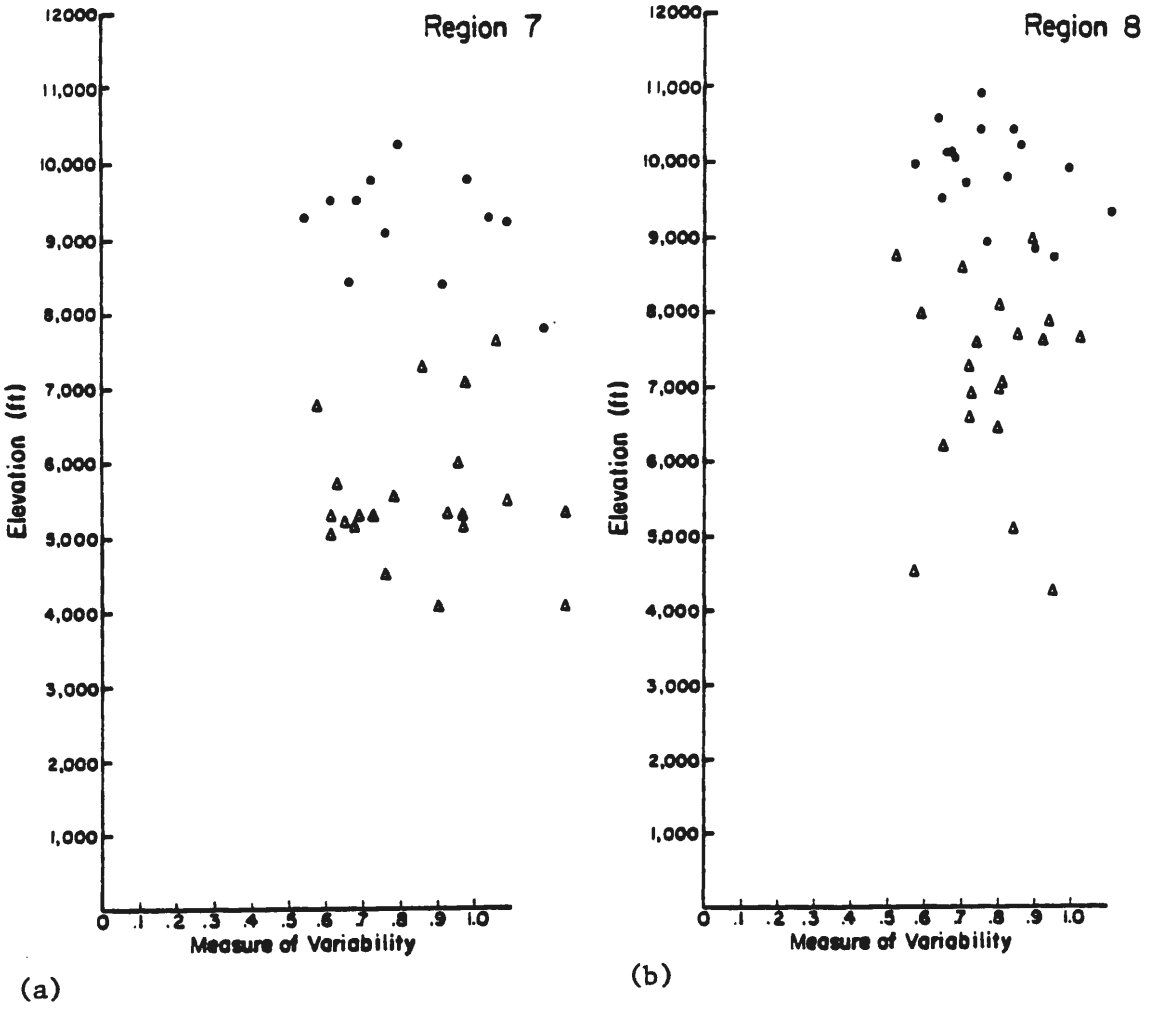

Figure IV.3 Same as Figure IV.1 except for a) region 7 and b) region 8.

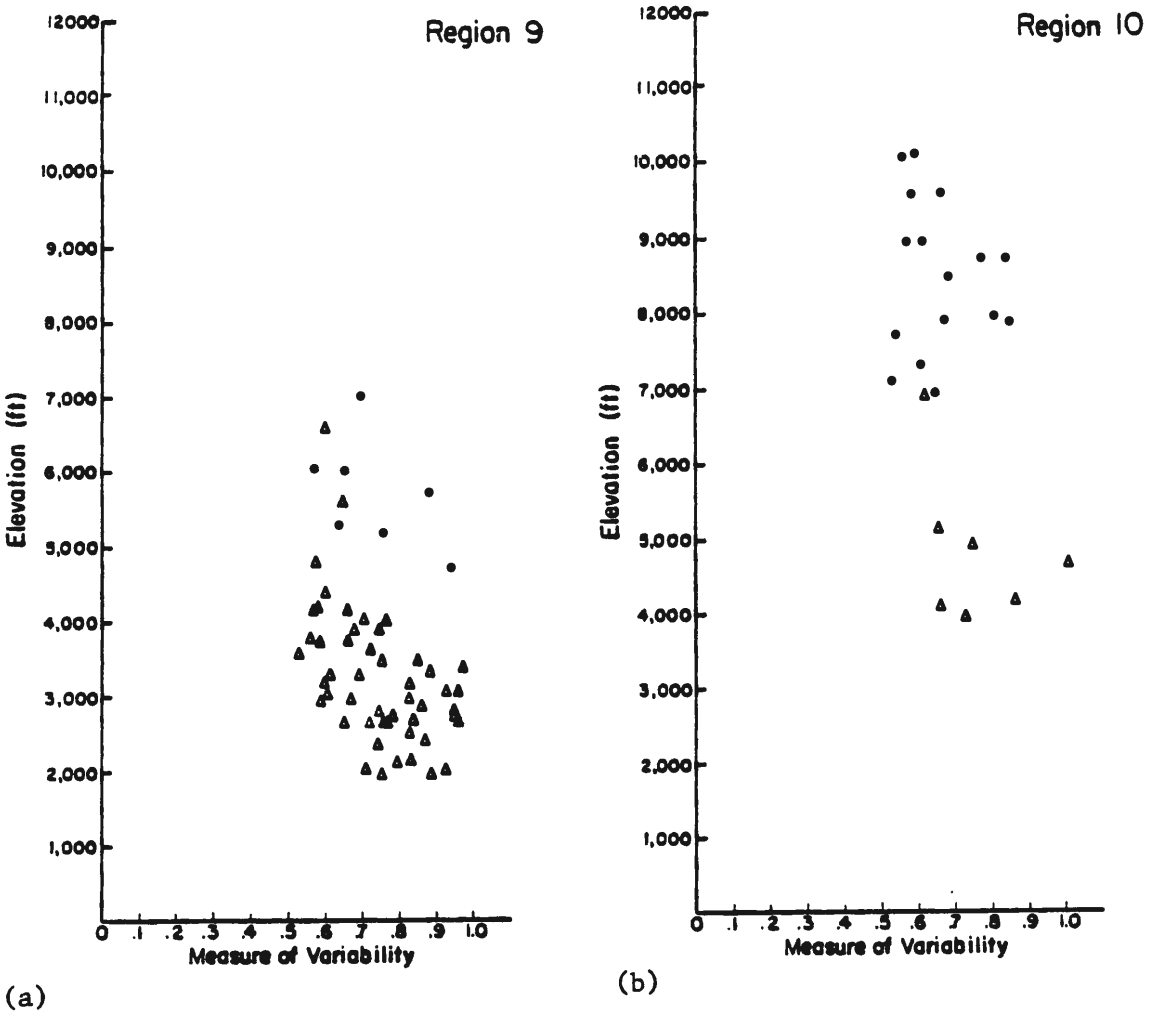

Figure IV.4 Same as Figure IV.1 except for a) region 9 and b) region 10.

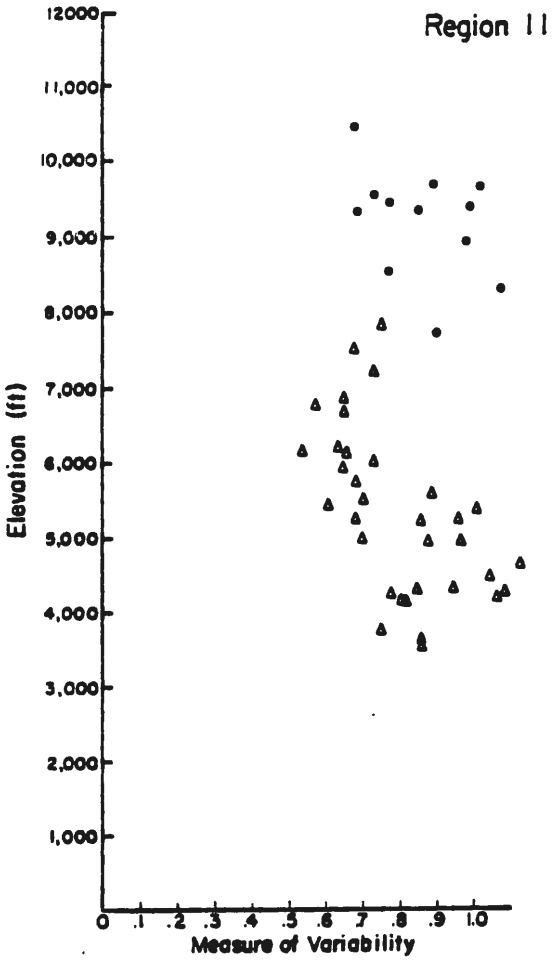

Figure IV.5 Same as Figure IV.1 except for region 11.

APPENDIX V

SPATIAL PATTERNS OF ANNUAL SN

In Chapter V spatial patterns of SN were described using objectively analyzed maps that showed the non-exceedence probabilities (based on 1951-1985 data) of SN. Figures 13-16, showed typical patterns for a wet year (1952), a dry year (1977), a north-to-south gradient year (1967), and an average year (1983). Figures V.1-V.16 show similar objectively analyzed maps for the other 31 years of the study.

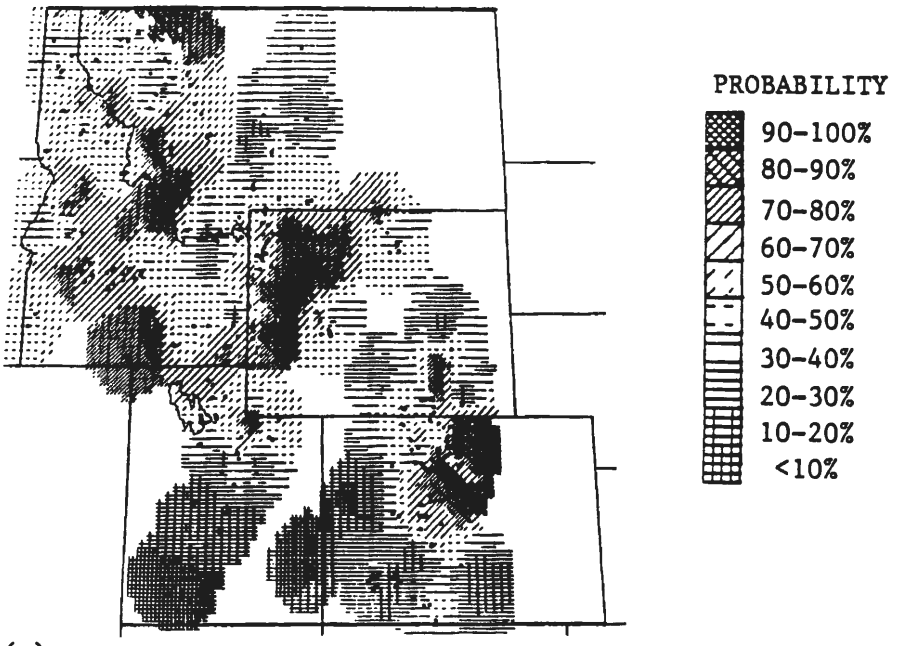

(a)

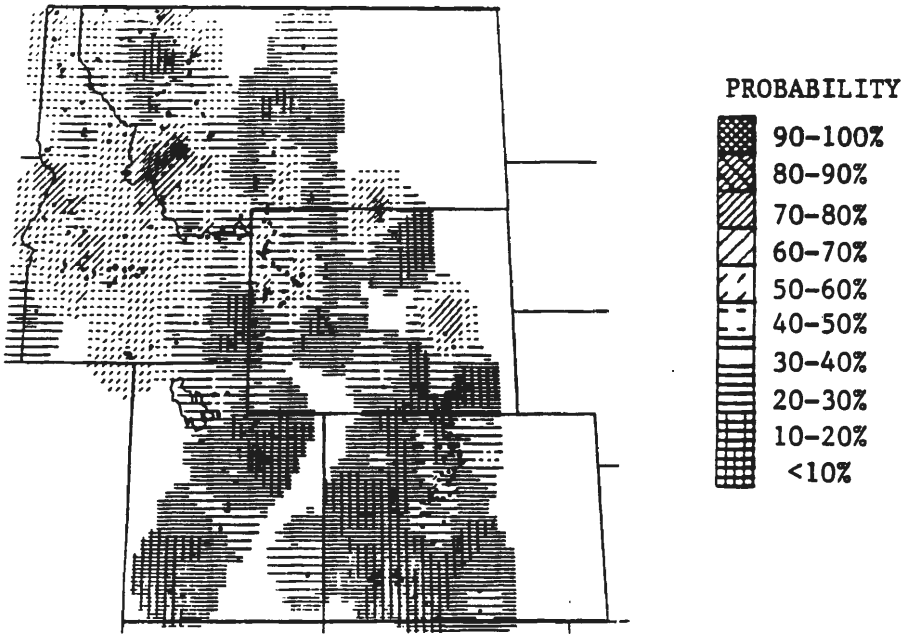

(b)

Figure V.1 Objectively analyzed map showing the non-exceedence probabilities (based on 1951-1985 data) of April 1 snowpack for a) 1951 (north-wet/south-dry pattern) and b) 1953 (dry pattern). Each of the 10 non-exceedence probability ranges are shaded differently.

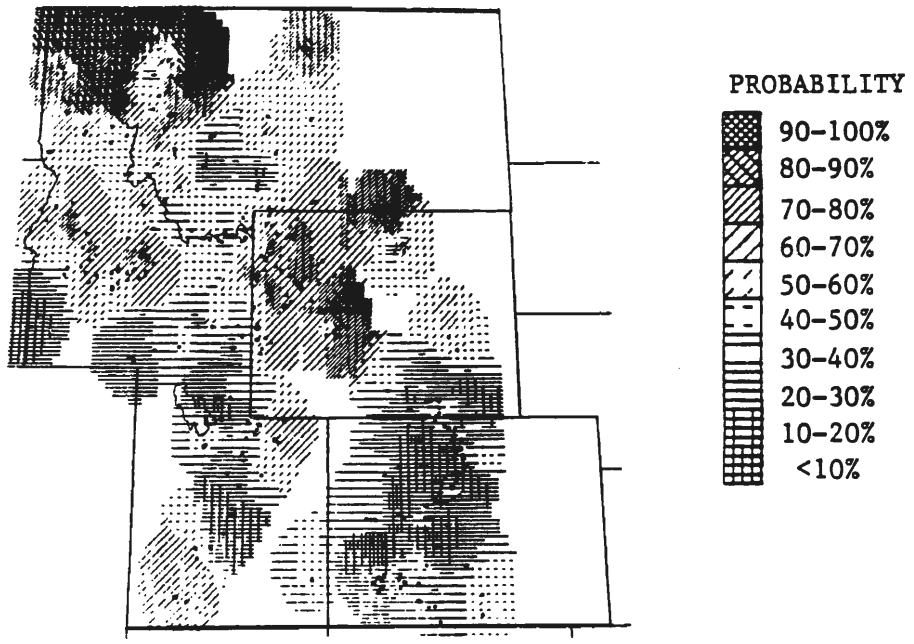

(a)

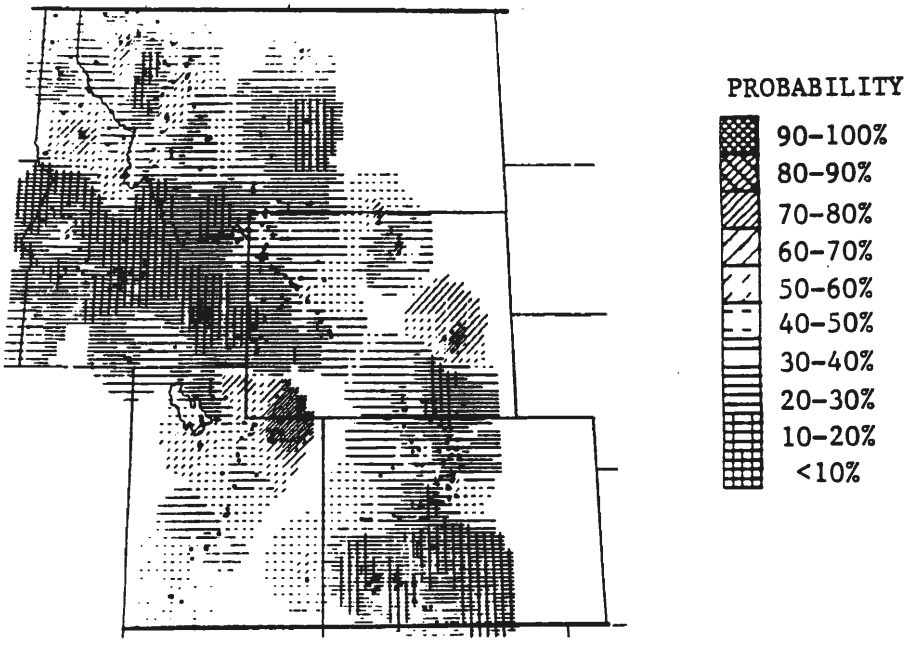

(b)

Figure V.2 Same as Figure V.1 except for a) 1954 (north-wet/south-dry) and b) 1955 (dry).

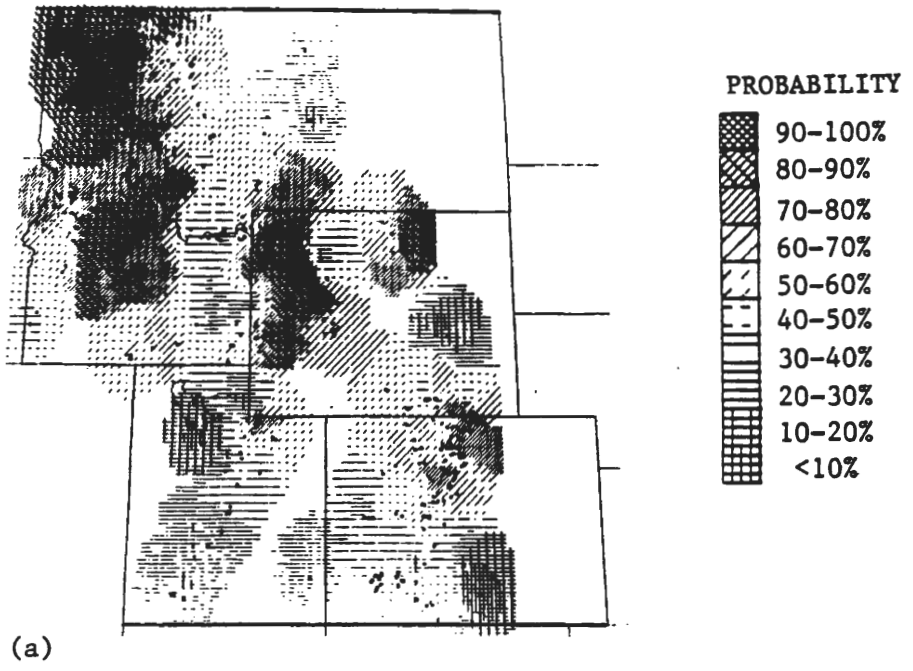

(a)

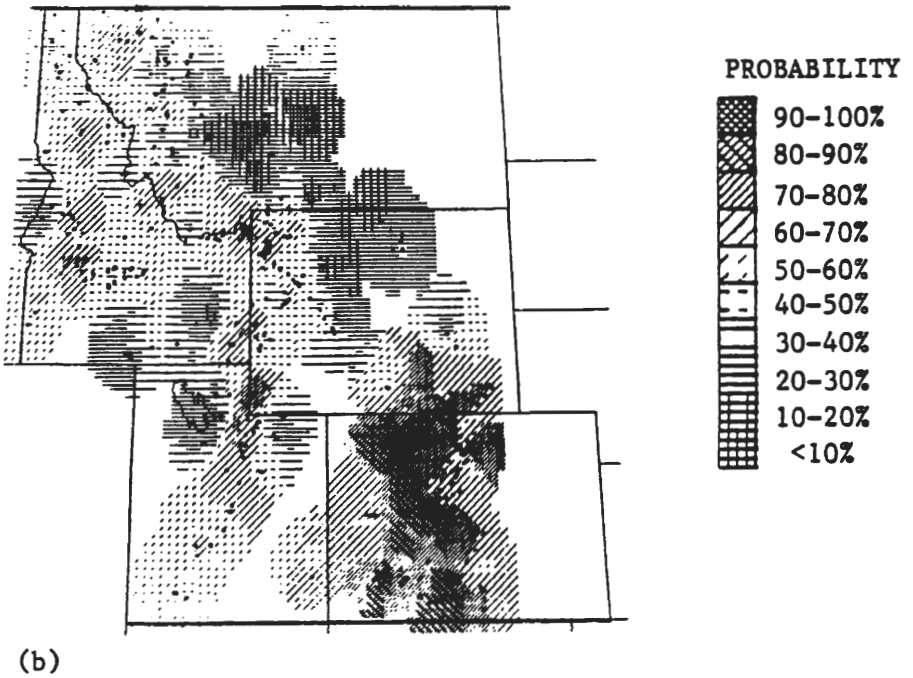

(b)

Figure V.3 Same as Figure V.1 except for a) 1956 (north-wet/south-dry) and b) 1957 (average).

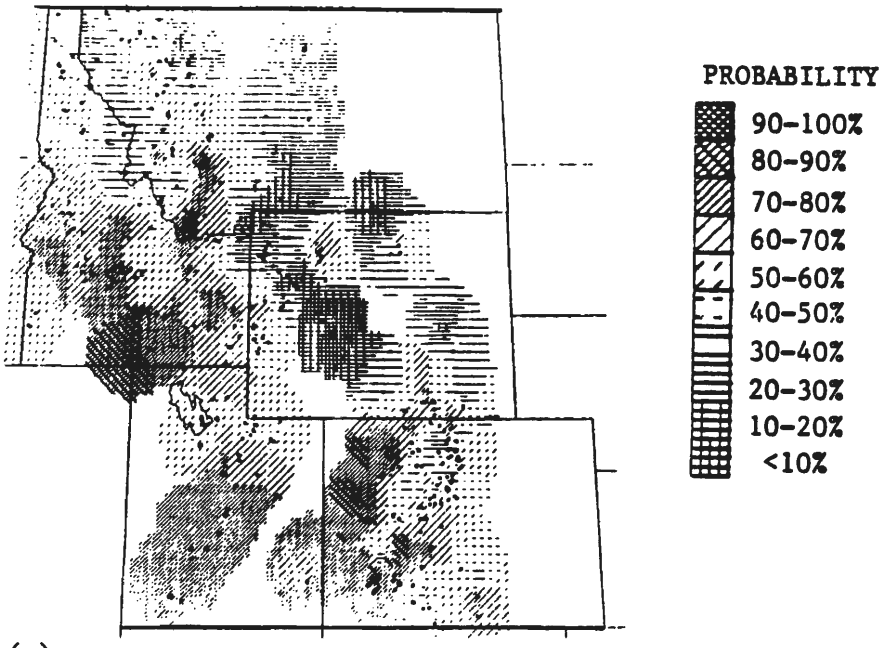

(a)

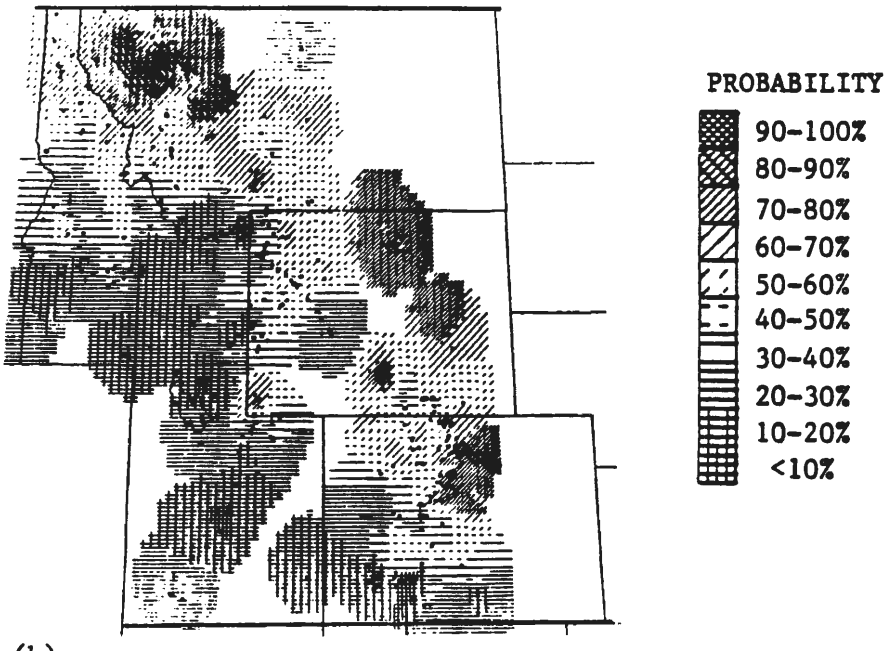

(b)

Figure V.4 Same as Figure V.1 except for a) 1958 (average) and b) 1959 (average).

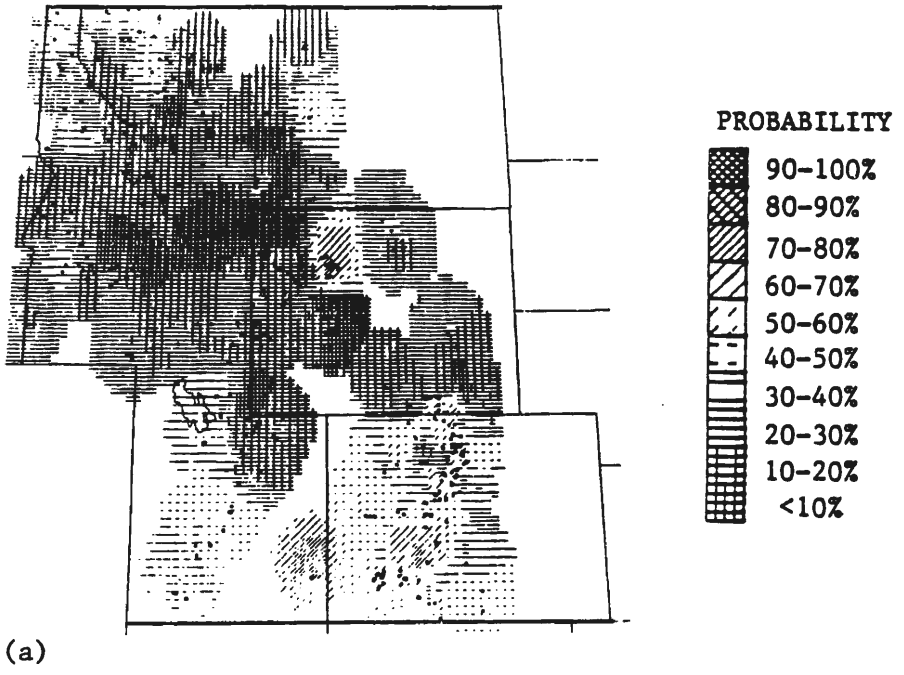

(a)

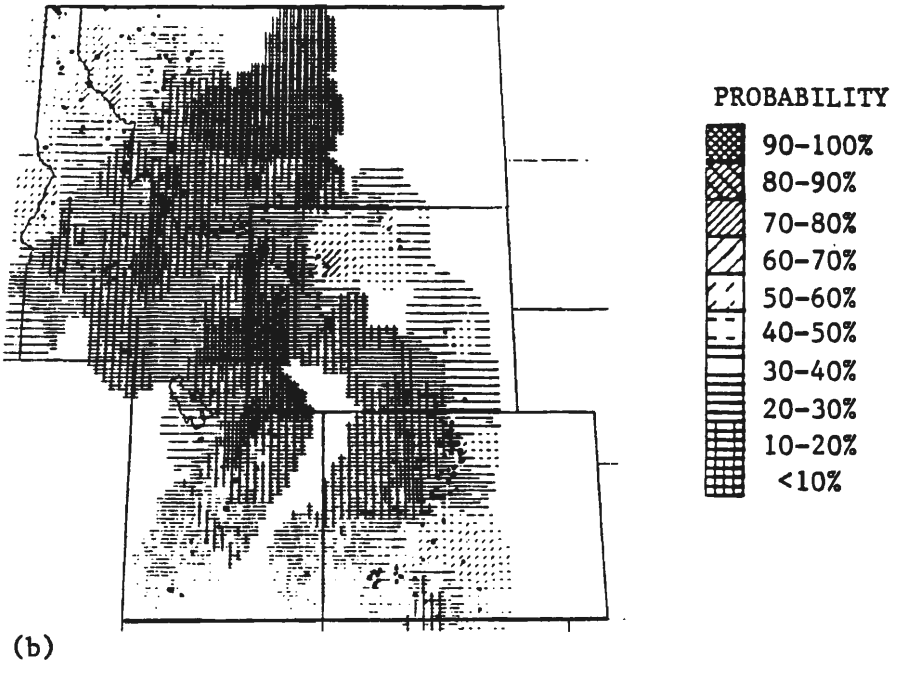

(b)

Figure V.5 Same as Figure V.1 except for a) 1960 (dry) and b) 1961 (dry).

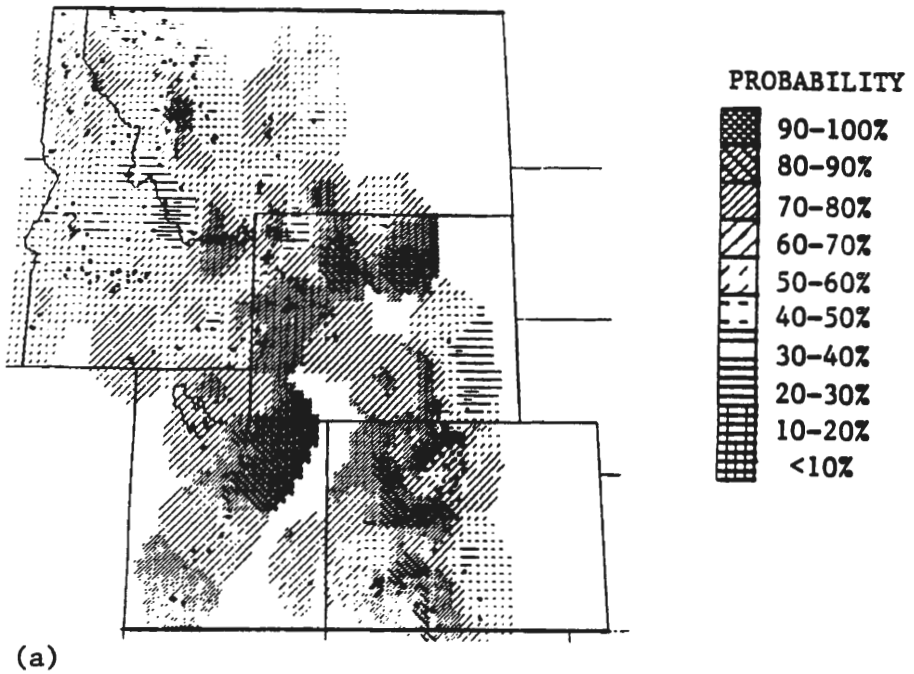

(a)

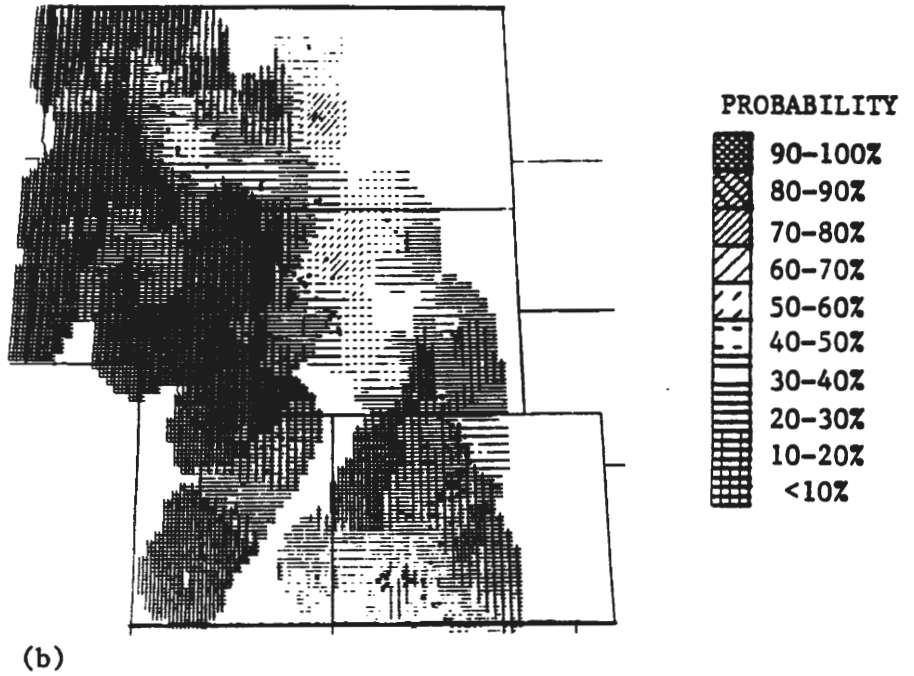

(b)

Figure V.6 Same as Figure V.1 except for a) 1962 (wet) and b) 1963 (dry).

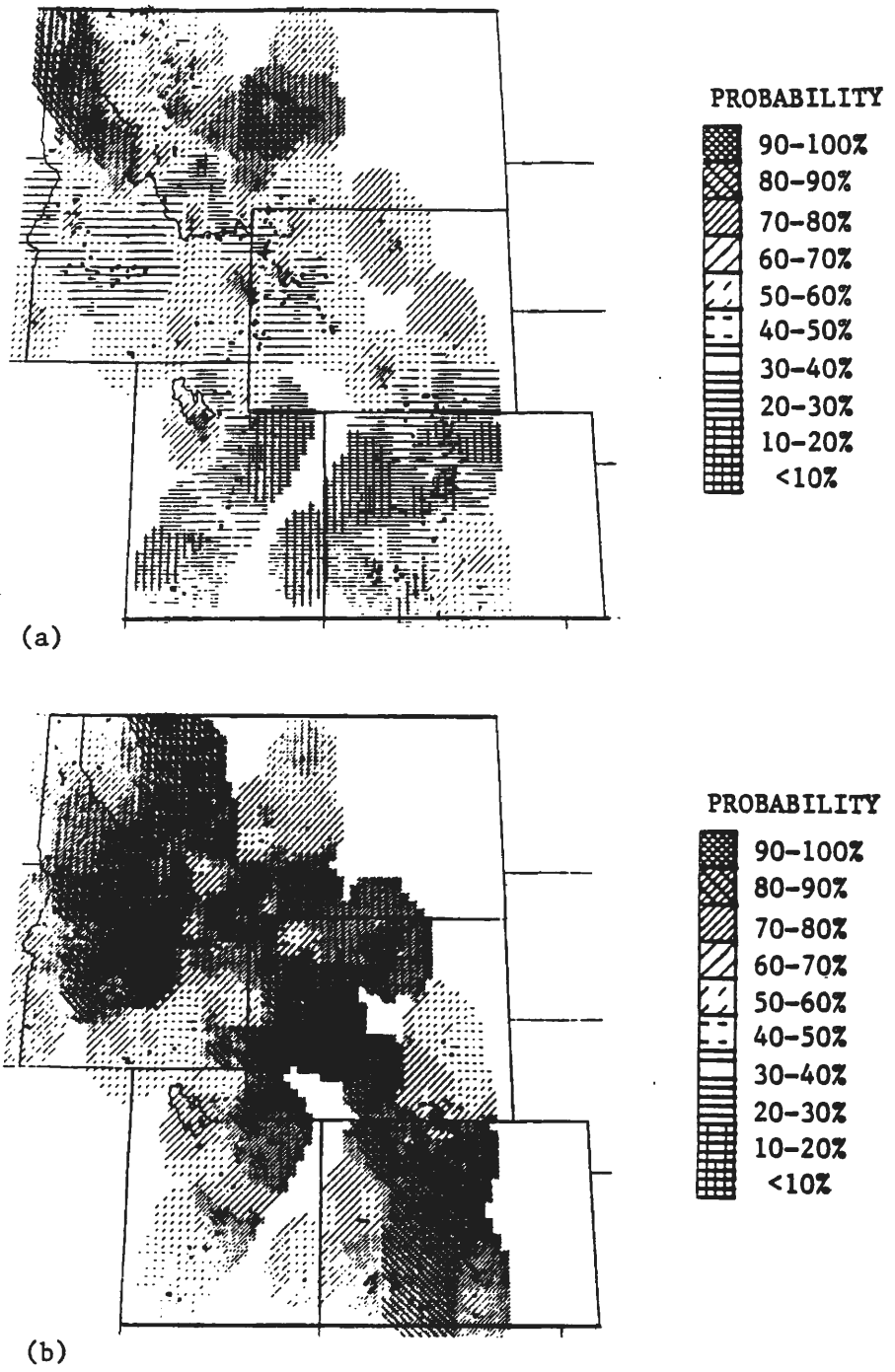

Figure V.7 Same as Figure V.1 except for a) 1964 (north-wet/south-dry) and b) 1965 (wet).

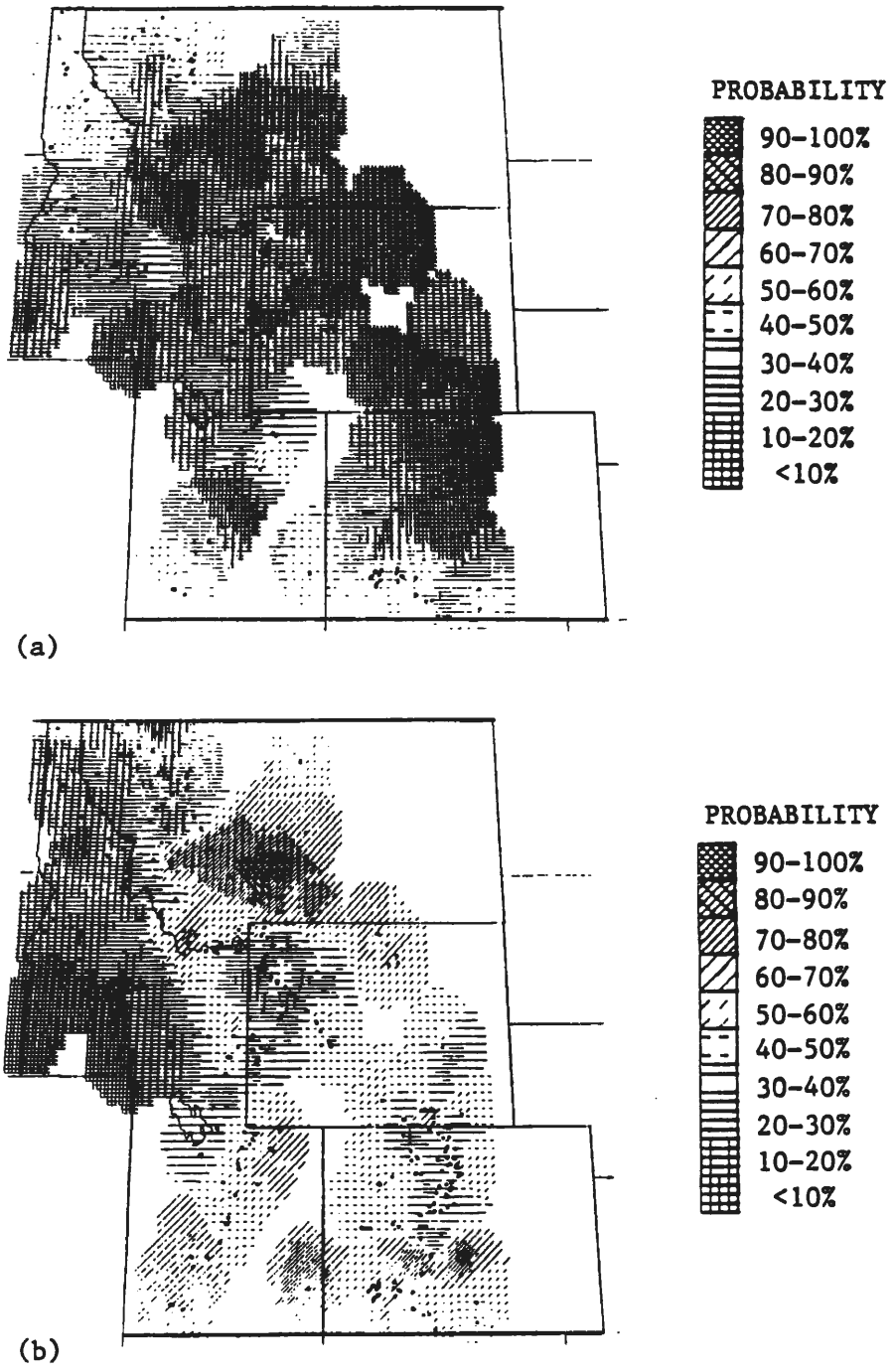

Figure V.8 Same as Figure V.1 except for a) 1966 (dry) and b) 1968 (average).

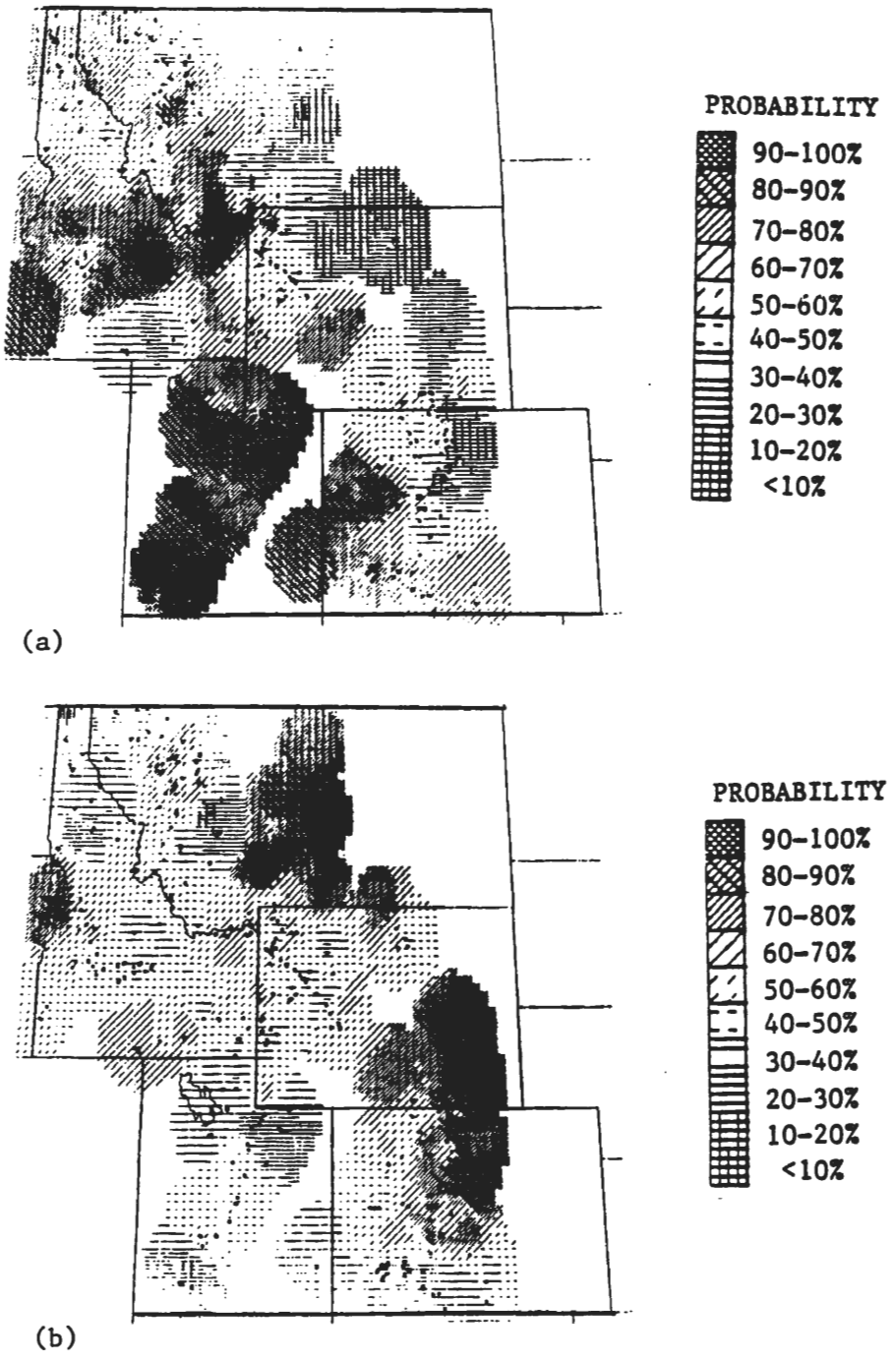

Figure V.9 Same as Figure V.1 except for a) 1969 (wet) and b) 1970 (average).

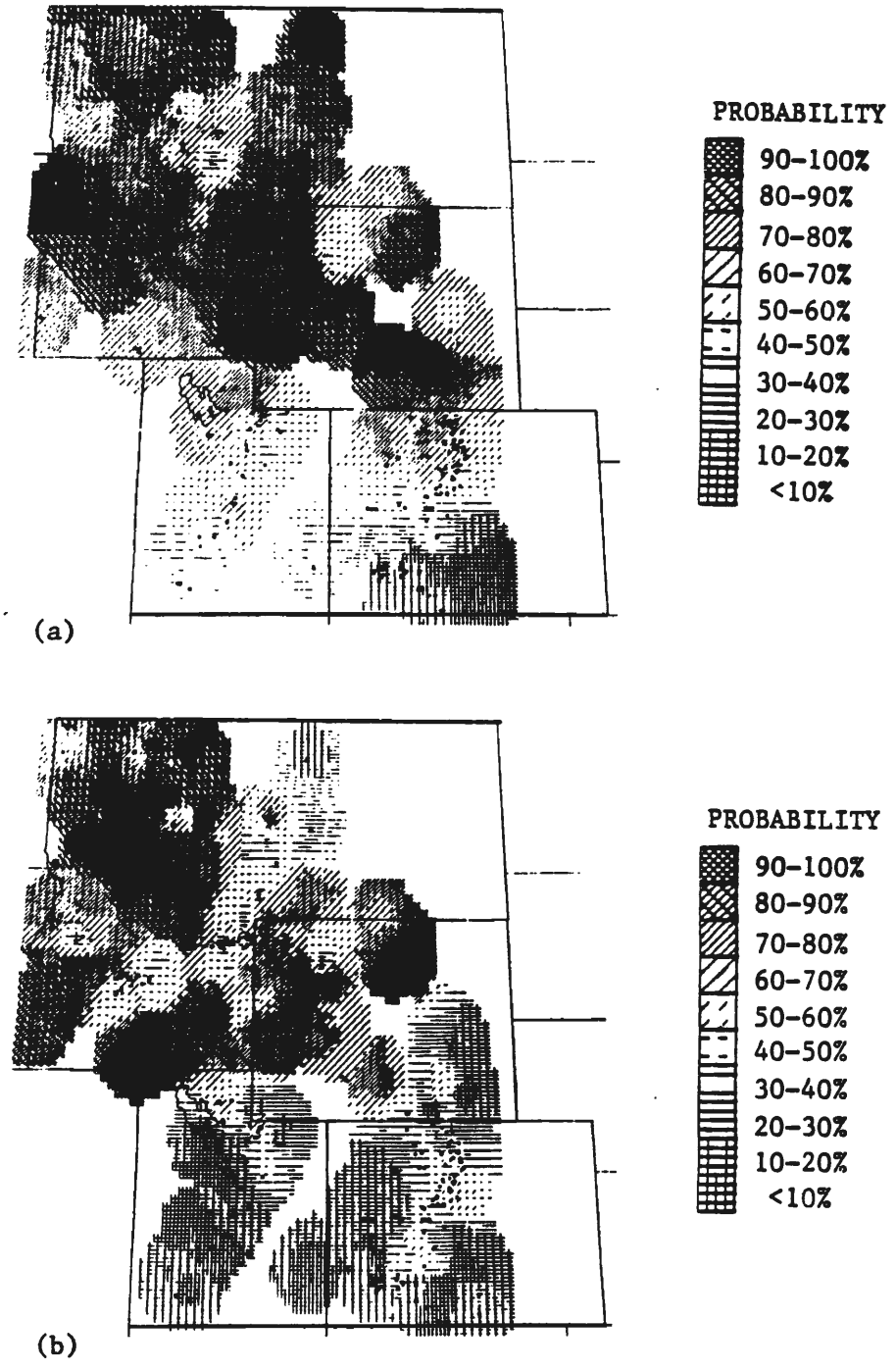

Figure V.10 Same as Figure V.1 except for a) 1971 (north-wet/south-dry) and b) 1972 (north-wet/south-dry).

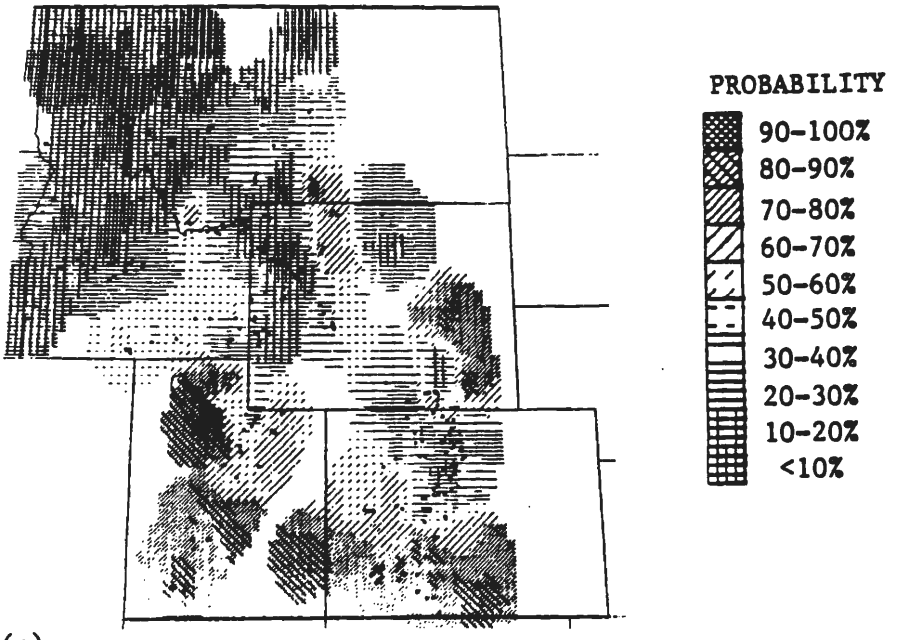

(a)

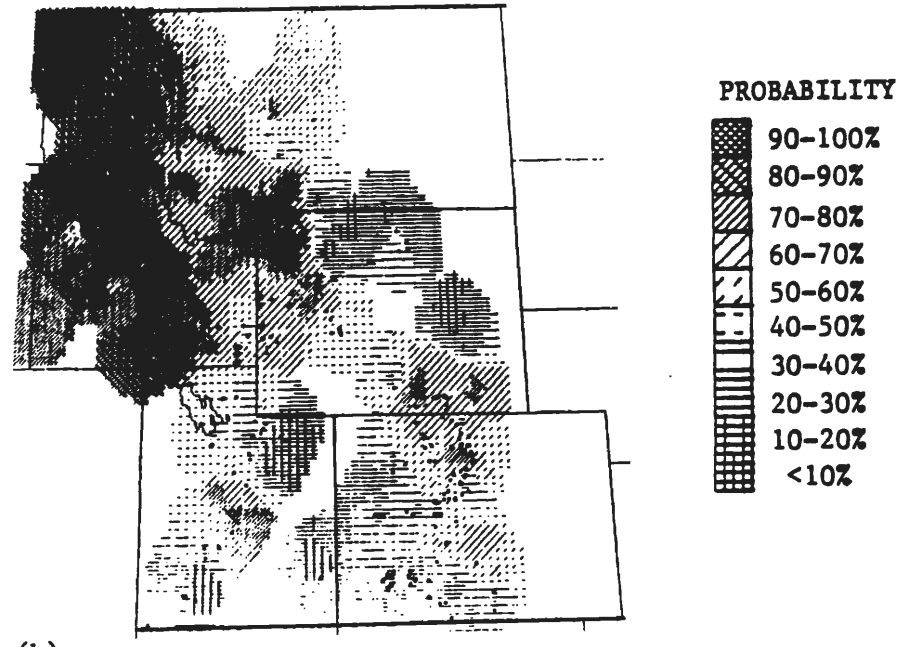

(b)

Figure V.11 Same as Figure V.1 except for a) 1973 (north-dry/south-wet) and b) 1974 (north-wet/south-dry).

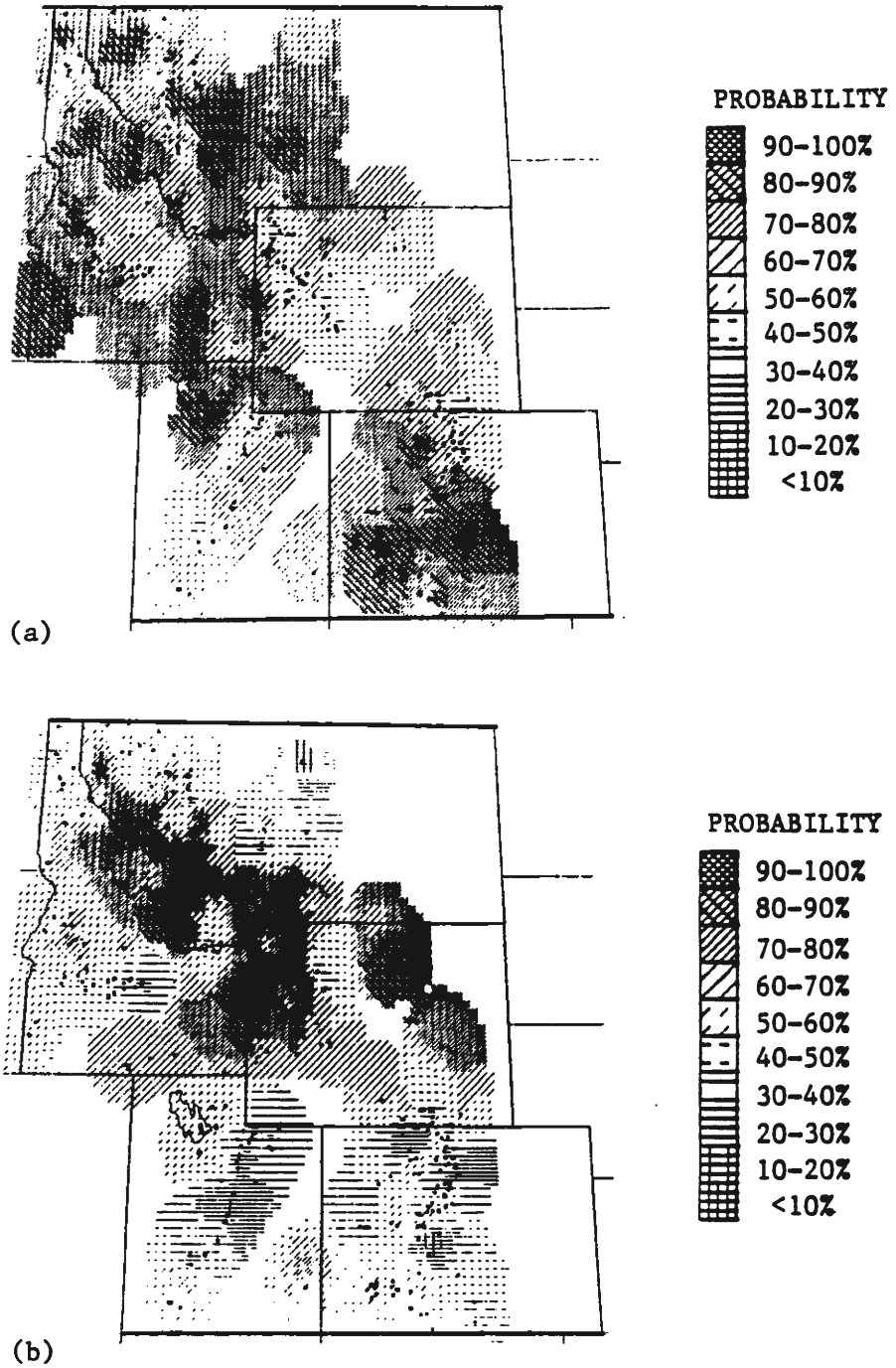

Figure V.12 Same as Figure V.1 except for a) 1975 (wet) and b) 1976 (average).

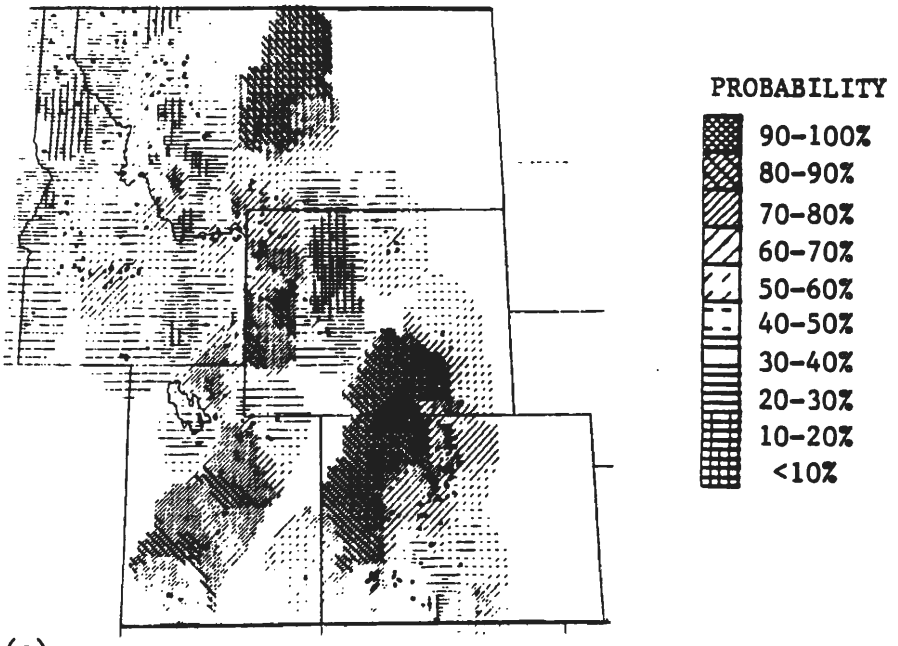

(a)

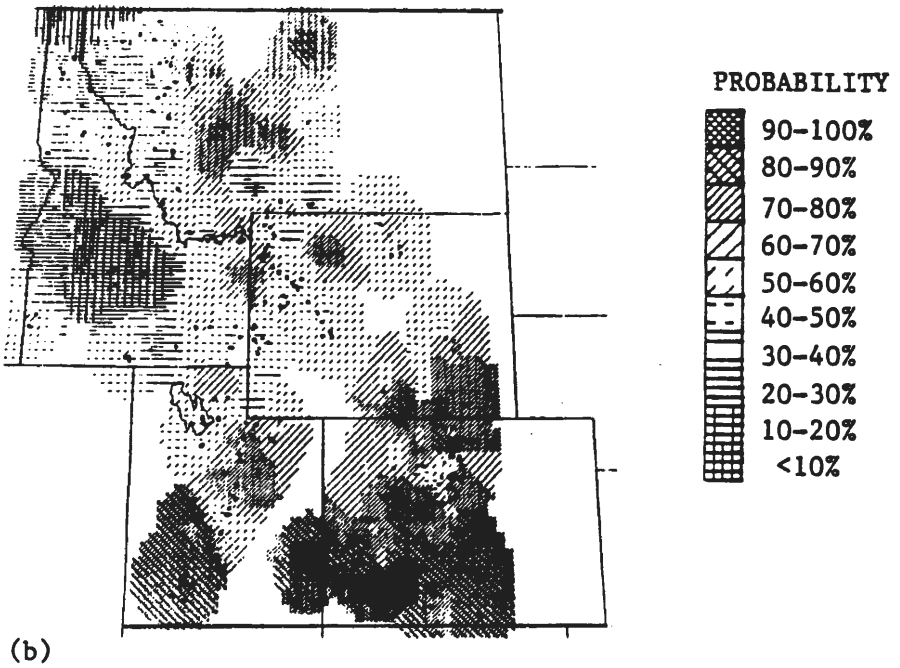

(b)

Figure V.13 Same as Figure V.1 except for a) 1978 (average) and b) 1979 (north-dry/south-wet).

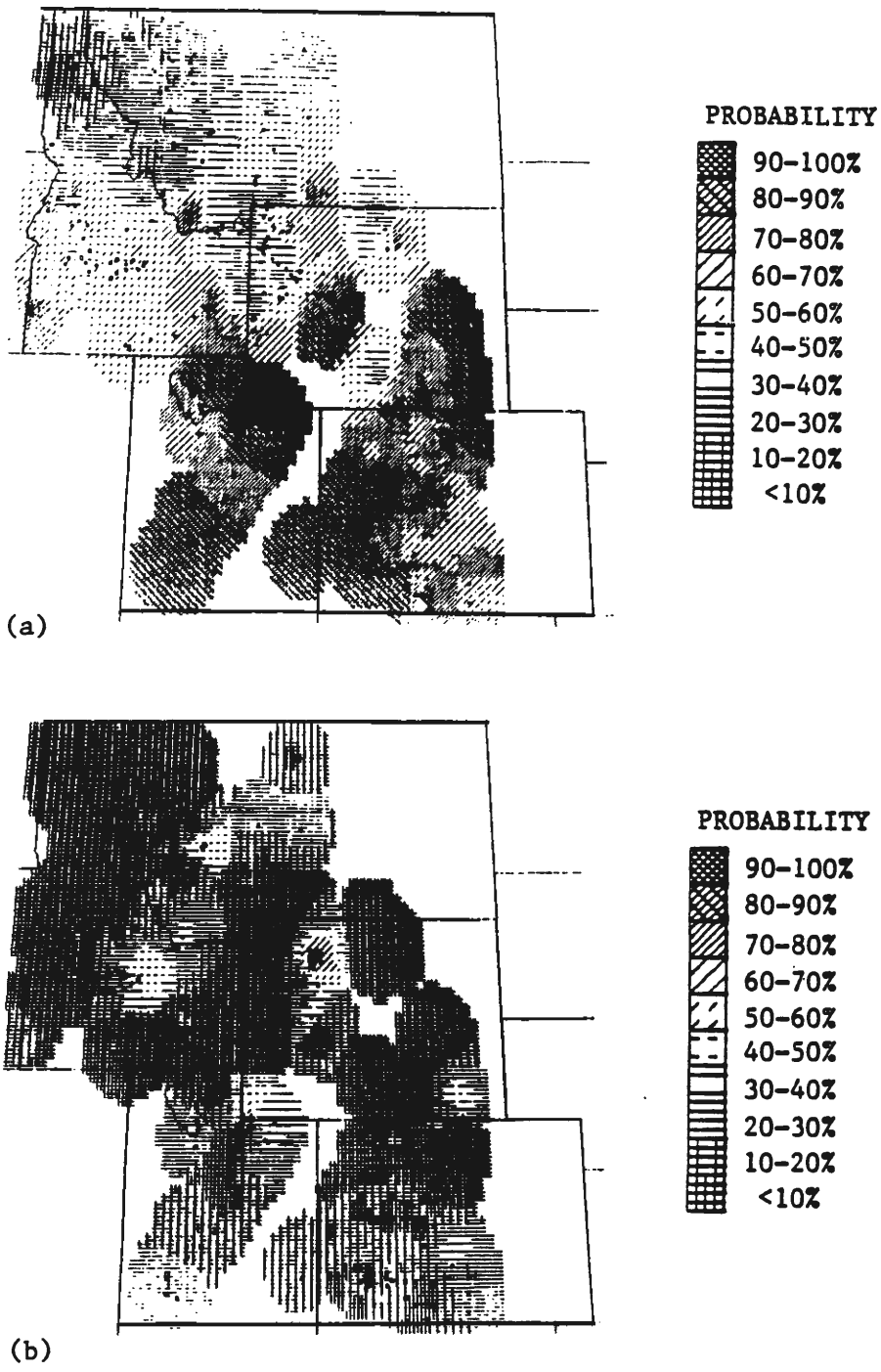

Figure V.14 Same as Figure V.1 except for a) 1980 (north-dry/south-wet) and b) 1981 (dry).

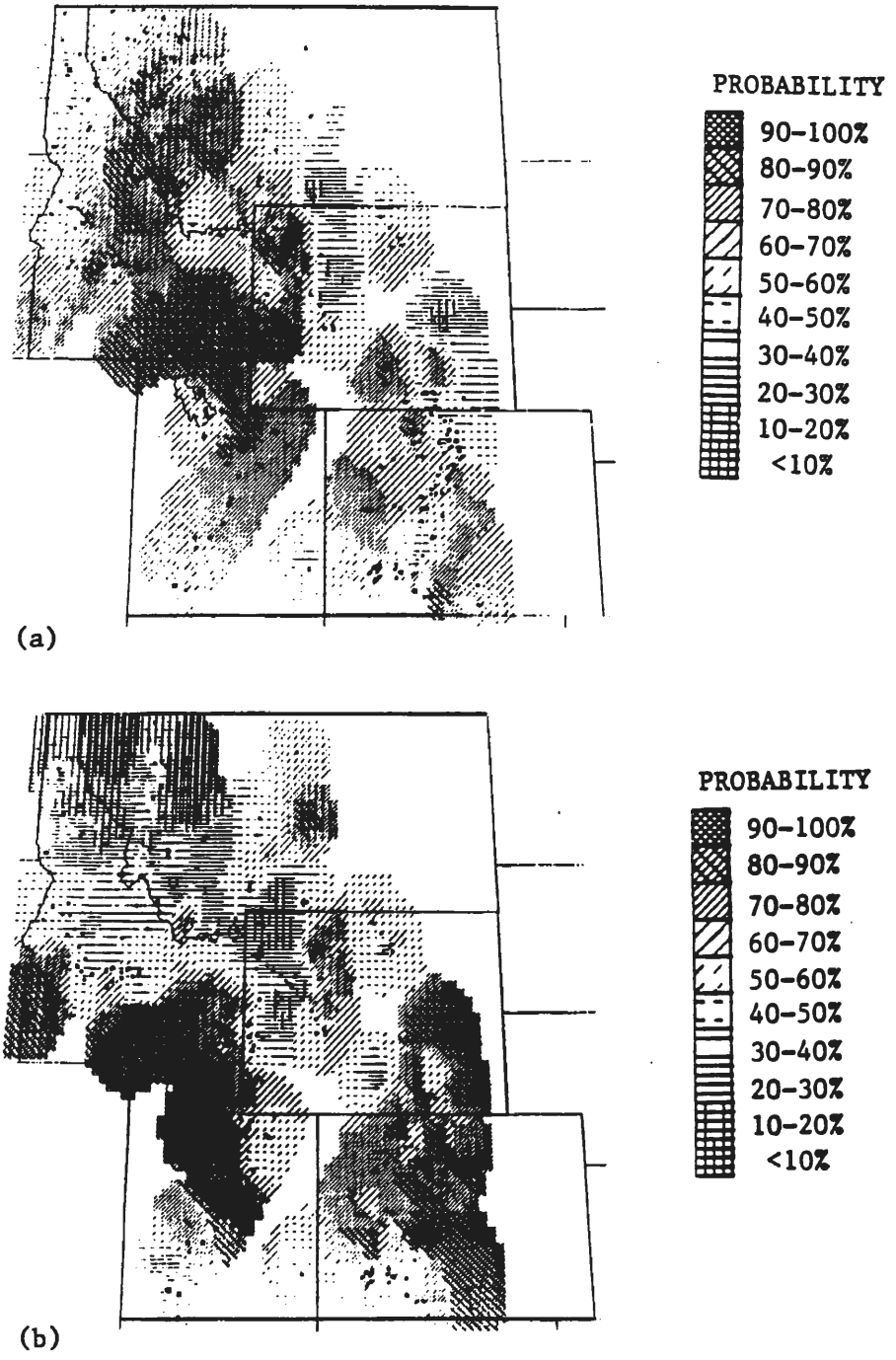

Figure V.15 Same as Figure V.1 except for a) 1982 (wet) and b) 1984 (north-dry/south-wet).

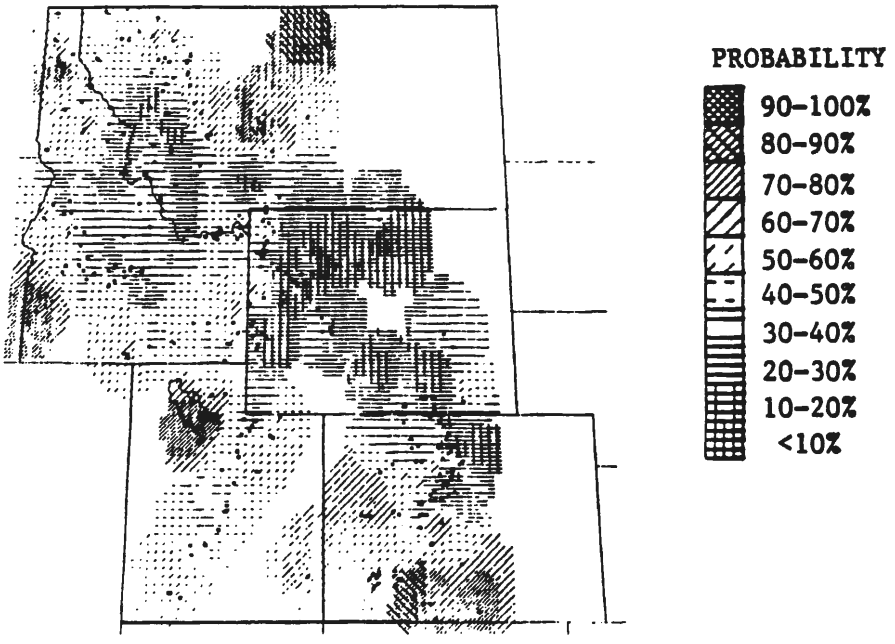

Figure V.16 Same as Figure V.1 except for 1985 (average).